Antecedent fluvial systems on an uplifted continental margin: constraining Cretaceous to present-day drainage basin development in southern South Africa

Janet Cristine Richardson

Submitted in accordance with the requirements for the degree of
Doctor of Philosophy

The University of Leeds
School of Earth and Environment

May 2016

The candidate confirms that the work submitted is her own, except where work which has formed part of jointly-authored publications has been included. The contribution of the candidate and the other authors to this work has been explicitly indicated below. The candidate confirms that appropriate credit has been given within the thesis where reference has been made to the work of others.

Chapter 7: Richardson, J.C., Hodgson, D.M., Wilson, A., Carrivick J.L. and Lang, A. Testing the applicability of morphometric characterisation in discordant catchments to ancient landscapes: a case study from southern Africa. Geomorphology, **201**, 162-176. DOI - doi:10.1016/j.geomorph.2016.02.026

Author contributions: Richardson, J.C – Main author. Responsible for data collection, collation and interpretation, and for writing the manuscript.

Hodgson, D.M, Wilson, A., and Lang, A – Data discussion, and detailed manuscript review.

Carrivick, J.L – Manuscript review.

Submitted: 26th September 2015

Available online: 23rd February 2016

Acknowledgments

I would like to thank my supervisors Dave Hodgson, Andreas Lang, Andrew Wilson and Jonathan Carrivick for their guidance and help throughout my project. I would especially like to thank Dave for the opportunity to do this PhD, for always being enthusiastic with my work (even if it meant turning into a geomorphologist!) and for 'helping' me to find wine!

I would like to thank the British Sedimentological Research Group and British Geomorphology Society for providing postgraduate funding for the cosmogenic dating and conference attendance. I would like to thank the Council of Geoscience, South Africa for providing geological tiles for the use in ArcGIS. Midland Valley Exploration Ltd. are thanked for providing the license for their proprietary software, Move. I would like to thank the farm owners of the Western Cape for allowing me onto their land to collect samples. I would also like to thank Veerle Vanacker for her help during laboratory work for cosmogenics and for guidance in interpreting the results. Thank you to Jérôme Schoonejans and Marco Brevin for their help in the laboratory.

I would like to thank Robert Duller, John Kavanagh and Barabara Mauz for the interesting talks when I spent time at Liverpool University at the start of my PhD.

I would like to thank STRAT group, for all the adventures, discussions and nights out. For their support and always helping me out when I came to visit (special thanks to Michelle, Hannah and Sarah for looking after me when I didn't live in Leeds and came to visit!). I would especially like to thank Claire Mellett for helping me start my PhD in Liverpool and to Yvonne Spychala for supporting me during the final months!

Finally I would like to thank my friends and family, for listening to my research and for providing support towards the final write up period. Thank you to Garry Power and the Geography department at St Michaels Catholic High school for inspiring me about Earth sciences from a young age. I would especially like to thank my aunt Daphne and uncle Richard for their continued support during my project and previous studies. Special thanks to Stephen McCann and family for their continued support and encouragement during my PhD.

Papers

Several chapters within this thesis (Chapters 4 – 8) were written as papers which were submitted to various geoscience journals for publications. The status of these papers are below.

In print:

Richardson, J.C., Hodgson, D.M., Wilson, A., Carrivick, J.L. and Lang, A., 2016. Testing the applicability of morphometric characterisation in discordant catchments to ancient landscapes: A case study from southern Africa.*Geomorphology*, *261*, pp.162-176.

Under review:

Chapter 5: Richardson, J.C, Hodgson, D.M, Paton, D., Rawcliffe, A., Lang, A. Reconstruction of the erosional landscape development of southwestern Africa since the late Jurassic: implications for offshore sediment budgets, drainage basin evolution and the Mesozoic exhumation of southern Africa: where is all the sediment? Gondwana Research, in review.

Author contributions:

Richardson, J.C – Main author. Responsible for data collection, collation and interpretation, and for writing the manuscript. Repeating Rawcliffe's 3DMove work and applying further constraints.

Hodgson, D.M – Data discussion, and detailed manuscript review.

Lang, A, Paton, D – Data discussion and manuscript review.

Rawcliffe, A. – Manuscript review and initial 3DMove work as part of M.Geol project (Appendix 1).

Chapter 6: Richardson, J.C., Vanacker, V., Lang, A., and Hodgson, D.M. Constraining landscape evolution using cosmogenic nuclide dating in an ancient setting: the pediments of the Western Cape, South Africa. ESPL, in review.

Author contributions:

Richardson, J.C – Main author. Responsible for data collection, collation and interpretation, and for writing the manuscript.

Vanacker, V – guidance in the laboratory with data processing and interpretation, manuscript review.

Hodgson, D.M and Lang, A – Data discussion, and detailed manuscript review.

‘Rivers are the gutters, down which flow the ruins of continents’

Leopold et al., 1964

Abstract

Reconstructing drainage evolution has important implications for constraining long-term source-to-sink configurations. Furthermore, the analysis of ancient landscapes can support research in geomorphological concepts such as steady state and landscape evolution modelling. Techniques such as cosmogenic dating and morphometric analysis have rarely been applied to investigate the long-term drainage evolution of systems draining southern South Africa.

This study focusses on the large-scale antecedent Gouritz catchment, Western Cape. Integrating provenance, cosmogenic and geomorphological (planform / morphometric indices) evidence indicates the trunk rivers are Cretaceous or older in age (i.e. principal topography of Mesozoic age). The trunk rivers fed huge volumes of sediment offshore during large-scale Mesozoic exhumation of southern South Africa with remnant coeval deposits in onshore extensional basins. However, there is a mismatch of onshore exhumation and offshore deposition and material is now found on the Falkland Plateau; separating source-to-sink by 6000 km. During exhumation, large scale pediments formed that grade to individual base levels and should be taken as individual features, not 'surfaces' correlated across the continent. A second phase of pediment evolution occurred in the mid-Cenozoic, dissecting the pediments and eroding small catchments into the Cape Fold Belt. These smaller order streams are strongly affected by the tectonic grain of the fold belt, whereas the trunk rivers are not, which is shown by variation in morphometric indices. The lack of correlation between catchment properties and denudation rates indicate the system has decoupled and that allogenic factors are now dominant. Due to the low rates of denundation, weathering is currently the rate limiting factor. However, during the early evolution of the catchment, tectonic activity was more dominant than the present day. The ancient catchment is in geomorphic steady-state, and highlights the need for further research into long-term landscape evolution, and linkage to offshore depositional records.

Table of Contents

List of Figure

List of Tables

Chapter 1 Introduction

1.1 Project rationale

The landscapes of southern South Africa have long intrigued geomorphologists and geologists due to distinctive topography and the designation as a 'type' example of a passive margin (e.g., King, 1944; Fleming et al., 1999; van der Beek, 2002; Vanacker et al., 2007; Kounov et al., 2009). Much of the geomorphological research in the area is focussed on the formation and development of the Great Escarpment (e.g., King, 1953; Partridge and Maud, 1987; Brown et al., 2002), and the large diamondiferous drainage systems north of the escarpment (e.g., Dingle and Hendey, 1984; de Wit, 1999; Moore and Larkin, 2001; Goudie, 2005). However, south of the escarpment, the river systems supply multiple offshore sedimentary basins (McMillan et al., 1997) and have been widely overlooked, with limited application of recent advancements in geomorphological techniques such as cosmogenic dating.

Ancient landscapes, such as South Africa are also often overlooked in the literature, and there is a focus towards the more active, highly erosional settings that have high sediment flux (e.g., Vance et al., 2003; Safran et al., 2005; Schaller et al., 2005; Derrieux et al., 2014). Despite this lack of detailed investigation, ancient landscapes form large areas of the Earth's surface and have been argued to represent many 'Gondwana landscapes' (Fairbridge, 1968), including cratonic areas and passive continental margins (e.g., Australia: Ollier, 1991; Ollier and Pain, 2000; Twidale, 2007a,b). Ancient landscapes also deserve attention as they have the potential to offer insights into the long-term interactions and variations of controls such as tectonic uplift or climate (Bishop, 2007).

The landscape of southern South Africa has developed since the break-up of Gondwana in the Mesozoic (Moore and Blenkinsop, 2002; Hattingh, 2008), and there has been an absence of significant geodynamic activity since then (e.g., Partridge and Maud, 1987; Kounov et al., 2007; Scharf et al., 2013; Bierman et al., 2014). However, the region still exhibits extraordinary morphology in the form of deep discordant gorges that are incised into highly resistant quartzites in the '*Alpine-like*' Cape Fold Belt. There remains a first order debate about the age of the landscape (e.g., Meoszoic: Partridge, 1998; Brown et al., 2000; Brown et al., 2002; Doucouré and de Wit 2003; de Wit 2007; Tinker et al., 2008a; Kounov et al., 2015 / Cenozoic: Burke 1996; Green et al., 2016). Whilst some previous work has argued for major Cretaceous exhumation (e.g., Brown et al., 2002; Tinker et al., 2008a), the volume of material removed from southerly draining river systems, the switch from deposition to

incision, the rates of incision and the drivers of antecedence seen within the region remain fundamental unknowns.

More widely, knowledge on the onshore landscape evolution of ancient settings, will provide information regarding the development of events (e.g., exhumation), that have affected the redistribution of erosional material and the development of hydrocarbon reservoirs, thereby constraining source-to-sink concepts (Tinker et al., 2008b). Due to advancements in cosmogenic analysis, remote sensing and provenance, the long-term onshore reconstruction and evolution of southern South Africa can be compiled for the first time.

1.2 Thesis aims

The overall aim of this project is to constrain landscape evolution and geomorphic development of the Western Cape with specific emphasis on the Gouritz catchment from the Cretaceous to the present day. The thesis is framed by a series of research questions and their rationale, which will be returned to in the discussion chapter. The rationale provided in the following section are related to southern African research, but are under-pinned by global studies as explained in Chapter 2.

Question 1: How can reconstructing drainage development help constrain source-to-sink concepts and rift basin facies models within South Africa?

Rationale: In modern systems, the flux of sediment between drainage basins and sedimentary basins can be readily quantified. However, the analysis of the long-term development of drainage basins, and the linkage to the depositional archive in sedimentary basins, is challenging to constrain. The river systems south of the escarpment are often overlooked in geomorphological work (e.g., Rogers, 1903, Partridge and Maud, 1987) despite supplying multiple offshore sedimentary basins (McMillan et al., 1997). Previous work has indicated a mismatch between onshore exhumation volumes of the Cretaceous and offshore accumulation rates (e.g. Tinker et al., 2008b). However, this work did not taken into account drainage evolution. Conversely, deposits associated with the large-scale Mesozoic exhumation, and reported drainage networks have not been integrated within a provenance and drainage reconstruction framework (e.g., Lock et al., 1975). Furthermore, source-to-sink concepts and rift-facies models have not been integrated with long-term tectonic movement and drainage development e.g., formation of antecedent drainage with large-scale transverse river systems which are characteristic to the evolution of southern South Africa (e.g., Leeder and Gawthorpe, 1987; Schlische, 1992).

Question 2: What is the spatial and temporal variation in erosion rates across southern South Africa and the Gouritz catchment?

Rationale: Understanding the erosional history can help address fundamental questions such as the principal age of the landscape, the absolute and relative timing of when different landforms became active, and help constrain the switch from deposition to incision. This can then be used to infer the effects of climate or tectonic activity on the catchments (e.g., Brook et al., 1995; Burbank et al., 1996; Granger et al., 1997; Jackson et al., 2002; Margerison et al., 2005; Dunai et al., 2005; Owen et al., 2005; Wittmann et al., 2007; Willenbring and Blackenburg, 2010; Bellin et al., 2014; Vanacker et al., 2015) and assess landscape evolution models associated with southern Africa (e.g., King, 1944, 1953, 1967). The current geochronology research (e.g., Fleming et al., 1999; Cockburn et al., 2000; Bierman and Caffee, 2001; van der Wateren and Dunai, 2001; Kounov et al., 2007; Codilean et al., 2008; Dirks et al., 2012; Decker et al., 2011; Erlanger et al., 2012; Chadwick et al., 2013; Decker et al., 2013; Scharf et al., 2013; Bierman et al., 2014; Kounov et al., 2015) indicates a decrease in erosion rates since the Cretaceous to the present day rates. Rates of up to 175 mMa^{-1} are recorded using Apatite Fission Track in the Cretaceous (e.g., Gallagher and Brown, 1999; Cockburn et al., 2000; Brown et al., 2002; Tinker et al., 2008b; Kounov et al., 2009; Flowers and Schoene, 2010), which decrease to 62.3 – 0.85 mMa^{-1} in the Cenozoic, recorded using terrestrial cosmogenic nuclides (Fleming et al., 1999; Cockburn et al., 2000; Bierman and Caffee, 2001; van der Wateren and Dunai, 2001; Kounov et al., 2007; Codilean et al., 2008; Dirks et al., 2010; Decker et al., 2011; Erlanger et al., 2012; Chadwick et al., 2013; Decker et al., 2013; Scharf et al., 2013; Bierman et al., 2014; Kounov et al., 2015). Published data indicates variation between different landforms of southern Africa, with the highest erosion rates related to the retreat of the escarpment face (up to 62.3 mMa^{-1}; Fleming et al., 1999) and the lowest related to pediments (0.85 mMa^{-1}; van der Wateran and Dunai, 2001; Bierman et al., 2014; Kounov et al., 2015). However, few cosmogenic and apatite fission track studies have been completed south of the Escarpment (e.g., Tinker et al., 2008a; Scharf et al., 2013; Bierman et al., 2014; Kounov et al., 2015), which are vital in understanding landscape development in the Western Cape.

Question 3: How can advancements in geomorphic techniques and concepts help constrain landscape development in ancient settings?

Rationale: Ancient landscapes and landforms have long been recognised in the literature (e.g., Du Toit, 1954; King, 1956,b; Carignano et al., 1999; Demoulin et al.,

2005; Panario et al., 2014; Peulvast and Bétard, 2015), but modern advances in geomorphological techniques have not been applied. Typically, morphometric theories are applied to highly erosional 'young' landscapes (e.g., Snyder et al., 2000; Zhang et al., 2013; Antón et al., 2014; Ghosh et al., 2014), and cosmogenic analysis are biased towards these active settings (e.g., Vance et al., 2003; Safran et al., 2005; Schaller et al., 2005; Derrieux et al., 2014). The application of modern techniques (GIS, cosmogenics) to constrain ancient landscapes is an important test of the assumptions embedded in morphometric indices or cosmogenic analysis methods. Advancements in techniques such as GIS or cosmogenic dating can help to critically analyse traditional viewpoints such as steady-state landscapes (Whipple, 2001), landscape evolution concepts (e.g., Davis, 1889; King, 1953; Hack, 1960) and testing whether there is geomorphic equivalent to the increase in depositional rates with decreasing timescales as recorded by Sadler (1981); that erosion will increase over time. The Gouritz catchment provides an ideal setting to test commonly used techniques in a large-scale tectonically quiescent setting.

1.3. Thesis structure

This thesis comprises of three manuscripts that have been accepted, or submitted, for publication in international peer-reviewed journals (Chapter 5, 7 and 8). Each of the chapters addressed different research questions.

Chapter 2: Is a literature review and provides a wider general background of the themes discussed in this thesis and provides a framework for the discussion. This chapter identifies the wider rationale and research gaps related to the research questions.

Chapter 3: Regional settings: provides a framework for the discussion by providing information on the geologic, climatic and geomorphic setting of the study area within southern South Africa.

Chapter 4: Provides a methodology of the thesis, including morphometric analysis, ArcGIS and cosmogenic nuclide dating.

Chapter 5: *Reconstruction of the erosional landscape development of southwestern Africa since the late Jurassic: implications for offshore sediment budgets, drainage basin evolution and the Mesozoic exhumation of southern Africa: where is all the sediment?* – submitted to Gondwana research: this chapter calculates the volume of material removed from southern South Africa, and reconstructs the drainage

evolution by integrating geomorphological and sedimentological evidence, the sediment sink is then speculated by using tectonic reconstructions.

Chapter 6: *Catchment averaged denudation rates, in a large antecedent catchment, South Africa; does nature do the averaging?* – This chapter assess variation in erosion rates between the trunk rivers of the Gouritz catchment, and the incisional history into the Cape Fold Belt. The denudation history is used to assess whether nature does the averaging. This is a key assumption in calculating catchment average denudation whereby the rivers will naturally incorporate grains eroded at different rates and from different source areas (e.g., hillslope processes, bedrock erosion).

Chapter 7: *Constraining landscape evolution using cosmogenic nuclide dating in an ancient setting: the pediments of the Western Cape, South Africa* – submitted to ESPL; this chapter assess the exposure ages and lowering rates of pediments within the Gouritz catchment. The data is then presented in a wider lithological and geomorphologic perspective, to help benchmark the cosmogenic results.

Chapter 8: *Testing the applicability of morphometric characterisation in discordant catchments to ancient landscapes: a case study from southern Africa* – published in Geomorphology: this chapter tests the applicability of commonly used morphometric indices to an ancient setting. DOI - doi:10.1016/j.geomorph.2016.02.026

Chapter 9: Is an extended discussion that addresses the key scientific research questions outlined in Chapter 1.2.

Chapter 10: Conclusions, wider implications and further work are discussed.

Chapter 2 Literature review

This chapter provides further rationale for the research questions by providing a review of key literature from different tectonic settings and spatial scales, providing further information on techniques used to constrain landscape evolution and the wider implications of the thesis.

2.1 Long-term landscape evolution

Quantifying the drivers of topographic development (and resulting draining patterns) is a key focus of tectonic geomorphology (Wobus et al., 2010). Perturbations vary on differing temporal and spatial scales, which in turn complicate the development of the landscape system, especially within ancient settings (Bierman, 1994; Allen, 2008). External (allogenic) factors such as climate and tectonics are, in turn, modulated by internal (autogenic) factors such as vegetation, bedrock lithology, variation in geological structure, and drainage rearrangement (e.g., Tooth et al., 2004; Moore and Blenkinsop 2006; Jansen et al., 2010; Prince et al., 2011). The form of the landscape is therefore the 'critical interface' between the interactions of the internal system with the external system (Allen, 2008).

One of the central areas of research within long-term landscape evolution is the idea of 'steady state' (equilibrium) landscapes, in which tectonic uplift (which contains a horizontal and vertical component) is in balance with erosion of the landscape (Willet et al., 2001). Willet and Brandon (2002) distinguished between: 1) flux steady state, in which accretionary flux equals erosional flux; 2) topographic steady state, in which the distribution of elevations does not vary with time, although the authors argued that this is 'probably never achieved' due to the inherent unsteady nature of geomorphic processes; 3) thermal steady state, where the temperature field within the crust does not change and; 4) exhumation (geomorphic) steady state, in which cosmogenic data yields on average the same age within a region. The idea that a landscape will endeavour to reach steady state is used as the basis of many landscape models (Allen, 2008). Nonetheless, a system may be in steady state with regards to one chosen variable and in a transient state to another.

Landscape and drainage evolution involves the following processes; denudation, erosion, incision and exhumation which occur at different rates. Denudation incorporates geomorphic erosion (achieved by surface processes), weathering and tectonic denudation (which occurs through normal faulting, whereby there is a rapid removal of solid rock) (Burbank and Anderson, 2011). Denudation of the landscape is achieved primarily by surface processes such as weathering, hillslope processes

and erosive agents such as fluvial or glacial action (Summerfield, 1991). Erosion refers to the process by which soil and rock are worn away and moved by gravity or by an agent such as water (rivers), wind or ice (glaciers). Whereas, incision refers to the vertical removal of sediment or rock. Exhumation is a process by which a parcel of rock approaches the Earth's surface, which can occur by erosion or extensional tectonics (Ring et al., 1999). The rates of which these processes occur are normally reported as centimeters or meters per thousand years (cm/ ka^{-1} or mka^{-1}) for shorter time scales associated with active landscapes or metres per million years (mMa^{-1}) for ancient landscapes.

2.1.1 Classical geomorphology; theories of landscape evolution

Understanding geomorphic evolution of landscapes is a fundamental component of Earth science. Agassiz (1840) first pioneered the concepts of landscape development by assessing the impact of glaciation on a landscape in terms of form and process, as well as including the irreversible changes in overall configuration of landforms as a function of time. Classic landscape theories are based on qualitative assessments of the landscape, several key theories have saturated the literature.

1) Davis (1889, 1899) model – 'the geographical cycle'

Davis' geographical cycle ('cycle of erosion') model is a temporal framework that recognises that all landscapes are palimpsests overwritten by numerous tectonic and climatic processes (Figure 2.1A). Davis believed that there are sequential changes in landscapes through time (through youth, maturity and old age) in which the evolution is directed towards the development of a peneplain. The geographic cycle is a simple model, assessing how mean elevation and mean relief change as a landscape erodes. During the youth stage, the landscape has high mean elevation but low relief, with erosion concentrated in rivers, with deep narrow valleys forming. As maturity is reached, valleys lower to base level and then begin to widen laterally. During this stage, hillslope erosion becomes important as interfluves are rounded, with weathered material transported to the river by creep processes. The mean elevation and relief of the landscape decrease. During old age, valleys can no longer deepen or widen and all landscape lowering is accomplished by hillslope processes, resulting in the formation of a peneplain. The cycle is renewed due to tectonic or climate change. Davis (1930) also applied the cycle of erosion to arid environments, in which slope retreat becomes a dominant feature of the landscape. Davis's model assumed stable landscapes for long periods of time, however polycyclic landscapes (palimpsests) are likely to be the norm rather than the exception (Summerfield, 1991).

Additionally, isostatic uplift related to erosion will delay the attainment of full peneplanation. Davis' model also does not account for rapid climate change (e.g., Quaternary) and related sea level change. It is therefore highly unlikely that landscapes anywhere can be viewed as a simple unidirectional sequence of landforms (Summerfield, 1991).

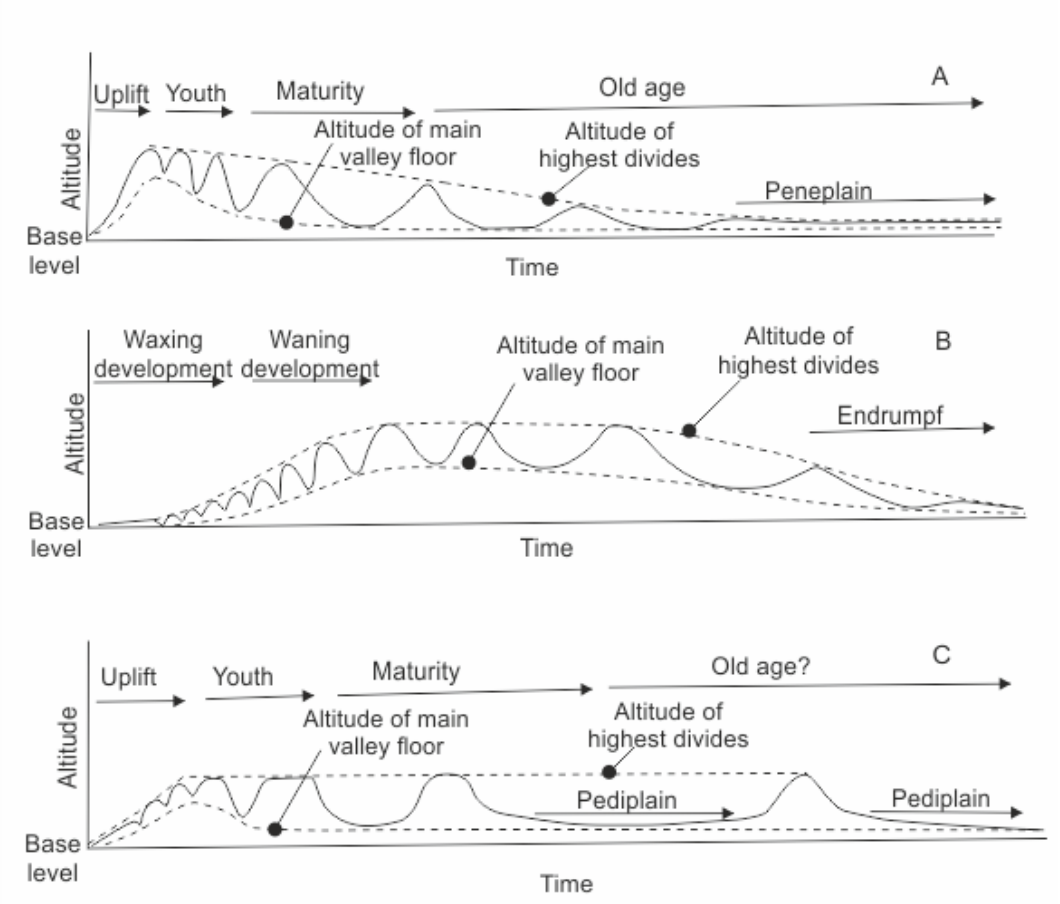

Figure 2.1 *– Schematic representations of the key elements of landscape models proposed by A) Davis; B) Penck and C) King (Summerfield, 1991). Davis believed that landscapes will evolve into peneplains, and that the time period associated with old age is many times longer than the stages of youth and maturity. Penck argued that landscape evolution is related to uplift and that development relates to waxing and waning phases. King argued for pediplanation, related to successive uplift related to tectonic rifting.*

2) Penck (1924, 1953) model – uplift and denudation

Penck's model is a direct challenge to that of Davis (1889, 1899), in which Penck argued that geomorphic forms are an expression of the *phase* and *rate* of uplift in relation to the rate of degradation (Figure 2.1B). The shape of hillslopes relates to the relative rates of valley incision by rivers and removal of debris, which is ultimately controlled by uplift. The landscape evolution model can be summarised as follows,

an initial surface is *gradually* uplifted, resulting in convex slopes, as uplift increases, benches are formed. As uplift rates decrease, there is transition from waxing development characterised by rapid downcutting to the waning stage, characterised by valley widening by the concept of slope replacement. The retreat of slopes leads to the formation of drainage divides, with inselbergs flanked by pediment surfaces, with slowly eroding concave slopes. Penck does not consider important factors such as the change in river discharge due to climate change, the influence of lithology, and the importance of weathering (Summerfield, 1991).

3) King (1953, 1967) – pediplanation

King's ideas are similar to Davis' (1889, 1899), but differ in the *mechanism* of slope retreat. King argued for parallel retreat due to successive uplift because of erosional isostatic unloading resulting in a decrease in base level (Figure 2.1C). Successive uplift results in nested escarpments, and the formation of pediments, which coalesced to form pediplains. Once pediments form, they exist indefinitely until consumed by younger cycles of escarpment retreat due to base level fall. As the surfaces are formed by escarpment retreat, the surfaces are diachronous and are progressively older away from the escarpment. King's model of landscape development has mainly been criticised due to the mechanisms of successive uplift, the rates needed for escarpment retreat from the coast and the inability to correlate surfaces across large areas (Summerfield, 1991). King's model is based on southern Africa and will be discussed again in Chapter 3.

4) Hack (1960) – dynamic equilibrium

Hack's ideas were based on that of Gilbert (1877), and argued for driving and resisting forces. Landscapes are essentially in dynamic equilibrium, whereby a time independent landscape will form given the same driving and resisting forces over time. The river and hillslopes are graded, with lowering occurring at the same rate between different landforms. The adjustment between driving (climate, tectonics) and resisting (lithology) forces are dynamic, and continually adjusting and therefore equilibrium is never truly reached. However, lowering rates between different landscapes may be occurring at the same rate in particular areas, it cannot occur over the entire catchment area in the long-term. As the rivers erode to base level, there is a reduction in gradient, and this will eventually propagate through the subcatchments. Hack also assumes a rapid response to variation in forcing conditions, however relict landforms survive in many areas (e.g. Gorelov et al., 1970; Gunnell et al., 2007; Bessin et al., 2015). Hack's ideas are most likely valid in ancient settings with slowly

eroding catchments, which have not experienced major climatic shifts and are isolated from base level changes.

2.1.2 Controlling factors

The interlinking factors controlling the rate of denudation within a landscape are tectonics and climate, modulated by geology (Whipple and Tucker, 1999; Anders et al., 2005; Wobus et al., 2006; Kamp and Owen, 2012). These factors not only influence the large-scale attributes of landscape development and fluvial networks but are also reflected in smaller scale changes in channel form (planform and cross sectional) and the formation of landforms such as terraces.

An understanding of these factors is therefore crucial to modelling all aspects of the landscape (DeVecchio et al., 2012). The relative importance of climate or tectonics in controlling the shape of the landscape is contentious; Portenga and Bierman (2011) state that 'it is difficult to predict how erosion rates will respond to changes in boundary conditions' (pg. 5).

2.1.2.1 Allogenic controls

The influence of tectonics (and subsequent orogenesis) has usually been distinguished using river planform, drainage patterns, or cross sectional dimensions (Burbank and Anderson, 2011). Tectonic perturbation can cause variation in stream power and, therefore, incision possibly leading to stream capture and terrace development. The influence of tectonics is clearer in tectonically active regions, however in quiescent settings tectonic perturbations can be long lived after the initial phase of tectonic activity. Debate surrounds the longevity of high elevation passive margins e.g. South Africa, western India and southeastern Australia (Bishop, 2007), with models relating to: downwarping or; downwearing and escarpment excavation or escarpment retreat (Bishop, 2007). The evolution of these margins such as South Africa is therefore, contentious.

Tectonic uplift also influences climatic patterns, with the formation of orographic rainfall. On the larger scale it has been argued that the uplift of mountains led to Cenozoic cooling and the development of ice ages (Raymo and Ruddiman, 1992) and the formation of the SE Asia monsoon (Hahn and Manabe, 1975). However, this view was challenged by England and Molnar (1990) who argued that as climate changed in the Cenozoic, enhanced erosion and valley incision caused isostatic adjustment. The relative importance and impact of these factors remains unclear.

Climate provides the driving force (discharge) for incision, which in turn modulates the sediment flux (which is also a function of climate in the form of weathering and sediment production) (Wobus et al., 2010). Climate also affects the amount of vegetation within the catchment, which will directly and indirectly impact on denudation rates. Bonnet (2009) argued that the drainage divide is an important component of a drainage basin and, therefore, the variation in precipitation needs to be considered in landscape modelling especially due to orographic precipitation. Trauerstein et al. (2013) studied 27 river catchments in the western flank of the central Andes (which was affected by Miocene uplift), and found that landscape metrics correlated with the north-south rainfall gradient; with average local relief values decreasing with mean precipitation. Trauerstein et al. (2013) argued precipitation provides a 'critical limit on the formative processes in the Western Andes' (pg. 25). Trauerstein et al. (2013) also argued that the type of process varies with the amount of precipitation; with bottom-up processes (e.g., detachment-limited system whereby channel incision outpaces hillslope processes) dominant in low precipitation regions and top-down processes (e.g., transport-limited system whereby hillslopes lower at the same rate or faster than fluvial incision) dominant where precipitation rates are higher. Trauerstein et al.'s (2013) data indicate a threshold of ~ 400 mm a^{-1} between these two situations. The impact of rainfall gradients has also been modelled in laboratory experiments in relation to the migration of drainage divides, which delineates domains in which precipitation and, therefore, hydraulic regime may directly influence topography and erosion rates (Bonnet, 2009). Bonnet (2009) argued that asymmetric topography (which is common to many orogens) within the Sierra Aconquija range, NW Argentina is not due to differential rock erodibility, as asymmetry does not coincide with lithological variations. Additionally, tectonic forcing has been negligible within the catchment. Bonnet (2009) therefore, argued that the asymmetry is due to the orographic rainfall gradient, which is shown to develop within their laboratory experiments.

Wobus et al. (2010) argued that by dating terraces the dominant control within a system can be distinguished. The impact of climate works downstream from the headwaters, with terraces becoming younger downstream, whereas tectonic perturbation works upstream from the mouth of the river, with terraces younging in an upstream direction. Both climate and tectonic perturbation cause incision due to local changes in sediment supply and transport capacity. Climate either decreases the sediment input due to a reduction in weathering or increases discharge, causing excess transport capacity and therefore incision. Whereas tectonics, increases

stream powers due to the gradient change causing incision. In the extreme case, tectonic perturbations can work downstream. Wobus et al. (2010) argued that climatically driven incision will result in a channel gradient that is less steep than the initial gradient, whereas tectonic perturbation will result in a steeper gradient and, therefore, even in the extreme case the forcing factor can be distinguished.

Nonetheless, the impact of tectonics can be localised, as shown by Kale et al. (1994) who researched an anastomosing bedrock reach of the Narmada River, India, which is an anomaly in terms of planform when compared to the rest of the river. Kale et al. (1994) distinguished three sub-reaches within their study: an upper sub-reach composed of a deep channel and fine sediments; a middle sub-reach composed of inter channel islands, boulder berms, and multiple incised channels and; a lower sub-reach comprising of rapids, high gradients, sandy bars with megaripples, boulder berms and abraded bedrock surfaces. The reach as a whole, is bounded by faults. However, the authors argued that the structural geology may control the reach as a whole, but does not explain the individual sub-reaches. Due to the variation in sediment sizes between the sub-reaches, high magnitude flooding events can explain the lower sub-reach, but the upper sub-reach containing fine sediments is problematic. Therefore, Kale et al. (1994) argued that tectonic processes (block or domal uplift) explain the sub-reaches studied. Uplift would have dammed the upper reaches due to an increase in bed level of the river, resulting in deeper flows and finer sedimentation. Downstream of the uplifted reach, the gradient of the river would increase, subsequently increasing stream power and, therefore, widening and deepen; resulting in the formation of rapids, knickpoints and formation of a deep gorge. The authors argued the anabranches formed in high magnitude flood events, whereby the river was devoid of sediment and able to incise. The multi-channel form was aided by the fracturing present in the granite lithology of the bedrock. Due to the lack of stream capture or drainage disruption, the authors argued the uplift was slow.

2.1.2.2 Autogenic controls

Jansen et al. (2010) researched the impact of substrate erodibility (which is non-uniform across the landscape) on channel form at a catchment scale and on the scale of individual reaches of rivers draining the Highlands, Western Scotland. The effects of quartzite outcrop within the study catchment areas was dominant although quartzite outcrops consisted only of ~7% of the catchments studied. A strong correlation was found between catchment size and the proportion of quartzite within the catchment, with smaller catchments containing the higher proportion of quartzite.

Rivers crossing quartzite are also narrower and steeper than those crossing other lithologies.

Within mixed bedrock-alluvial rivers, the bedrock reaches have been argued to be a dominant control on river development; acting as local base levels. Tooth et al. (2004) researched rivers on the South African Highveld (Klip River, Schoonspruit and Venterspruit which are left bank tributaries of the Vaal River) where the occurrence of resistant dolerite intrusions control the long term development of the river systems. Tooth et al. (2004) distinguished a three stage cycle (Figure 2.2) which is time progressive, and possibly repeats when another intrusion is encountered.

2.1.3 Drainage development

Research into erosional landscapes has deep roots within the literature. Playfair (1802) argued that equilibrium existed between erosion and sediment transport across the entire basin, which resulted in a stable landscape. Gilbert (1887) analysed stream networks and argued that erosional landscapes have divergent ridge networks and convergent stream networks, which are adjusted to dynamic equilibrium. Instability of channels results in migration of drainage divides, with spatial variation in drainage patterns due to differential resistance of lithologies, differential uplift, and the interaction of transport capacity and sediment supply (Gilbert, 1887). Strahler (1950) argued that erosional landscapes adjust their form to attain a time independent form; with landforms found in a narrow range of morphometric values. Hack (1960) argued that stream-hillslope systems are closely adjusted, and will erode at the same rate if the forcing conditions are constant.

Drainage development may be subject to the formation of transverse (or discordant) drainage and river captures. Transverse drainage has long been recognised in the literature (e.g., Oberlander, 1985) and could be a function of erosion along transverse faults, antecedence or superimposition. Erosion along transverse faults, involves stream captures due to headward erosion (e.g., Stokes and Mather, 2003). Antecedence (Figure 2.3) is the concept that the river systems existed prior to uplift of a mountain belt, whereby the rivers have enough energy to erode down and keep pace with uplift, as has been argued for rivers of the Alps, Cascades and Himalayas (e.g., Summerfield, 1991; Bracciali et al., 2015; Ghosh et al., 2015). Whereas superimposition (Figure 2.3), in which drainage has developed on sedimentary cover and eroded down onto underlying geology, with the initial drainage being discordant (Summerfield, 1991) has been argued for the Suan Juan River, Colorado (e.g., Pederson et al., 2002).

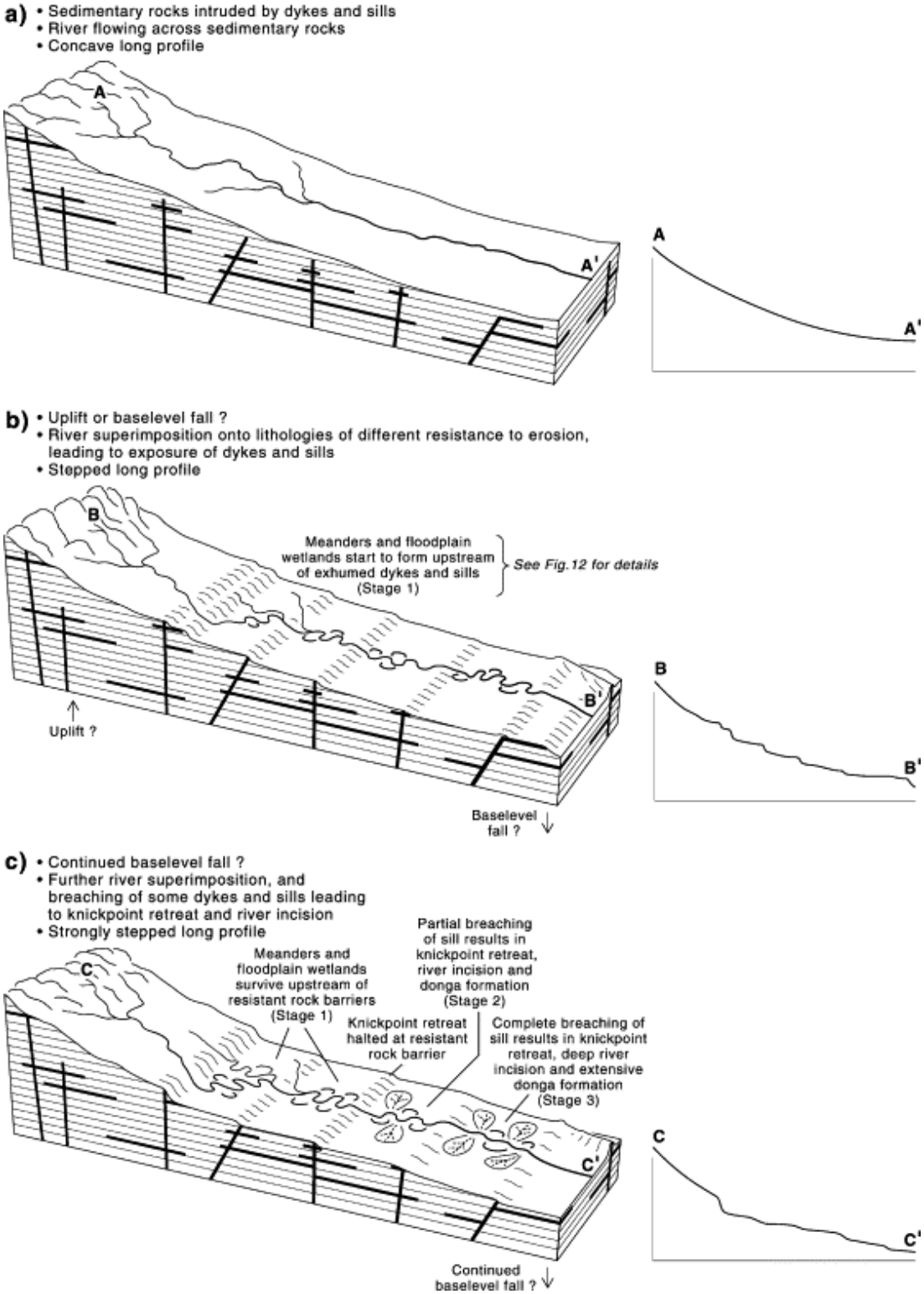

Figure 2.2 *– Long term river and landscape development in sedimentary basins which have been extensively intruded by dolerite sills and dykes. The dolerites provide a local base level of the river and have a key control on the landscape evolution; related to the formation of knickpoints and the successive breaching and exhumation of dolerite sills and dykes. Figure from Tooth et al. (2004).*

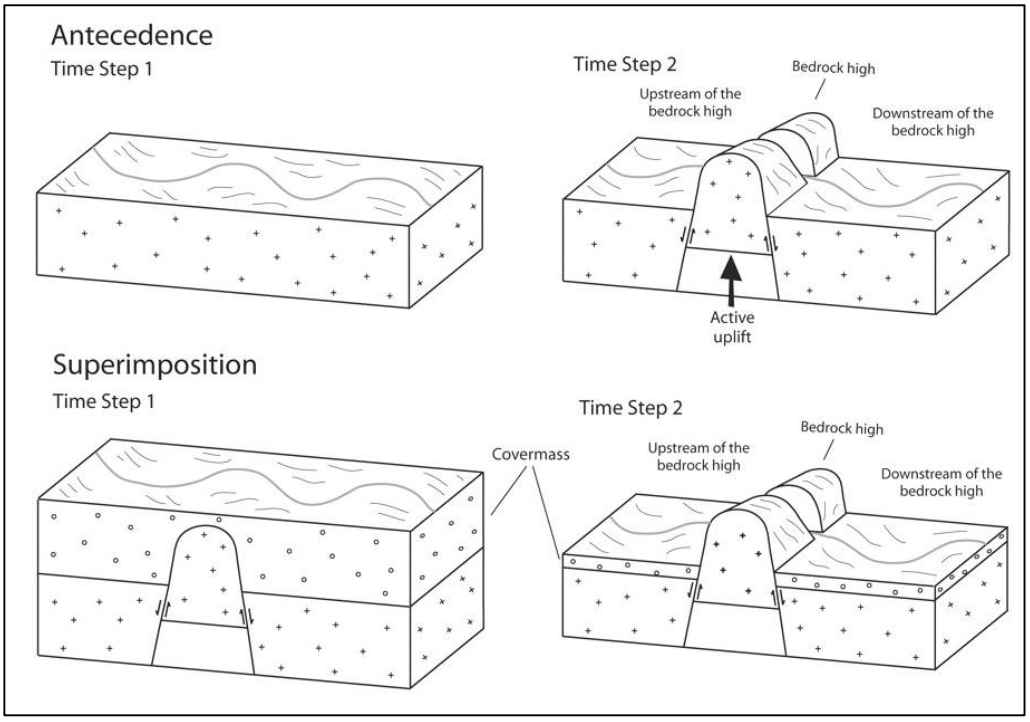

Figure 2.3 *– Schematic diagram of antecedent and superimposed drainage development (Douglass et al., 2009). Antecedence occurs when the pre-existing river is able to keep pace with tectonic uplift. Whereas superimposition occurs when rivers exhume underlying tectonic structures and keeps its pre-existing planform. In both cases the river is discordant to underlying tectonic structure.*

River capture (piracy) was first identified by William Morris Davis (1889), and has been widely cited as a key aspect of landscape evolution (Figure 2.4). Stream capture occurs when an adjacent stream has a greater erosive power (which could be due to a range of factors including tectonic and climatic variation) within the headwaters, that erodes back and 'captures' the drainage from the adjacent river. Due to the diversion of river courses, not only is the hydrological regime affected but also the sediment budget and provenance (Bishop, 1995). Rust and Summerfield (1990) argued for large scale rearrangement of the Orange Catchment to account for the sediment volume variation offshore. Stream capture does not always result from tectonic or climatic forcing, Hasbargen and Poala (2000) emphasised that the autocyclic nature of stream capture must be recognised, as stream capture occurred in their experiments without changes in climate or tectonic forcing. Due to the impact of stream capture on drainage area and slope it may represent an important internal control on the rate of denudation. Prince et al. (2011) investigated the impact of stream capture on the Roanoke River, USA, and concluded that stream capture (coupled with the creation of asymmetric drainage divides) can act as an internal

driver of transience long after tectonic forcing stops and independent of climatic forcing.

2.2. Recent advances in landscape evolution research

A recent trend in geomorphological investigations have been to attempt to quantify landscape dynamic. In addition, the realisation of global-scale interactions between parameters, such as climate, surface processes and tectonics, has shown a lack of constriants in bedrock channel system dynamics in comparison to alluvial river systems (Whipple, 2004). The increasing knowledge of bedrock systems (see Tinkler and Wohl, 1998; Sklar and Deietrich, 2001; Finnegan et al., 2005; Turowski et al., 2008; Whipple, 2004; Attal et al., 2011; Hodge et al., 2011) has allowed the quantification of bedrock channel systems in relation to external and internal controls. Quantifying the dynamics of river erosion is fundamental to long-term landscape evolution models (Section 2.3) interpretation of erosional topography, dating techniques such as AFFT (Cockburn et al., 2002), and controls on sediment supply (Tucker and Slingerland, 1996).

Long-term erosion has often been modelled in terms of excess stream power, specific stream power or shear stress for detachment-limited systems. In these cases, sediment supply is seen as a second order effect (Whipple and Tucker, 2002). Alternatively, transport-limited models have been proposed, which assume an infinite supply of mobile sediment, in which transport capacity and supply are balanced (e.g., Tucker and Slingerland, 2002). Hybrid models also exist, which account for the role of sediment flux in transitions from bedrock to alluvial, and in controlling the rate of particle detachment from a resistant substrate (Whipple and Tucker, 2002).

2.2.1 Stream power law

The detachment-limited stream power law (Howard and Kerby, 1983) has been argued to be the most satisfying law in terms of physical erosion (Whipple and Tucker, 1999) and is the most common erosion law applied. The stream power law is fundamental for landscape evolution models (Section 2.3, Croissant and Braun, 2014) and has been used in a range of studies to question the impact of boundary change on catchment morphometrics and to assess how landscapes evolve over time (e.g., Anderson, 1994; Howard, 1994; Tucker and Slingerland, 1996; Whittaker, 2012; Croissant and Braun, 2014). The stream power law (Eq. 2.1) relates incision to drainage area, a proxy for local discharge and local slope:

$$\frac{\partial h}{\partial t} = -KA^m S^n \qquad \text{Eq. 2.1}$$

Where, *h* is the elevation of a stream channel relative to the underlying rock column, *t* is time, *S* is channel gradient, *A* is drainage area, and *K* is an erosional efficiency factor related to lithology, climate, channel geometry and potentially sediment supply (Whipple and Tucker, 1999).

The parameters *m* and *n* depend on geomorphological, climatic and tectonic activity within the region and have not been defined fully (Whipple and Tucker, 1999). The range in values is shown below (Croissant and Braun, 2014):
$0 < m < 2$

$0 < n < 4$

Additionally, the component *K* varies by an order of magnitude and incorporates lithology, climate, sediment flux, and river channel dimensions, as well as the variation in *m* and *n* (Croissant and Braun, 2014). A problem of the stream power law, despite its wide application, is the fact that the *K* value is normally held as a constant and sediment flux is rarely integrated and is either ignored or subsumed in the exponent (Tucker and Whipple, 2002). Further, as *K* is constant this implies the assumption that no other variables can change in response to uplift, apart from slope. However, several variables do vary including the channel width, and coverage of alluvial/colluvial material (Whipple and Tucker, 1999).

Detachment-limited equations assume that erosion rates are limited by the rate at which substrate can be removed via plucking and abrasion (Whipple et al. 2000) rather than the rate at which it can be transported. Whipple and Tucker (1999) investigated the sensitivity of the stream power law, and concluded that slope is the critical unknown component. The magnitude and timescale of bedrock channel response to a perturbation is largely governed by the erosion number raised to a power determined by slope. Additionally, the m/n ratio only affects the shape of the river profile (which will impact response time) but does not affect the sensitivity of the channel. Whipple and Tucker (1999) stated that the m/n ratio is restricted to a narrow range of 0.35 – 0.6.

Recently, landscape evolution models have been used to constrain the exponents (e.g., van Der Beek and Bishop, 2003). Croissant and Braun (2014) applied a

surface model process and an inversion method on the Whataroa catchment, Central Southern Alps and found that the optimum values for *m* is 0.3 and *n* is 0.5. The analysis indicated that steady-state exists in some parts of the landscape, however that the stream power law is only a first order parameterisation but cannot represent '*many and varied physical processes at play*' (pg. 164) such as the effects of sediment delivery.

Analysis of the stream power law by Tucker and Whipple (2002) showed that, within detachment limited models, large-scale escarpment retreat occurs when $n \leq 1$. When *n* is greater than 1, the model predicts the dissection of the plateau and the formation of smooth river profiles; there is no definite scarp. This infers that down-wearing is of greater importance (e.g., Davis' geographical cycle, Section 2.1.1) than back-wearing (e.g., King's landscape model, Section 2.1.1).

The stream power law can be used to assess the assumptions of steady-state landscapes (see Section 2.1), in a steady-state, uplift will balance with erosion and uplift rates can be reflected as the steepness index (Eq. 2.2).

$$S = K_s A^{-\theta} \qquad \text{Eq. 2.2}$$

Where, S is slope, Ks is the steepness index, A is area and θ is the ratio of m/n.

The equation above can be utilised to derive patterns of differential uplift and the steepness index has been shown to correlate with uplift in a range of environments (e.g., Kirby and Whipple, 2001; Sklar and Dietrich, 2004; Di Biase et al., 2010). The concept of steady-state (See Section 2.1) is idealised, and while, a useful concept, it is likely that throughout geological time, most landscapes exists in a state of perturbation away from steady-state due to boundary condition changes. Steady-state analysis is often focused on geologically recent orogens such as mountain ranges in Taiwan (Whipple, 2001). Rapid climate fluctuations within the Quaternary have limited the ability of these modern landscapes to reach steady state. Steady-state assumptions have not been applied to South Africa (Chapter 6). Knickpoints are one of the easiest identifiable catchment responses when there has been a change in boundary conditions.

2.2.2 Knickpoint characterisation

Knickpoints are relatively steep sections of channel long profiles that relate to the reaction of the channel to forcing, and represent non-equilibrium landforms (Miller,

1991; Jansen, 2006; Phillips and Lutz, 2008). Knickpoints have been argued to account for the principal means of bedrock lowering (Stock and Montgomery, 1999l; Hayakawa and Matsukura, 2003; Whipple, 2004; Bishop et al., 2005) and long-term river development (Turowski, 2010). Knickpoints display equifinality, and, therefore, knickpoints within a catchment can form from different forcing factors and evolve independently (Larve, 2008).

The formation and retreat of knickpoints has been analysed mathematically, and stems from the research of the stream power law, which has been applied to knickpoint retreat (e.g., Rosenbloom and Anderson, 1994; Seidl et al., 1994, Strock and Montgomery, 1999); equation 2.3 indicates that during a sudden decrease in base level a knickpoint will propagate upstream, at an ever decreasing rate from the point of disturbance without attenuation (Whipple and Tucker, 1999). The celerity of knickpoints has also been assessed as power law function of upstream drainage area and local slope (e.g., Rosenbloom and Anderson, 1994; Whipple and Tucker, 1999).

$$C_e = -Kk_a^m x^{hm} s^{n-1} \qquad \text{Eq. 2.3}$$

Where C_e is the kinematic wave speed, K_a is a co-efficient of erosion, and h, m and n are exponents.

The equation above, therefore, assumes that a change in boundary conditions (e.g., tectonic uplift) will cause knickpoints to be found at the same elevation across the landscape. If several knickpoints of similar elevation are found within a catchment, this can be related to one pulse of change in the boundary conditions. However, multiple knickpoints (Crosby and Whipple, 2006) are often observed within catchments and it can be hard to tease out the dominant controls, especially when tectonics or climate change occurs within the same time period (e.g., within South Africa, see Chapter 3). Further, static knickpoints related to resistant lithologies (Chapter 8) or bed armouring can be found in catchments and have to be differentiated before analysis begins (Whipple and Tucker, 2002).

2.3 Ancient settings

Long-lived ancient landscapes (Bishop, 2007) have long been recognised (Crickmay, 1975; Twidale 1976; Ollier, 1991) and many ‘Gondwana landscapes’ (Fairbridge, 1968) have been identified covering large parts of the planet, including cratonic areas

and passive continental margins, such as Australia (e.g., Ollier, 1991; Ollier and Pain, 2000; Twidale, 2007a, 2007b), southern South Africa (e.g., Du Toit, 1954; King, 1956a), and South America (e.g., King, 1956b; Carignano et al., 1999; Demoulin et al., 2005; Panario et al., 2014; Peulvast and Bétard, 2015). Long-lived landforms and surfaces have also been argued to form parts of Russia (Gorelov et al., 1970), India (Gunnell et al., 2007), Sweden (Lidmar-Bergström, 1988), and western France (Bessin et al., 2015).

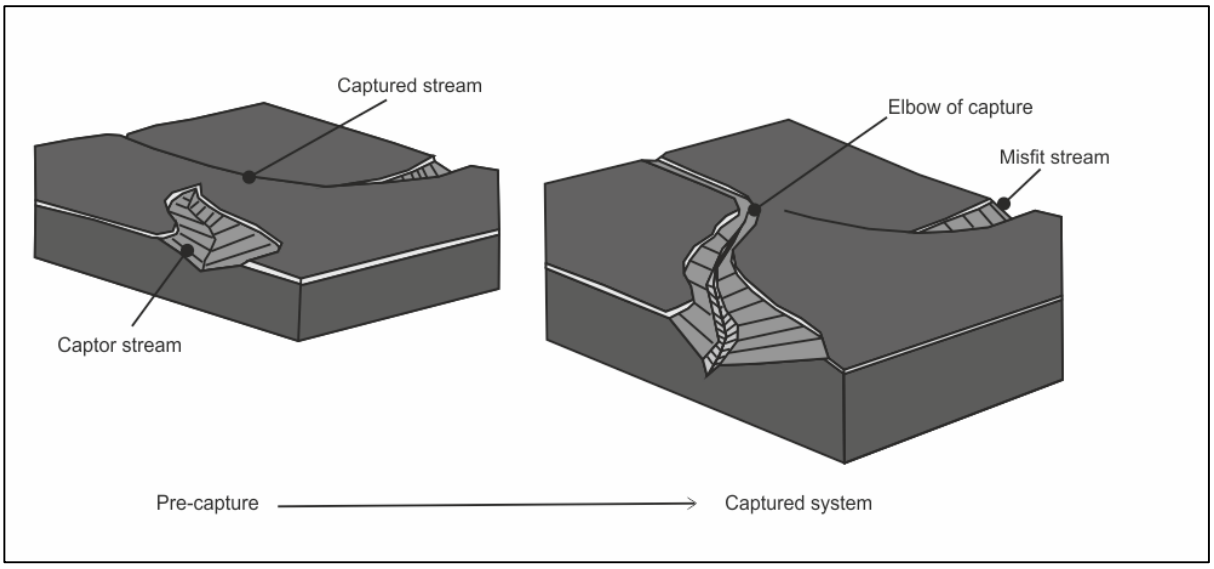

Figure 2.4 *– Schematic diagram showing the process of river capture (after Schumm, 1977). The captor stream erodes headward and captures a nearby stream resulting the formation of wind gaps, elbows of capture and misfit streams.*

Despite the prevalence of ancient landscapes, geomorphological research has mainly focused on youthful landscapes with high erosion rates (e.g., Coughlin et al., 1998; George et al., 2001; Grimmer et al., 2002; Vance et al., 2003; Safran et al., 2005; Schaller et al., 2005; Coutand et al., 2006; Zheng et al., 2006; Derrieux et al., 2014), with geochronology rarely applied. Rabassa (2010) argued that landscapes need to be reassessed with a 'Gondwanic vision' instead of an 'Andean vision'. Whilst Bishop (2007) emphasised the need to reconcile landscape evolution over different timescales and in different tectonic settings.

Research of ancient landscapes has focused on the southern hemisphere, in which specific landforms have been associated with ancient settings e.g., duricrusts, inselbergs, etch surfaces and pediplains (Rabassa, 2010). Early research of ancient landscapes was qualitative, relying on descriptions to support theories (e.g., King, 1953, Chapter 3). Later work incorporated geomorphic, stratigraphic and topographic

considerations to assign ages to a landscape (e.g., Twidale and Campbell, 1988; Twidale and Vidal Romani, 1994). More recently, with the development of geochronology, terrestrial cosmogenic nuclides have been used to quantify and date landscapes (e.g., Bishop, 1985; Bierman and Turner, 1995; Bishop and Goldrick, 2000; Cockburn et al., 2000; Bierman and Caffee, 2001; Matmon et al., 2002).

Much work has been completed in Australia. Twidale (1976, 2007a,b), Twidale and Campbell (1988), Twidale et al. (1996) assessed the ages of landscapes by comparing with geomorphic, stratigraphic and topographic information to infer Mesozoic ages of many landforms e.g., Gawler Ranges (Twidale, 2007). Twidale (2007a,b) argued the formation of the Gawler Ranges, Australia, was formed by the melting of the Permian ice sheets. During the early Jurassic, there was deep weathering and planation forming the Beck Surface. The surface originally had a thick regolith, however tectonic uplift in the Cretaceous caused partial denudation and the removal of the regolith due to river rejuvenation. The Beck Surface was then removed due to the formation of the younger Nott Surface in the Early Cenozoic, with small remnants only found in a few locations. Bierman and Turner (1995) quantified ages using ^{10}Be and ^{26}Al, with *minimum* exposure ages indicating the landscape of the Eyre Peninsula was older than the Pleistocene. Bierman and Turner (1995) highlighted that minimum exposure ages and the actual age of the landscape could vary by an order of magnitude or two. Within ancient landscapes the use of cosmogenic dating becomes difficult and is discussed in Chapter 9.

Ancient landscapes are closely linked to the theories of tropical geomorphology, due to the formation of deep weathering and duricrusts, with a weathering front up to 1000 m in depth (Ollier and Pain, 1996). However, the ability of landscapes to persist has been met with contention (e.g., Thornbury, 1969), especially by those who believe in Huttonian continuous change (Hutton, 1795) and Davis' views of ubiquitous degradation (Davis, 1899). The majority of landscapes are regarded as 'youthful', with a maximum age of late Cenozoic (e.g., Stokes and Mathers, 2003). However, persistence of landscapes has been argued for multiple places (e.g., Australia, South Africa) due to long term stability, aridity and the resistance of the lithologies (e.g., Bierman et al. 1995, Scharf et al. 2013). The analysis of ancient landscapes is also complicated by the lack of modern day analogues for the climatic conditions required to form the deep weathering; the landscapes are often interpreted using information from highly active settings or current day climatic conditions which are not capable of forming such landscapes ('non-analogue' landscapes; Bloom, 2002). Ollier (1979) argued that landscape evolution should be taken from the last glaciation; the

Quaternary for the northern hemisphere (e.g., Europe) and the Permian glaciation for southern Africa and Australia.

The quantification of landscapes has allowed the rates of landscape evolution to be assessed. Thornbury (1954, 1969) argued that the Earth's topography is very young, and not older than the Pleistocene and argued that the existence of ancient landscapes is dubious due to high erosion rates. However, as Young (1983) argued, Thornbury (1969) studied glaciated regions in the northern hemisphere, with high erosion rates, likely to be one end of the spectrum, with low rates experienced in non-glaciated and tectonically quiet settings. Rates of erosion in these locations, as recorded by cosmogenic nuclides range from 5 – 10 mMa^{-1} (Bishop, 1985; Bishop and Goldrick, 2000; Cockburn et al., 2000; Bierman and Caffee, 2002; Matmon et al., 2002; for studies related to South Africa see Chapter 3), but can be as low as 0.14 m Ma^{-1} for the dry valleys in Antarctica (e.g., Nishiizumi et al., 1991; Summerfield et al., 1999a,b). It is unlikely landscapes can persist from the Cambrian as stated by Stewart et al. (1986) and Ollier et al. (1988) and geochronology has allowed the identification of exhumed surfaces and features (e.g., Belton et al., 2004; Tinker et al., 2008a). Apatite fission track thermochronology (AFFT) is a technique which give estimates of exhumation rates based on the cooling history of apatite as the host rock moves from depth to the surface by denudation (for a more in depth explanation see Gallagher et al., 1998; Gleadow and Brown, 2000; Ehles and Farley, 2003; Reiners and Ehlers, 2005). This technique has allowed the evolution history of landscapes to be assessed deeper into time (e.g., Cretaceous). House et al., (1998) used AFFT to discover that the major valleys and ridges of the Californian Sierra Nevada mountains are Cretaceous in age. AFFT has been used in other ancient settings such as in the Transantartic Mountains, Antarctica, resulting in identification of phases of increased denudation (Early Cretaceous, Later Cretaceous and Cenozoic) that have been related to tectonic activity (Fitzgerald and Stump, 1997).

Landscape evolution models, such as SIBERIA, CAESAR and CHILD **(**see Beaumont et al., 2000; Coulthard, 2001; Willgoose, 2005 and; Codilean et al., 2006 for reviews) have allowed specific concepts to be tested (e.g., Kooi and Beaumont, 1996) and the evolution of specific areas to be modelled (e.g., van der Beek et al., 1999). Models allow tectonic processes and geomorphic processes to be merged over long time-scales. However, these models are very simplistic as it is not yet possible to incorporate full physical law-based formulas of tectonics and landscape process; a process law approach is therefore taken. van der Beek et al. (1999) applied the CASCADE (Figure 2.5) model (Braun and Sambridge, 1997) to the southeastern

Australian highlands, under the assumption that the highlands were elevated throughout the Mesozoic and that rifting in the late Jurassic – early Cretaceous caused a drop in base level. The model predicts that the topography can be explained without large-scale uplift in the Cretaceous or Cenozoic (Bishop, 1988; Bishop and Goldrick, 1998). There is drainage rearrangement of an initially northwest drainage network due to base level fall related to rifting to the east and south of the study area. Drainage has remained stable in the area since the Mesozoic rifting. The model also predicts 1.5 – 2 km of denudation on the coastal plain in the post-mid Cretaceous, which is consistent with fission track data, if higher geothermal gradients are used.

2.4 Source-to-sink

The concept of source-to-sink was first introduced qualitatively by Meade (1982), and concepts have expanded in recent years due to the availability of remote sensing data and development of new tools which can fully integrate onshore and offshore data. Source-to-sink concepts comprise all components of a system that contribute to erosion, transport and deposition; from catchment headwaters to submarine basin-floor fans (Sømme et al., 2009a). Within the literature there is a dominance of source-to-sink studies utilising provenance of zircons for analysing onshore drainage development. Detrital zircons are a minor constituent of clastic sedimentary rocks, however their physiochemical resilience and high concentration of key trace elements (e.g., U-Pb) have allowed zircon analysis to be an important part of source-to-sink analysis (e.g., Liang et al., 2008; Carwood et al., 2012; Yang et al., 2013). Whitchurch et al. (2011) used detrital zircons to reconstruct the evolution of the south central Pyrenees and to assess sediment routing patterns. By using zircon cooling ages Whitchurch et al. (2011) were able to establish the change of drainage patterns that are coeval with orogenesis. Parallel river systems dominated in the late Cretaceous-Palaeocene during the onset of mountain building, with a change towards transverse

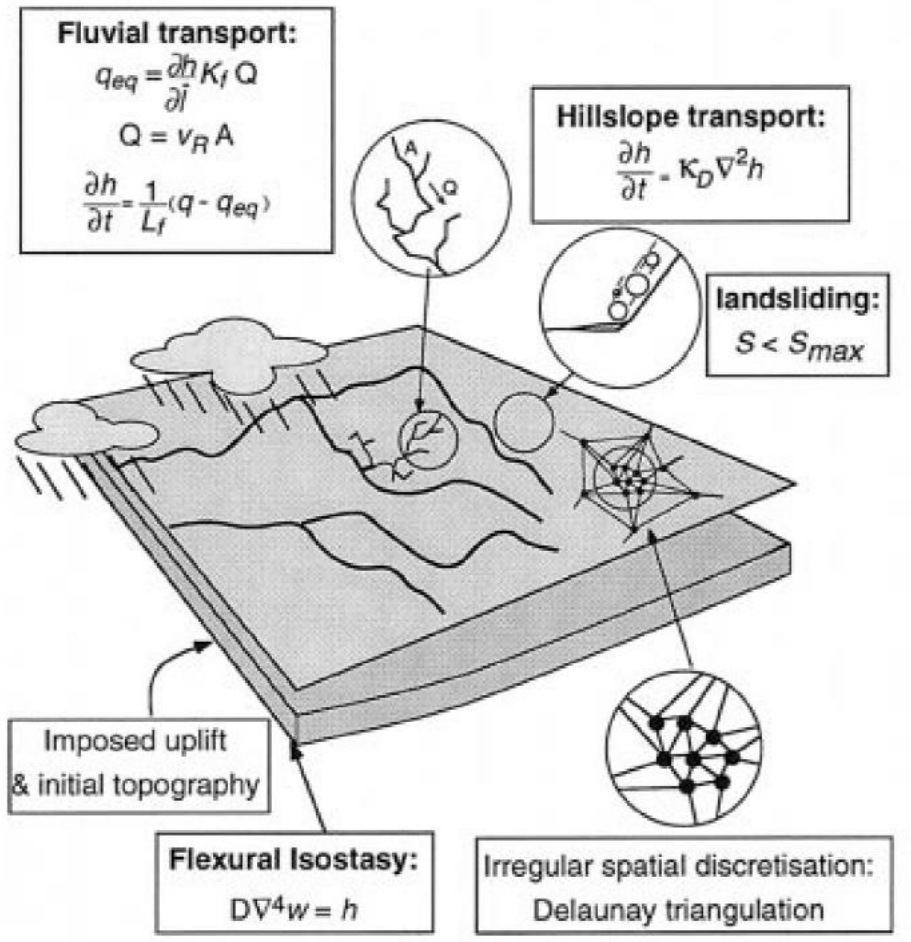

Figure 2.5 *– CASCADE landscape evolution model and the input parameters. Where, the hillslope transport includes continuous, slow processes (e.g., creep, soil wash) which are modelled by a linear diffusion equation in which the rate of denudation (∂h/∂t) is proportional to slope curvature ($\nabla^2 h$), K_D is a diffusion coefficient. Mass wasting is modelled by imposing a threshold (S_{max}), when the threshold is exceeded slope material is moved from higher grid points to lower grid points. Fluvial capacity (q_{eq}) is a linear function of discharge (Q), which is measured by the area of the channel (A) and velocity of the water (V_r), local slope (∂h/∂l) and a fluvial transport parameter (K_f). q is sediment flux and the imbalance between q-q_{eq} controls deposition and erosion. Lf is either the erodibility of bedrock or length scale for alluvial deposition. Flexural rigidity (D) is modelled by the upward deflection of a 2D thin elastic sheet (van der Beek et al., 1999).*

river systems, which were fully established by the Late Eocene-Miocene (Whitchurch et al., 2011). Detrital zircons have also been used to reconstruct the drainage development of Eastern Himalayas (e.g., Liang et al., 2008) and the Tian Shan ranges, Asia (e.g., Yang et al., 2013). Carwood et al. (2012) showed that the zircon signatures change depending on tectonic settings, and therefore, zircons can be used to assess the original basin's tectonic setting even when a small outcrop remains, with no other information about the system. Within convergent margins there are a large proportion of zircon ages close to the depositional age of the sediment, whereas

in collisional, extensional or intracratonic settings there are a greater proportion of zircons with older histories that reflect the evolution of the underlying basement. The distribution of difference between the crystallisation ages (CA) of the individual zircon grains and the depositional age (DA) of the sediment can be used to differentiate between tectonic settings.

Numerical models have also been utilised to assess the redistribution of onshore denudation and sediment routing to offshore basin accumulation (e.g., Granjean and Joseph, 1999; Paola, 2000; Syvitski and Bahr, 2001; Syvitski et al., 2003; Syvitski and Milliman, 2007). Syvitski and Milliman (2007) investigated sediment flux to the coastal zone using the 'BQART model', which integrates geomorphic, tectonic (e.g., basin area, relief), geography (e.g., temperature, runoff), geology (e.g., lithology, ice cover) and human activity (e.g., reservoir trapping, soil erosion). The model was applied to 488 rivers world-wide and successfully predicted 96% of variation in the long-term (30 years) sediment yields of the catchments. Furthermore, the model allows the identification of the dominant factors on sediment yield; 65% of sediment production can be related to geological factors (e.g., lithology, area), 14% can be related to the variation in climate (e.g., precipitation) and 16% can be related to anthropogenic activities (e.g., damming). Although the model successfully predicted sediment yields, the periodicity of sediment transport could not be modelled (Syvitski and Milliman, 2007); this is because the influence of typhoons and earthquakes are hard to predict, furthermore sediment transport is a complex process related to several interlinking factors such as climate, geology and stream hydraulics (Sømme et al., 2009a).

Source-to-sink studies that link the segments of the system together are rare. The components of the system are genetically linked (Moore, 1969), for example erosion in one part of the system will be reflected in morphological modification in another segment downstream. This process-response relationship is fundamental to source-to-sink concepts, and varies at many temporal and spatial scales within the system due to both external and internal controls (Section 2.1.2). Few studies have integrated segments from the entire system, instead focussing on particular aspects, for example river response to climate (e.g., Meade, 1982; Allen and Densmore, 2000; Zhang et al., 2001; Molnar, 2004; Quigley et al., 2007) or deep marine basins (e.g., Metivier and Gaudemer, 1999; Galloway et al., 2000; Paola, 2000). Sømme et al. (2009) researched 29 systems to decipher relationships between each segment of the source-to-sink system including the fluvial domain, shelf, slope and basin floor.

For the fluvial segment, the hypsometry (area-elevation) of the system is important in controlling sediment transport and storage, smaller systems with small floodplains (and accommodation space) respond rapidly to perturbations and are reactive (Allen, 2008). Small Californian catchments were very reactive to storms, hurricanes and El Nino forcing, transporting 50% of their sediment load during a short time period (Warrick and Milliman, 2003; see also Wolman and Miller, 1960; Meade et al., 1990; Meybeck et al., 2003). Whereas larger catchments have the ability to buffer the impact of perturbations due to larger catchment areas and floodplains; Metivier and Gaudemer (1999) found floodplain reaction times in South East Asia, of 10^4 – 10^6 Ma. Larger catchments transport greater sediment loads (e.g., Milliman and Meade, 1983; Milliman and Syvistski, 1992), and only large scale external perturbations affect the catchment, for example flooding in the headwaters may not propagate down the entire system (Matthai, 1990). Over the longer-term (>10^6 Ma) catchment evolution becomes the dominant control on sediment dispersal, whereas factors such as hypsometry, drainage pattern, lithology, vegetation and climate are important at shorter time scales (10^0 – 10^5 Ma) (Sømme et al., 2009a). The continental shelf controls the distribution of material supplied by the river catchments to the slope and basin floor fans. Sediment distribution is controlled by currents on the shelf, wave regime, climate (wind direction and strength), tidal and long-shore currents as well as the shelf type and dimensions, which is dependent on the relative sea level. Slope length shows a strong correlation with the trunk river length of onshore catchments. Further, the basin floor fan area is strongly correlated to catchment area. Morphometric analysis such as Sømme et al.'s (2009a) has not often been undertaken in source-to-sink studies. Sømme et al.'s (2009a) technique has been applied successfully in Møre Basin, Norway (Sømme et al., 2009b) and the Paleocene Ormen Lange System, Norweigian shelf by Martinsen et al. (2010).

Modern studies of source-to-sink have often focused on large scale basins of tectonically active settings e.g., Brahamaptura (e.g., Einsele et al., 1996; Goodbred and Kuehl, 1999; Goodbred, 2003) / Mississippi (e.g., Belmont et al., 2011) utilising gauging data, sediment budget analysis, or GIS. Blum and Roberts (2009) reconstructed the sediment budget of the Mississippi delta for the last 1200 years by integrating the area of the delta with sediment thicknesses to decipher sediment volumes. Blum and Roberts (2009) argued that inevitable drowning of the delta will occur due to sea level rise and the reduction of 50% of the sediment delivery due to damming. Climate change has been a key strand of sediment delivery rates research (e.g., Blum and Tornqvist, 2000) and much of Blum's work has focused on the source

areas of the system. Leeder and Gawthorpe (1987) first integrated the development of the drainage basin and the impact of offshore deposition in a rift basin setting. Leeder and Gawthorpe (1987) produced facies models and analysed the impact of tectonic tilting on different landform segments. For example, the alluvial fans will become segmented, axial rivers and delta lobes will migrate or avulse towards the axis of maximum deformation, and the submarine fans in the footwall pass offshore into small submarine fans. Out of the facies models created, the continental basin with axial through drainage is the most applicable to this study (Figure 2.6). Gawthorpe and Leeder (1987) argued that axial rivers are the main transporters of sediment, with small transverse systems present that drain the footwalls or high relief areas, forming fans. In this sense, the transverse rivers provide the material that the axial rivers transport away. Due to tectonic movement the axial rivers will migrate across the floodplain successfully to the fault zone and area of maximum subsidence, and the transverse rivers may exploit fault relay zones. The transverse rivers never increase in drainage area over the size of the axial systems.

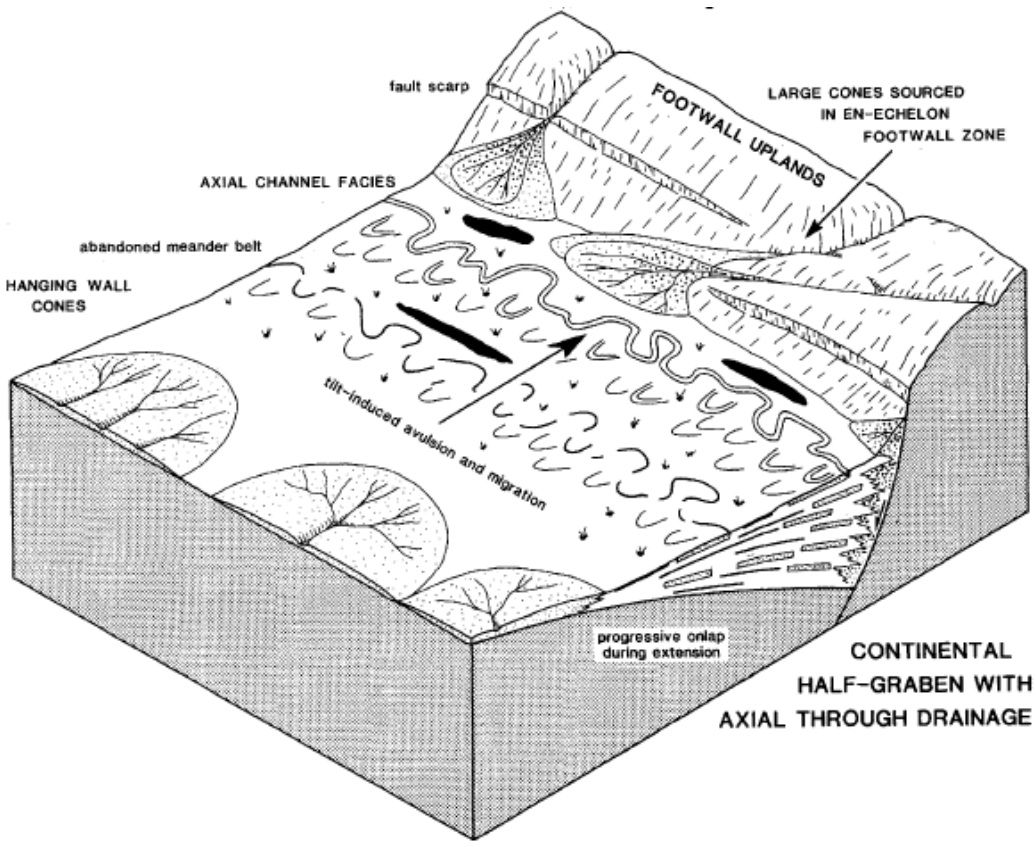

Figure 2.6 *– Isometric diagram of Leeder and Gawthorpe's (1987) rift basin facies model related to continental basins with large scale axial river systems. Transverse systems may utilise relay ramps producing large scale alluvial fans, but the catchment areas never exceed those of the axial systems.*

Onshore erosion rates can be constrained further using terrestrial cosmogenic nuclides (e.g., Chapell et al., 2006), which will be discussed further in Chapter 6, 7 and 9. Analysis of source-to-sink concepts in ancient settings in passive margins has often been overlooked in the literature (e.g., Tinker et al., 2008b) as it is difficult to constrain (Martinsen et al., 2010), but provide an important case study to assess the concepts of uniformitarianism, in which Sømme et al.'s (2009a) study relies on.

2.5 Summary

This literature review covers key aspects of the subject background in order to frame the scope of the thesis in a wider context. Ancient settings remain an understudied element of geomorphology, with little research utilising modern techniques such as cosmogenic analysis and GIS (Research Question 3). Ancient settings are complicated by the processes of erosion removing evidence, overprinting of different forcing factors, and the time periods considered. However, they can offer important insights into the main controls on landscape evolution, and help constrain evolution models. Furthermore ancient settings can help refine engrained theories related to geomorphology such as steady-state or the dominance of autogenic or allogenic factors (Research Question 3). The analysis of ancient landscapes can help improve source-to-sink concepts by providing vital quantitative data for numerical models (Research Question 1), assessing how denudation rates vary over time (Research Question 2), and how the eroded material was routed (Research Question1). Southern Africa offers a unique location, whereby offshore and onshore data can be integrated over timescales up to the Cretaceous. Southern Africa has intrigued geomorphologists since the early 1900s; this research is discussed in the following chapter.

Chapter 3 Regional settings

This chapter provides a framework for the thesis and research questions. The geologic and climatic settings of southern South Africa are discussed, before focusing on geomorphologic studies related to southern South Africa. The main study area is discussed and relevant literature provided.

3.1 Geology

3.1.1 Lithology

The age of the geology of southern South Africa ranges from Pre-Cambrian to Cenozoic deposits. The Pre-Cambrian stratigraphy of southern Africa comprises the Gamtoos, Kaaimans, Malmesbury and Cango Cave Groups (Figure 3.1), which crop out as inliers and are locally important (Chapter 8). The Gamtoos Group is composed of phyllites, greywacke, limestone and dolomites (Rozendaal et al., 1999). The Kaaimans Group is composed of massive quartzites, limestones, quartz schists and phyllites (Rozendaal et al., 1999), whilst the Gamtoos Group is composed of deformed and metamorphosed marine shales (Rozendaal et al., 1999). These groups represent distal facies of a rift-succession associated with pull-apart basins during break-up of Rodinia and opening of the Adamaster Ocean (Rozendaal et al., 1999). Towards the coastal areas, the Cape Granite Suite (Figure 3.1) formed of Neoproterozoic to Cambrian batholiths and smaller plutons outcrop as inlier remnants. The Cape Granite Suite was emplaced during the formation of Gondwana, and the granites are intrusive into the Saldania Belt (Da Silva et al., 2000).

The geology of southern South Africa is dominated by the Cape and Karoo Supergroups, which represent two large-scale episodes of subsidence and sedimentation within the interior of Gondwana (Tankard et al., 2009). The Cape Supergroup (Figure 3.2) is a siliciclastic sequence composed of the Table Mountain, Bokkeveld and Witteberg groups (Broquet, 1992). The quartzitic Table Mountain Group, which forms the backbone of the Cape Fold Belt, represents sedimentation on a subsiding shelf (Broquet, 1992), with deposits including conglomerates, sandstones, mudstones and shales. The argillaceous Bokkeveld Group represents deep-marine sedimentation (Broquet, 1992). The Witteberg Group comprises sand-prone shelf sediments, which are now quartzites, and mudstones (Broquet, 1992). The Cape Supergroup stratigraphy has been metamorphosed; temperatures of up to middle greenschist facies conditions (~400°C) were reached during pre-Cape orogeny, whereas lower greenschist conditions (~ 300°C) prevailed during the Cape Fold Belt orogeny (Frimmel et al., 2001).

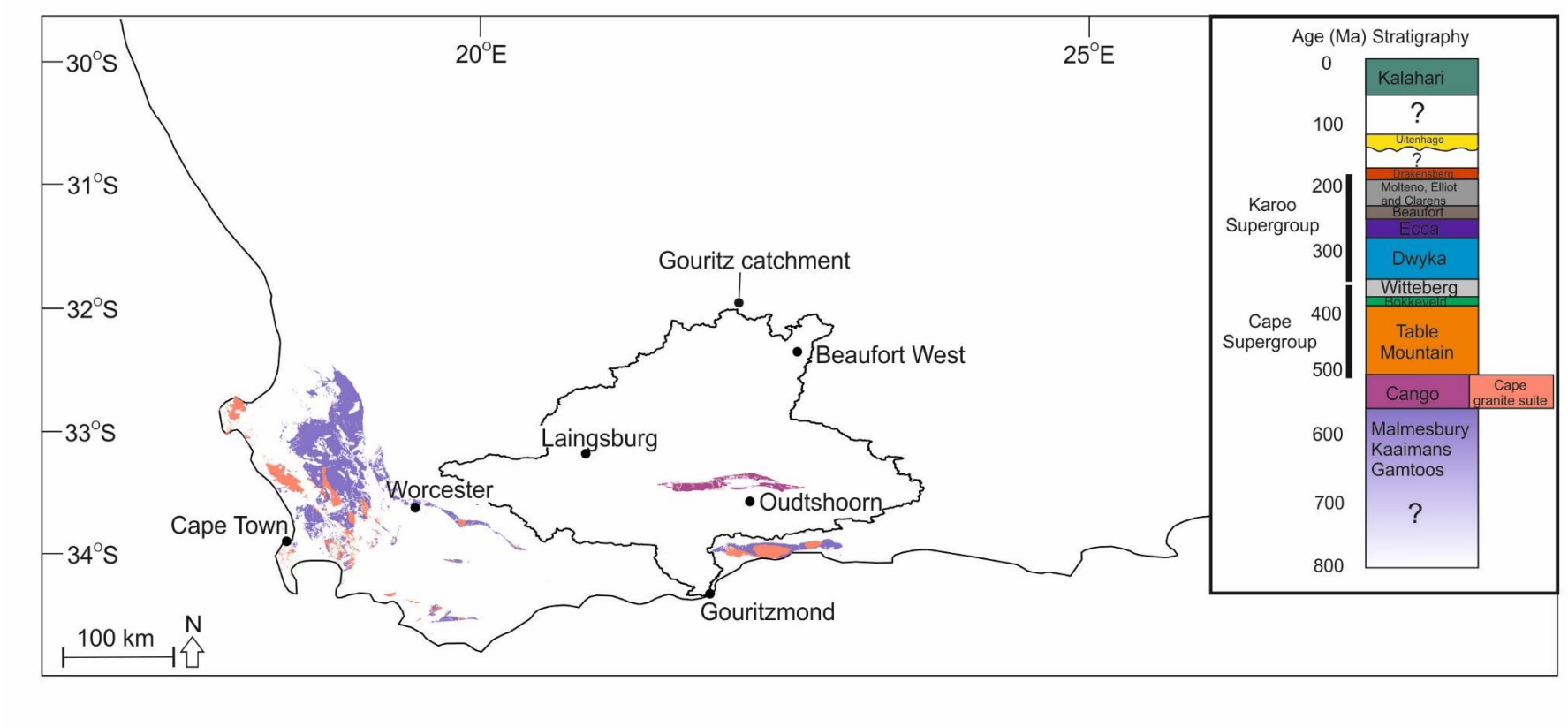

Figure 3.1 *– Pre-Cambrian stratigraphy of southern South Africa.*

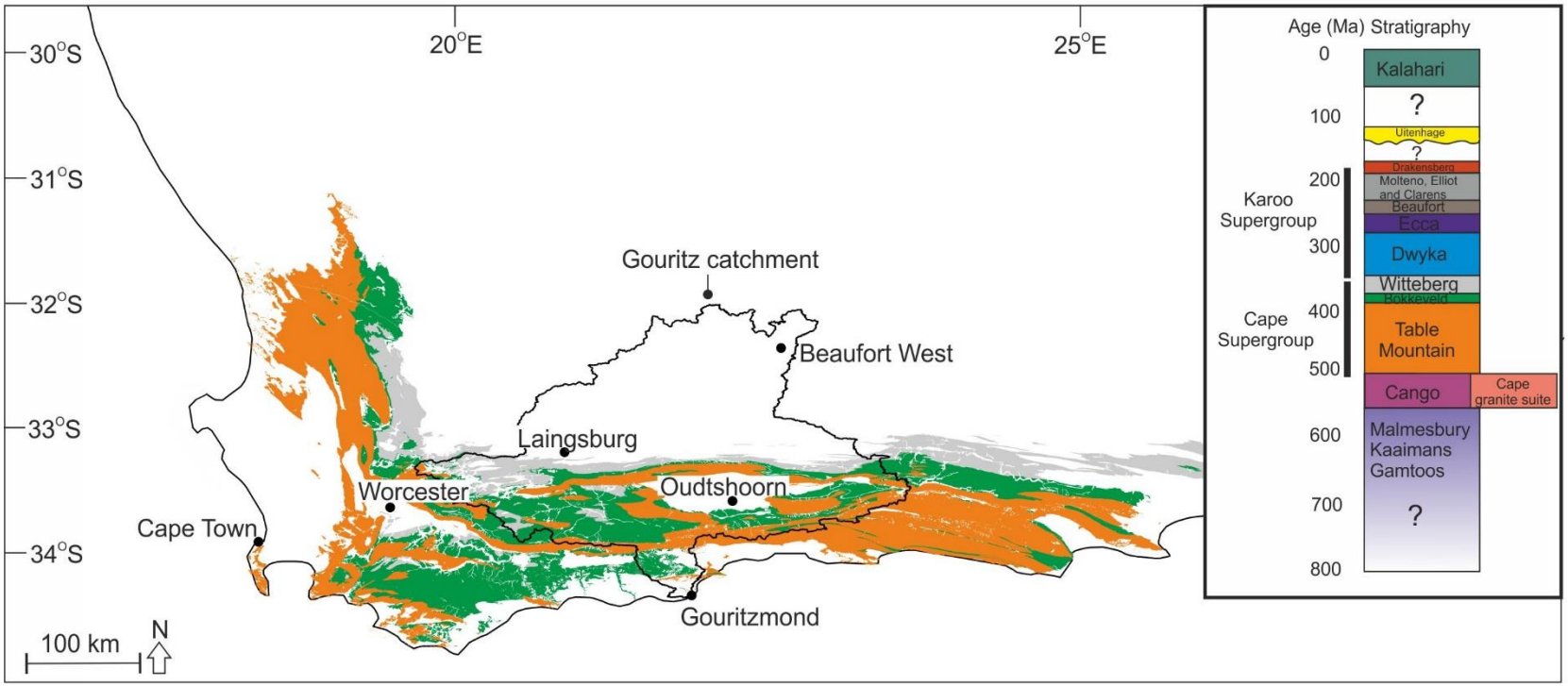

Figure 3.2 *– Distribution of the Cape Supergroup lithologies.*

The Karoo Supergroup (Figure 3.3) was deposited in the large-scale Karoo Basin, which has previously been interpreted as a retro-arc foreland basin that developed behind an inferred magmatic arc and fold-thrust belt (e.g., Catuneanu et al., 1998; Johnson et al., 2006). However, more recent work has argued that the Cape Fold Belt (CFB) was not emergent at the time of the deposition of the Karoo infill. Petrographic and geochemical studies (e.g. Johnson, 1991) suggest little or no contribution from the Cape Fold Belt to the Karoo Basin sediments, with a first cycle granitic source proposed (Van Lente, 2004) roughly 600 km away (King et al. 2009; Brunt et al., 2013). Additional evidence is provided by apatite fission track theromochronology (AFTT) work. The CFB was not exhumed (i.e., a surface feature) until the Cretaceous (Tinker et al., 2008a; Scharf et al., 2013).

The Karoo Supergroup comprises the Dwyka, Ecca and Beaufort groups. The Dwyka Group comprises tillite related to four major glaciation cycles (Visser et al., 1997). The Ecca (e.g., Wickens, 1994; Goldhammer et al., 2000; Rozman, 2000; Johnson et al., 2001; van der Werff & Johnson, 2003; Hodgson et al., 2006, 2009; Prélat et al., 2009; Wild et al., 2009; Hofstra et al., 2015; Spychala et al., 2015) and lower Beaufort (e.g., Smith, 1987; Smith 1993; Gulliford et al., 2014; Wilson et al., 2014) contain claystone, siltstone, and sandstone. The deposits represent an overall shallowing-upward succession from basin-floor and submarine slope, through shelf, to fluvial and lacustrine depositional environments (Johnson et al., 1996; Flint et al., 2011).

By the time of deposition of the lower Beaufort Group, terrestrial conditions prevailed across the Karoo Basin (e.g., Smith, 1987; Smith 1993; Gulliford et al., 2014; Wilson et al., 2014). The Stormberg Group contains mudstones and sandstones, and represents sub-aerial and fluvial deposition (Johnson et al., 1996). The Drakensberg Group contains flood basalts and dolerites associated with the initial rifting of Gondwana (Visser, 1984) and represent the end of infill of the Karoo Basin (Tankard et al., 2009). Ar^{40}/Ar^{39} dates on the flood basalts and intrusions represent a short period of magmatism (185 – 180 Ma; Duncan et al., 1997; Jourdan et al., 2005).

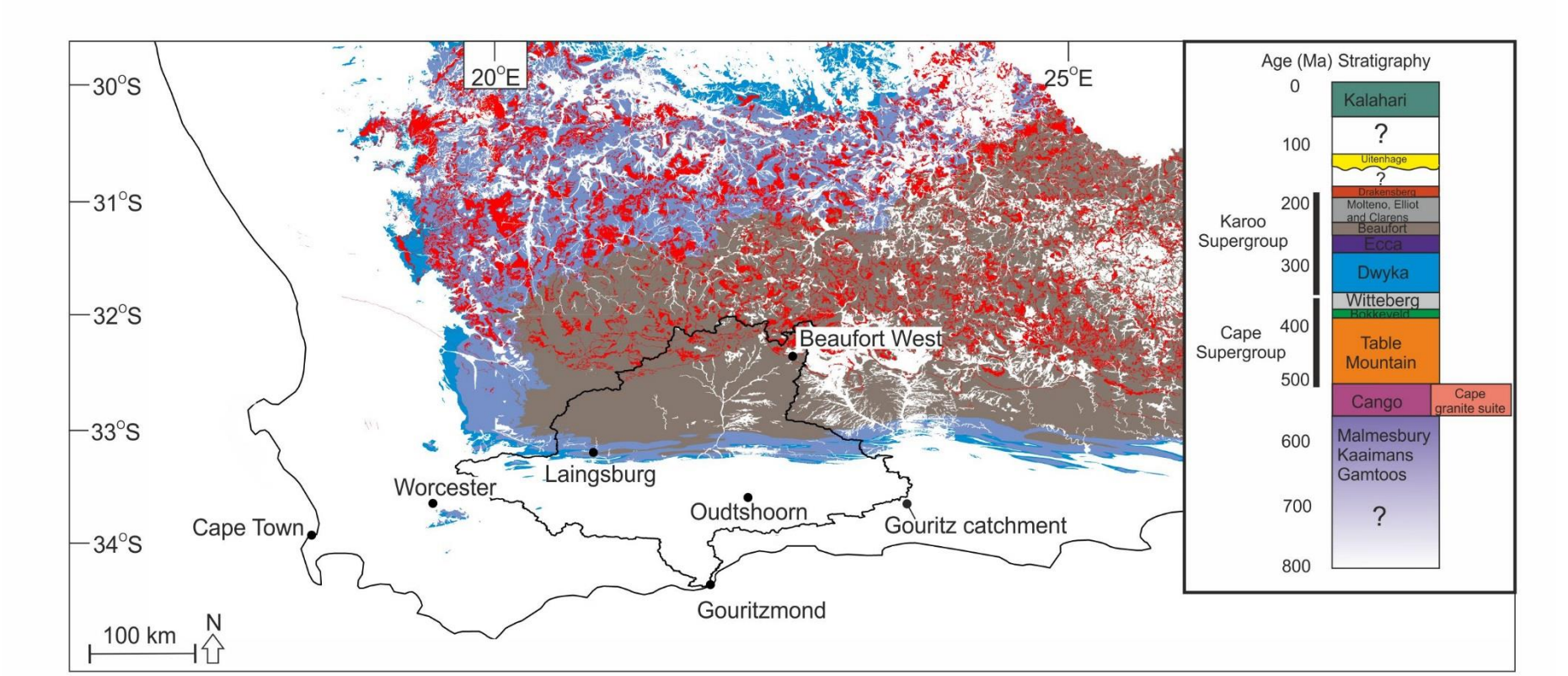

Figure 3.3 *– Distribution of the Karoo Supergroup lithologies.*

Mesozoic deposits within South Africa comprise the Uitenhage Group (Figure 3.4), which are associated with the large-scale exhumation of southern South Africa and are related to continental rifting and associated uplift. The Uitenhage Group comprises fluvial sandstones and mudstones deposits and alluvial fan conglomeratic deposits (Shone, 2006) associated with alluvial fan formation (Hill, 1972; Rigassi and Dixon, 1972; Winter, 1973) and rapid denudation across South Africa (Dingle, 1973; Lock et al., 1975). The Mesozoic deposits are discussed further and analysed in Chapter 5.

The onshore Cenozoic deposits (Figure 3.5) of South Africa are sparse and relate to the Kalahari Group, coastal limestones along the south coast, duricrusts (silcrete, ferricrete, calcrete) and superficial deposits (e.g., alluvium, soil). The Kalahari Group is composed of aeolian sands, and has been deposited in an internally drained basin, mainly fed by the Okavango River (Stankiewicz and de Wit, 2005). Silcretes of Cenozoic age are found on the coastal plain (Helgren and Butzer, 1977), which has been subject to marine transgressions and regressions.

3.1.2 Structure

Southern Africa is underlain by tectonic blocks, which have subsided due to mantle processes and are responsible for the formation and development of the Cape and Karoo Basins (Tankard et al., 2009). The main structural expression in the Western Cape is the Cape Fold Belt (Figure 3.6). The backbone of the Cape Fold Belt is formed by the east-west orientated anticlines of the Swartberg and Langeberg ranges, but also contains several transverse ranges such as the Cederberg range (Figure 3.6). The fold belt was formed in the Triassic (Tankard et al., 2009) and exhumed during the Cretaceous (Tinker et al., 2008a; Scharf et al., 2013). The geomorphic expression of the CFB reaches a maximum height of 2325 m in the Seweweekspoort, however the associated E-W folds decrease in amplitude towards the north (Paton, 2006; Spikings et al., 2015).

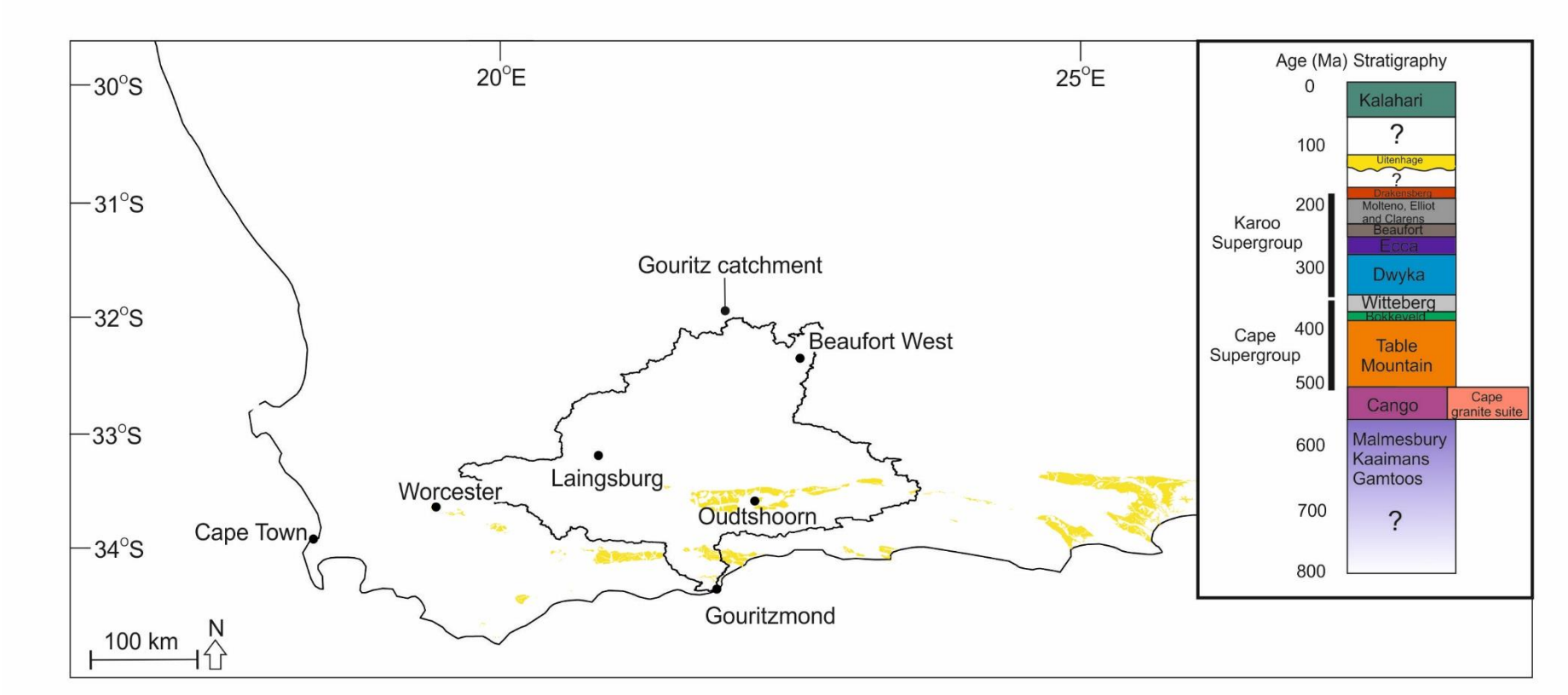

Figure 3.4 *– Mesozoic deposits of southern South Africa.*

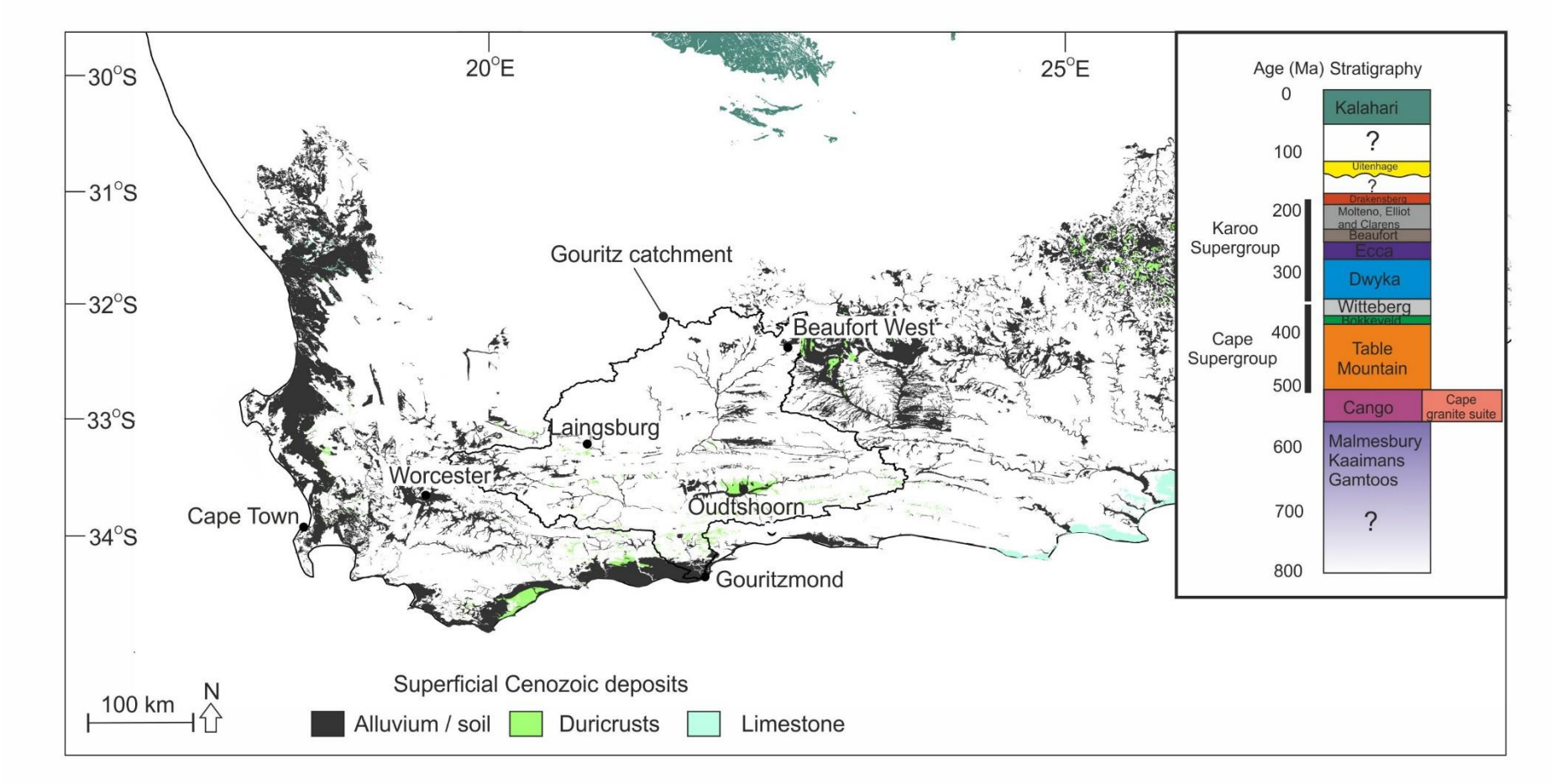

Figure 3.5 *– Cenozoic deposits of southern South Africa.*

Paton et al. (2006) split the Cape Fold Belt area into two broad domains. Thin-skinned deformation (Figure 3.7), in which surface thrusts coalesce and become shallower at depth, which dominates the northern domain of the Cape Fold Belt, and thick-skinned deformation (Figure 3.7) dominates the southern domain and coastal region of the Cape Fold Belt (Paton et al., 2006). Thick-skinned deformation involves the basement, and deformation is primarily controlled by the presence and geometry of crustal scale high angled structures (e.g., Coward, 1983).

The structural geology of South Africa is dominated by large-scale reactivated normal faults of the Cape Fold Belt (Figures 3.6, 3.8), which were reactivated due to the rifting of Gondwana (Paton, 2006; Paton et al., 2006). Selective reactivation occurred due to the orientation of the extensional stresses during the development of onshore Mesozoic basins (Paton and Underhill, 2004; Paton et al., 2006).

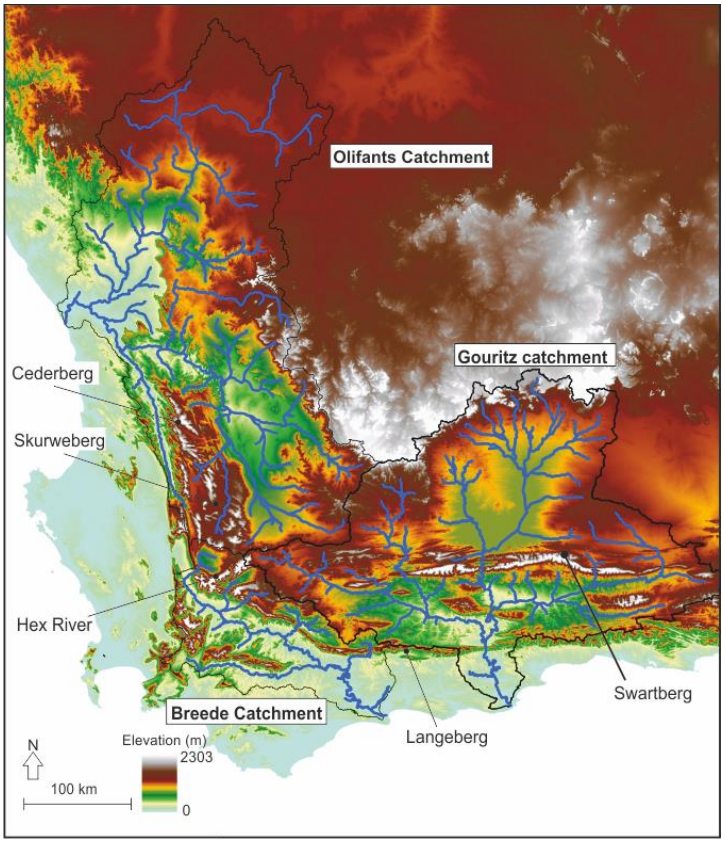

Figure 3.6 *– Ranges of the Cape Fold Belt and major drainage systems of the Western Cape.*

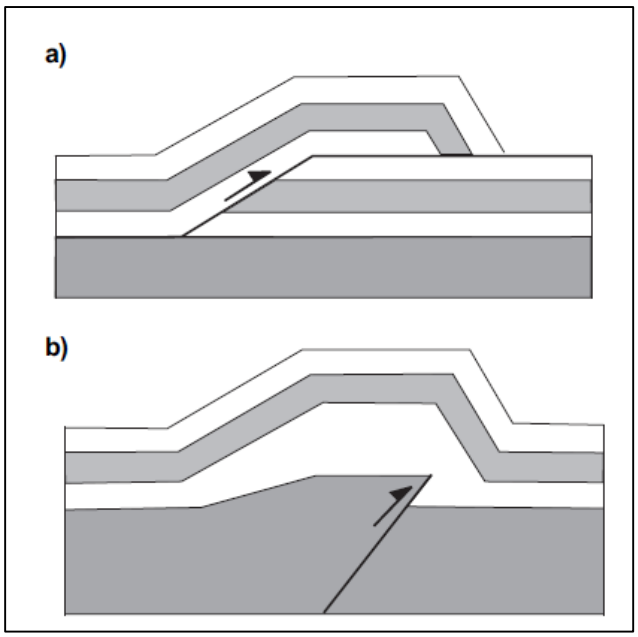

Figure 3.7 *– Schematic of a) thin and b) thick skinned deformation (Paton et al., 2006).*

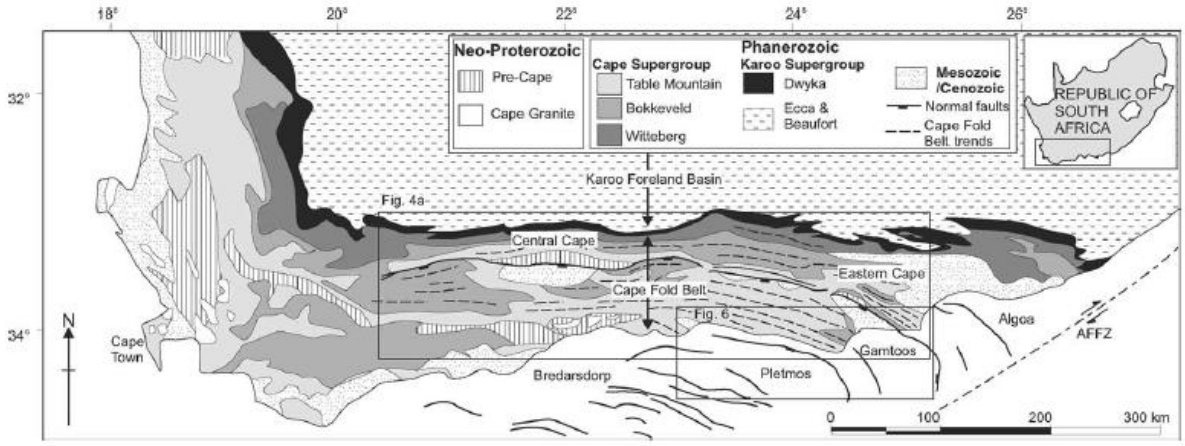

Figure 3.8 *– Geological map of southern South Africa with the reactivated extensional faults. The correlation in trend of the structural fabric and extensional faults is particularly evident to the SW, where there is a change in trend from an E-W orientation to a NW-SE trend (Paton, 2006).*

The reactivated faults are composed of long splays, rather than segmented portions, and maximum throw on the faults vary with the largest displacement ~ 6 km on the Worcester Fault (Tankard et al., 2009). Smaller faults are inherent within the CFB (Manjoro, 2014), but cannot be mapped at a 125,000 scale.

Epeirogenic uplift caused by large-scale denudation has been argued to have occurred in the Cretaceous (Brown et al., 1990). South Africa is currently tectonically quiescent with low seismic activity (e.g., Bierman et al., 2014) and sediment production (e.g., Tinker et al., 2008b). However, the recent uplift history of southern South Africa is contentious, with uplift histories deduced through the study of the

geomorphology of landforms such as erosional surfaces. Burke (1996) argued for uplift at ~30 Ma when the African plate came to rest with respect to the underlying mantle. The resulting uplift caused the formation of the Great Escarpment (discussed further in Section 3.3.1). Partridge and Maud (1987) argued for 150 – 300 m of uplift during the late Miocene to Pliocene, resulting in the tilting of South Africa towards the west. Partridge (1998) argued for a further 900 m of uplift in the Late Pliocene due to epierogenic uplift, causing rejuvenation and incision of east coastal rivers, further evidence is shown by the convex-up river profiles, marine sediments now 300m above sea level near Port Elizabeth and warping of erosional surfaces (Partridge, 1997). Roberts and White (2010) used a simple 1D inverse algorithm of long profiles to extract uplift histories of rivers. Roberts and White (2010) assumed that the shape of the long profile is controlled by uplift rates and the moderated erosional response, and using their analysis argued for Cenozoic uplift. Inversion of long profiles in the coastal Eastern Cape rivers (Figure 3.9) indicated uplift consistent with those predicted by Partridge and Maud (1987) at ~35 – 10 Ma. However, the model assumes that: 1) one single profile can be used to indicate uplift for the region; 2) planform is fixed in time and space; 3) no drainage capture events occurred; 4) there is no pre-existing topography and that uplift is only a function of time; 5) other controls such as climate, discharge and lithology are ignored.

Uplift proposed by Partridge and Maud (1987) was disputed by Brown et al. (2002) and van der Beek et al. (2002). Based on Apatite Fission track thermochronology (AFTT), there is no signal for a recent period of uplift (Brown et al., 2002). Furthermore, there is a lack of timing constraints of the original evidence, coupled with a modelled subsidence in the Port Elizabeth area, resulting in raised marine sediments (van der Beek et al., 2002). However, the Cenozoic uplift event may not have produced a significant amount of denudation to affect AFTT results. Nonetheless, Green et al. (2016) argued for Cenozoic uplift of the Swartberg Range (CFB) using AFTT data.

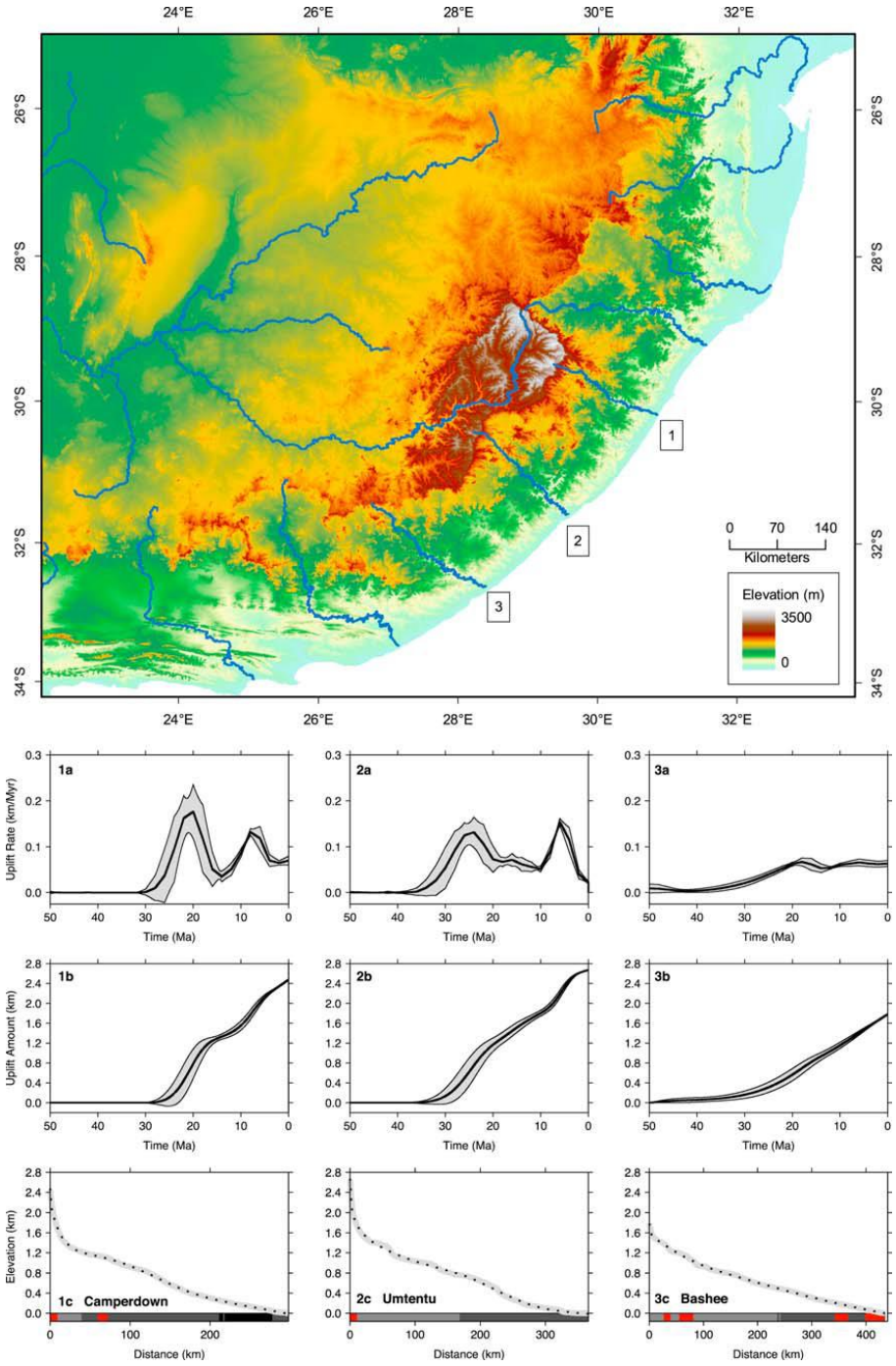

Figure 3.9 *– Long profile analysis of the Eastern Cape rivers: 1) Camperdown River; 2) Umtentu River; 3) Bashee River. a) Thick black line and grey envelope show mean uplift rate history and its uncertainty which were calculated by Monte Carlo inverse modelling of river profiles; b) Cumulative uplift history calculated from uplift rate history; c) Long profile analysis – showing the bedrock lithology, black – Precambrian basement, grey – Paleozoic/Mesozoic sedimentary rocks, white – Cenozoic sedimentary rocks and red – igneous rocks (Roberts and White, 2010).*

3.2 Climate

The Cretaceous period was warm and humid (Dingle et al., 1983; Partridge and Maud, 2000), with deep weathering occurring globally (Bardossy, 1981; Valeton, 1983). Significant desiccation of the soils occurred during the transition into the

Cenozoic, causing saline soil and the precipitation of silcretes (Partridge and Maud, 2000). The climate evolution of South Africa has not been studied in great detail, and what work has been done has focussed on the Holocene period (e.g., Holmgreen et al., 1999; Gasse et al., 2008). During the Cenozoic, the climate became cooler and drier, with increasing aridity (Partridge and Maud, 2000). Proxy data including pollen (e.g., Zhao et al., 2003; Scott and Woodborne, 2007), tree rings (e.g., Hall, 1976; Dunwiddie and LaMarche, 1980; Thackeray, 1996), stalagmites (e.g., Talma and Vogel, 1992) and offshore sediment accumulations (e.g., Gasse et al., 2008) have been used to reconstruct the Holocene climatic record.

The major variations in the Holocene climate relate to warm and cold phases with the stalagmite record dominated by the Little Ice Age period, where temperatures decreased to the lowest in 1700 AD (Holmgren et al., 1999). The present day climate of the Western Cape is primarily semiarid (Dean et al., 1995). The region has a clear split between summer and winter rainfall regimes, with late summer to winter rainfall in the Great Escarpment and central Karoo region, winter rainfall in the western CFB, late summer to winter rainfall in the southern CFB, and summer and winter rainfall in the coastal areas (CSIR, 2007). The lower coastal region has a Mediterranean-type climate (Midgley et al., 2003).

3.3 Geomorphology

Much debate surrounds the uplift history and geomorphic evolution of southern Africa. The landscape of southern Africa is atypically elevated (~ 1km) compared to other cratonic regions that have average elevations of between 400 – 500 m particularly given the passive continental margin setting (Lithgow-Bertelloni and Silver, 1998; Gurnis et al., 2000). The dominant geomorphic feature is the Great Escarpment, which separates an interior plateau of low relief and high elevation, from a coastal region of high relief and low average elevation (Fleming et al., 1999; Tinker et al., 2008b; Moore et al., 2009). Debates surrounding the landscape relate to the mechanisms of formation, the evolution of the landscape, and the age of landscape.

3.3.1. Mechanisms of formation

The anomalous height of South Africa has received the attention of geophysicists and geomorphologists alike, with the main mechanisms of formation being proposed explained by mantle plume concepts or plate tectonics;

1) Mantle plume concepts

The anomalously high topography of southern Africa has often been related to the 'African superswell' where exceptional tectonic uplift has occurred. Evidence for thermal perturbations are related to geological observations (e.g., Cenozoic rifting in E Africa and volcanism; Ebinger and Sleep, 1998), geochemical anomalies (Ebinger and Sleep, 1998), and geophysical evidence such as gravity field anomalies (Nyblade and Robinson, 1994) related to the central and northern part of the continent. The source of the superswell heating has been argued to have been from movement of the continent over Mesozoic hotspots (upper mantle; Nyblade and Robinson, 1994), as well as the production of a low velocity anomaly zone formed by active upwelling from the core-mantle boundary seen in tomographic models (Lithgow-Bertelloni and Silver, 1998; Gurnis et al., 2000). Numerical modelling of plumes have shown that the location of continental flood basalts may not coincide with the location of the plume head, but correlate well with the distribution and timing of magmatism (Ebinger and Sleep, 1998). Moore and Blenkinsop (2002) argued that superimposition of plumes of different ages and overprinting has caused a dominant eastward drainage pattern, and accounts for the pre-Gondwana drainage. Conversely, Cox (1989) argued that in the Karoo volcanic province the drainage is radial, with antecedence within the rivers seen because of topographic highs formed by the plume activity (e.g., Orange River).

2) Plate tectonics

Moore et al. (2009) suggested that the dynamic topography predicted by the plume related models do not correspond with the actual topography of southern Africa. The modelled low elevation areas are actually the highest e.g., Drakensberg Mountains (Lithgow-Bertelloni and Silver, 1998) and the predicted radial drainage (Cox, 1989) does not dominate in river planforms. Tankard et al. (2009) argued there is a '*conspicuous lack of direct evidence to support a mantle plume model*' (pg. 1404). Moore et al. (2009) researched the current horseshoe-shaped (Du Toit, 1933; King, 1963; Moore, 1999) drainage divides that dominate southern Africa (Figure 3.10), the drainage divides do not follow geological boundaries or structural lineaments (Figure 3.11) and have been related to axis of epierogenic uplift (Du Toit, 1933; King, 1963; Moore, 1999). Three major divides are seen within southern Africa; 1) Escarpment axis and towards the north 2) Etosha-Griqualand-Transvaal (EGT) axis, and 3) Ovambo-Kalahari-Zimbabwe (OKZ) axis (Figure 3.11). The axes are argued to have been activated at progressively younger ages inland (Moore et al., 2009) based on river planform analysis, sedimentary flux to deltas, and AFTT data.

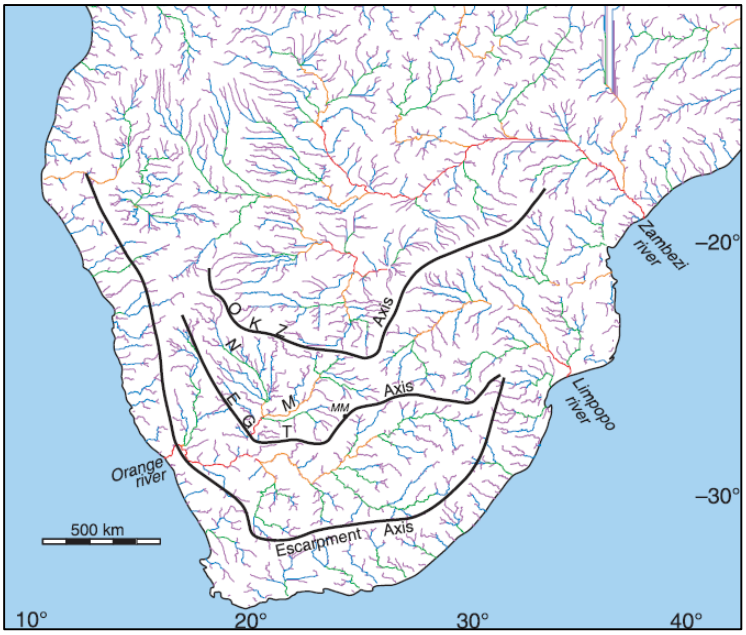

Figure 3.10 *– Drainage patterns of southern Africa and flexure axis (Moore et al. 2009). With the main 'horseshoe shaped' continental drainage divides corresponding with the axis of uplift. The colours of the streams relate to stream order number, purple 1, blue 2, green 3, orange, 4 and red 5.*

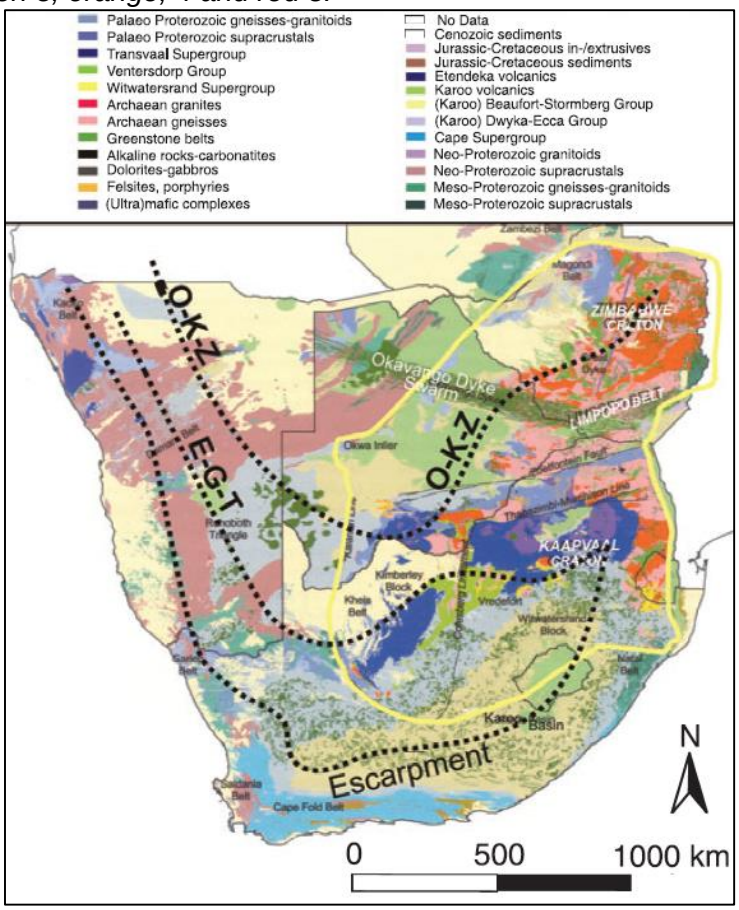

Figure 3.11 *– Relationship between axis and geology (Moore et al., 2009).* Etosha-Griqualand-Transvaal (EGT) axis and Ovambo-Kalahari-Zimbabwe (OKZ) axis.

The Escarpment axis is relevant to this study and has been argued to have formed at the rifting of Gondwana, due to continental instability following the separation of the

Agulhas Bank and the Falklands Plateau and the initiation of the Indian and Atlantic Oceans (~ 126 Ma); which caused the coastal plain to be eroded and the axis to migrate inland as isostatic flexure (Gilchrist and Summerfield, 1991). This flexure is still present, but is uplifting at very slow rates (Fleming et al., 1991; Brown et al., 2002).

3.3.2 Landscape evolution models and rates of change

King's (1953, 1963) ideas of polycyclic erosion cycles have dominated the literature on southern Africa (Figure 3.12). King argued that southern Africa is dominated by planation surfaces, which form in response to phases of rapid uplift, followed by long periods of regular back wearing. Numerous regional surfaces relate to separate erosion cycles and, thus, represent separate uplift events. A key aspect of King's viewpoint is that the Great Escarpment originated at the coast, after initial rifting and retreat due to base level fall. Partridge and Maud (1987) endorsed the escarpment viewpoints of King, but they argued that fewer erosional surfaces could be delineated than King identified. Acceptance of plate tectonic theory led to development of alternative views to those of King. For example, Gilchrist et al. (1994) did not include landscape cycles, instead arguing that rifting is more important. Rifting reorganised the drainage patterns and resulted in an exterior and interior catchment. Exterior catchments experienced isostatic uplift, reducing the impact of denudation whilst interior catchments deposited less sediment in inland basins compared to the external catchments. Due to erosion, the exterior catchments drainage divide migrates inland and breaches the inland marginal divide causing river capture (Gilchrist et al, 1994). Additional rejection of King's hypothesis is related to how the episodic uplift could have occurred. Gilchrist and Summerfield (1990, 1991) demonstrated that the formation of a coastal plain by scarp retreat would result in continuous isostatic adjustment and that there is an absence of a suitable mechanism to account for episodic uplift. However, Moore et al. (2009) argued that episodic uplift due to plate tectonics (Section 3.3.1.1), could have provided the successive episodic uplifts described in King's model. Subsequent modelling by Gilchrist and Summerfield (1990, 1991) argued rather that the formation of the coastal plain by escarpment retreat would cause continuous isostatic adjustment and not a pulsed uplift as King envisaged. King's surfaces have also been disputed as it is difficult to extrapolate interpretations from discrete remnants on a regional, or sub-continental scale (e.g., Summerfield, 1996; Brown et al., 2000). Furthermore, assigning relative ages to each surface is tenuous (e.g., Summerfield, 1996; Brown et al., 2000).

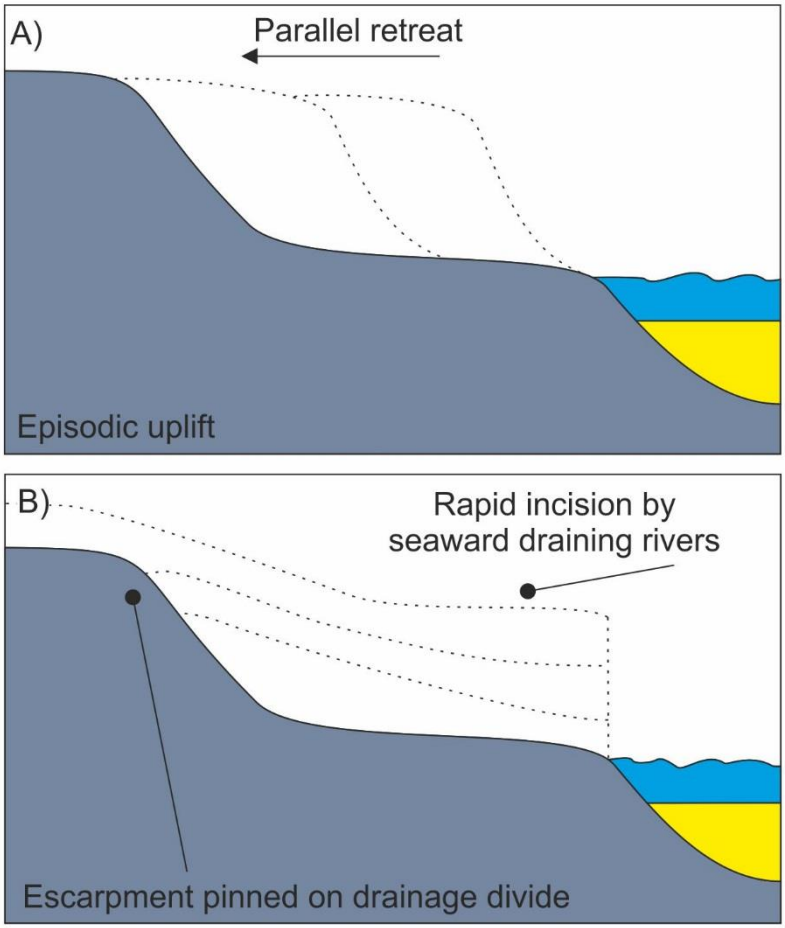

Figure 3.12 *– Models of landscape evolution: A) King's model (*1953*) and B) Gilchrist et al.'s (1994) model based on a pinned drainage divide. Kings (1953) model shows parallel retreat of the escarpment from the coast after successive uplift, whereas Gilchrist et al. (1994) argued for limited retreat of the escarpment, which is pinned on a drainage divide. Seaward of the escarpment, the land is rapidly incised by small seaward draining systems.*

Unravelling the landscape development of southern South Africa has recently been aided by the development of cosmogenic dating (Figure 3.13), AFTT and numerical modelling, which has allowed rates of erosion to be calculated and methods of development constrained. Brown et al. (2002) used AFTT on samples in a transect across eastern South Africa, and found accelerated incision between ~91 – 69 Ma with the removal of 3 km of crustal section at a mean rate of 95 mMa^{-1}. This rate refutes King's hypothesis because retreat of the escarpment from the coast would require constant rates of over 1000 mMa^{-1}. Additionally, a much later phase of accelerated denudation, than recorded by Brown et al. (2002) would be expected at the Swartberg borehole as the escarpment retreated past. Brown et al. (2002) argued for an internal drainage divide controlling incision rates. Rivers that formed at the coast eroded the escarpment due to rifting, which accounts for the first phase of

accelerated incision at the coast. The later phase of incision shown by the Swartberg borehole, as the escarpment retreats could also be related to the rivers headward erosion. A new escarpment would form at the inland divide, and the escarpment would slowly retreat (Brown et al., 2002). van der Beek et al. (2002) numerically tested the hypothesis of a post-break up drainage divide and found that an escarpment could form at the drainage divide, and only retreat a short distance. Moore and Blenkinsop (2006) argued resistant lithologies do not necessarily erode when associated with an inland drainage divide, with a possible decrease in erosion rates related to the development of angiosperms in the area in the mid-late Cretaceous, binding the soil. However, the authors stated that this is somewhat speculative. The influence of lithology is compounded by the shift in climate to a more arid environment since the Cretaceous (Bakker and Mercer, 1986). Moore and Blekinsop (2006) state that Brown et al.'s (2002) model does not include any transient effects of tectonic uplift, which Cox (1989) argued has a first order control on post-Gondwana drainage systems. Moore and Blenkinsop (2006) argued that the evolution of the escarpment (Drakensberg) could relate to both King's model of retreat and the occurrence of an inland drainage divide; with the occurrence of an inland drainage divide as a subordinate factor not fully disregarded.

There is a general consensus that large-scale exhumation of southern Africa occurred in the Cretaceous (e.g., Gilchrist et al., 1994; Gallagher and Brown, 1999; Cockburn et al., 2000; Brown et al., 2002; Tinker et al., 2008a; Kounov et al., 2009; Flowers and Schoene, 2010). Tinker et al. (2008a) used AFTT across a north-south transect across the southern margin of South Africa (Figure 3.13), and found two periods of increased denudation; Early Cretaceous and Mid-Late Cretaceous. Tinker et al. (2008a) argued that '*if the entire Karoo sequence, up to and including the Karoo volcanics, originally covered the Southern Cape region, then a potential maximum of ~6-7 km of sediment and volcanic rock may have been eroded from this area since ~181 Ma*' (p. 89).

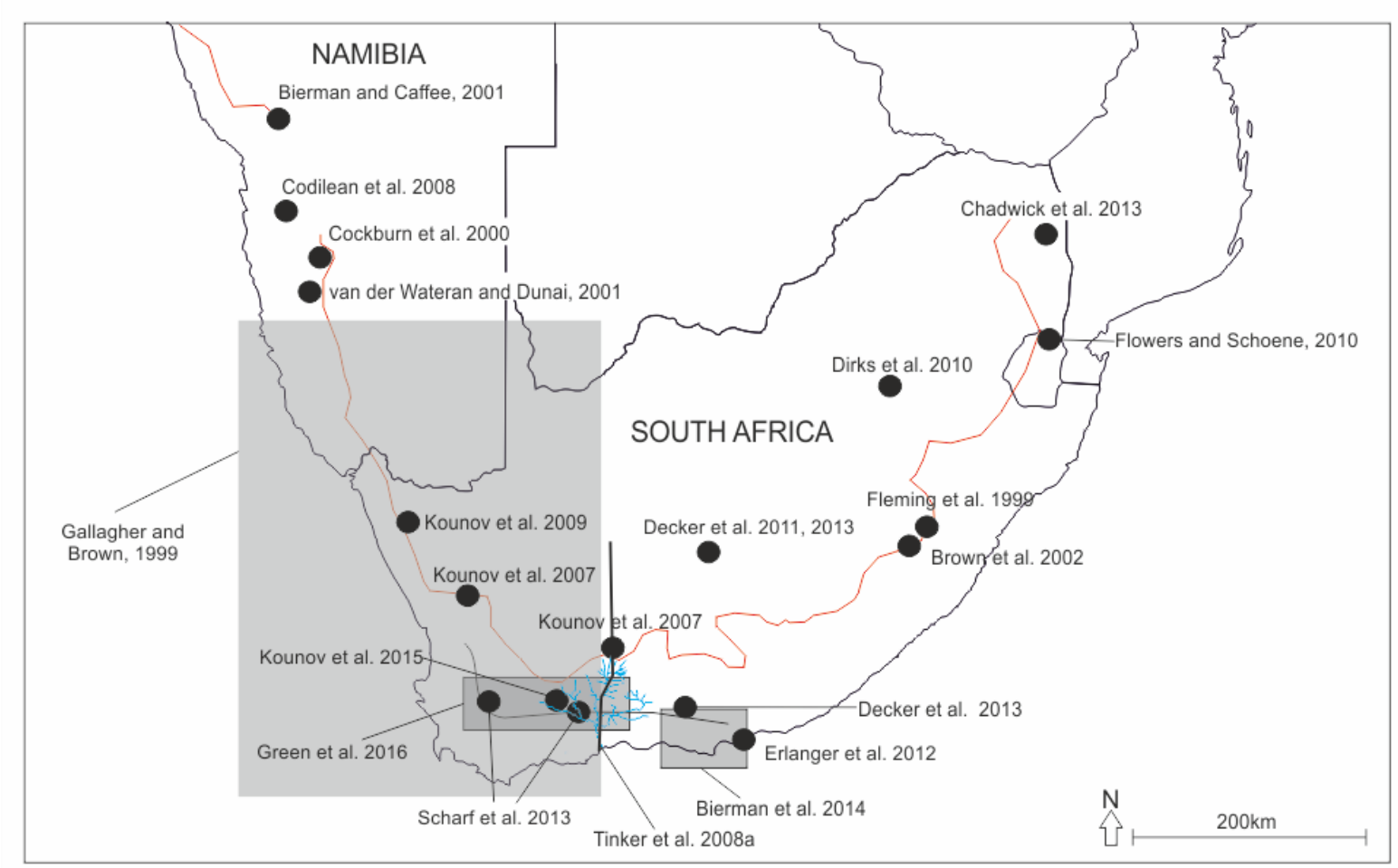

Figure 3.13 *– Location of cosmogenic and apatite fission track studies within southern Africa. The Gouritz drainage network is shown in blue and the Great Escarpment in red. The grey boxes represent the area analysed using apatite fission track.*

Table 3.1 *– Cosmogenic (^{36}Cl, ^{10}Be, ^{21}Ne, ^{3}He, ^{38}Ar, ^{26}Al) and apatite fission track data; rates of erosion in southern Africa.*

Location	Technique	Rate mMa^{-1}	Landform	Time integration (Ma)	Reference
Drakensberg escarpment	^{36}Cl	55.05	Escarpment Face	0 – 1	Fleming et al. 1999
Namib Desert	^{10}Be	7.08	Escarpment Face	0 – 1	Cockburn et al. 2000
South-central Karoo	^{3}He, ^{21}Ne, ^{38}Ar	4.02	Escarpment Face	0 - 1	Decker et al. 2011
Namib Desert	^{10}Be	7.20	Escarpment Ridge	0 – 1	Cockburn et al. 2000
South-central Karoo	^{3}He, ^{21}Ne, ^{38}Ar	70.57	Escarpment Ridge	0 – 1	Decker et al. 2013
South-central Karoo	^{3}He, ^{21}Ne, ^{38}Ar	4.24	Escarpment Summit	0 – 1	Decker et al. 2013
Drakensberg escarpment	^{36}Cl	11.25	Escarpment Summit	0 – 1	Fleming et al. 1999
Southern/southwestern coastal escarpment	^{3}He, ^{21}Ne	1.20	Escarpment Summit	0 – 1	Kounov et al. 2007
Highveld	^{10}Be	3.63	Escarpment Summit	0 – 1	Dirks et al. 2010
Namib Desert	^{3}He, ^{21}Ne, ^{38}Ar	2.23	Escarpment Summit	0 – 1	Decker et al. 2013
Drakensberg escarpment	^{10}Be	4.63	Coastal inselbergs	0 – 1	Cockburn et al. 2000
Namib Desert and escarpment	^{10}Be	3.55	Inselbergs	0 – 1	Bierman and Caffee, 2001
South-central Karoo	^{3}He, ^{21}Ne, ^{38}Ar	1.75	Inselbergs	0 – 1	Decker et al. 2011
South-central Karoo	^{3}He, ^{21}Ne, ^{38}Ar	1.78	Low relief plain	0 – 1	Decker et al. 2011
Namib Desert	^{21}Ne	0.46	Pediment/gravel plain	0 – 1	van der Wateran and Dunai, 2001
Eastern Cape	^{10}Be	0.92	Pediment	0 – 1	Bierman et al. 2014
Western Cape	^{21}Ne	0.81	Pediment	0 – 1	Kounov et al. 2015

Namib Desert	^{21}Ne	0.61	Strath terrace	0 – 1	van der Wateran and Dunai, 2001
South-central Karoo	^{3}He, ^{21}Ne, ^{38}Ar	1.00	Strath terrace	0 – 1	Decker et al. 2011
Eastern Cape	^{26}Al, ^{10}Be	16.10	Strath terrace	0 – 1	Erlanger et al. 2012
Western Cape, CFB	^{10}Be	3.30	Bedrock river	0 – 1	Scharf et al. 2013
Namib Desert	^{21}Ne	0.91	Bedrock river	0 – 1	van der Wateran and Dunai, 2001
Western Cape	^{21}Ne, ^{10}Be	10.24	Bedrock river	0 – 1	Kounov et al. 2015
Highveld	^{10}Be	53.00	Bedrock river	0 – 1	Dirks et al. 2010
South-central Karoo	^{3}He, ^{21}Ne, ^{38}Ar	1.76	Bedrock river	0 – 1	Decker et al. 2011
Western Cape, CFB	^{10}Be	5.13	River sediment	0 – 1	Scharf et al. 2013
Eastern Cape	^{10}Be	4.54	River sediment	0 – 1	Bierman et al. 2014
Namib Desert and escarpment	^{10}Be	11.56	River sediment	0 – 1	Bierman and Caffee, 2001
Namib Desert	^{10}Be	9.98	River sediment	0 – 1	Codilean et al. 2008
Highveld	^{10}Be	5.45	River sediment	0 - 1	Chadwick et al. 2013
Namibia	AFTT	7-36	Bedrock river	140 – 0	Gallagher and Brown 1999
Namib Desert	AFTT	40	Bedrock river	130 – 36	Cockburn et al. 2000
Namib Desert	AFTT	5	Bedrock river	36 – 0	Cockburn et al. 2000
Coastward of drakensberg escarpment	AFTT	≥ 35	Bedrock river	130 – 0	Brown et al. 2002
Coastward of drakensberg escarpment	AFTT	95	Bedrock river	91 – 69	Brown et al. 2002
Inland of drakensberg escarpment	AFTT	15-28	Bedrock river	78 – 0	Brown et al. 2002

Inland of Drakensberg escarpment	AFTT	82	Bedrock river	78 – 64	Brown et al. 2002
Coastward of southern escarpment	AFTT	125-175	Bedrock river	100 – 80	Tinker et al. 2008
Coastward of southern escarpment	AFTT	10-15	Bedrock river	80 – 0	Tinker et al. 2008
South Africa western margin coastal plain	AFTT	60-108	Bedrock river	115 – 90	Kounov et al. 2009
South Africa weatern margin interior plataeu	AFTT	<40	Bedrock river	115 – 90	Kounov et al. 2009
Eastern Drakensberg escarpment	AFTT	11-14	Bedrock river	65 – 0	Flowers and Schoene 2010

The apatite data is within this predicted range, with Early Cretaceous denudation accounting for the differences. Tinker et al. (2008a) note that the drivers for the Cretaceous denudation remain unclear, however they argued that both time periods coincide with mantle activity forming large igneous provinces / kimberlite activity.

Green et al. (2016) collected 73 samples from the Western Cape area for AFTT (Figure 3.13), and found five periods cooling (exhumation) since the Mesozoic: 1) 205 – 180 Ma (lower Jurassic); 2) 145 – 130 Ma (lower Cretaceous); 3) 120 – 100 Ma (lower-upper Cretaceous); 4) 85 – 75 Ma (upper Cretaceous) and; 5) 30 – 20 Ma (Cenozoic). The lower Jurassic exhumation is regional and related to the rifting of Gondwana. The lower Cretaceous exhumation was identified near Oudtshoorn, related to the Mesozoic formation of fault bounded basins (Section 3.1) depositing the Uitenhage Group, in which a significant thickness of sediment is missing (lower-upper Cretaceous). Exhumation of the Uitenhage Group occurred in the upper Cretaceous, forming the remnants that are seen today (Section 3.1). Cretaceous exhumation is in agreement with other published work (e.g., Gilchrist et al., 1994; Gallagher and Brown, 1999; Cockburn et al., 2000; Brown et al., 2002; Kounov et al., 2009; Flowers and Schoene, 2010). However, Green et al. (2016) argued for Cenozoic exhumation in the Swartberg Mountain range, forming the transverse rivers seen in the region. Furthermore, the Great Escarpment is a Cenozoic feature not related to continental break-up (*cf.* Brown et al., 1990; Gilchrist et al., 1994; Kounov et al., 2009), which is pinned on dolerite due to differential exhumation of the area in the Cenozoic (last 30 Ma) as shown by cooling in samples collected from Beaufort West. However, the escarpment is not pinned on dolerite in all locations, but is a dominant feature of the Western Cape where samples were taken. Green et al. (2016) argued this viewpoint is supported by kimberlite pipe research of Stanley et al. (2013), which shows Cenozoic exhumation. Stanley et al. (2013) did find evidence of Cenozoic exhumation, but the exhumation recorded does not need regional uplift. The kimberlite pipes are near a palaeochannel of the Orange River system (De Wit, 1999), and Stanley et al. (2013) argued for river incision causing the exhumation.

Cosmogenic dating suggests a decrease in erosion rates since the Cretaceous (e.g., Fleming et al., 1999; Cockburn et al., 2000; Bierman and Caffee, 2001; van der Wateran and Dunai, 2001; Kounov et al., 2007; Codilean et al., 2008; Dirks et al. 2010; Decker et al., 2011; Erlanger et al., 2012; Chadwick et al., 2013; Decker et al., 2013; Scharf et al., 2013; Bierman et al., 2014; Kounov et al., 2015; Table 3.1). Fleming et al. (1999) used cosmogenic ^{36}Cl in basalt samples from the Drakensberg escarpment and found that denudation has actively been occurring over 10^5-10^6

years; King's (1953, 1962 and 1963) erosional surfaces would not have survived this erosion. The rates of denudation are also an order of a magnitude less than needed for an escarpment retreat from the coast (*cf*. King, 1953, 1962, 1963).

The Cape Fold Belt, which is outboard of the Great Escarpment, yields some of the lowest denudation rates worldwide, and highlighted that rugged topography does not necessarily result in high denudation rates (Scharf et al., 2013). Scharf et al. (2013) proposed that the persistence of the fold belt and the low denudation rates are a function of the lithological resistance of the quartzites and metamorphosed sediments. They considered that the belt therefore represents a post-orogenic case of steady state topography with uplift due to isostasy caused by denudation. The catchments studied are detachment limited (lacks in channel sediment load, or "tools"), and although bedrock is bare and able to be incised (without a sediment cover having to be removed beforehand); the authors used the lack of tools (or sediment within the system that can erode the underlying bedrock) to explain the low denudation rates. Scharf et al. (2013) do not find evidence of uplift to support Partridge and Maud (1987), and concluded that tectonic stability has prevailed in South Africa throughout the Cenozoic.

Low erosion rates have been reported elsewhere in southern Africa such as in the Namib Desert, where denudation rates vary between 1 and 16 m Ma^{-1}. Bierman and Caffee (2001) argued against King's (1953, 1962 and 1963) style of escarpment retreat from their cosmogenic dating using paired nuclides (^{10}Be and ^{26}Al). Bierman and Caffee (2001) concluded that there has been little geomorphic change over 10^5 to 10^6 years and, therefore, the landscape represents a steady state form. The authors identified no significant spatial distribution in erosion rates, despite a precipitation gradient with the influence of fog drip, which an important moisture source on the coastal plain. Like the Cape Fold Belt, the geology of the Namib Desert is strongly influenced by post-orogenic mountain belts with metamorphosed lithologies. The rivers that originate in the area are ephemeral in nature (Bierman and Caffee, 2001), therefore, even during flooding little geomorphic work is accomplished, perhaps due to the lack of 'tools' (or transported sediment within the river) within the basin similar to Scharf et al.'s (2013) study.

Decker et al. (2013) argued that climate is a dominant factor accounting for the low Cenozoic denudation rates within the African Plateau, with denudation rates of the Karoo dolerite surfaces reflecting chemical weathering rates and, therefore, are climate limited. The reduction in Cenozoic denudation rates reported by other workers (Fleming et al., 1999; Cockburn et al., 2000; Bierman and Caffee, 2001; van der

Wateren and Dunai, 2001; Kounov et al., 2007; Codilean et al., 2008; Dirks et al., 2012; Decker et al., 2011; Erlanger et al., 2012; Chadwick et al., 2013; Decker et al., 2013; Scharf et al., 2013; Bierman et al., 2014; Kounov et al., 2015) is therefore due to climate. Although tectonic activity cannot be ruled out, the reduction of erosion rates since the Cretaceous may also reflect fluvial systems becoming adapted to lithological and structural controls. Romer (2010) also argued that weathering is an important component affecting how systems respond over long timescales. Nonetheless, Brown et al. (1992) disregarded climate as a primary control on the reduction of erosion of the escarpment between the Cretaceous and Cenozoic. Roberts and White (2010) also argued that climate, and in particular weathering, is not an important constraint on river profile shape in their study of river profiles draining African topographic swells.

3.3.3 Offshore sedimentation

Denuded sediment is preserved in offshore basins and provides an important archive of the timing and rates of onshore incision. Rouby et al. (2009) researched the Orange and Walvis basins along the Southern Africa and Namibian Atlantic margin. The offshore sediment volumes indicate that the major episodes of denudation occurred during the post-rift Early Cretaceous and the Late Cretaceous, with rates decreasing thereafter. The initial high rates of incision can be attributed to rift-related tectonic activity. However the persistence of sedimentation (and, thus, incision) needs an explanation and requires a rejuvenation event 50 Ma after the rifting event. The rejuvenation could be attributed to a change in lithological resistance (Rouby et al., 2009) or by drainage rearrangement. Coastal streams developed by the rifting could have captured the previously internal plateau drainage (Rouby et al., 2009). Although re-organisation has been attributed to the Orange Basin, Rouby et al. (2009) argued that this would not increase the drainage area enough to explain the high sedimentation rates. Topographic and relief reorganisation has been used by Rouby et al. (2009) to explain an increase in denudation at 80 Ma shown by apatite data. Climate change could be an important factor, however the available palaeoclimatic reconstruction does not indicate this (Rouby et al., 2009). Rouby et al. (2009) concluded that offshore data is a reliable estimation of denudation but is subject to caveats.

Tinker et al. (2008b) used offshore wells in the inner and outer Outeniqua Basin (central southern Africa, Figure 3.14), relating the offshore accumulation to denudation histories. The timings of increased sedimentation match with the timings of increased denudation, but there is a mismatch with the volume of sediment found

versus that calculated to have been eroded (Figure 3.15). The discrepancies may arise from the fact that onshore denudation rates neglect chemical weathering, which could be significant for the Karoo basalts, whilst offshore results are always underestimated due to the volumetric difference between sediment accumulation and deposition due to compaction. In addition, sediment may have bypassed the shelf as slope turbidity currents (Tinker et al. 2008b). The data nonetheless indicates increased activity in the Mesozoic and, therefore, topographic development of southern Africa. Sonibare et al. (2015) researched the Bredasdorp Basin and found increased deposition during the Mesozoic.

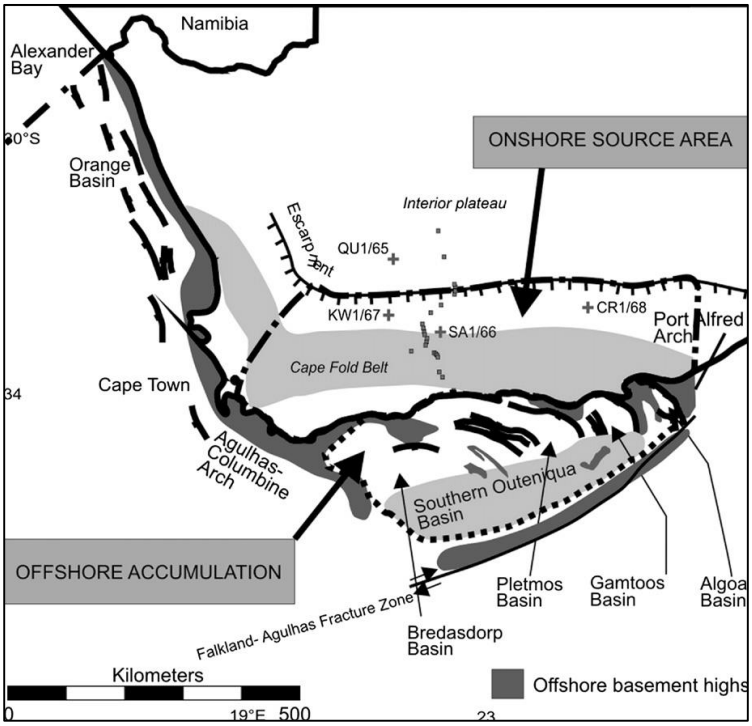

Figure 3.14 *– Outeniqua Basin location and contributing source areas (dot-dash line). The dark grey fill shows basement highs. The location of Tinker et al. (2008a) AFTT samples is also shown (squares, showing outcrop samples and crosses, showing borehole samples) (Tinker et al., 2008b).*

3.3.4 Age of the landscape

There is much debate in the literature about the age of the formation of the present day topography within South Africa, with researchers arguing for both a Cretaceous and Cenozoic age. The majority of researchers argue that large-scale exhumation and topographic formation had finished by the end of the Cretaceous on the basis of AFTT (Gilchrist et al., 1994; Gallagher and Brown, 1999; Cockburn et al., 2000; Brown et al., 2002; Tinker et al., 2008a; Kounov et al., 2009; Flowers and Schoene, 2010),

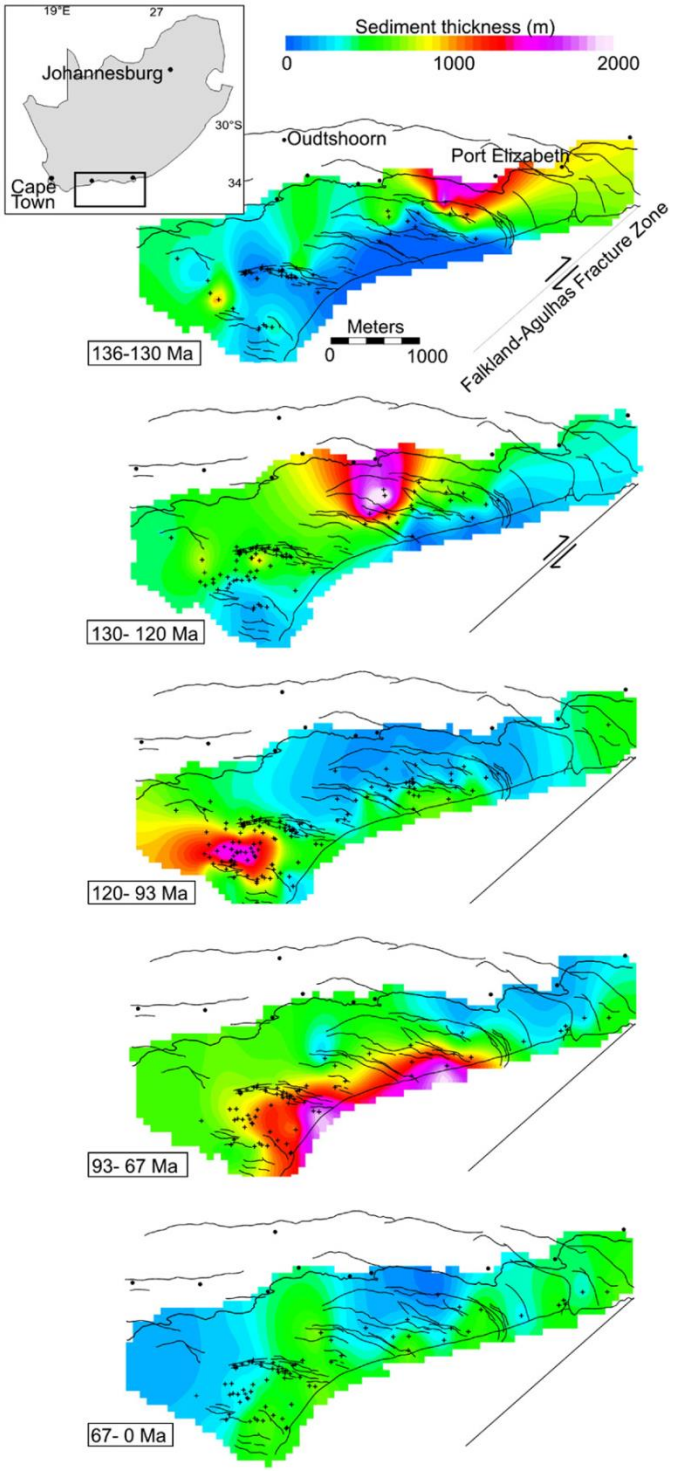

Figure 3.15 *– Sediment thickness time slices (Tinker et al. 2008b).The data shows pulses of increased sedimentation in the Cretaceous from the Port Elizabeth area in the Early Cretaceous to offshore in the Late Cretaceous, accumulation rates are low during the Cenozoic.*

forming the present day topography, which has changed little since (Partridge, 1998; Brown et al., 2000; Brown et al., 2002; Doucouré and de Wit 2003; de Wit, 2007; Tinker et al., 2008a; Kounuv et al., 2015).

Additional evidence is shown by a reduction in offshore sediment volumes (Tinker et al., 2008 b; Hirsch et al., 2010; Dalton et al., 2015; Sonibare et al., 2015), low Cenozoic cosmogenic erosion rates (e.g., Fleming et al., 1999; Cockburn et al., 2000; Bierman and Caffee, 2001; van der Wateran and Dunai, 2001; Kounov et al., 2007; Codilean et al., 2008; Dirks et al., 2010; Decker et al., 2011; Erlanger et al., 2012; Chadwick et al., 2013; Decker et al., 2013; Scharf et al., 2013; Bierman et al., 2014; Kounov et al., 2015; Table 3.1, Figure 3.14) and differential erosion of kimberlite pipes (Hawthorne, 1975; Gilchrist et al., 1994; de Wit, 1999). Although, offshore sedimentation in the Cenozoic is locally significant, large-scale deposition is not seen to the scale of the Mesozoic deposits (e.g., Tinker et al., 2008b; Hirsch et al., 2010; Dalton et al., 2015; Sonibare et al., 2015).

Large-scale exhumation and topographic formation being a primarily Cretaceous process has been disputed by Burke (1996) and Green et al. (2016). Burke (1996) considered that the topography and Great Escarpment was formed due to uplift at 30 Ma, related to the African plate coming to rest with relation to the underlying mantle. Burke (1996) also argued that Cretaceous South Africa was covered in marine sediments, but the crater facies of kimberlite pipes indicate lacustrine conditions based on fossil evidence (Hawthorne, 1975; Smith 1986). In contrast, Green et al. (2016) proposed a younger age of landscape development based on AFTT data arguing that the bedrock gorges within the Cape Fold Belt were formed during the Cenozoic, when there was differential denudation with higher erosion within the Swartberg Mountain range (CFB) as shown by Cenozoic cooling (30-20 Ma). Green et al. (2016) also suggested that the escarpment is not related to continental break-up but Cenozoic erosion.

3.5 Study Area

The study area of this research covers the Western Cape (Figure 3.16) however, there is a specific emphasis on the Gouritz catchment (Figure 3.17). The Gouritz catchment comprises six main trunk rivers; Traka, Touws, Buffels, Olifants, Dwyka and Gamka rivers, which are often ephemeral south of the Cape Fold Belt (Figure 3.17). The source regions for many of the main tributaries are hillslopes to the south of the Great Escarpment, with the Gouritz system reaching the Atlantic and Indian oceans at Gouritzmond (Figure 3.17). The majority of the rivers are bedrock or mixed bedrock-alluvial in nature, with common steep-sided valleys and bedrock-confined

gorges (Figure 3.18). Unfortunately there is no river gauging record showing bedload data available, but boulder to sand grade material is found in many bedrock reaches. The substrate of the catchment is Cape and Karoo Supergroups (Section 3.1).

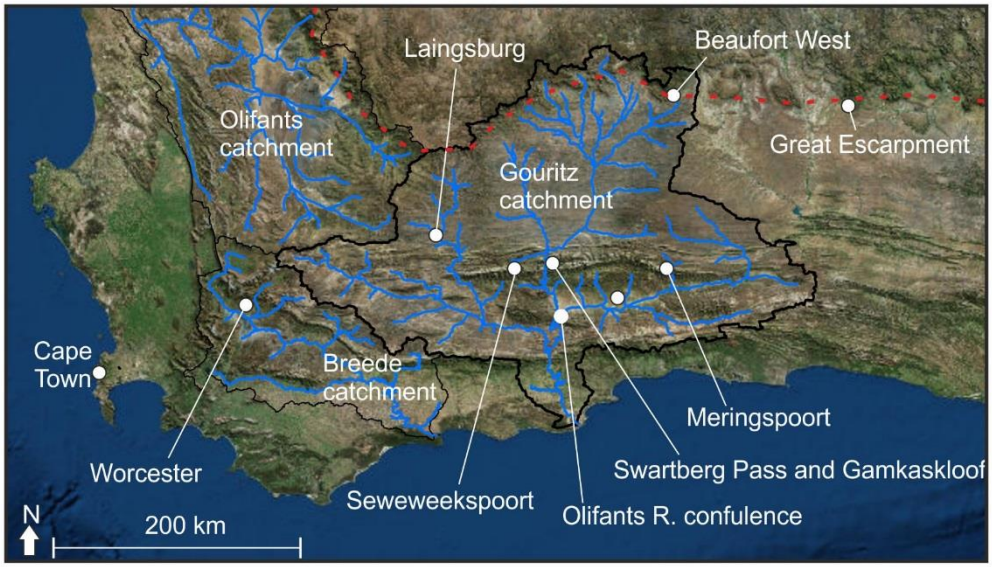

Figure 3.16 – Main drainages of the Western Cape and location of the Great Escarpment. The photo locations of Figure 3.18 are shown; the Olifants R. confluence, Seweweekspoort, Swartberg Pass, Gamkaskloof and Meringspoort.

3.5.1 Relevant literature

The Gouritz catchment is often overlooked in the literature (Rogers, 1903; Davis, 1906). Previous drainage reconstructions have argued that the Cape Fold Belt acted as a sediment conduit towards the east (Lock et al., 1975) or that the planform of the catchment has remained remarkably similar to the current planform since the Cretaceous, with extension of the upper catchment as the Great Escarpment retreated (Figure 3.19; Partridge and Maud, 1987).

The Gouritz catchment drainage pattern is rather peculiar, because meandering rivers transect the structural grain of the Western Cape (Figure 3.20). The main debate within the Gouritz catchment, therefore, relates to the planform and the formation of gorges or ‘poorts’ within the Cape Fold Belt. Previous workers have correlated gravel surfaces and discussed the Uitenhage Group, but the correlation has not been constrained using modern techniques.

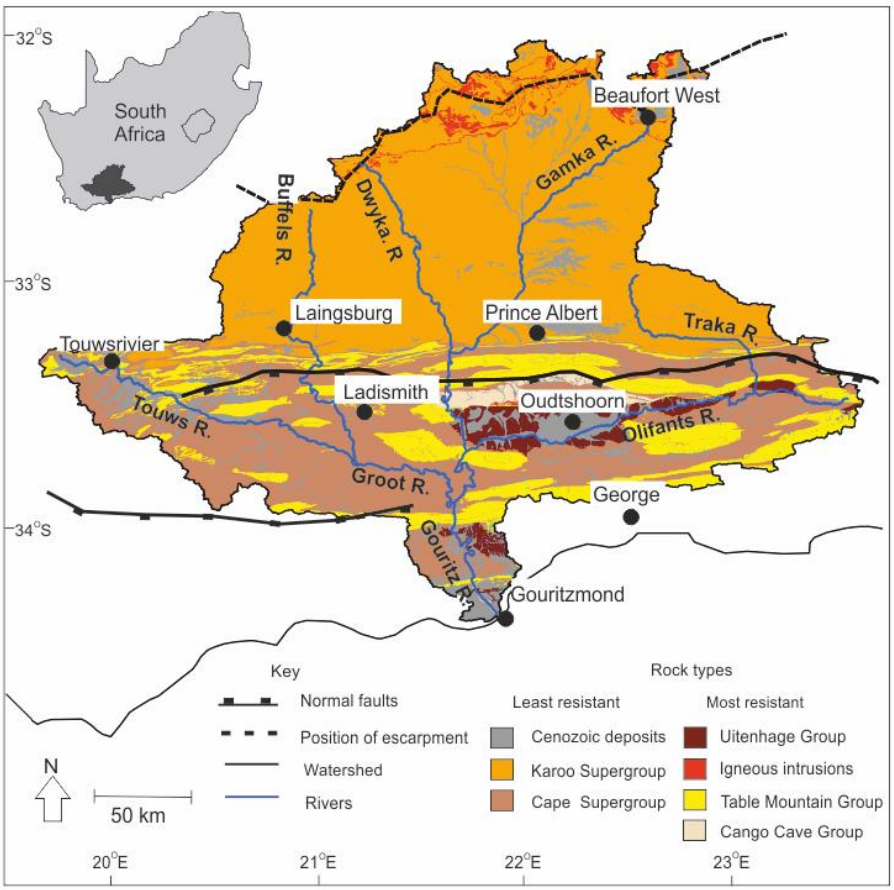

Figure 3.17 – Gouritz catchment, showing the main tributaries. The large scale faults are also highlighted and a simplified geology map.

Formation has been related to antecedence, superimposition and headward erosion (e.g., Rogers, 1903; Davis, 1906; Du Toit, 1954; Taljaard 1948, 1949; King, 1951; Maske, 1957). Both Rogers (1903) and King (1951) argued that the Gouritz system was superimposed on the underlying Cape Fold Belt by the Late Cretaceous to Early Cenozoic, after incising through the Uitenhage Group lithologies, which provided a low gradient plain. Du Toit (1954) argued that the E-W systems routed through the Cape Fold Belt, were redirected through N-S synclines due to synclinal warping forming the present day pattern after superimposition. Davis (1906 a, b) favoured headward erosion, with the rivers that breach the Cape Fold Belt possibly related to antecedence, of which he argued there is no field evidence. Davis (1906a, b) argued the present day drainage could have formed post-Cretaceous and possibly in the mid-Cenozoic, due to cyclic erosion. Taljaard (1948, 1949) also favoured headward erosion along master joints, with the Touws and Gamka rivers argued to have formed in the late-Cretaceous and the Seweweekspoort to have been mid- to late-Cenozoic in age.

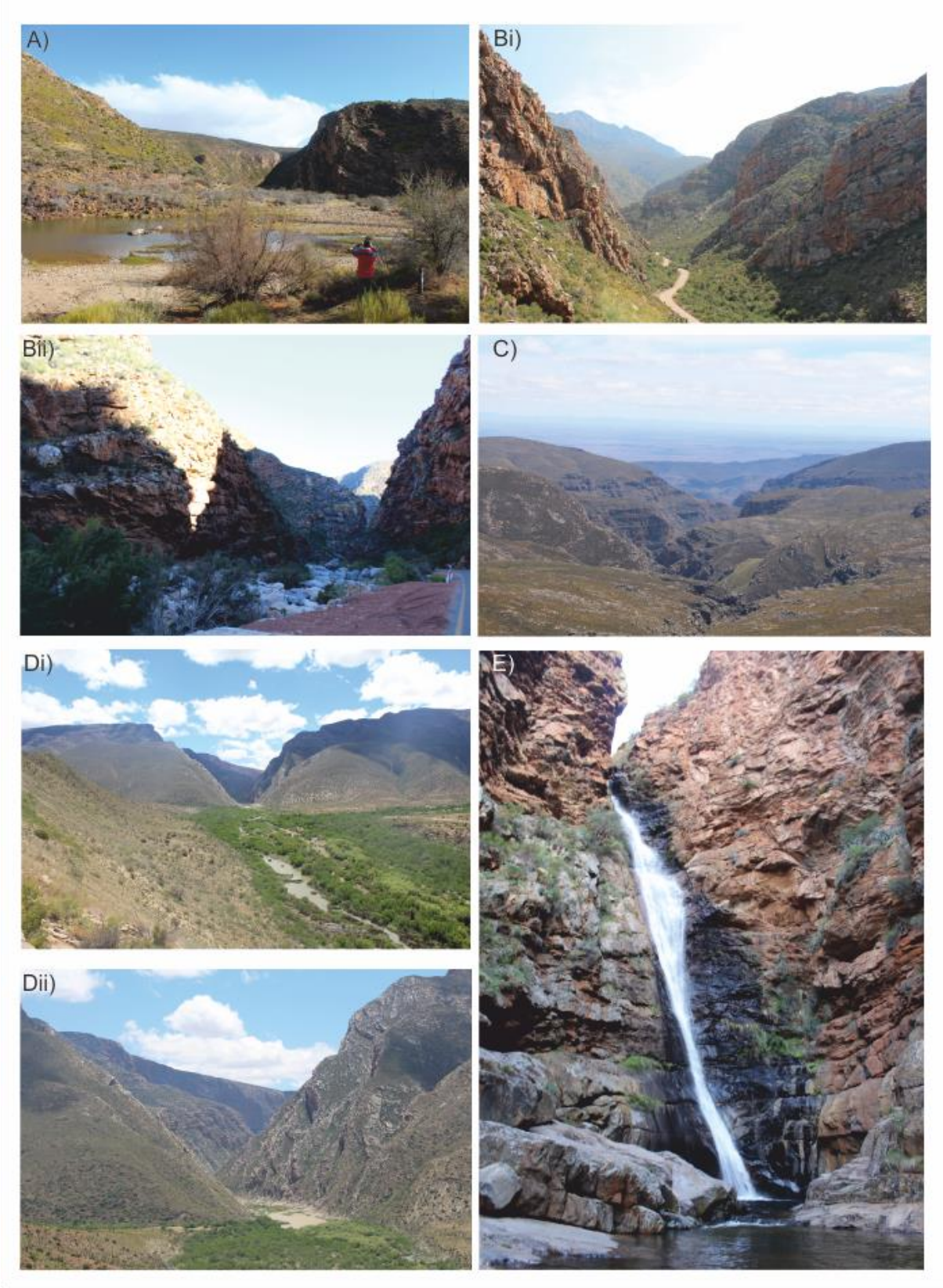

Figure 3.18 – Bedrock confined gorges within the Gouritz catchment; A) River Olifants, near the confluence with the River Gamka; B) Seweweekspoort; C) Swartberg Pass; D) Gamkaskloof – River Gamka; E) Meringspoort; see Figure 3.16 for photo locations.

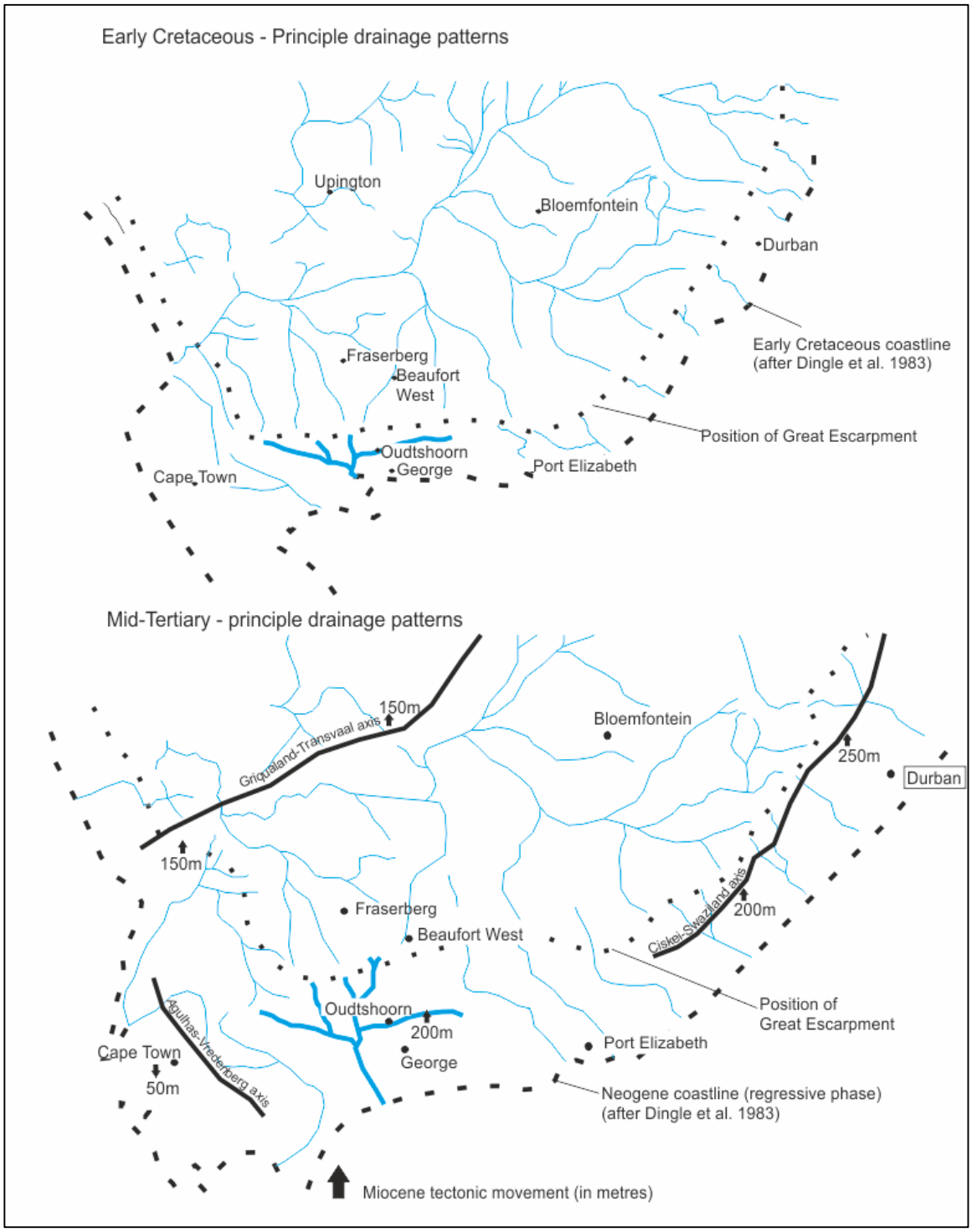

Figure 3.19 *– Early Cretaceous and mid-Tertiary drainage patterns (Partridge and Maud, 1987). The Gouritz catchment is shown in bold.*

Lenz (1957) correlated multiple erosion surfaces, and argued for erosion along joint sets like Taljaard (1948, 1949) and Davis (1906 a, b) with the Gouritz River breaching the Cape Fold Belt in the Cretaceous, and the Gamka River in the Eocene-Oligocene. Maske (1957) also favoured headward erosion, stating the relative age of the Cape Fold Belt Orogeny (Permo-Triassic) and the age of the Uitenhage deposits (Late

Cretaceous) refutes the antecedence theory. Maske (1957) argued that the main Cretaceous drainage was E-W and structurally controlled, with the N-S systems becoming dominant due to headward erosion associated with the break-up of Gondwana, which caused N-S warping within the Cape Fold Belt.

On the basis of AFTT, Tinker et al. (2008a) showed the Cape Fold Belt was exhumed, and that the superimposition of the meanders (antecedence) was possible, and points to the river canyons to be late-Cretaceous in age. However, recent work by Green et al. (2016) argued that two canyons in the Cape Fold Belt (Seweweekspoort and Meringspoort, Figure 3.16) are Cenozoic in age, when differential uplift occurred within the Swartberg mountain range (Figure 3.20).

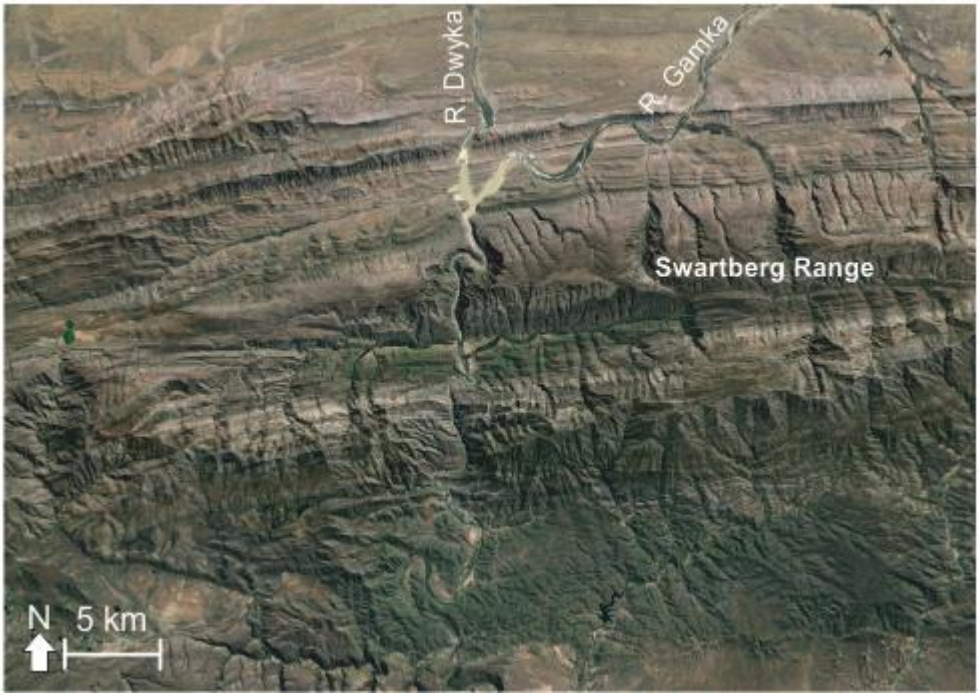

Figure 3.20 *– Incised meanders and transverse drainage of the Gouritz catchment.*

3.6 Summary

The geologic and geomorphic history of southern Africa remains contentious with the causes of uplift, timing of uplift and landscape development disputed. Classical models such as King's (1953, 1962, 1963) are being reassessed using modern techniques such as geochronology, numerical modelling and advancements in geophysical interpretations. There is a general consensus of large-scale exhumation forming the topography of southern Africa during the Cretaceous, with a subsequent reduction in erosion rates and corresponding offshore sedimentation accumulation rates since then. Nonetheless, drainage systems south of the Great Escarpment are often overlooked, with much of the research in the Gouritz catchment related to the

formation of poorts, the mechanisms of which remains contentious. The drainage evolution of the catchment has not been assessed in detail.

Chapter 4 Methodology

Analysis of the evolution of ancient landscapes rarely accesses recent geomorphological concepts and techniques. This chapter offers additional methodological information of techniques employed in this research that was beyond the scope of the accompanying submitted and published manuscripts.

4.1 Morphometric Indices

Morphometry is defined as '*measurement and mathematical analysis of the configuration of the Earth's surface and the shape and dimensions of its landforms*' (Clarke, 1966) and has been used by geomorphologists since the 1940's to characterise drainage basins and to extract information on catchment evolution (e.g., Horton, 1932; Miller, 1953; Schumm, 1956; Chorley, 1957; Strahler, 1964). Morphometric analysis has had a recent revival in physiographic research because of the increased availability of high-resolution topographic data (e.g., from satellite sensors such as Shuttle Radar Topography Mission [SRTM], Advanced Spaceborne Thermal Emission and Reflection Radiometer [ASTER] etc.), which can be processed in ArcGIS (e.g., Walcott and Summerfield, 2008; Antón et al., 2014). Morphometry is often used to elucidate the influence of climate change or tectonic activity on landscapes (e.g., Montgomery et al., 2001; Walcott and Summerfield, 2008; Antón et al., 2014), but also has wider implications for soil loss (e.g., Hlaing et al., 2008); landslide susceptibility (e.g., Leoni et al., 2012), and catchment management (e.g., Mitchell and McDonald, 1995).

4.1.1 Linear and areal properties

Horton (1945) quantified the hierarchal arrangement and density of drainage networks and reported linear measurements such as stream number, stream length and bifurcation ratio, and areal measurements such as basin area, drainage density and stream frequency. Horton's Laws are as follows: 1) the number of streams of different orders tend to follow an inverse geometric sequence; 2) the average lengths of streams increase as order number increases and; 3) there is a geometric decrease in channel slope with increasing stream order.

4.1.2 Long profiles and stream length gradient

Long profiles allow insight into fluvial incision within the catchment but can also indicate the geomorphic history of the catchment area as well as lithological controls (Hack, 1973). The analysis of long profiles can highlight knickpoints within the system. Knickpoints represent '*relatively steep sections of channel separating reaches of lower gradient, irrespective of whether produced by tectonic deformation, base level*

fall, or variable rock resistance' (Jansen, 2006; pg.44) and are the principal method of channel lowering within bedrock channels (Whipple, 2004).

In order to quantify the geometry of the long profiles, the stream gradient index was extracted (50-m reaches). The stream gradient index (SL) developed by Hack (1973) assess the level of grading within a river and is calculated by the following equation.

$$SL = (\Delta H/\Delta Lr)\Delta Lsc \qquad \text{Eq. 4.1}$$

Where ***ΔH*** is change in altitude, ***ΔLr*** is length of the reach and ***ΔLsc*** is the horizontal length from the watershed divide to the midpoint of the reach.

The stream length gradient is approximately constant within a graded long profile within a homogenous lithology, with deviations from the average caused by forcing factors such as tectonics (Keller and Pinter, 2002), lithology (Hack, 1973) or migrating knickpoints (Bishop et al., 2005).

4.1.3 Hypsometry

Hypsometry is the study of the area of land surface per elevational band/bin/range. The use of hypsometry was first introduced by Strahler (1952) who argued that the hypsometric integral (H.I.) can be used to assess the 'age' of the landscape with regards to Davis' landscape concepts (1889, 1899). Strahler (1952) argued that hypsometric integrals > 0.6 characterise catchments that are in dis-equilibrium, with catchments with hypsometric integrals between 0.4 and 0.6 being in equilibrium. More recently, hypsometry has been used for a wide range of investigations including landscape evolution (Hancock and Willgoose, 2001), effect on precipitation and runoff (Montgomery et al., 2001), and inferring tectonic evolution of catchments (Ohmori, 1993). The influence of basin properties on the hypsometric integral has received mixed results, with researchers arguing for both correlation (Hurtrez et al., 1999; Chen et al., 2003) and no correlation (Walcott and Summerfield, 2008). The hypsometric curve (Figure 4.1) has been used to give '*an insight into the key geomorphic processes dominating a region'* (Lowman and Barros, 2014 pg.1326). Strahler (1952) maintained that catchments try to maintain a convex or sinusoidal curve, with erosion of the transitory concave "monadnock" phase returning the curve to a sinusoidal curve (Figure 4.1).

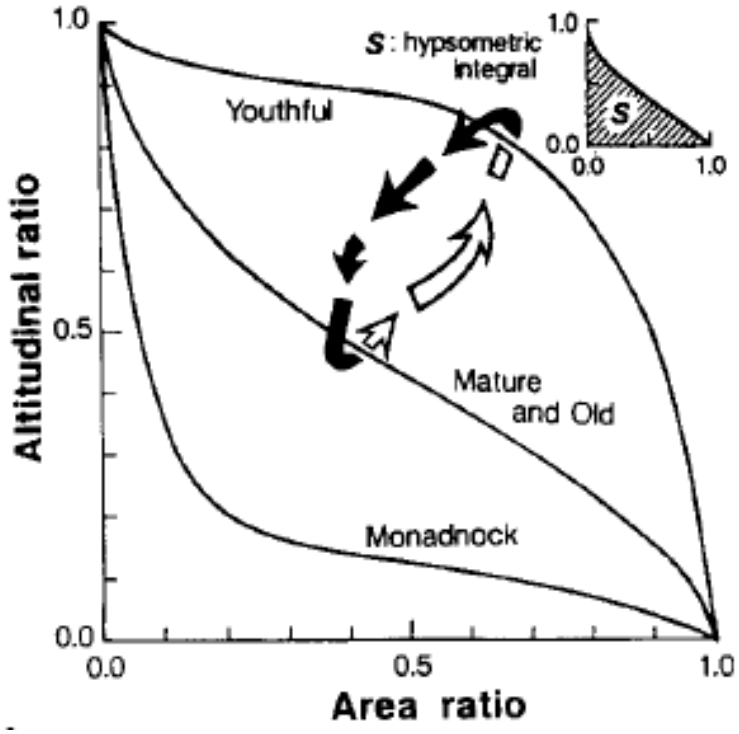

***Figure 4.1** – Hypsometric curves for different landscape 'ages' (Ohmori, 1993).*

4.2 ArcGIS

ASTER is one of five remote sensing devices on board the Terra satellite, which collects high-resolution images of the Earth over the electromagnetic spectrum in 14 bands (ranging from visible to thermal infrared light; Hirano et al. 2003). Stereo-images are then processed and used to create a digital elevation models (DEM) using the principals of photogrammetry (Jacobsen and Lohmann, 2003; Cuartero et al., 2004). The purpose of ASTER data is to investigate the interactions of the geosphere, hydrosphere, cryosphere and atmosphere (Yamaguchi et al., 1993; Yamaguchi et al., 1998).

For this research, the ASTER 30 m resolution DEM of South Africa was downloaded from the NASA reverb and processed in ESRI's ArcGIS 10.1. Geology polygons of South Africa including structural information were supplied by the Council of Geoscience, South Africa under the Academic Research License for use in this study.

4.2.1 Catchment delineation

The DEM was filled in order to remove sinks (and peaks) within the data; which are associated with the resolution of the data or rounding of elevations to the nearest integers. Sinks need to be filled in order to successfully delineate drainages. The filled DEM was processed using the hydrology toolbox, in order to constrain drainage patterns and delineate watersheds (Figure 4.2). In order to constrain drainage

patterns, a “con” value of 3000 was used (representing an upstream contributing area of 3.35 km^2), which shows both ephemeral and perennial rivers, which are a component of the Gouritz catchment (Chapter 8).

4.2.2 Morphometric indices

ArcGIS was used to extract morphometric indices for the Gouritz catchment, which were assessed on the catchment and sub-catchment scale (Chapter 8).

Linear and areal measurements: The data can be found within the attribute table e.g. area and stream length.

Slope: The slope of the sub-catchments was extracted using the ‘slope tool’ within ArcGIS.

Long profiles: The extracted drainage patterns were digitised, with data points added every 1 m along the stream lengths, heights were then assigned to the data points, and long profiles extracted. The data were extracted for the stream length gradient in 50 m reaches for the main trunk rivers, and normalised to allow comparison between the trunk-rivers.

Hypsometric integral and curve: The hypsometric integrals (Eq. 4.2) of the catchment and sub-catchments were extracted by downloading an ESRI ‘hypsometric tool’ add-on by Davis (2010). This allows the individual hypsometric integrals to be delineated and the curve data to be extracted. Hypsometric integrals were then compared to catchment properties such as circularity (the ratio of the perimeter of the basin with the perimeter of a circle with the same area), area, relief (Eq. 4.3) and dissection (Eq. 4.4). The DEM data points were extracted and processed in order to calculate relief and dissection, by extracting the maximum, minimum and mean height values.

$$H.I. = \frac{mean\ elevation - minimum\ elevation}{maximum\ elevation - minimum\ elevation} \quad \text{Eq.4.2}$$

$$Relief = maximum\ elevation - minimum\ elevation \quad \text{Eq.4.3}$$

$$Dissection = mean\ elevation - minimum\ elevation \quad \text{Eq.4.4}$$

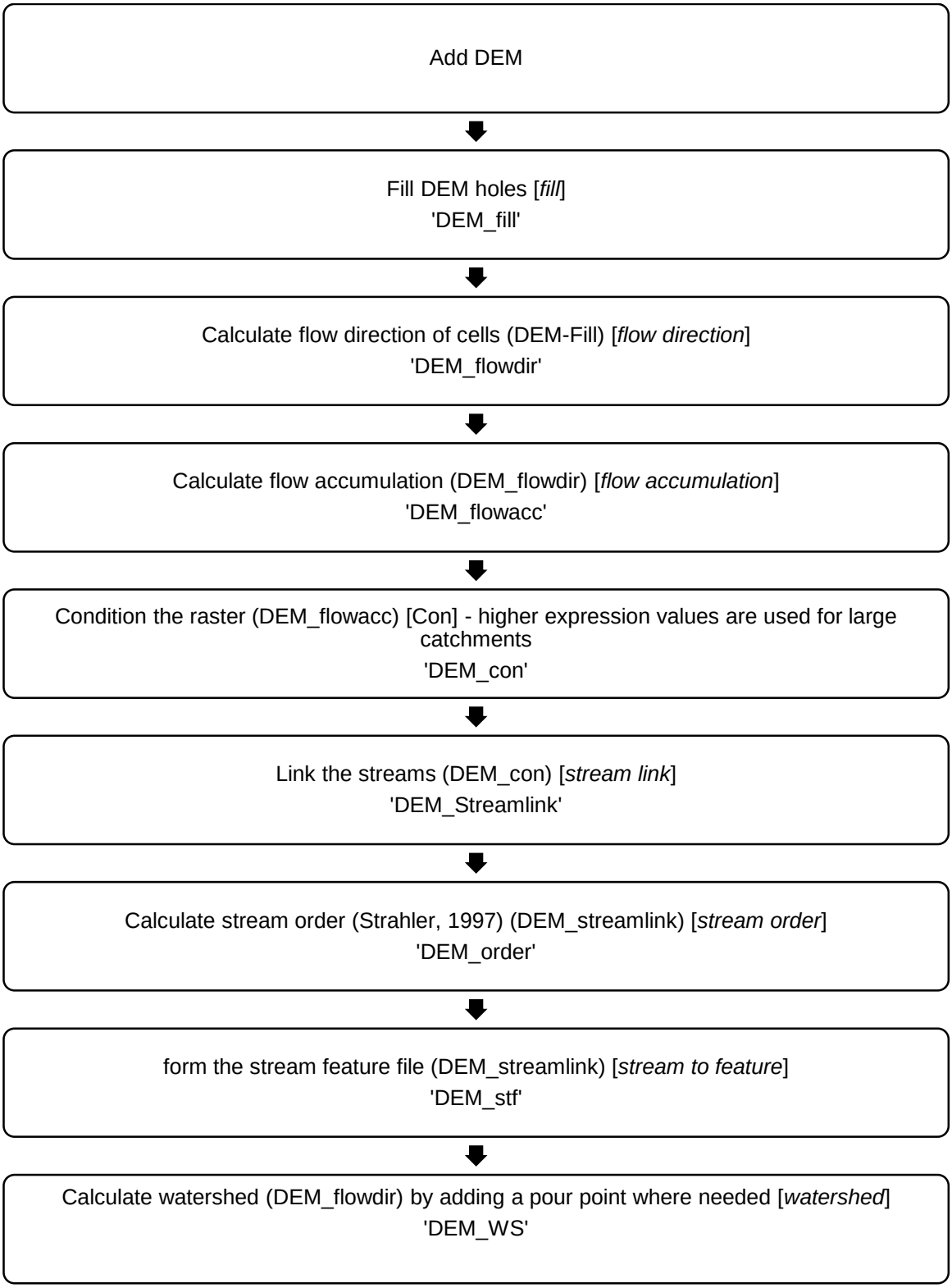

***Figure 4.2** – Hydrology toolbox method to extract catchments. Square brackets and italics are the tool function used*, parentheses *are the file used in the tool function, and quotation marks are the output raster or polygon file.*

Hypsometric curve geology: In order to constrain the influence of lithology on the hypsometric curves extracted, the geology at each normalised height was analysed. The individual lithological unit polygons were extracted from the geology tile, and the corresponding DEM cut; allowing the heights of the individual lithological units to be extracted. This data was then exported and processed (i.e., constraining to each normalised height unit group), and applied to the hypsometric curves (Figure 4.3).

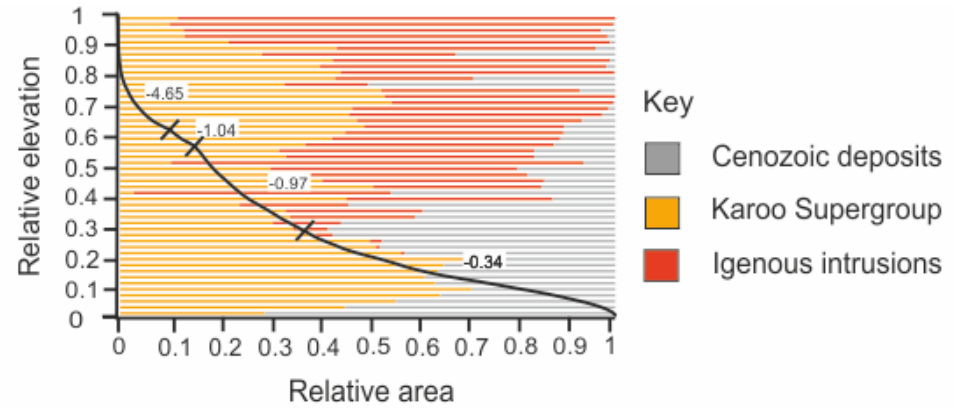

Figure 4.3 *– Example hypsometric curve with geology percentage at each height bin, the numbers in the white box relate to the gradient of sections of the hypsometric curve.*

4.2.3 Volume of material removed

The minimum eroded volume (Figure 4.4), was used to i) analyse how 'misfit' bedrock streams are (Figure 4.5; Chapter 5); ii) quantify the erosion of sub-catchments in the CFB (Chapter 7) and; iii) quantify the eroded volume around the pediment surfaces (Figure 4.6; Chapter 7). It is noted that the method used to extract the minimum eroded volume may represent an underestimation, as the watershed and interfluve areas would have been lowered due to erosion (Brocklehurst and Whipple, 2002; Bellin et al., 2014;).

i. Misfit streams are streams that are either too big or small to have eroded the current valley and are often associated with glacial regions (e.g., Clapperton, 1968). Misfit streams can be related to climate or tectonic change or due to stream capture (e.g., Dury, 1958; Stankiewicz and de Wit, 2006), and therefore offer important insights into landscape evolution. Misfit streams are often analysed using the ratio of meandering on the floodplain with underlying deposits (e.g., Dury, 1958, 1960). However in a bedrock setting, with low or no accommodation, this cannot occur. In order to assess how misfit a catchment is the minimum eroded volume was extracted and compared to the

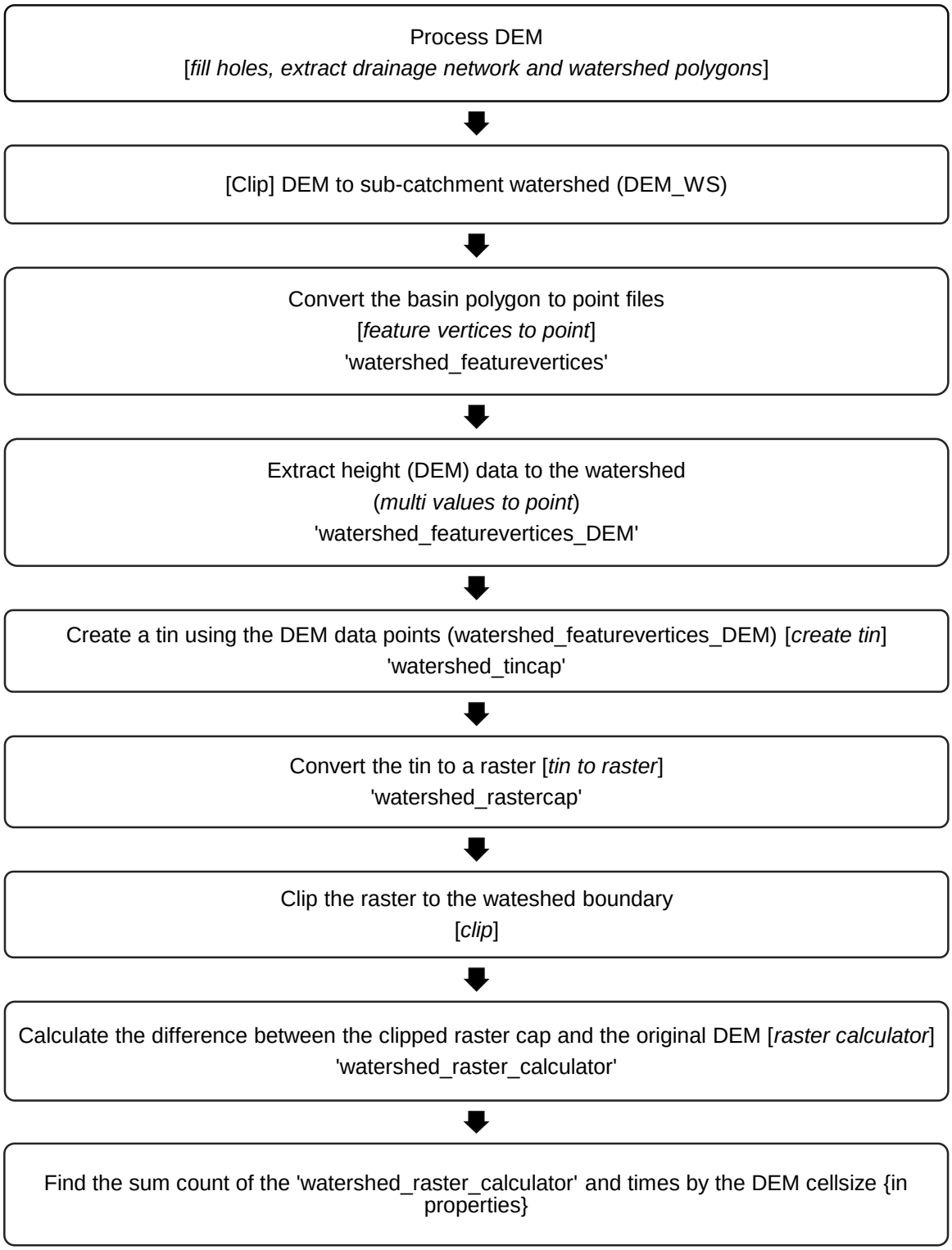

Figure 4.4 *- Minimum eroded volume method using ArcGIS. Square brackets and italics are the tool function used*, parentheses *are the file used in the tool function, curly brackets are where you can find the information, and quotation marks are the output raster or polygon file.*

catchment area. Bellin et al. (2014) showed a significant correlation between minimum eroded volume, and catchment area, which was then compared to cosmogenic erosion rates.Therefore, minimum eroded volumes are expected to correlate with area. If the area is too large or small for the extracted eroded volumes, the catchment may be misfit. In order to constrain the catchments within South Africa, data points (area, minimum eroded volume) for 10 catchments (Table 4.1) of various sizes from a range of tectonic and climatic settings were extracted using global ASTER DEM data using the same method as Figure 4.4.

ii. Sub-catchments of the CFB: Small catchments in the CFB have formed by headward erosion, dissecting the pediments analysed in Chapter 6. The sub-catchment volumes were extracted, converted into equivalent lithological thickness (Eq. 4.5) and compared to published cosmogenic data in order to constrain the length of time needed to form the catchment. This information was then used to constrain landscape evolution of the pediments within the Gouritz catchment.

$$Lithological\ thickness\ (Km) = \frac{Volume\ of\ material\ (Km^3)}{Cross\ sectional\ area\ (Km^2)} \qquad \text{Eq.4.5}$$

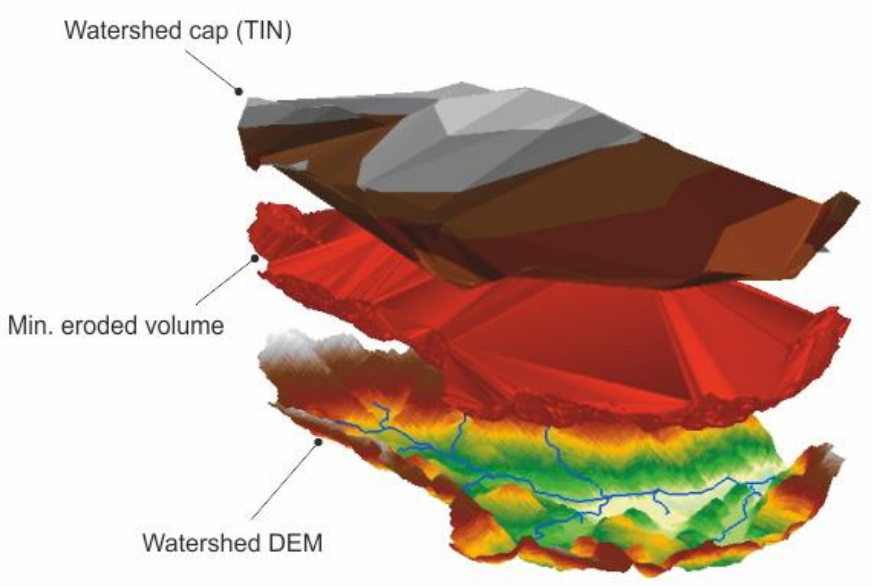

Figure 4.5 *– Minimum eroded volume example, whereby the current watershed is used to cap the drainage basin and the volume of material eroded extracted.*

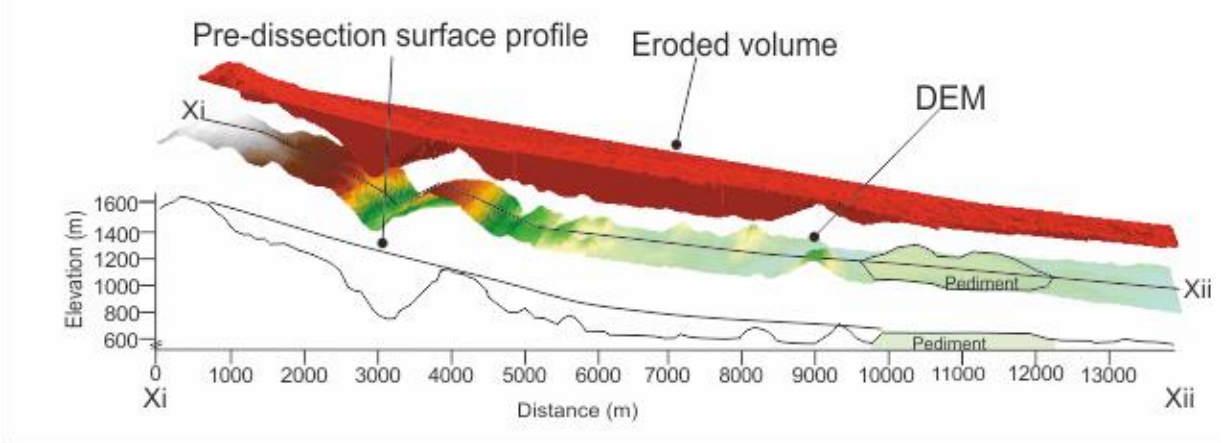

Figure 4.6 *– Example of eroded volume removed around a pediment surface, the volume of material removed is calculated using the DEM and the pre-dissection profile.*

iii. Post-pediment formation dissection: Quantification of pediment dissection has not occurred within the literature, with basic morphometric and areal measurements reported (e.g. slope, area; Tator 1952; Cooke, 1970; Cooke and Mason 1973, pg. 193, Thomas 1974; Bierman et al., 2014; Kounov et al., 2015). The pediments of the Gouritz catchment are deeply dissected; ArcGIS was used to reconstruct the palaeosurface of the individual pediments (Figure 4.6). The volume between the reconstructed surface and current DEM was then extracted (Figure 4.7), and converted into lithological thickness (Eq. 4.5), and compared to published cosmogenic data. This was used to constrain the development time-frame of the pediments with regards to the calculated cosmogenic data, in order to estimate the time taken for the post-pediment formation dissection.

***Table 4.1** – Global data to compare how misfit the streams in South Africa are.*

Location	Latitude	Longitude	Area (km^2)	Erosion rate (mMa^{-1})	Reference
Namibian desert and escarpment	-21.304	16.217	1090.92	8.63	Bierman et al. 2007
Queensland Escarpment, Australia	-16.852	145.648	1991.83	17.19	Bierman et al. 2009
Stanley, Virginia, US	38.532	-78.603	3305.63	6.59	Duxbury 2008
Tin Can Creek, Australia	-12.453	133.270	387.33	10.09	Heimsath et al. 2009
Peradeniya, Sri Lanka	7.261	80.595	1071.80	15.09	Hewawasam et al. 2003
Nahal Yael, Isreal	29.580	34.930	0.46	34.28	Clapp et al. 2000
Bredbo River, Australia	-36.000	149.500	135.82	31.41	Heimsath et al. 2006
Rio Azero, Bolvia	-19.610	-64.080	3929.84	107.68	Insel et al. 2010
Little River, Tennessee US	35.664	-83.592	100.43	35.88	Matmon et al. 2003
Northern Flinders Range, Australia	-30.187	139.428	79.09	37.57	Quigley et al. 2007b

4.3 Midland Valley 3D MOVE

Midland valleys 3D MOVE is a structural geology programme that is often used to reconstruct the tectonic evolution of systems e.g., the amount of shortening associated with a fold (e.g., Borraccinni et al., 2002; Tanner et al., 2003; Spikings et al., 2015). In this study MOVE was used in order to constrain the volume of material removed in the Western Cape during the Cretaceous (Chapter 5).

Cross sections: 9 cross sections were constructed using published geological maps of South Africa. The cross sections were digitised and imported into 3D MOVE (Figure 4.8). Several assumptions were utilised when constructing the cross sections (Chapter 5).

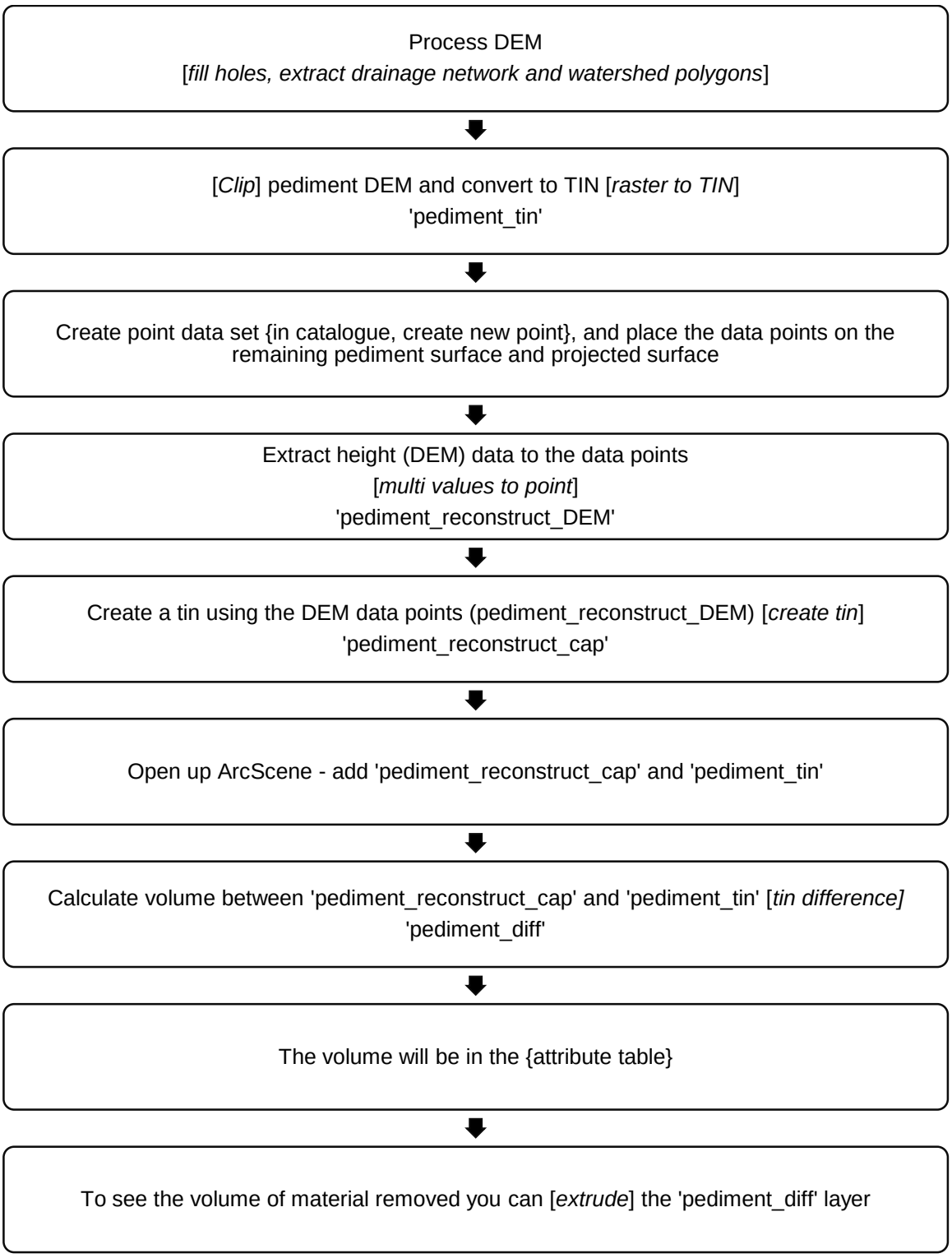

Figure 4.7 *– Pediment reconstruction volume extraction method using ArcGIS and ArcScene. Square brackets and italics are the tool function used, parentheses are the file used in the tool function, curly brackets are where you can find the information, and quotation marks are the output raster or polygon file.*

3D Move: The ASTER DEM of South Africa was imported into MOVE, and represents the lowest boundary condition for volume extraction. In the oceanic area, the average

height of South Africa was used to 'complete' the horizon level. The cross sections were digitised within MOVE and tied together at cross section intersections with additional structural data, in order to create a full horizon level.

The upper horizons represent the digitised top of the cross sections (e.g. Drakensberg, Stormberg etc). The difference between the upper and lower horizons represent the volume of material removed (extracted using the geo-cellular volume function). Only large-scale faults (e.g. Worcester fault) were digitised, and tied between the corresponding cross sections (Figure 4.8).

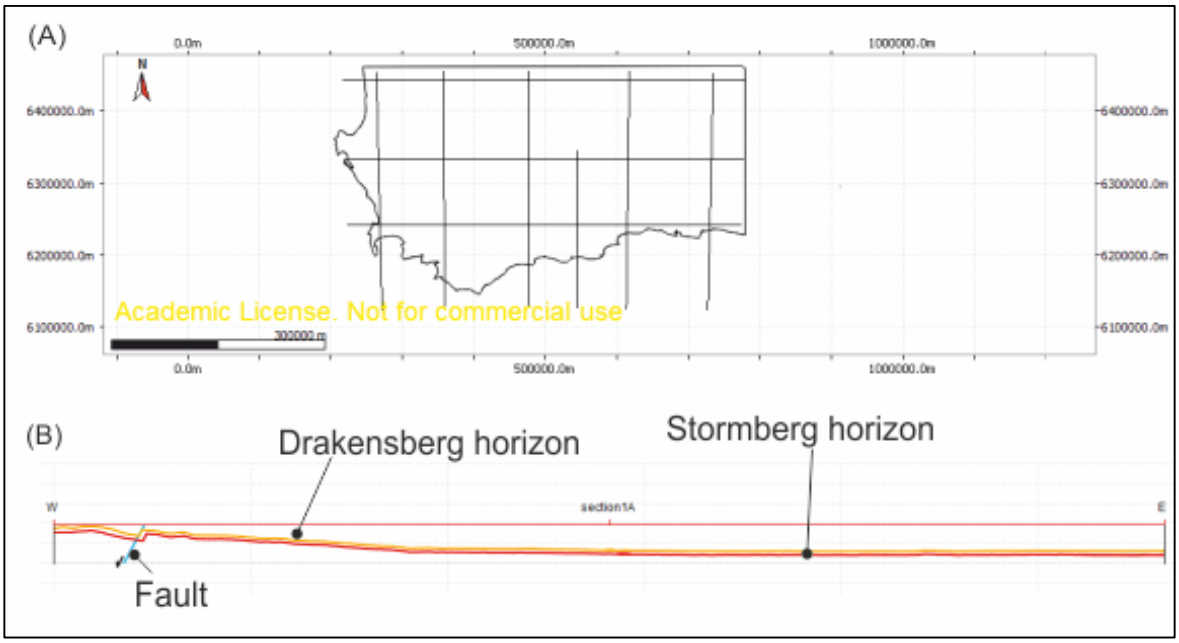

Figure 4.8 *– A) location of cross sections in MOVE (for more detail see Chapter 4) and; B) example of a digitised cross section.*

Data extraction: The horizons (e.g. Drakensberg) were converted into a surface using the ordinary kringing method (in which the horizons can be manipulated to follow certain structural trends), and the geo-cellular volume was extracted between the top lithological surface and the lower DEM surface. The geo-cellular volume was converted into lithological thickness by dividing the study area (~140 000 km^2). The extracted volume was cut to the current DEM surface, as well as constraining the volume removed to the western draining catchments; the different scenarios reported constrain the level of error associated with the method.

4.4 Dating: Cosmogenics

This project is concerned only with application of the cosmogenic method to an ancient catchment and not to methodology improvements and validation. Therefore only a brief background to cosmogenic dating and the associated methods are reported. Further information and a more in-depth review can be found in Gosse and

Phillips (2001); Cockburn and Summerfield (2004); Ivy-Ochs and Kober (2008); Dunai (2010) and; Granger et al. (2013).

Geochronology allows the quantification of rates erosion and ages of landforms (Darville, 2013). Cosmogenic analysis is effective over 10^2 - 10^5 year time frames, and bridges the gap between longer term apatite fission track studies and recent geomorphological records such as sediment trapping and gauging (e.g, Binnie et al., 2006; Palumbo et al., 2009). Terrestrial cosmogenic nuclide (TCN) dating, relies on the predictable decay of rare isotopes (Dunai, 2001). Common isotopes used are ^{10}Be, ^{26}Al, ^{36}Cl, ^{14}C, ^{3}He and ^{21}Ne, which are produced in common mineral lattices such as quartz (Dunai, 2001). TCNs have been widely utilised in landscape development studies due to the range of geomorphic units that can be studied e.g., alluvial river terraces (e.g., Phillips et al., 1997; Repka et al., 1997; Schaller et al., 2002; Bookhagen et al., 2006), bedrock terraces of rivers and shorelines (e.g., Leland et al. 1998; Alvarez-Marrón et al., 2008; Kong et al., 2011), glacial moraines (e.g., Philips et al., 1990; Brook et al., 1993; Kaplan et al., 2004; Owen et al., 2005), catchment average denudation rates (e.g., Binnie et al., 2006; Vanacker et al., 2007; Bellin et al., 2014). For a wider list of published cosmogenic studies please refer to Daville et al. (2013).

TCNs form due to the interaction of cosmic rays produced in supernova events with the upper meters of the Earth's surface (Dunai, 2010). The cosmic rays consist largely of protons (87%) and alpha-particles (12%). As the cosmic rays enter the Earth's atmosphere, a nuclear cascade forms where the primary rays are converted into secondary rays (Figure 4.9), forming nucleonic and mesonic components that are responsible for the production of TCNs within mineral lattices such as quartz. The nucleonic and mesonic components interact with the lattice of the minerals by processes such as spallation and muonic reactions (Dunai, 2010). The concentration of TCNs can be used to calculate erosion rate or exposure ages, as the half-life of the nuclides is known.

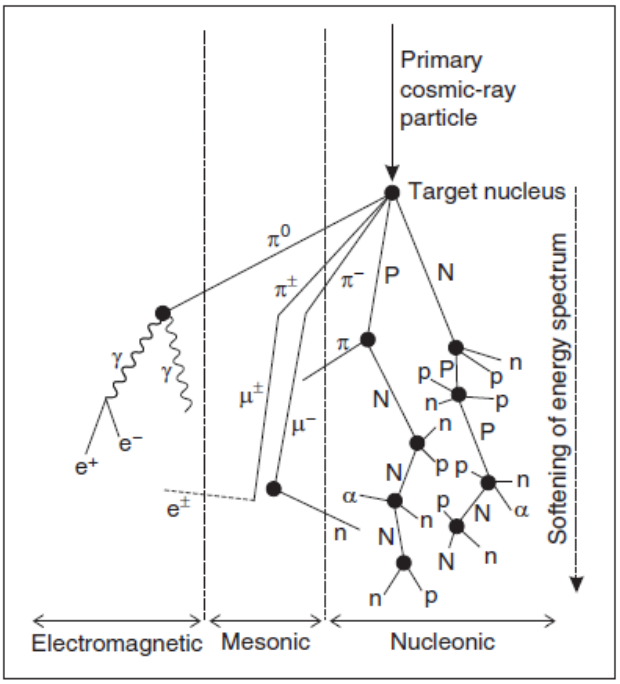

Figure 4.9 *– Nuclear cascade of cosmic rays. Abbreviations used: n, neutron, p, proton (capital letters for particles carrying the nuclear cascade), a, alpha particle, $e^{\pm}$, electron or positron, γ, gamma-ray photon, p, pion, m, muon (Dunai, 2001).*

4.4.1 Sampling

Samples for cosmogenic analysis were collected from pediment surfaces (Figure 4.10), the pediment colluvial material (depth sample; Figure 4.11), strath terraces (Figure 4.12) and river channels (Figure 4.13) within the Gouritz catchment (Figure 4.14). The samples were collected to ascertain the rates of erosion and age of formation of surfaces. Quarzitic boulder samples were collected from the top of the boulders using a lump hammer (Figure 4.10), whereas river sediment (gravel size and below) was collected from channel bars (Figure 4.13). Additional photos of samples can be found in Chapters 6 and 7. The strath terrace samples were dated, however produced anomalous values and therefore, the catchment average denudation was compared against terrace height in Chapter 6.

Figure 4.10 *– Example sample of a quarzitic boulder used for cosmogenic analysis on a pediment surfaces.*

Figure 4.11 *– Depth profile location, Laingsburg.*

Figure 4.12 *– Example strath terrace sampling site, Seweweekspoort.*

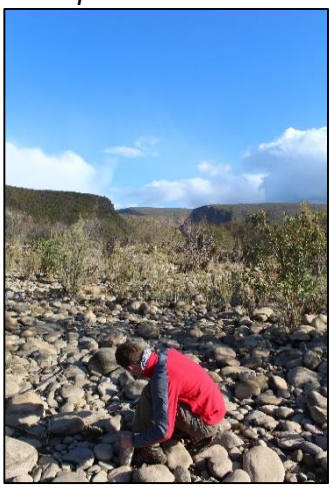

Figure 4.13 *– Example river sediment sampling; A) study site - Touws River and; B) sampling of the Olifants River*.

4.4.2 Methods in laboratory

The boulder samples were crushed using a mechanical crusher and sieved. The river sediment samples were sieved. In both cases the 250 to 500 µm grain fraction was processed under the supervision of Dr. Veerle Vanacker (e.g., Vanacker et al., 2007) at the *Université catholique de Louvain, Belgium* following the protocols shown in Figure 4.15.

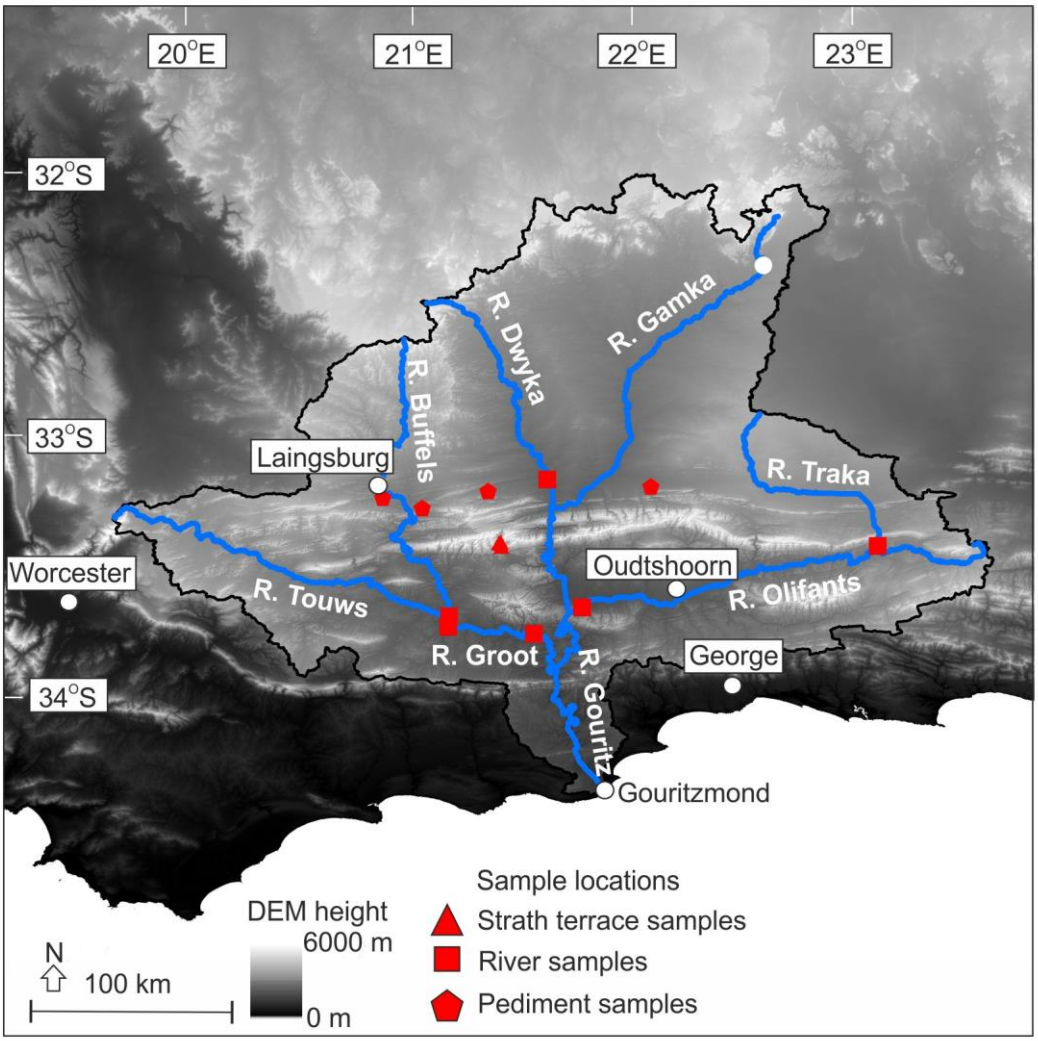

Figure 4.14 *– Sample locations within the Gouritz catchment, squares represent river samples, circles pediment samples and triangles bedrock strath samples. Samples were collected from the Gamka and Gouritz Rivers, however they were very 'dirty' and did not have enough of the 250 to 500 µm grain size fraction required in this study.*

Once the Beryllium was extracted (Figures 4.16, 4.17, 4.18), the targets (Figure 4.19) were sent to ETH Zurich (*Kubik and Christl, 2010*) where mass-spectronomy was used to ascertain the ratio between ^{10}Be and ^{9}Be isotopes (the data was normalised to the in house S2007N standard). As the samples were spiked with a known ^{9}Be concentration, the ^{10}Be concentration can be calculated.

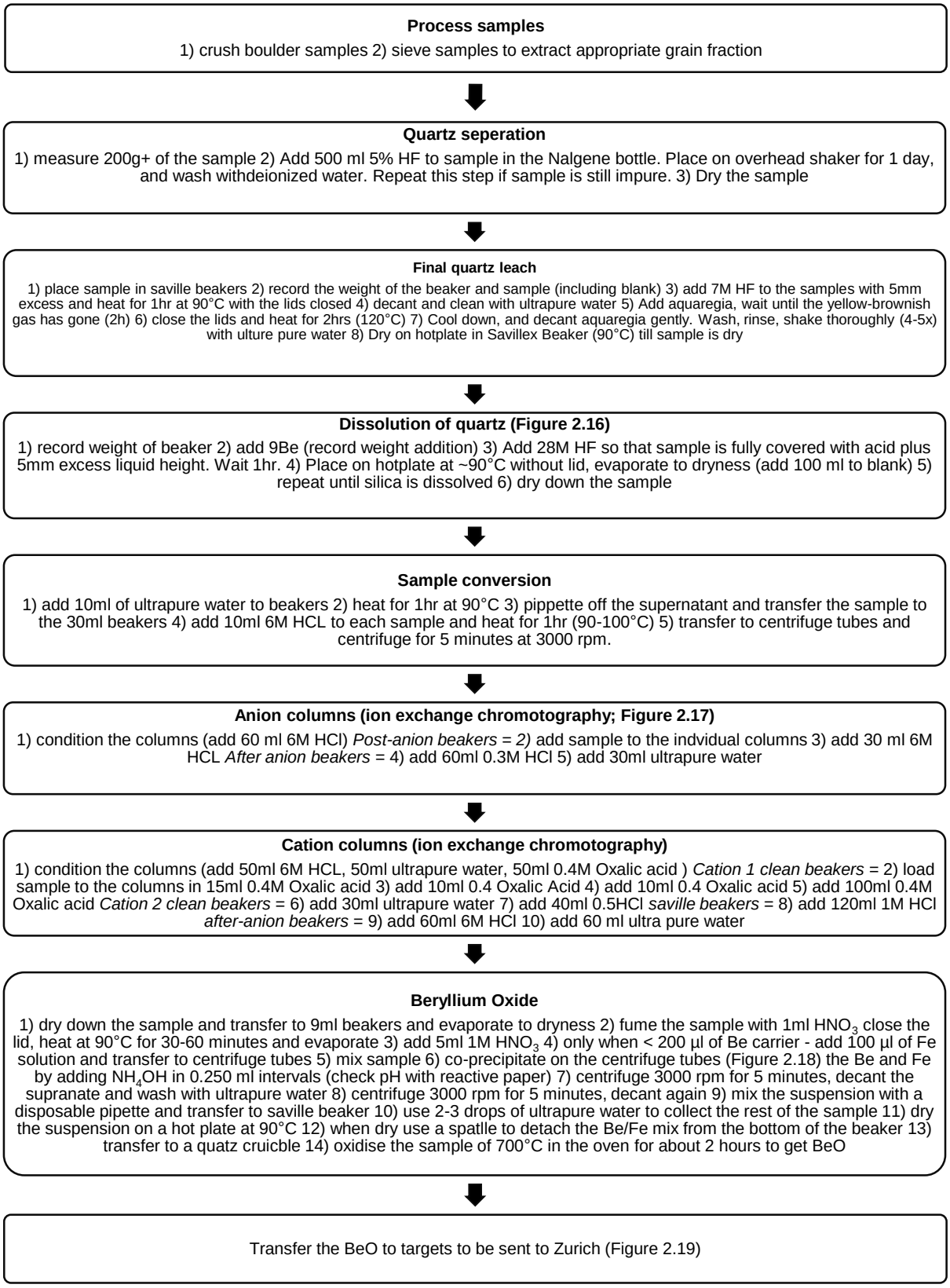

Figure 4.15 *– Beryllium extraction: cosmogenic analysis.*

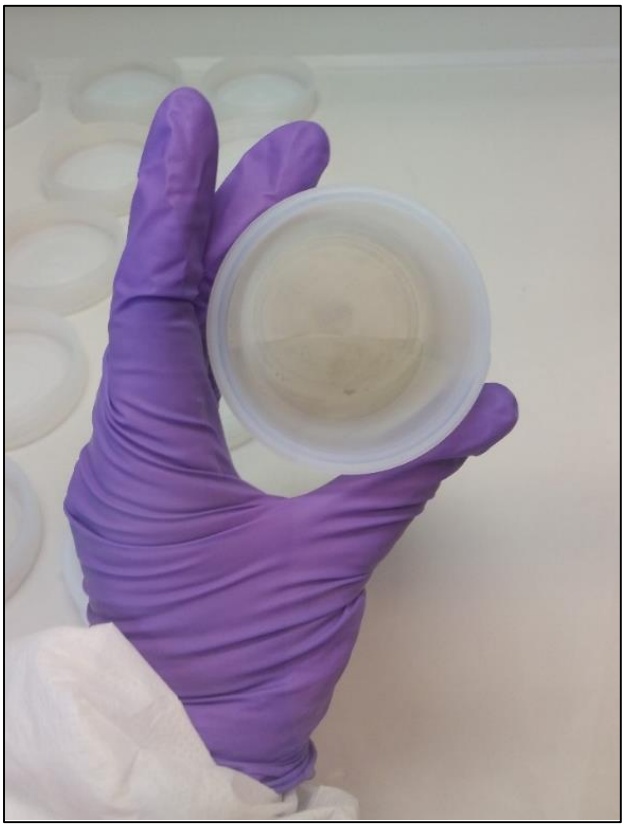

Figure 4.16 *– Samples after quartz dissolution, the black dots represent heavy minerals, which will be removed during further HF addition and ion exchange chromatography.*

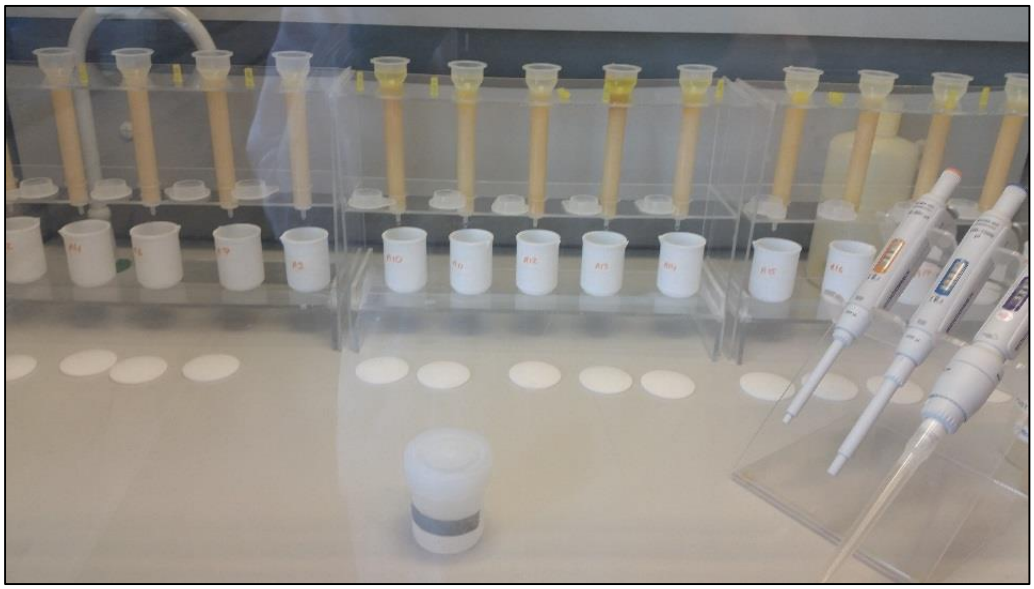

Figure 4.17 *– Ion exchange chromatography – anion columns.*

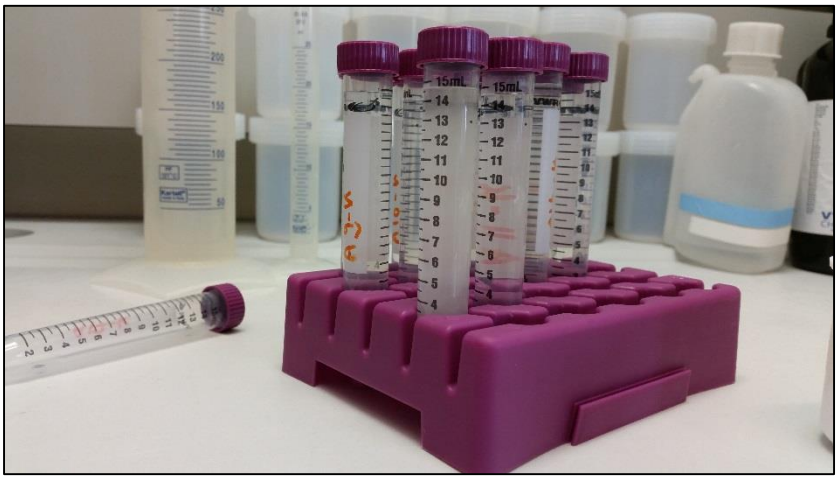

Figure 4.18 *– Centrifuge tubes with sample inside.*

Figure 4.19 *– Processed samples in targets to be sent to Zurich.*

4.4.3 Data processing

The results from ETH Zurich were processed and the accelerator mass spectrometry (AMS) error propagated; the error (due to laboratory contamination, as measured by the 'blank sample') on cosmogenic samples was low (<40%). The corrected ^{10}Be concentration and associated error data was then used in the CRONUS calculator (Balco et al., 2008). To calculate the erosion rate, the CRONUS calculator uses the: 1) longitude/ latitude of the sample (Figure 4.20); 2) the elevation (Figure 4.20) and elevation standard; 3) sample thickness; 4) shielding correction; 5) ^{10}Be concentration; 6) uncertainty on the ^{10}Be concentration; 7) name of the ^{10}Be standardisation.

The latitude/longitude and elevation data (Figure 4.20) are important as the cosmogenic flux rate varies towards the poles and increases as elevation increases (Dunai, 2010). The cosmic rays only infiltrate the top few metres of the Earth's surface (muons can penetrate the furthest), therefore sample thickness is important for TCN

concentration (Dunai, 2010). Shielding (Figure. 4.20) refers to the topographic, slope and local rock (Gosse et al., 1995) effects on the reduction of cosmic rays reaching a sample; if the shielding value is 1, there is no reduction on the amount of cosmic rays reaching the sample. The lower the number, the greater the influence of shielding and reduction in cosmic rays reaching the sample. Shielding has to be corrected for, especially when reporting age data, otherwise the result will be erroneously low. The data presented in this thesis uses the Dunai (2001) scheme (^{10}Be standardisation - S2007N). Dunai's (2001) scheme is similar to Lal (1991), however incorporates the non-dipole component of the Earth's magnetic field, shorter attenuation lengths more applicable to the Earth's surface and uses atmospheric pressure as a proxy for atmospheric depth as atmospheric depth does not simply decrease linearly with altitude. Dunai (2001) was chosen over Desilets and Zreda (2003), Lifton et al. (2005) and Desilets et al. (2006) as it is simpler to apply, and the long term variation of the Earths magnetic field is not fundamental to the time spans considered in this thesis.

The CRONUS calculator is also used to calculate the exposure ages of the samples, in which the erosion rate is assumed to be 0 m Ma^{-1}; this is because very low erosion rates cannot be solved by the Monte Carlo simulation associated with the calculator as the input has to be in cm yr^{-1}.

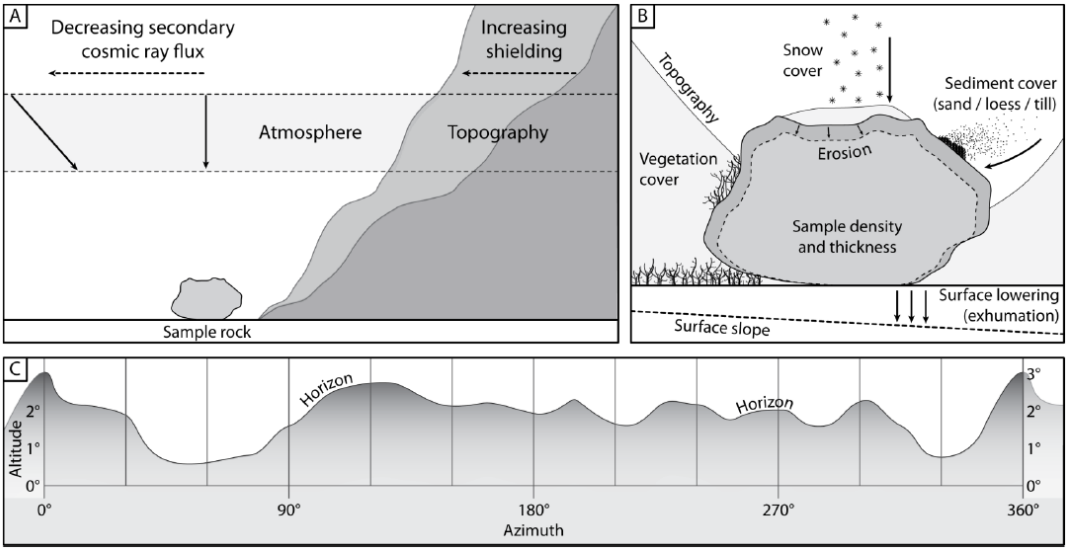

Figure 4.20 *– The influence of multiple factors on cosmogenic accumulation, A) cosmic ray flux decreases if it passes through a greater amount of atmosphere (latitude/longitude) and steeper topography (shielding) will affect the cosmogenic flux; B) local factors which alter the shielding of a sample and; C) topographic shielding calculated for a full 360°, where the angle (altitude) to the nearest horizon is measured (Darville et al., 2013).*

The depth profile sample was solved numerically following the method of Braucher et al. (2003; Eq. 4.6), whereby the concentration at a given depth is composed of two components: 1) the post-depositional concentration and; 2) inherited concentration. The inherited concentration is taken from the lowest sample collected in the depth profile. The depth profile is then solved numerically, based on a chi-squared model fitting between the observed and simulated ^{10}Be depth profiles (Figure 4.21). As the depth profile is from a deposit, the shielding factor used for the CRONUS (Balco et al., 2008) calculator must incorporate the shielding for the whole catchment, which was calculated using Arc-GIS using the method of Norton and Vanacker (2009).

$$N(z,t) = \frac{P(z)}{\lambda+\frac{E}{z*}} e^{-(z_0-Et)/z*}\left(1-e^{-(\lambda+\frac{E}{z}*)t}\right) + N_{inh}e^{-\lambda t} \qquad \text{Eq. 4.6}$$

where *P(z)* is the rate of production, *λ* is the decay constant (ln 2 /$t_{1/2}$), z_0 is the initial shielding depth, and *E* is the post-depositional erosion rate (cm a^{-1}) of the top of the terrace.

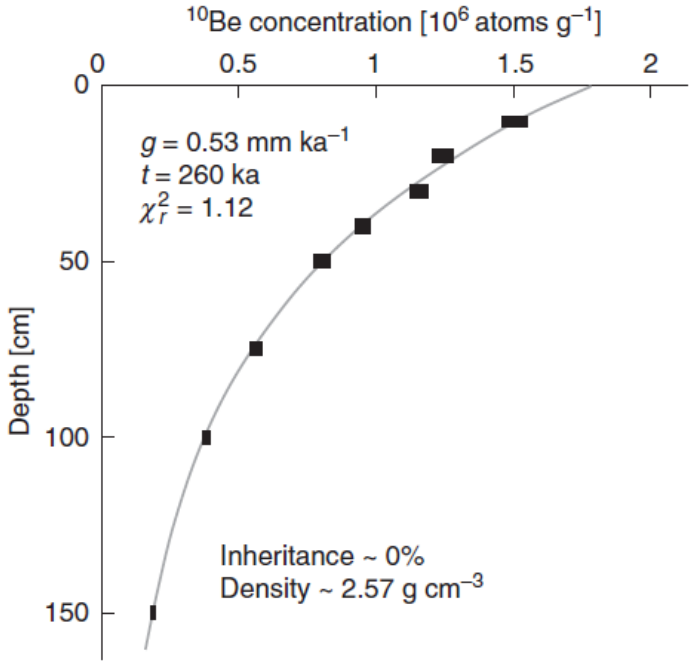

Figure 4.21 *– Depth profile using ^{10}Be, the size of the black rectangle represents the uncertainty associated with each sample. The grey line is a simulated profile using an erosion rate of 0.53 mm ka^{-1} and an exposure age of 260 ka. Chi squared (1.12) indicates a good fit between the sampled and modelled curve (Dunai, 2001 after Hein et al., 2009).*

Chapter 5 Reconstruction of landscape development in southwestern Africa since the late Jurassic: implications for offshore sediment budgets

5.1 Abstract

Quantifying the rates and timing of landscape degradation provide a means to constrain the flux of sediment to offshore basins. The late Mesozoic evolution of drainage basins in southwestern Africa is poorly constrained despite the presence of several small onshore and four large offshore sedimentary basins. The volume of material exhumed since the Early Cretaceous has been constrained by constructing structural cross sections and extrapolating maximum and minimum thicknesses of key lithostratigraphic units. Calculated eroded volumes from southwestern Africa range from 2.52 $x10^6$ km^3 (11.30 km of lithological thickness) to 8.87 $x10^5$ km^3 (4 km of lithological thickness). For the southward draining systems, a volume of 7.81 $x10^6$ – 2.60 $x10^5$ km^3 has been removed, which is far greater than the volumes of sediment recorded in offshore basins (2.69 $x10^5$ km^3). Reconstruction of the drainage systems using geomorphic indicators and clast provenance of the Uitenhage Group, as well as extrapolated cosmogenic dates, indicate the southern draining systems were active by the late Jurassic with coeval activity in axial and transverse systems. The improved understanding of routing patterns, and the long-lived nature of the main transverse systems, allow the 'missing' sediment to be interpreted to have been deposited on the Falkland Plateau as it moved past the offshore basins during the late Mesozoic. Therefore, the sink is separated from its source by 6000 km.

5.2 Introduction

Reconstructing onshore routing patterns and landscape development is an important stage in the analysis of ancient source-to-sink configurations (Clift et al., 2006, Romans et al., 2009; Covault et al., 2011; Macgregor, 2012; Sømme and Jackson, 2013). This relationship can been challenging to constrain and quantify when assessing configurations in deep-time, and close to active plate boundaries (Romans et al., 2009; Romans and Graham, 2013). Advances with techniques such as *in situ* cosmogenic dating (e.g., Gosse and Phillips, 2001; von Blackenburg and Willenbring, 2014) and apatite fission track thermochronology (AFTT) (e.g., Green, 1988; Gleadow et al., 1983, 1986; Gallagher et al., 1998) provide a means of constraining onshore drainage basin configurations through time more accurately (e.g., Bierman, 1994; Gallagher and Brown, 1999; Cockburn et al., 2000). When

combined with advances in remote sensing techniques this approach can aid offshore analysis as catchment areas and drainage evolution can be linked (e.g., McCauley et al., 1986; McHugh et al., 1988; Ramasamy et al., 1991; Blumberg et al., 2004; Gupta et al., 2004; Griffin, 2006; Youssef, 2009; Abdelkareem and El-Baz, 2015; Breeze et al., 2015).

Offshore southern South Africa there are four sedimentary basins (Bredasdorp; Pletmos (Infantaya Embayment), Gamtoos and Algoa basins) (McMillan et al., 1997). Despite the presence of these basins, the onshore drainage development of river catchments south of the Great Escarpment is often overlooked (Rogers, 1903; Partridge and Maud, 1987). Landscape evolution research in South Africa has often focussed on the development and retreat of the Great Escarpment (e.g., King, 1953; Partridge and Maud, 1987; Fleming et al., 1999; Brown et al., 2002; Moore and Blenkinsop, 2006) and large-scale drainage systems such as the Orange River (e.g., Dingle and Hendry, 1984; Rust and Summerfield, 1990; de Wit et al., 2000).

During the Cretaceous there was large-scale exhumation of southern Africa, recorded by AFTT studies (Brown et al., 1990; Tinker et al., 2008a). At the same time, large rift basins developed offshore due to the fragmentation of Gondwana (Macdonald et al. 2003). Tinker et al. (2008a) documented 6.0 - 7.5 km of exhumation using AFTT sampling and identified two pulses of exhumation in the Early- and Mid-Late-Cretaceous. The mechanisms of the large scale exhumation remain contentious (e.g. Doucouré and de Wit, 2003; de Wit 2007; Paton, 2011), with Tinker et al. (2008a) noting that both periods of exhumation in the Cretaceous are related to mantle activity and the formation of large igneous provinces and kimberlites. The Uitenhage Group represents the only onshore depositional representation of the Jurassic-Cretaceous exhumation event. Previously, however, drainage reconstructions have not linked with geomorphic development of the region or with sedimentological studies on the Uitenhage Group.

This study aims to reconstruct the drainage history of two large drainage basins in the Western Cape, using both sedimentology and geomorphology, in order to: (1) calculate the volume of material removed in the Western Cape and compare this to known offshore sediment volumes; (2) examine the geomorphic indicators of river evolution and reconstruct the drainage evolution using geomorphological and sedimentological evidence, and (3) discuss where the ‘missing’ sediment was deposited during Mesozoic exhumation of southern Africa.

5.3 Regional settings

5.3.1 Study area

The study area encompasses four onshore Mesozoic extensional basins in the Western Cape: the Oudtshoorn (study site - Kruisrivier Valley and N12), De Rust (study site - R341), Worcester (study site – Rooikrans) and Nuy (study site – Nuy Road) basins (Figure 5.1). The onshore sedimentary basins are within two large discordant catchments in the Western Cape Province: the Gouritz and the Breede (Figure 5.1), which have been developing since the Mesozoic break-up of Gondwana (Moore and Blenkinsop, 2002; Goudie, 2005; Hattingh, 2008).

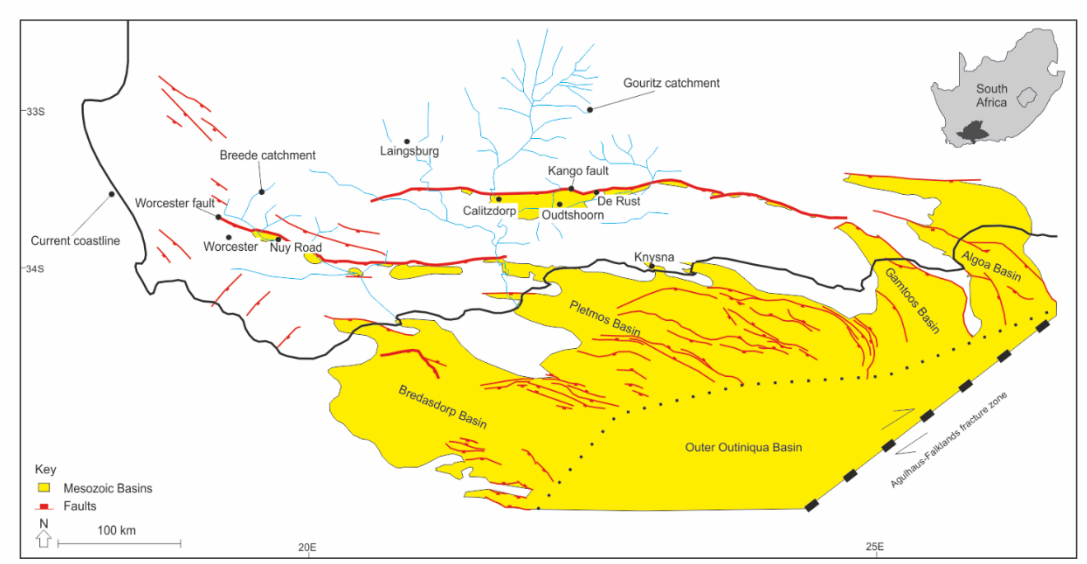

Figure 5.1 *– Location map of study sites and Mesozoic basins of southern South Africa. The current day planforms of the Breede and Gouritz catchments are shown.*

The Mesozoic sedimentary basins have been deeply dissected (Figure 5.1; Green et al., 2016). The Oudtshoorn Basin is the largest onshore Mesozoic basin, is bounded by the Kango fault, and is currently 80 km in length across the E-W strike and up to 21 km wide (Figure 5.1). The De Rust Basin is also bounded by the Kango fault, is 37 km in length (E-W strike) and has a maximum width of 8 km. The Worcester and Nuy basins are bounded by the Worcester fault. The Worcester Basin is highly dissected, and is ~27 km in length and 3 km in width, and the Nuy Basin 15 km in length and 7 km in width. Hereafter, the Worcester and Nuy basins are referred to as the Worcester Basin.

5.3.2 Geology

The Cape and Karoo Supergroups are extensively exposed in southern Africa, with minor Pre-Cambrian metasediments (the Malmesbury, Kaaimans and Gamtoos

groups) and granites (the Cape Granite suite) (Figure 5.2). The Cape Supergroup is a siliciclastic sequence composed of the Table Mountain, Bokkeveld and Witteberg groups (Broquet, 1992).

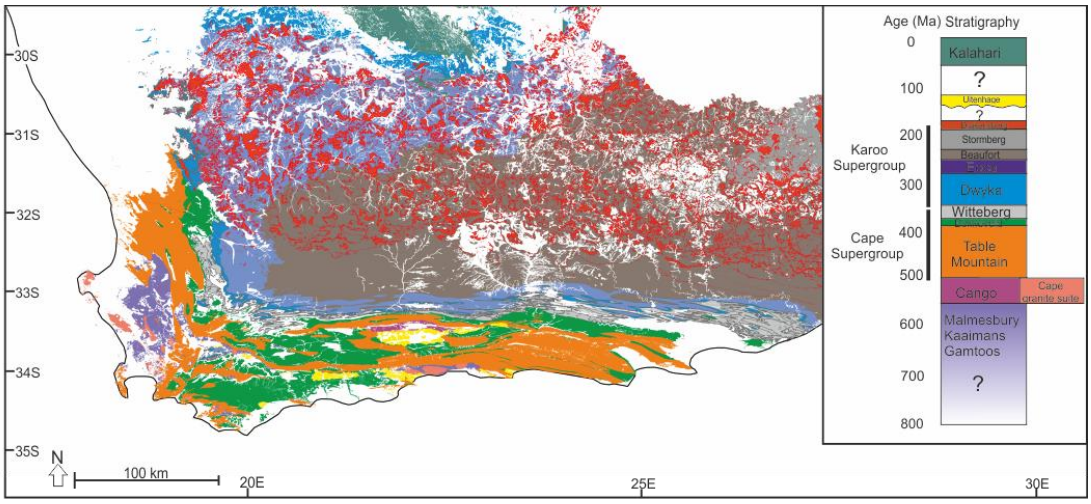

Figure 5.2 *– Geological map of southern South Africa showing key stratigraphic units used in the cross section construction. The current day distribution of the Drakensberg volcanics are towards the north.*

The quartzitic Table Mountain Group represents sedimentation on a subsiding shelf, with deposits including conglomerates, sandstones, mudstones, quartz arenites and shales. The argillaceous Bokkeveld Group represents deep-marine sedimentation. The Witteberg Group contains shelf sedimentation of quartzites and mudstones (Broquet, 1992). The Karoo Supergroup comprises the Dwyka, Ecca, Beaufort, Stormberg and Drakensberg groups. The Dwyka Group represents glacial sedimentation and comprises tillite. The Ecca and Beaufort contain claystone, siltstone, and sandstone. The deposits represent an overall shallowing-upward succession from basin-floor and submarine slope, through shelf, to fluvial and lacustrine depositional environments (Johnson et al., 1996; Flint et al., 2011). The Stormberg Group contains mudstones and sandstones, and represents sub-aerial and fluvial deposition (Johnson et al., 1996). The Drakensberg Group contains flood basalts and dolerites associated with the initial rifting of Gondwana (Visser, 1984). The Uitenhage Group comprises deposits associated with the large-scale exhumation of southern South Africa during uplift and extension, and contains the Enon, Kirkwood and Sunday River formations. The Enon and Kirkwood formations crop out in the study areas, and are remnants of a once thicker and more laterally extensive extensional basin-fill successions (Figure 5.1) (Shone, 1978). The Enon Formation is conglomeratic with silty/sandy matrix (Shone, 2006), which interfinger with sandstone layers (McLachlan and McMillan, 1976). This has been interpreted

as an alluvial fan deposit (Rigassi and Dixon, 1972; Hill, 1972; Winter 1973). Deposition of the Enon Formation was coeval with rapid denudation as shown by the high sediment concentrations and boulder beds (Dingle, 1973; Lock et al., 1975). The Kirkwood Formation is variegated silty mudstone and sandstone, and represents a meandering fluvial environment (Shone, 2006).

Dating control within the Uitenhage Group is sparse, and relies on biostratigraphy. The Marine River Formation, of which there is no equivalent in the Oudtshoorn Basin (Shone, 1978), contains ammonites, dated as upper Valanginian to Hauterivian (~140-130 Ma) (McLachlan and McMillan, 1976). McLachlan and McMillan (1976) propose a Lower Valanginian to Berriasian age for the Enon and Kirkwood formations (~144-137 Ma). Green et al. (2016), on the basis of Shone (2006) and Dingle et al. (1983), assign a Tithonian to Valanginian age (151-136 Ma). No onshore sediments of Jurassic age have been dated (McLachlan and McMillan, 1976); nonetheless Partridge and Maud (1987) assign an upper Jurassic age. An unpublished radiometric age for the underlying Suurberg Group, based on K-Ar whole rock age from a single basalt sample, is dated as 162 +/- 7 Ma and represents the maximum age of the Uitenhage Group (McLachlan and McMillian, 1976). However, due to erosion or non-deposition, caution is needed with this date. The Drakensberg volcanics are dated at 183 +/- 1 Ma using ^{40}Ar-^{39}Ar (Duncan et al., 1997) and can also be used to constrain the age of the Uitenhage Group and Gondwana rifting.

The offshore sedimentary basins (Figure 5.1) are interpreted as extensional pull apart systems that formed during rifting of East and West Gondwana and the subsequent break-up of the southern Atlantic (Brown, 1995; McMillan et al., 1997; Paton, 2006; Tinker et al., 2008b; Sonibare et al., 2015). Tinker et al. (2008b) calculated an order of magnitude difference between the amount of sediment exhumed onshore and the volume of sediment in the inner Outeniqua Basin, the collective name for the Bredasdorp, Pletmos, Gamtoos and Algoa basins (Figure 5.1) and outer (Southern) Outeniqua Basin. The offshore accumulation was estimated to account for 860 m of onshore exhumation (Tinker et al., 2008b).

Offshore deposition of conglomerates in the Uitenhage Group have been recorded in the major sedimentary basins of the inner Outeniqua Basin. The timing of initial deposition is diachronous across the offshore sedimentary basins (Dingle and Scrutton, 1974). The first appearance of conglomerate offshore in the Bredasdorp

Basin is the Late Jurassic (Sonibare et al., 2015), Early Cretaceous in the Pletmos Basin (Brink et al., 1993), and Late Jurassic to Early Cretaceous in the Gamtoos Baisn (Thomson, 1999) and Algoa Basin (Dingle, 1973).

5.3.3 Structure

Structurally, the Western Cape is dominated by the exhumed Cape Fold Belt (CFB), which is a compressional mountain range that formed in the late Permian and Triassic (e.g. Tankard et al., 2009; Flint et al., 2011). The CFB comprises resistant quartzite, as well as psammites and metamorphosed mudstones, of the Cape Supergroup (Shone and Booth, 2005). Metamorphism within the Cape Supergroup reaches lowermost greenschist to anchizonal grade (Frimmel et al., 2001; Hansma et al., 2015). Greenschist facies form across a wide range of burial depth (8-50 km). However, considering the continental geothermal collision setting, and assuming the density of overlying sediment of 2.6 g cm $^{-3}$, 12-15 km of overburden was estimated to reach 300°C (Frimmel et al. 2001).

Southern South Africa can be split into two broad tectonic domains defined as thick- and thin-skinned, for the southern and northern domain respectively (Paton et al. 2006). Uitenhage Group sediments accumulated in the hanging-wall of WNW-ESE trending half-graben basins formed by trending extensional faults during rifting (Paton, 2006). These were reactivated CFB thrust faults that originally formed during late Palaeozoic/early Mesozoic orogeny (Paton et al., 2006; Stankiewicez et al., 2007). The reactivated faults originated as long planes rather than individual segments, resulting in uplift across the entire planar surface (Paton, 2006). The Kango and Worcester faults have had displacements of 6-10 km (Dingle et al., 1983; Tankard et al., 2009). The onshore basins (e.g., Oudtshoorn, Worcester, Heidelberg, Swellendam; Robertson) have not been assessed in detail (e.g., Söhnge, 1934; De Villiers et al. 1964; Du Preez, 1994; Lock et al., 1975), but contain Mesozoic sediment accumulations of up to 3000 m (e.g., Oudtshoorn Basin).

5.3.4 Geomorphology

The major drainage basins in the Western Cape are superimposed (Rogers, 1903), with deeply incised bedrock meanders in resistant quartzite lithologies and courses that are discordant to the major geological structures (e.g., the folds and faults of the CFB). Although the Western Cape catchments have not been assessed in detail, the Eastern Cape and Northern Cape rivers have undergone major drainage reversals via stream capture events (de Wit et al., 2000; Hattingh, 2008). Major

drainage reorganisation has occurred in the Orange River catchment (de Wit et al., 2000) due to continental uplift, as well as denudation onto the underlying structured pre-Karoo topography, which would also have affected catchments towards the south. Gilchrist et al. (1994) proposed that at the time of Gondwana rifting, two drainage basin types developed in southern Africa: internally draining catchments (e.g., Kalahri and Karoo rivers) separated by the Great Escarpment from externally draining catchments to the sea, which formed as Gondwana rifted. The distance of retreat and formation of the escarpment are contentious. King (1966) argued the escarpment formed at the coastline and has since retreated to its current position. However, geochronometric dating and numerical modelling have concluded the escarpment formed near its present day position, with much of the retreat occurring in the Cretaceous and limited retreat thereafter (e.g., Fleming et al., 1999; van der Beek et al., 2002; Brown et al., 2002; Kounov et al., 2007). Published retreat rates and distances are shown in Table 5.1 using AFFT and cosmogenic data, given the data the escarpment has retreated a maximum of 29 km to its current day position (Brown et al., 2002). In contrast, Green et al. (2016) argue on the basis of AFFT, that the Escarpment is the remnant of denudation in the Cenozoic (20-30 Ma) based on 7 samples from the Beaufort West area (Figure 5.3). There is variation in the retreat rate around the Great Escarpment, with higher rates in the Drakensberg range. The Drakensberg escarpment is underlain by basalt, whereas in Namibia, the escarpment is formed on quartzites. In addition, the Drakensberg area has a higher rainfall which could account for the higher rates (Tinker, 2005). The retreat of the escarpment has affected the upper catchment of the current Gouritz drainage basin (Figure 5.3).

Table 5.1 *– Published data on the retreat of the Great Escarpment.*

Reference	Nuclides	Material	Region	Lithology	Landform	Denudation rate (m/Myr)
Fleming et al. 1999	36 Cl	Basalt	Drakensberg (se) escarpment	Basalt	Face	50 -95
Cockburn et al. 1999/2000	10 Be, 26 Al	Quartz	Central Namibian (western) margin	granite-gneiss	escarpment faces and ridges	10
Bierman and Caffee, 2001	10Be, 26Al	Quartz	Central Namibian (western) margin	granite, granite-gneiss, quartzite, pegmatite	outcrop, including inselbergs	3.2
				sediment	escarpment	16
					highlands	5
					coastal plain	8
						6.4
Kounov et al. 2007	3He, 21Ne	Quartz	Southwestern Karoo	Quartzite	Plateau surfaces	1.5-3
		Pyroxene	Southwestern Karoo	Dolerite	Plateau surfaces	1-2.1
Decker et al. 2011	3He	Pyroxene	South-central Karoo and north east KwaZulu-Natal	Dolerite	Scarps, summits, plains and ridges	0.5-4
Brown et al. 2002	AFFT	Apatites	Drakensberg Escarpment			100-200

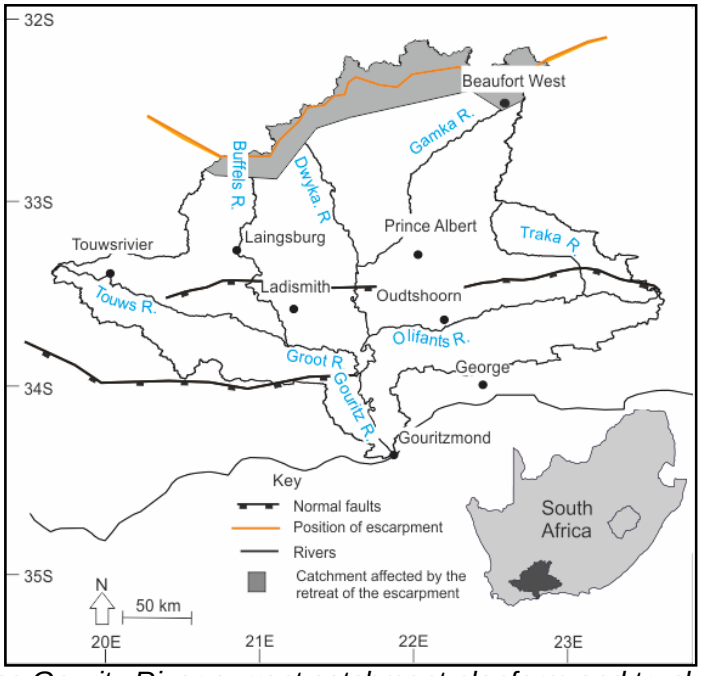

Figure 5.3 *– The Gouritz River current catchment planform and trunk river location.*

Apatite Fission Track work has shown that large-scale exhumation has occurred in South Africa. Using cored boreholes, Tinker et al. (2008a) conclude that 3.3 - 2.5 km of exhumation took place in the mid-late Cretaceous, and argued for a maximum of 7 km could have been exhumed if the Karoo volcanics are taken into account with erosion in the Early Cretaceous accounting for this. Green et al. (2016) argued for three phases of exhumation and sediment accumulation within the Cretaceous, with a regional cooling event in the Late Cretaceous (85-75 Ma).

Timing of offshore basin sedimentation indicate southward drainage was established by the late Jurassic in the Western Cape. The change from net deposition to net erosion in the Western Cape area is related to Gondwana rifting and lowering base levels of the continent. This caused intense denudation and exhumation of the Karoo Basin-fill and CFB, and the development of southward draining rivers (Gilchrist et al., 1994). The exact location and number of mantle plumes, and the relative movement of plumes is contentious (Pik et al., 2006). An elevation gain of 2 km (Cox, 1989), associated with plume activity, could have provided the activation energy to drive the change from deposition to erosion (Cox, 1989; Nyblade and Sleep, 2003). However, researchers have also argued that the topography of South Africa is not related to dynamic topography related to the plumes, and invoke epeirogenic uplift and plate tectonic driven uplift (Moore and Blenkinsop, 2002; Moore et al., 2009). The reactivation of faults during rifting

(Paton, 2006) reduced local base level and enhanced incision into resistant Cape Supergroup lithologies.

Drainage reconstructions using the Uitenhage Group have not been integrated with the long-term geomorphic development of the region. Previous drainage reconstructions using the Uitenhage Group have argued for connection between downdip basins, with lows in the surface relief of the CFB acting as sediment corridors (Lock et al., 1975). However, this is disputed by Rigassi and Dixon (1972), who argue that the similarity between the basins is due to the same type of depositional environment prevailing across southern South Africa. Also, Paton (2006) argued that the downdip basins of the Oudtshoorn area were separated by pre-rift strata.

Rogers (1903) argued for a complicated drainage history of the Gouritz catchment whereby the Groot River captured the Buffels and Touws rivers (Figure 5.3). Rogers (1903) incorporated the Uitenhage Group deposits into the reconstruction, and argued that because there are no Uitenhage Group deposits in the transverse river valleys (e.g., Gamka River), they were not active at the time of deposition. The reconstruction of the Gouritz drainage basin by Partridge and Maud (1987) has a planform similar to the present day, with extension of the tributaries to the north as the escarpment retreated. The lower portion of the catchment is also affected by variation in relative sea level, with the river extending further onto the continental shelf in the mid-Cenozoic when eustatic sea level lowered. Partridge and Maud (1987) integrated the presence of marine deposits and duricrusts into their reconstructions. Recently, Green et al. (2016), argued that the incision of the Gouritz Catchment into the Swartberg range is a Cenozoic event (30-20 Ma) that was driven by uplift on the basis of AFFT data.

5. 4 Methodology

5.4.1 Volume of material removed

Nine structural cross sections (6 N-S and 3 E-W) were constructed across the Western Cape (study area of ~224 200 km^2) using 1:250 000 geological map sheets (Figure 5.4). Key structural units were then extrapolated across the sections using maximum and minimum thickness data recorded within the literature using the arc method (Busk, 1929), where constant lithological thickness are maintained (Table 5.2). Using Midland Valley's 3DMove software, a 3D model was constructed of the key intervals across the study area (Figure 5.4). This model permits the volume of

material removed to be calculated, over the study area of ~224, 200 km^2 (Figure 5.5).

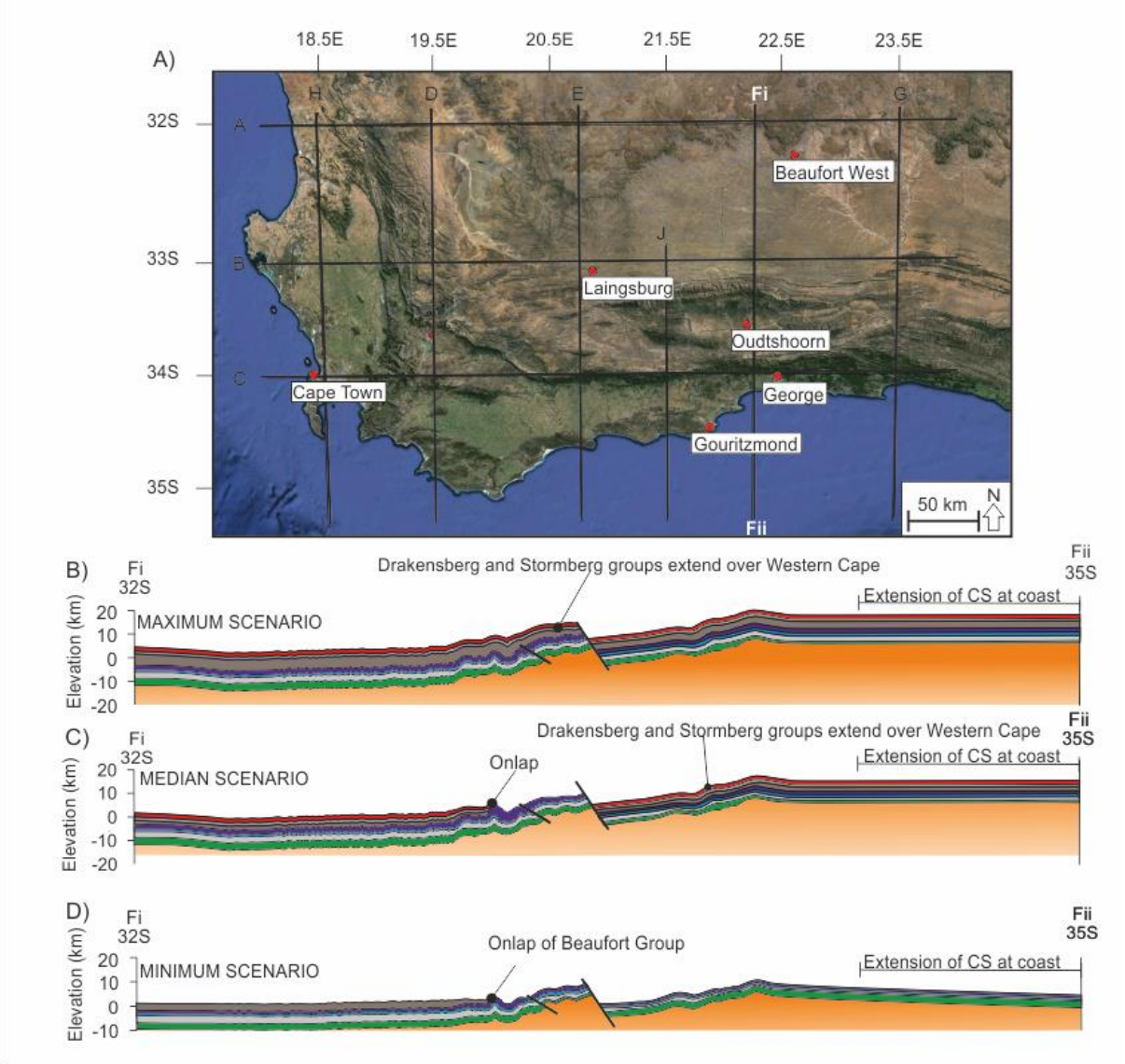

Figure 5.4 *– A) Location map of the 9 cross sections used in 3D Move to calculate maximum and minimum exhumation volumes. B) Cross section F using the maximum assumptions, the top surface represents the maximum lithological extent prior to erosion. C) Median Scenario schematic. D) Cross section F using the minimum assumptions.*

This uses the difference between a base horizon, which is a combination of the digital elevation model (DEM) of the present-day topography for the land surface and the average height of the study area where the cross sections are extended at the coast, and the top horizon, which is the top of individual cross sections. The estimated **maximum** and **minimum** volumes of material removed require a number of assumptions that relate to the original tectono-stratigraphic configuration of the area prior to exhumation. These assumptions are as follows:

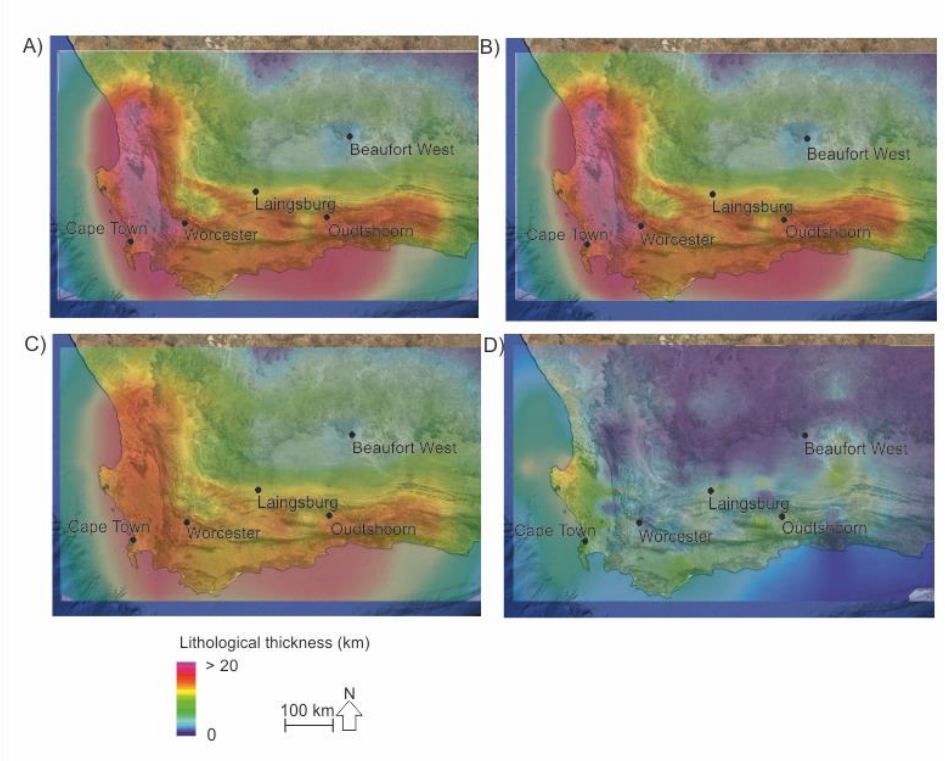

Figure 5.5 *– Result output from 3D MOVE showing the lithological thickness variation in southern South Africa. A) Maximum scenario with Drakensberg lithologies present, B) maximum scenario without Drakensberg lithologies present C) median output and D) minimum assumption scenario.*

Table 5.2 *– Thicknesses of key lithologies used in the geological cross sections.*

Group	Max Thickness (m)	Reference	Min thickness (m)	Reference
Drakensberg	1,400	Catuneanu et al., 2005		
Stormberg	1,400	Johnson, 1976		
Beaufort	3,000	Adams et al., 2001	3,000	Adams et al 2001
Ecca	1,800	Adams et al., 2001	1,800	Adams et al., 2001
Dwyka	1,300	Rowsell and De Swardt, 1976	600	Rowsell and De Swardt, 1976
Witteberg	2,000	Ros March 03	1,700	Ros March 03
Bokkeveld	2,000	1:250,000 Map Data	2,000	1:250,000 Map Data
Table Mountain	2,500	Shone and Booth, 2005	2,500	Shone and Booth, 2005

1. The extent of the Drakensberg volcanics, which currently do not crop out in the Western Cape, and were either absent at the time (minimum) or extended into the study area at a similar thickness to their present day occurrence in the east (maximum). Xenoliths in kimberlites have been used to reconstruct palaeo-geomorphological evolution in central South Africa, and it is argued that ~1500 m of the Drakensberg Group lithologies (mainly Lesotho Formation) were in the Kimberly area at the time of eruption (183 Ma) (Hanson et al. 2009). It is highly likely, therefore, that the Drakensberg volcanics extended across the entire Karoo Basin. Additionally, AFFT work by Green et al. (2016) found a high chlorine content in the Uitenhage Group sandstones, indicative of volcanogenic sources.
2. Only lithologies older than Cretaceous are included in the cross sections, as the main exhumation occurred during the Cretaceous (Tinker et al., 2008a). Although the Uitenhage Group deposits are locally thick, they are minor compared to the volume of material removed. For example, the volume of Cretaceous deposits in the Oudtshoorn Basin, assuming a maximum fill of 3000 m (McLachlan and McMillian, 1976), is 6900 km^3.
3. The cross sections were constructed either with all post-Carboniferous deposits (the Karoo Supergroup) onlapping against the folds of the CFB (minimum) or with all the eroded lithostratigraphic units conformable and maintaining a constant thickness across the CFB to the present day coastline (maximum), which assumes that all folding is post-depositional. There is no evidence beyond the present shoreline to constrain the upper lithological bounding surface.

Due to these uncertainties when calculating volumes of landscape erosion, several scenarios were developed to minimise the associated error.

5.4.2 Sedimentological logs and clast analysis

Five representative sedimentary logs (cumulative thickness of 67.4m) and 950 clast measurements were taken in the Oudtshoorn, De Rust and Worcester Basins. The main purpose of the data was to assess provenance and sedimentary environments, therefore, clast lithology, size and roundness was recorded. Imbrication was also measured if seen within the outcrop.

5.4.3 Remote sensing

River planform can also indicate the evolutionary history of the catchment and can give important insight into the geological development of the region (Twidale, 2004). Aster 30m DEM was obtained from NASA Reverb (2015) for southern South Africa

and analysed using ArcGIS. Present-day river patterns and catchment areas were extracted using the hydrological toolbox using a con value of 3000 showing both perennial and ephemeral rivers (Abdelkareem et al., 2012; Ghosh et al., 2015). Evidence of stream capture was identified to constrain drainage evolution (Summerfield, 1991). Elbows of capture are indicated by sharp changes in channel direction (~90°). Commonly, the previous river course of a beheaded stream leaves a dry 'upstream' reach of the previous course and fluvial deposits in an abandoned river valley (wind gaps) (Summerfield, 1991). Stream reversal can be shown by barbed confluences, whereby the tributary joins the main river at an anomalous angle (Haworth and Ollier, 1992). Misfit streams are valleys that have anomalous cross sectional areas compared to the streams that currently occupy them (Dury, 1960). Misfit streams can form by variation in discharge (Dury, 1960) caused by extrinsic factors such as climate change and tectonic activity, or intrinsic factors such as stream capture (Summerfield, 1991). In alluvial settings, identification of misfit streams uses the degree of meandering and the underlying floodplain deposits (Dury, 1960), however due to the lack of accommodation in bedrock settings this cannot occur. In bedrock settings, to assess how misfit a stream is, the *minimum bulk catchment erosion* was calculated using ArcGIS, whereby a horizontal 'cap' is placed on the catchment to compare the volume of material removed from the catchment area. Catchment area has been shown to have a strong correlation with cosmogenic data and rates of erosion (Bellin et al., 2014), therefore *minimum bulk catchment erosion* is expected to correlate with catchment area and provides an approach to quantify how misfit a stream is when deposits are lacking . If the catchment area is too small or large for the extracted volumes, the catchment may be misfit. In order to constrain how misfit the catchments in the study area could be, data (catchment area / minimum bulk catchment erosion) from 10 catchments from different tectonic and climatic settings from a range of locations (Table 5.3) were extracted and compared to the study location data. The *minimum bulk catchment erosion* method represents an underestimation of material removed as the watershed and interfluve areas would have been lowered due to erosion (Brocklehurst and Whipple, 2002; Bellin et al., 2014).

Table 5.3 *– Global data extracted to see how misfit the valleys of the study area are.*

Location	Latitude	Longitude	Area (km^2)	Minimum bulk catchment erosion (km^3)	Reference
Namibian desert and escarpment	-21.304	16.217	1251.873	0.106	Bierman et al. 2007
Queensland Escarpment, Australia	-16.852	145.648	2296.749	2.269	Bierman et al. 2009
Stanley, Virginia, US	38.532	-78.603	5430.284	1.659	Duxbury 2008
Tin Can Creek, Australia	-12.453	133.270	403.6931	5.348	Heimsath et al. 2009
Peradeniya, Sri Lanka	7.261	80.595	1165.496	9.059	Hewawasam et al. 2003
Nahal Yael, Isreal	29.580	34.930	0.447029	9.576	Clapp et al. 2000
Bredbo River, Australia	-36.000	149.500	20.97207	4.269	Heimsath et al. 2006
Rio Azero, Bolvia	-19.610	-64.080	4432.853	0.003	Insel et al. 2010
Little River, Tennessee US	35.664	-83.592	149.4539	22.268	Matmon et al. 2003
Northern Flinders Range, Australia	-30.187	139.428	103.945	6.740	Quigley et al. 2007

5.4.4 Cosmogenic nuclide dating

Cosmogenic dating using *in situ* produced nuclides provides information to help constrain the exposure ages of surfaces including erosional strath terraces. The highest accessible erosion surface in Gamkaskloof (Figure 5.6) was dated using *in situ* ^{10}Be. The sample was crushed and the 0.25 - 0.5 mm grain fraction extracted and treated using standard lab procedures (Von Blanckenburg et al., 1996, 2004). The ^{10}Be/^{9}Be ratios were measured in BeO targets with accelerator mass spectrometry at ETH Zürich (Kubik and Christl, 2010). The sample was normalised to the ETH in-house secondary standard S2007N, 0.162 g of ^{9}Be carrier was added to the sample and uncertainties were propagated from AMS counting statistics and the 38% uncertainty on the blank sample. Incision rates were calculated using CRONUS (Balco et al., 2008), which calculates on the basis of the ^{10}Be concentration, using the known decay rates of ^{10}Be (and integrates sample information such as elevation, latitude and longitude, shielding and sample density).

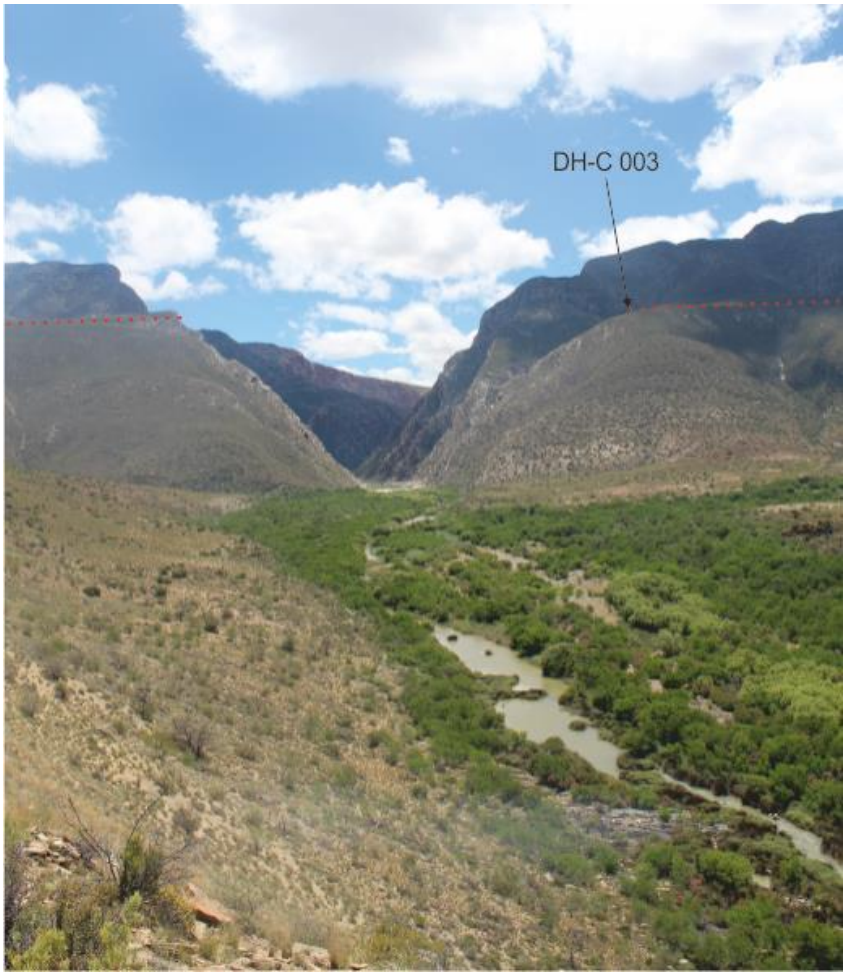

Figure 5.6 *– Gamkaskloof erosional surfaces and sampling point for cosmogenic dating. The transverse Gamka River can also been seen dissecting the Cape Fold Belt.*

The age of the drainage systems in the Western Cape, including the deeply incised gorges, are poorly constrained (e.g., Rogers, 1903; Davis, 1906; Maske, 1957; Green et al., 2016), but are vital to improve understanding temporal links between drainage basins and sedimentary basins. The sample used in this study was from the highest accessible surface within Gamkaskloof (Figure 5.6), which is one of three breaches of the CFB within the Gouritz drainage basin, and marks where the Gamka River (the confluence with the Dwyka River is 9 km upstream) transverses the resistant quartzites of the Cape Supergroup. The incision rate was then used to extrapolate exposure ages to the highest elevation point of the Swartberg. The extrapolation of the age of incision uses data from the highest sampled strath terrace, and provides an approximate long-term averaged incision, which would have varied from the Cretaceous to present day.

5.5 Results

5.5.1 Amount of erosion

Table 5.4 shows the volumes of material removed and the corresponding average lithological thickness calculated from a range of different scenarios using the uncertainties outlined above. Using the DEM of South Africa as the base horizon, with the presence of the Drakensberg Group, an absolute maximum amount of 2.52 x 10^6 km^3 of material removed, relating to an average of 11.3 km lithological thickness removed across the study area. This is expected when considering the metamorphic grade of the Cape Supergroup (Frimmel et al., 2001). Using the minimum assumptions, a volume of 8.87 x10^5 km^3 equating to 4.0 km has been eroded in the study area, constraining this to the Western Draining catchments this value is reduced to 2.60 x10^5 km^3 relating to 1.2 km of thickness removed. This is much lower than expected from the metamorphic grade of the Cape Supergroup.

The median (using the maximum and minimum scenario assumption, and calculating a surface in 3D Move) value indicates up to 7.60 km of material has been removed (equivalent volume of 1.71 x10^6 km^3) when including the Drakensberg Group, this decreases to 6.8 km (volume of 1.53 x10^6 km^3) when the Drakensberg Group is not present. Constraining the data to the southerly draining catchments, 2.3 km of material has been removed with the Drakensberg Group present, or 2.1 km (4.06 x10^5 km^3) without the Drakensberg group. The variation in lithological thickness removed is shown in Figure 5.5, with maximum thicknesses over the CFB and in western South Africa.

Table 5. 4 *– Volume of material removed from southern South Africa, data from 3D Move.*

Scenarios	Volume (km^3)	Lithological thickness (km)
	MAXIMUM	
	Extended at the coastline	
With Drakensberg	2.52 $x10^6$	11.30
Without Drakensberg	2.18 $x10^6$	9.70
	To current coastline	
With Drakensberg	1.40 $x10^6$	6.30
Without Drakensberg	1.17 $x10^6$	5.30
	Southerly draining catchments	
With Drakensberg	7.81 x 10^6	3.50
Without Drakensberg	6.72 $x10^6$	3.00
	MEDIAN	
	Extended at the coastline	
With Drakensberg	1.71 $x10^6$	7.60
Without Drakensberg	1.53 $x10^6$	6.80
	To current coastline	
With Drakensberg	9.34 $x10^5$	4.20
Without Drakensberg	8.18 $x10^5$	3.60
	Southerly draining catchments	
With Drakensberg	5.21 $x10^5$	2.30
Without Drakensberg	4.06 $x10^5$	2.10
	MINIMUM	
Extended at the coastline	8.87 $x10^5$	4.00
To current coastline	4.67 x 10^5	2.10
Southerly draining catchments	2.60 $x10^5$	1.20

5.5.2 Sedimentology

5.5.2.1 Sedimentary facies

Sedimentary logs of the red-coloured Enon Conglomerate (Figure 5.7), the oldest unit of the Uitenhage Group, were collected from the Oudtshoorn and De Rust

basins adjacent to the Kango fault, whereas the Worcester conglomerate exposures are located farther from the boundary fault (the Worcester fault). Facies one (F1) comprises poorly-sorted to rare normally graded clast-supported conglomerate with coarse sand to gravel grade matrix in 1-5 m thick beds with erosional bases common (Figure 5.7). Commonly, the individual clasts have deeply weathered crusts (Figure 5.7).

Clast imbrication in the Worcester Basin suggests a dominant southeastward palaeoflow (Figure 5.8). Facies two (F2) comprise poorly–sorted lenticular conglomeratic beds (up to 3 m) with a coarse sand matrix (Figure 5.7). Facies three (F3) comprise structureless to weakly laminated lenticular coarse sand to gravel beds that range in thickness from 0.10 to 1.2 m. Locally, beds contain dispersed clasts (up to 10 cm; Figure 5.7). Facies 4 (F4) comprises lenticular medium- and coarse-grained sandstones with pebble stringers (Figure 5.7) that pinch out laterally within < 1m. There is no distinct difference in roundness or clast size between the different conglomeratic facies; however there is regional variation (Table 5.5). The standard deviation of clasts measured in the Oudtshoorn Basin shows a wide spread of data points in the a, b and c axis (Table 5.5). The clast roundness is dominated by clasts that are sub-rounded to sub-angular (Figure 5.8). The clasts in De Rust are dominantly sub-rounded and rounded. The Worcester Basin clasts are smaller than those in Oudtshoorn or De Rust. There is a larger spread of clast sizes within the Rooikrans study site compared to the Nuy Road study site as shown by the standard deviation values.

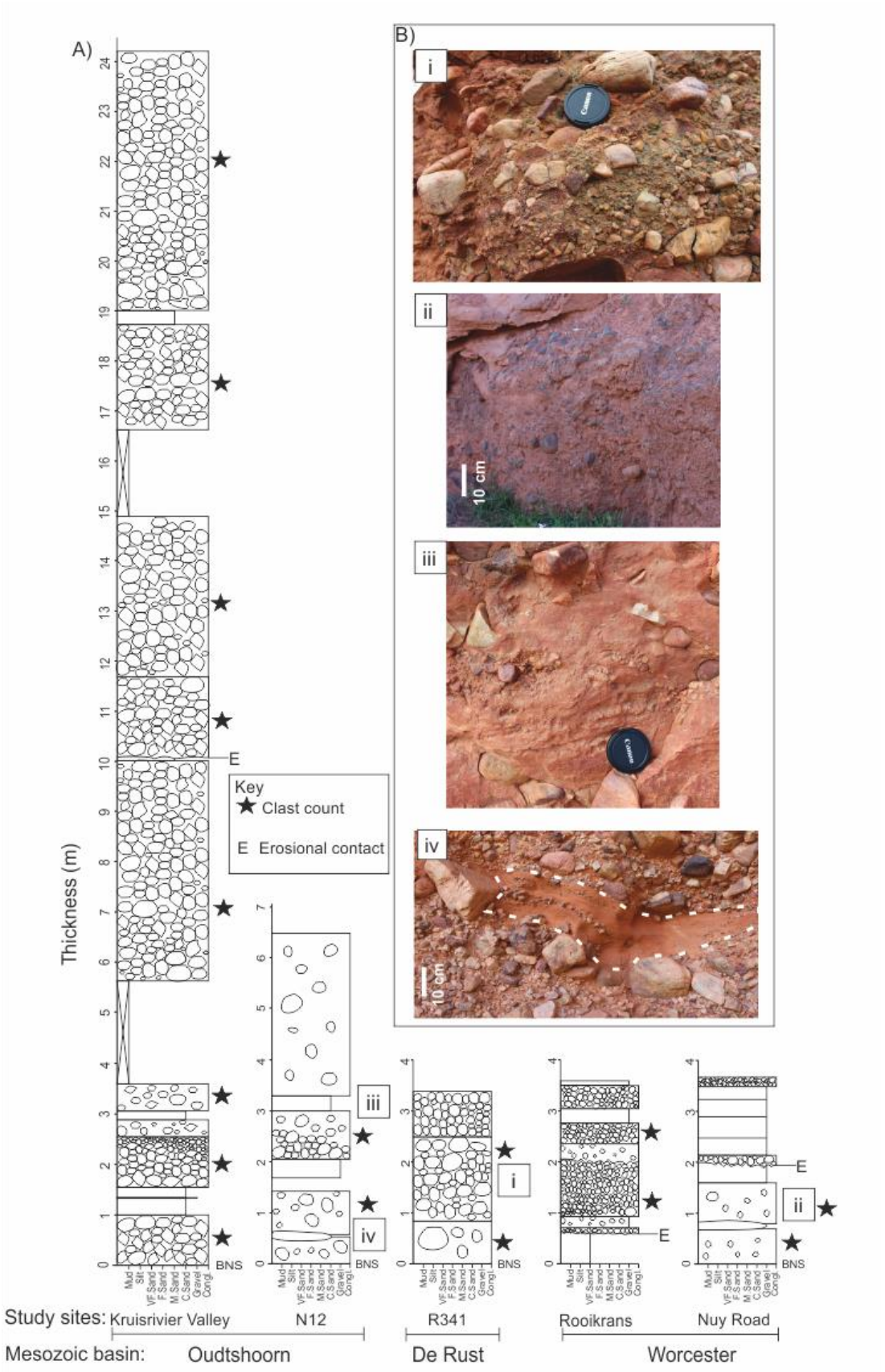

Figure 5.7 *– Facies descriptions and sedimentary logs from the Mesozoic basins.*

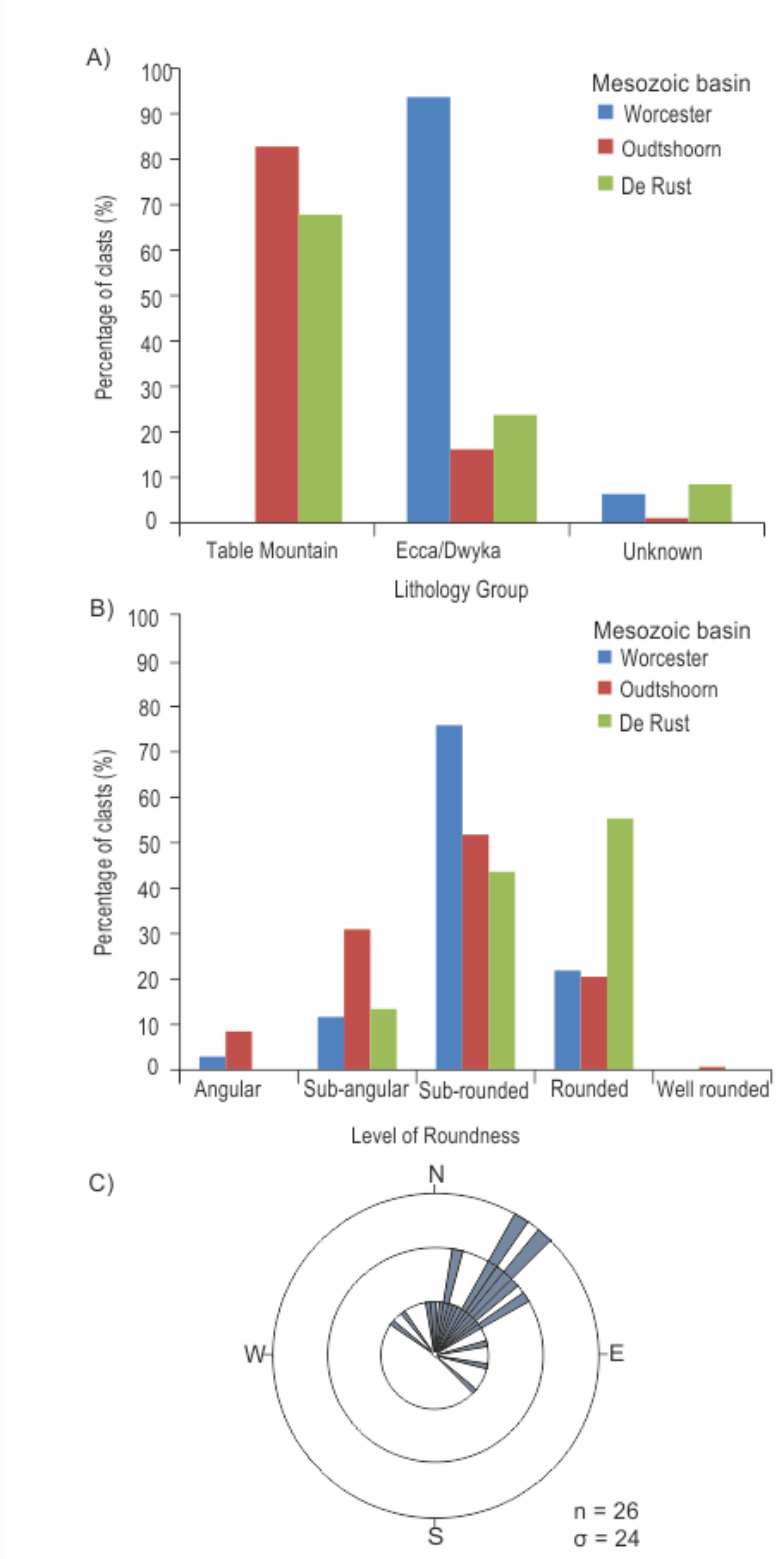

Figure 5.8 *- Clast characteristics of the Worcester (Nuy and Rooikrans study sites), Oudtshoorn and De Rust Basins: A) clast lithology; B) clast roundness and; C) rose diagram of clast imbrication measured from Rooikrans study site.*

Table 5.5 *– Clast size data and standard deviation (in brackets*).

Study Site	A axis (cm)	B Axis (cm)	C Axis (cm)
Worcester – Rooikrans	34 (6.99)	33 (5.05)	24 (3.73)
Worcester – Nuy Road	10 (1.72)	6 (1.19)	5 (0.95)
Oudtshoorn – Kruisrivier	39 (6.19)	29 (4.11)	18 (2.96)
Oudtshoorn – N12	22 (5.34)	10 (3.11)	10 (2.28)
De Rust	52 (9.55)	33 (6.83)	28 (5.04)

5.5.2.2 Clast provenance

The clasts in the Oudtshoorn and De Rust Basins are dominated by quartzites of the Cape Supergroup (Figure 5.8). The clasts within the Worcester Basin (Figure 5.8) are primarily sandstones, mudstones anddiamictite (Karoo Supergroup), but no quartzite clasts are found. No volcanic or dolerite clasts are observed.

5.5.2.3 Depositional environment

The bi-modal clast data (Figure 5.8) at Oudtshoorn suggest deposition in alluvial fans by highly active streams, with short travel distances from the source to the basin (Shone, 2006; Hattingh, 2008). Some of the deposits are well-rounded quartzites with weathered surfaces, which represent reworked sediment. The De Rust (Figure 5.8) deposit is more rounded than at Oudtshoorn and suggests greater transport distance from the source area. The Worcester deposit (Figure 5.8) is more fluvial in nature, as shown by the higher proportion of rounded clasts and the dominance of graded and laminated sandstone/gravel beds and erosion surfaces (Rastall, 1911).

5.5.3 Geomorphological evidence

The Gouritz and Breede catchments are dominated by rivers with courses that are discordant to the underlying tectonic fold structures and extensional faults. These are ancient rivers that are superimposed onto the underlying strata (Figure 5.9), with deeply incised meanders into resistant quartzite of the Cape Supergroup. Anomalous bends are seen with the catchments (Figure 5.9), with angles of up to 90°, and barbed confluence. The anomalous bends are not formed by meandering as they are inset within the bedrock. The high angles of changes in river orientation observed are consistent with stream capture (e.g., Morisawa, 1989; Gardner and Sevon, 1989; Standford, 1993; Thomas and Shaw, 1992; Bishop, 1995; Mather et al., 2000; Willet et al., 2014). Further, high level gravels have been identified and associated with capture sites (e.g., Rogers, 1903), however the gravel deposits are

not mapped at the scale of 1:250, 000. In the absence of mapping the gravels, the anomalous bends are interpreted as stream capture sites over alternative mechanisms, such as geological control causing anomalous bends, as no faults cross the sites of capture as mapped by the 1:250 000 geological maps. The stream capture site evidence is supplemented by misfit stream analysis, sedimentological clasts data, structural geology and the previous study on the Gouritz Catchment by Rogers (1903).

Three large-scale misfit streams are identified along the watershed of the Gouritz catchment (Figures 5.9, 5.10). Two of the catchments (Figures. 9a, c) have higher *minimum bulk catchment eroded volumes* than global catchments of similar sizes and even larger catchments (Table 5.3; Figures 5.1, 5.10).

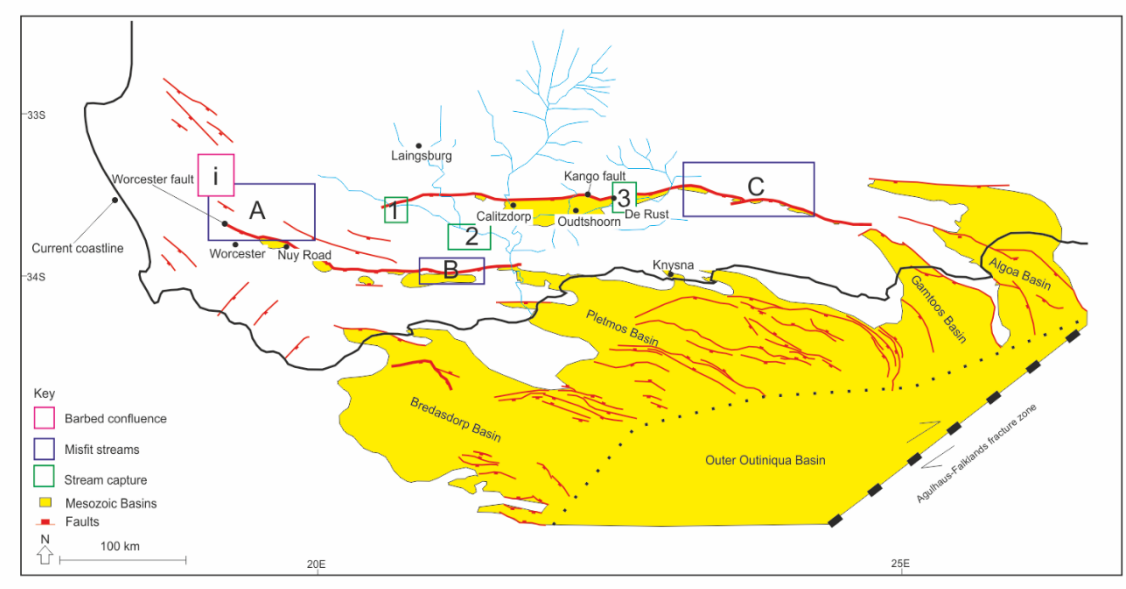

Figure 5.9a *- Geomorphic evidence of drainage reorganisation: insets A), B) and; C) misfit streams; 1), 2) and 3); stream capture points and i), barbed confluences can be found on Figure 5.9b.*

The one exception is a catchment in Bolivia (Insel et al., 2010), in which the erosion rates are extremely high in this location due to the tectonic activity of the Andes. The catchment at Garcia Pass (Figure 5.9, inset a), does not have an anomalous volume, however Rogers (1903) identified a wind gap at this location related to the previous Buffels River course. Our data indicates that the stream capture took place prior to the full exhumation of the Cape Supergroup.

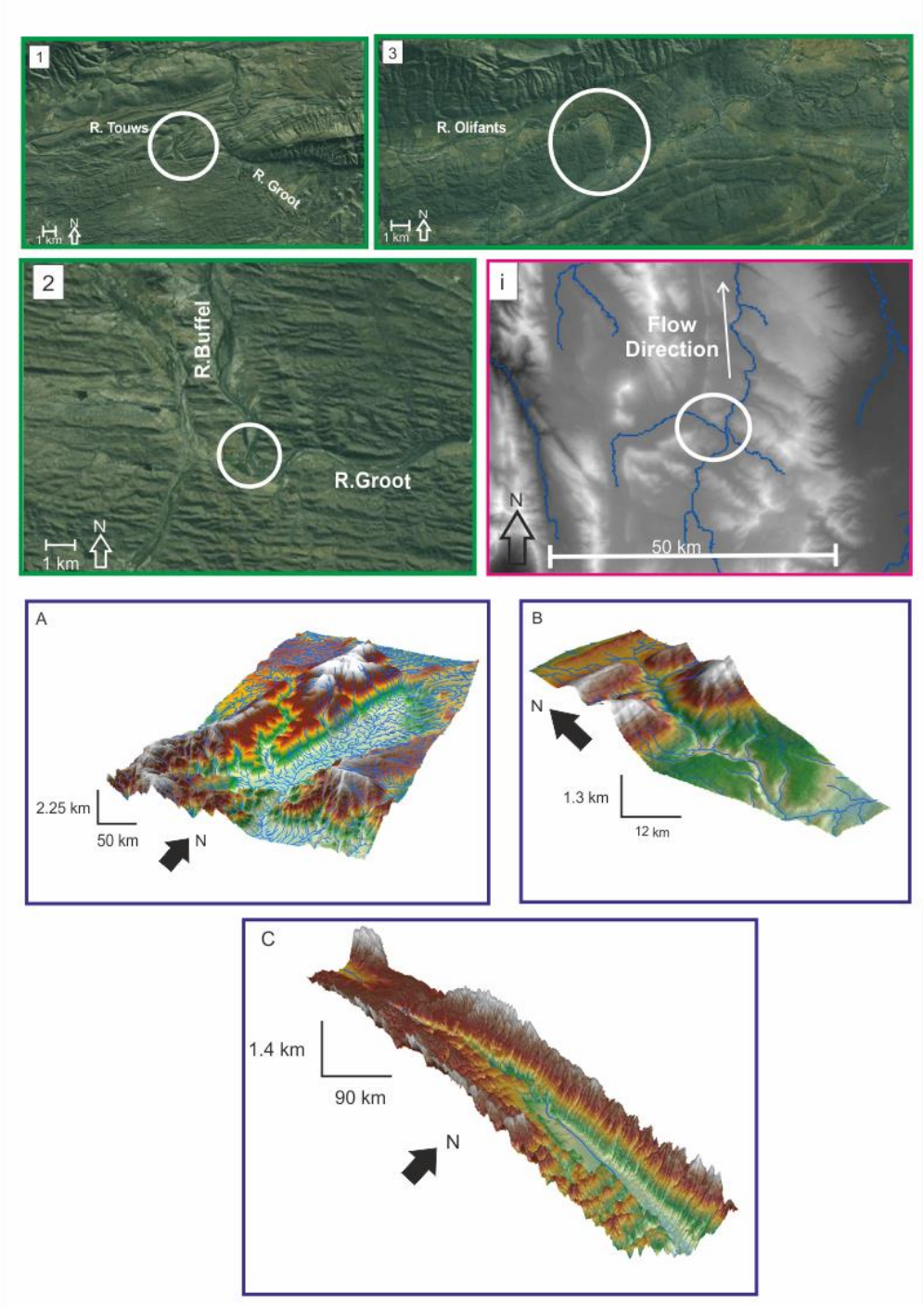

Figure 5.9b *- Geomorphic evidence of drainage reorganisation: insets A), B) and; C) misfit streams; 1), 2) and 3); stream capture points and i), barbed confluences, locations can be found on Figure 5.9a.*

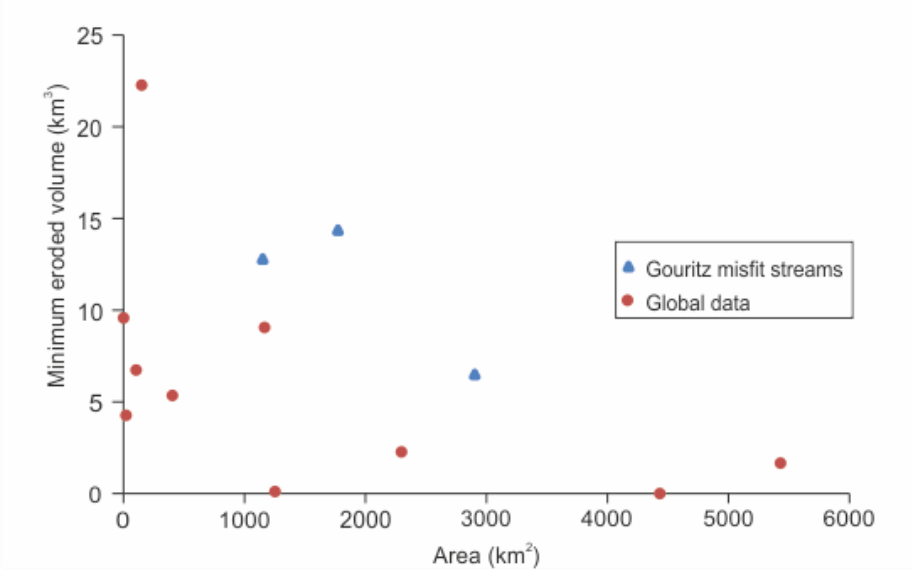

Figure 5.10 *- Comparison of how misfit the valleys in South Africa are compared to worldwide examples. The world wide sample data information can be found in Table 5.3.*

5.5.4 Cosmogenic dating

The strath terrace dated at Gamkaskloof (Swartberg Range), is at a height of 90 m above the current day river, with incision rates of 1.22 mMa^{-1} +/- 0.02 (Figure 5.6). This indicates that the incision from the strath height to the current river took ~73 Ma. Incision of the material above the sample location must have been occurring by the start of the Cretaceous or earlier, and does not account for the removal of overlying stratigraphy at this location. Despite this crude calculation and variation in incision rates, it does indicate that the Gamka River was most likely in place during the Cretaceous. Alternatively, the Gamka River could have formed more recently (30-20 Ma) (Green et al. 2016), with ~1 km incision into the resistant Cape Suerpgroup (Swartberg Range). However, this rapid incision does not support published AFTT or cosmogenic studies (e.g., Tinker et al., 2008a, b; Scharf et al., 2013; Kounov et al., 2015), or offshore depositional record, and is discussed later.

5.6 Discussion

5.6.1 Antecedence of the catchment

The rivers in southern South Africa have undergone significant re-organisation since the break-up of Gondwana (Partridge and Maud, 1997; De Wit et al., 2000; Goudie 2005), and this is the case for the Gouritz catchment. As Gondwana started to rift, reactivation of thrust faults as long extensional faults (Paton et al., 2006) led to the development of half-graben systems with sedimentation and the initiation of net southward draining river systems on the rift margin (Gilchrist et al., 1994). The small coastal draining rivers would have eroded headward, due to the reduction of base

level at the newly formed coastline capturing internal draining catchments (Gilchrist et al., 1994) that eroded into the youngest unlithified shallowly buried deposits.

Prior to the full exhumation, the large southerly drainage systems are interpreted to have been in place and are antecedent as shown by their superimposed planform into resistant quartzites (Rogers, 1903), bedrock meanders with high gradients (Chapter 8), and the deeply incised confluence of the Olifants and Gouritz rivers. Additional support comes from estimates using cosmogenic dating of terraces in Gamkaskloof, in which the rivers had incised down 90m above the present day river by the end of the Cretaceous.

Superimposition, supported by AFTT analysis (e.g., Tinker et al., 2008a), requires a vertical component of incision (Maw, 1866; Gilbert, 1877; Rogers, 1903; Partridge et al., 2010), and is unlikely to have been formed solely by headward erosion from the coast (e.g., Gilchrist et al., 1994). The evidence stated above clearly shows that the main trunk rivers are ancient. Further evidence is shown by the drainage capture sites, which indicate a long-time period of catchment evolution, especially when considering the resistant lithologies of the catchment. The capture sites support interpretations of the drainage evolution of the surrounding area and can be supplemented by the sedimentological observations of the conglomerates. In a more recent setting, capture sites are more obvious (e.g., Mather et al., 2000), however since the main period of catchment evolution discussed below is the Cretaceous much of the evidence of drainage rearrangement has been eroded, and can be speculative in some cases. However, by incorporating sedimentology, misfit streams, and cosmogenic dating, the uncertainty associated with interpreting stream capture sites can be reduced.

5.6.2 Evolution of onshore sedimentary basins

The onshore basin-fills are remnants of half-graben subsidence, in-filling up to 2 km (Green et al., 2016) and incision (Figure 5.11). The number of cycles and relative timing of different half-graben remains elusive. The clast composition of the remnant fill can be used place constraints on the different evolutionary histories in relation to exhumation of the Karoo and Cape supergroups, and potential source areas. Karoo Supergroup clasts dominate the Worcester Basin (Figure 5.2). This suggests that at the time of deposition, the depth of exhumation had not reached the Witteberg Group quartzites, which would have produced larger and more resistant clasts than the Karoo Supergroup (Figure 5.8). The present-day distribution of Karoo

Supergroup outcrops supports the presence of a drainage basin farther north (Figure 5.2). The absence of dolerite clasts may be used to place a northern limit to the source area (Figure 5.2). Karoo Supergroup rocks are unconformably overlain by the Uitenhage Group conglomerates in the Worcester Basin indicating exhumation before accumulation during the formation of the Worcester Basin. The small clast size and clast roundness, and the large amount of sand, suggests reasonable transport distances. The absence of material in the Worcester Basin indicating local Cape Supergroup provenance could be due to erosion (Green et al., 2016). No clasts of the upper Beaufort Group are found within the conglomerate, this could be a function of the shallowly buried and weakly lithified siltstone / sandstone sediments, which are easily eroded as matrix. The lack of Drakensberg clasts in the conglomerate does not prove that the Drakensberg lithologies did not extend into the Western Cape (Hanson et al., 2009; Green et al., 2016), as volcanic material would be easily removed during the large scale exhumation (Tinker, 2005). The Oudtshoorn and De Rust basin clasts are primarily Table Mountain Group quartzites, which crop out at the basin margins (Figure 5.2) and indicates deeper exhumation at this location at the time of basin formation and filling compared to the Worcester Basin.

5. 6.2 Drainage basins reconstruction

In the late Jurassic – Early Cretaceous (after Gondwana rifting), the rivers meandered (as shown by the superimposed planform, Figure 5.11) and incised into the youngest infill of the Karoo Basin, shallowly buried volcanic (westward equivalent of Drakensburg) and fluvial deposits of the upper Beaufort Group. During incision, and net southward drainage, the rivers encountered increasingly deeply buried and more resistant rocks (Tinker et al., 2008a). The precise relationship between incision and local uplift and subsidence patterns during fault reactivation, is largely speculative. Nonetheless, the superimposed river systems, deposition of the Enon conglomerate and published apatite fission track studies (Brown et al., 1990; Brown et al., 2002; Tinker et al., 2008a) and offshore basin stratigraphy (Dingle, 1973; Brown, 1995; McMillan et al., 1997; Paton and Underhill, 2004; Tinker et al., 2008b; Sonibare et al., 2015) indicate large volumes of material exhumed and transported offshore in the Early Cretaceous. The exhumation was by efficient and well established fluvial networks that were established early (Figure 5.11; e.g., similar to the Eastern Cape - Hattingh, 2008).

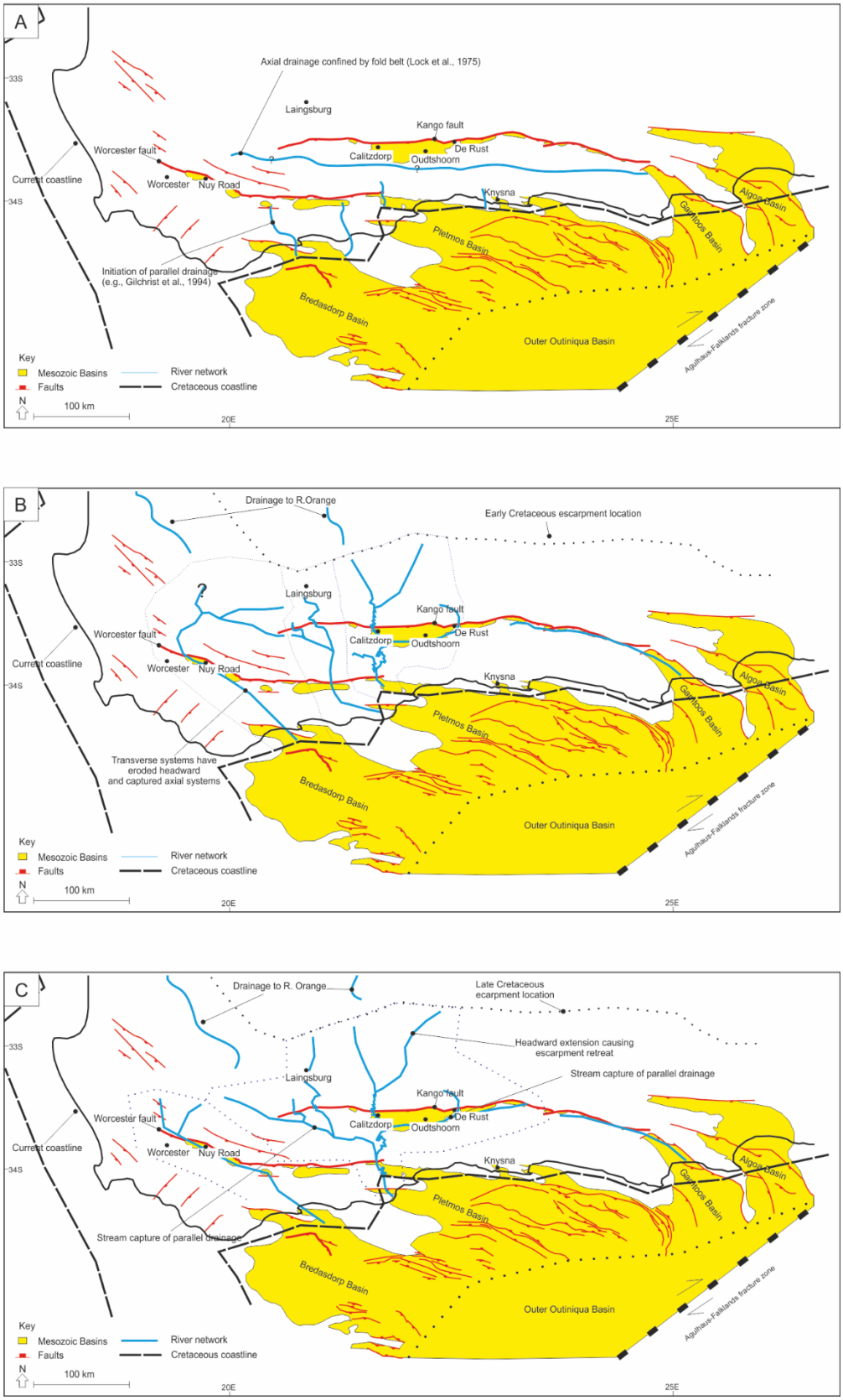

Figure 5.11 *– Drainage evolution of southern South Africa during the a) pre-rifting of Gondwana; b) early Cretaceous and; C) Late Cretaceous. The synthesis draws on aspects of modelling by Gilchrist et al., 1994 and the belief that the palaeodrainage was to the south in the pre-Cretaceous (Lock*

et al., 1975), as well as work by Rogers, (1903). These studies have been integrated into the data found within this chapter.

The deposition of the Mesozoic conglomerate in onshore half-graben basins was coeval with the large-scale exhumation and incision of the Cape Supergroup. In the case of the western Oudtshoorn Basin, this suggests that transverse and axial drainage systems, and large-scale erosion of the bedrock and sediment accumulation, was penecontemporaneous but <1 km apart. Coeval axial and transverse drainages are well documented in tectonically-active settings, with relief increasing due to tectonic activity related to the early stage of mountain growth) and are feature of many mountain ranges of the world (e.g., Davis, 1889; Oberlander, 1985; Hovius, 1996; Ramsey et al., 2008; Babault et al., 2012; Grosjean et al., 2015). The interplay between axial and transverse rivers is not well-documented using deposits alone (Szwarc et al., 2015). Many facies models related to basins in continental rift settings emphasise a large component of axial deposition with minor flank-draining transverse systems (e.g., Leeder and Gawthorpe, 1987; Schlische, 1992). These models do not take into account large cross-cutting transverse river systems (e.g., Gawthorpe and Leeder, 2000) that can be a large component of rift settings after headward erosion of transverse systems and integration of the entire drainage net (axial and transverse systems) (e.g., Gilchrist et al., 1994). In the case of the Gouritz catchment, there was large-scale net deposition within the axial river system and net erosion within the large transverse river system during the Cretaceous due to the position of drainage networks with respect to areas of uplift (erosion) and subsidence (deposition). We speculate that the integration of the drainage net occurred rapidly in this location. The lack of deposits in the transverse rivers is due to the low preservation potential within bedrock channels due to high stream powers and the net erosional setting (Hancock et al., 1998). This leads to efficient bypass of sediment to the offshore basins and does not indicate that the transverse systems were inactive during the deposition of the Uitenhage Group as postulated by Rogers (1903).

During the Early Cretaceous, there were drainage divides within the Olifants River, due to pre-rift strata (Paton, 2006). Stream capture sites and a large-scale misfit stream suggest that part of the river system drained through the Oudtshoorn Basin to the confluence with the Gamka River, and part drained eastward and discharged

into the Indian Ocean at Jeffreys Bay (Figures 5.9, 5.10). Drainage divides are interpreted to have been present in the Touws River area, with westward stream flow to the Worcester Basin (Breede River), and partly to the east into the Buffels River, as supported by the provenance of the Mesozoic conglomerates in the Worcester Basin (Figure 5.8). The Buffels River drained south, and influenced the onshore Heidelberg Basin as a conduit for sediment, as shown by the wind gap at Garcia Pass (Rogers, 1903).

Apatite fission track work by Green et al. (2016) concluded that there was 1.5 km or more of deposits that covered the remnant Enon conglomerate outcrops in the Oudtshoorn Basin (Figure 5.11). The material above the Enon conglomerate could represent one phase of net deposition, although Green et al. (2016) speculate the material could be detritus from the Cango Inlier or related to post-Drakensberg volcanism as the Uitenhage Group shows high chlorine content, which is related to a volcanic source. The deposition of this material could have diverted the Olifants River within the floodplain, or formed epigenetic gorges (e.g., Ouimet et al. 2008). However, exhumation of the Cape Supergroup, and the CFB as a geomorphic feature towards the south, would have limited the space into which the river could have migrated. The Gamka River was able to incise the Cape Supergroup and was likely to continue as a conduit of sediment bypass during this period of sedimentation in the Outdshoorn Basin. Green et al. (2016) also argued for episodic block uplift, however, this would not change the overall regional gradient of the Western Cape and the rivers would still drain southward. The record of episodic uplift can no longer be seen in the current river morphometric indices (Chapter 8). However, at the time of block uplift, propagating knickpoints would have formed during river adjustment to new regional base levels (e.g., Seidl et al., 1994, 1997; Wohl et al., 1994; Weissel and Seidl 1998; Stock and Montgomery, 1999), with faster response times to larger tectonic perturbations (Whittaker and Boulton, 2012). In addition, due to the high erosive power of the rivers during this time as documented by the Enon Conglomerate (Hattingh, 2008) and the formation of transverse drainage systems, it is likely the rivers would have been able to keep pace with this uplift rather than be deflected by it (e.g., Westaway et al., 2006; Stokes et al., 2008; Douglass et al., 2009). This is due to the large catchment areas of the transverse trunk rivers, resulting in high stream power and knickpoint development (e.g., Burbank et al., 1996; Bishop et al., 2005). During uplift, large trunk rivers will try to maintain their gradients, which could result in aggradation upstream (Burbank et al., 1996). If aggradation keeps pace with, or exceeds, uplift

then the river will remain discordant to the structure due to the maintenance of the long profile gradient and resulting impacts on stream power (Burbank et al., 1996, Humphrey and Konrad, 2000). There is no evidence of upstream aggradation remaining within the catchment, due to the large-scale denudation of southern South Africa (Tinker et al., 2008a; Green et al., 2016). If uplift exceeds aggradation then the transverse rivers must erode the block. In this case, the resistance of the block becomes a dominant control on the development of discordant rivers (Burbank et al., 1996). The trunk rivers were capable of incising deeply into quartzite, which indicates the rivers were powerful and likely to have eroded more easily the younger less resistant stratigraphy above the Table Mountain Group (Figure 5.2). The morphometric indices of the Gouritz catchment indicate that the smaller stream order catchments are structurally-controlled within the CFB with trellised stream patterns, whereas the trunk rivers simply dissect the fold belt, with straight sections of the long profiles seen within the CFB region (Chapter 8). Furthermore, incising rivers can control deformation and isostatic adjustment (e.g., Simpson, 2004) and therefore control the landscape development of the uplift zone.

The Groot River is interpreted to have captured the Buffels and Touws rivers, as indicated by the right-angled confluence (Figure 5.9) (Rogers, 1903). Stream captures could have occurred within the Olifants River (Figure 5.9), most likely resulting in a large-scale misfit stream towards the east (Figure 5.9). The climate of the Western Cape Province has not changed significantly since the Cretaceous (Bakker and Mercer, 1986) and the area is relatively stable tectonically compared to the Cretaceous as shown by the lack of scarps and reduction in sediment production (e.g., Tinker et al., 2008b; Bierman et al., 2014). Therefore, stream capture is the preferred mechanism to explain the misfit streams. Further development towards the north of the Gouritz catchment due to the retreat of the escarpment extended the catchment and caused capture of the Orange River catchment area. Stream capture of the Hex River by the Touws River (Gouritz catchment) has reduced the size of the Breede catchment since the Cretaceous.

Many researchers argue on the basis of AFTT that large-scale exhumation had finished by the end of the Cretaceous (Gilchrist et al., 1994; Gallagher and Brown, 1999; Cockburn et al., 2000; Brown et al., 2002; Tinker et al., 2008a; Kounov et al., 2009; Flowers and Schoene, 2010), with minor changes to the present day physiography (Partridge, 1998; Brown et al., 2000; Brown et al., 2002; Doucouré and de Wit 2003; de Wit 2007; Tinker et al., 2008a; Kounov et al., 2015). Additional

evidence is shown by a reduction in offshore sediment volumes (Tinker et al., 2008 b; Hirsch et al., 2010; Dalton et al., 2015; Sonibare et al., 2015), low Cenozoic cosmogenic erosion rates (e.g., Fleming et al., 1999; Cockburn et al., 2000; Bierman and Caffee, 2001; van der Wateran and Dunai, 2001; Kounov et al., 2007; Codilean et al., 2008; Dirks et al., 2010; Decker et al., 2011; Erlanger et al., 2012; Chadwick et al., 2013; Decker et al., 2013; Scharf et al., 2013; Bierman et al., 2014; Kounov et al., 2015) and differential erosion of kimberlite pipes (Hawthorne, 1975; Gilchrist et al., 1994; de Wit, 1999). Locally, offshore sedimentation in the Cenozoic is significant, but is minor compared to Mesozoic deposition (e.g., Tinker et al., 2008 b; Hirsch et al., 2010; Dalton et al., 2015; Sonibare et al., 2015). Despite the evidence above, this scenario has been disputed by Burke (1996) and Green et al. (2016) who argue for a younger age of landscape development. Burke (1996) argued the topography and Great Escarpment was formed due to uplift at 30Ma, and related to the African plate coming to rest with relation to the underlying mantle. Burke (1996) also argued that the Cretaceous South Africa was covered in marine sediments. However, the crater facies of kimberlite pipes indicate lacustrine conditions based on fossils (Hawthorne, 1975; Smith 1986). Green et al. (2016) argued for younger active landscape development based on AFTT data, and argued that the deep bedrock gorges within the CFB were formed during the Cenozoic, when there was differential denudation with higher erosion within the Swartberg Mountain range (CFB) as shown by Cenozoic cooling (30-20 Ma). However, Green et al.'s (2016) samples were not collected near the large cross-cutting transverse rivers of the Gouritz catchment (e.g., Gouritz River), and were from smaller subcatchments that dissect the CFB (with current catchment areas of 179 km^2 and 1060 km^2). The samples showing Cenozoic cooling were taken at the base of the Swartberg Mountain, near the current river bed, and do not indicate that the large trunk rivers were not already active, and eroding the ~1 km of material above the sample. Green et al.'s (2016) data can only be used to indicate that there was additional uplift at 30-20Ma, whereby the lower section of the gorges were cut in the Cenozoic. The CFB is an exhumed mountain belt that formed in the Permo-Triassic (Tankard et al. 2009), and the uplift implied from the AFTT data represents the latest stage of landscape development to affect the region after denudation leading to exhumation of the mountain chain. Therefore, successively younger ages towards the base of a mountain are to be expected. The localised nature of the samples and the proposed uplift probably relates to fault relaxation or isostatic uplift due to the large amount of Cretaceous exhumation; the recent tectonic pulse is not seen within morphometric indices of the Gouritz Catchment (Chapter 8). Based on

the above considerations, it is therefore argued that by the end of the Cretaceous the current watershed of the Gouritz catchment was mostly in place with the main trunk rivers active and depositing material offshore South Africa (Figure 5.11).

5.6.3 Crustal implications of large-scale exhumation

Using the median exhumation values, ~ 15 km of exhumation has occurred across southern South Africa, with the largest amount of exhumation over the CFB. This result is within the constraints provided by the metamorphic facies of the CFB (Frimmel et al., 2001). AFFT studies also show large-scale denudation, but values are not as high as using the cross sectional reconstruction method used in this study (e.g., Tinker et al., 2008a). This could be because of the thermal gradient used and the altitude of the samples for the fission track analysis. Furthermore, the method used places constraints on the absolute upper limit of exhumation. Such large-scale exhumation has important implications for crustal unloading, and could lead to a positive feedback where exhumation leads to further uplift and dissection (e.g., Brown et al., 1990; Simpson, 2004). Coupled with the uplift related to Gondwana rifting, isostatic uplift provides an additional mechanism to explain the anomalous height of southern Africa and the debated uplift history (e.g., Partridge and Maud, 1987; Nyblade and Robinson, 1994; Burke, 1996; Ebinger and Sleep, 1998; Lithgow-Bertelloni and Silver, 1998; Gurnis et al., 2000; Brown et al., 2002; van Der Beek et al., 2002; Doucouré and de Wit, 2003; de Wit 2007; Moore et al., 2009; Tankard et al., 2009).

5.6.4 Where is the ‘missing’ sediment?

The maximum estimated volume of 7.81 x 10^5 km^3 material eroded from the southern drainage basins is larger than the volume of major long-lived submarine fan systems, such as the Amazon Fan, and if point-sourced would result in a fan up to 400 km long (e.g. Sømme et al. 2009). However, there is a mismatch between the estimated onshore erosion and offshore accumulation of sediment. In the Outeniqua Basin and southern Outeniqua Basin, there is a volume of 268 500 km^3 of material (Tinker et al., 2008b). Therefore, ~5.13 x 10^5 km^3 of sediment ‘missing’ (Table 5.4). If the southward draining catchments were active at least in the Early Cretaceous, the missing volume could have been transported deeper offshore via sediment gravity flows (Tinker et al., 2008b).

During rifting, and the deposition of the Uitenhage Group, the Falkland Plateau was located offshore South Africa (Macdonald et al., 2003, Figure 5.12). Adie (1952) first

stated that the Falkland Plateau was in a rotated position east of South Africa, and formed part of the missing SE corner of the Karoo Basin. The amount and timing of Falkland Plateau rotation remains contentious (e.g., Richards et al., 1996; Macdonald et al., 2003; Stone et al., 2009; Richards et al., 2013) and is beyond the scope of this work.

As the Falkland Plateau moved westward along the south side of the Falkland-Agulhus transform fault in the Late Jurassic to Early Cretaceous, the Falkland Plateau Basin developed (Macdonald et al., 2003; Figure 5.12). The Falkland Plateau Basin formed the distal extension of the Pletmos and Bredasdorp basins in the early Aptian (Martin and Hartnady, 1986; Fouché et al., 1992; Ben-Avraham et al., 1993, 1997; Macdonald et al. 2003) or Albian (Ludwig, 1983). A second phase of rifting occurred in the Early Cretaceous resulting in the North Falkland Basin, and the drifting apart of the plateau and the African continental plate (Richards et al., 1996; Fish, 2005; Figure 5.12). Ludwig (1983) argued that the large change in depositional environment on the Maurice Bank from black shales to oxygenated nannofossil claystone is due to the plateau moving past the tip of Africa.

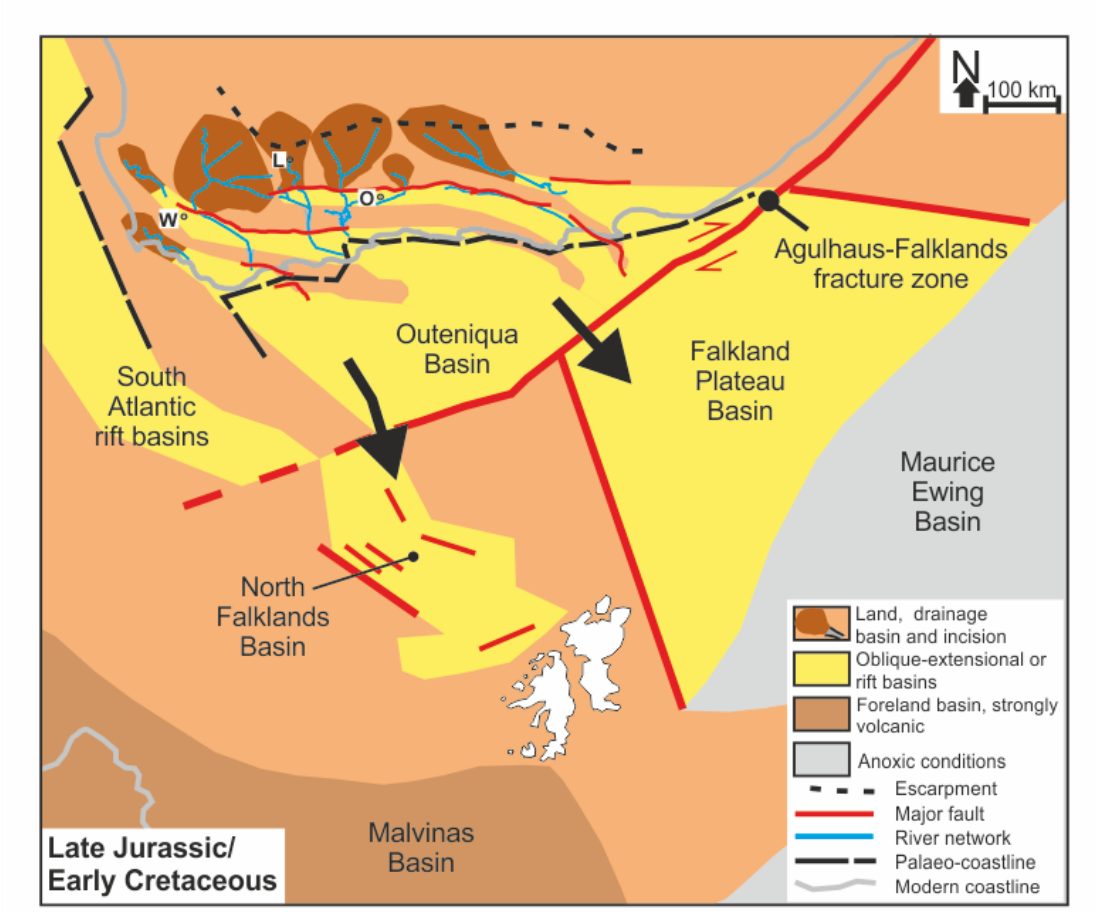

Figure 5.12 *– Palaeogeographic reconstruction of the Late Jurassic to Early Cretaceous of the southern South Atlantic region based on Macdonald et al. (2003; their Figures 11, 13). Note that the Falkland Plateau Basin and the North Falkland Basin could both have been downstream depocentres of the Outeniqua Basin.*

Recent research on the Sea Lion Main Complex (SLMC) discovery in the North Falkland Basin has identified an Early Cretaceous fluvial prodeltaic and turbidite succession in a lacustrine syn-rift sequence (Farrimond et al., 2015; Griffiths 2015). The basin has large amounts of sand deposits (Bunt, 2015; Williams, 2015) and comprise multiple basin-floor fans that offlap into a deep lake basin (Griffiths, 2015). Radiogenic U^{238}/Pb^{206} zircon ages suggest that the SLMC accumulated over <250 ka during the early Aptian. If the Falkland Plateau was offshore South Africa with erosion from the continent and transverse and axial sediment routing then this configuration could account for the large and rapid accumulations of sand in the syn-rift lake basins (Figure 5.12). The SL 10 and 20 fans are ~87 m thick and extend over areas of 115 km^2 (Bunt, 2015). Extra-basinal material is predominantly coarse material of volcanic and metamorphic origin, with rivers draining the sub-aerial basement to the east (Williams, 2015). Williams (2015) states the Sea Lion Main Complex sands are derived largely from a co-existing shallow water system, which we postulate were supplied by the southerly draining river systems of southern South Africa (Figure 5.12). Several authors have commented on the similarity between the stratigraphy of the Falkland Plateau Basin and the offshore Mesozoic basins of southern South Africa (Martin et al., 1981; McMillian et al., 1997). Martin et al. (1981) also argued that between the Late Jurassic and Early Cretaceous, during the rift to drift period, the Bredasdorp, Pletmos-Infanta, Gamtoos, and Algoa basins were the proximal tongues of the large Falkland Plateau Basin (Macdonald et al. 2003). In summary, we posit that the implication of this configuration is that a large proportion of the ‘missing’ sediment exhumed during the Late Jurassic and Early Cretaceous is represented by deposits in rift basins of the northern Falkland Basin and the Falkland Plateau Basin. Indeed, on global sediment thickness maps (Divins, 2003, Figure 5.13) the Falkland Plateau is distinctive due to the thickness of sediment cover and lack of adjacent significant landmass. This configuration means that the sedimentary basins are dislocated by ~6000km from their drainage basins. This highlights the challenges of constraining and quantifying source-to-sink relationships in deep-time and close to active plate boundaries (Romans et al., 2009; Romans and Graham, 2013).

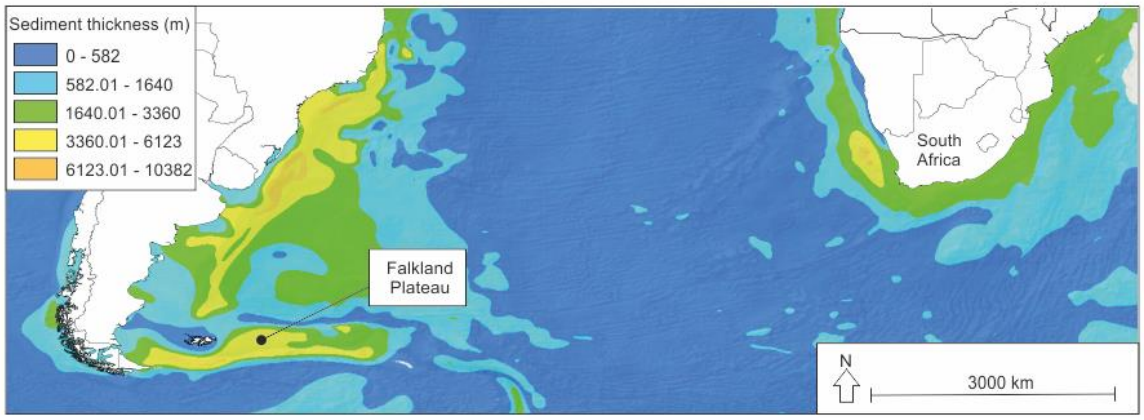

Figure 5.13 *– Sediment thickness map for present-day southern South Atlantic from Divins (2003) and Whittaker et al. (2013). Note the marked disparity of sediment thickness and small land area on the Falkland Plateau. Thickness is in metres.*

5.7 Conclusion

Large-scale exhumation (up to 11 km) during Early Jurassic and Late Cretaceous rifting in southwest South Africa resulted in the deposition of the Uitenhage Group, the only onshore representation of a major phase of landscape denudation. A major mismatch in the volumes of material exhumed onshore and the volume of sediment deposited in offshore basins has been identified by construction of structural cross-sections. Using sedimentology, geomorphology and cosmogenic dating, evolutionary histories of two large-scale discordant basins in the Western Cape have been deciphered for the first time. The catchments have had a complicated history and multiple reorganisations due to stream capture in the Cretaceous. However, the main transverse trunk rivers of the catchments have been long-lived features (up to 145 million years), resulting in extensive offshore sediment deposition. By reconstructing sediment routing patterns and timing of exhumation, we interpret that the location for much of the ‘missing’ sediments is the North Falklands Basin and Falkland Plateau Basin. If this is the case, then the source has been separated from its sink by 6000 km. In order to verify this, further work is needed to analyse the deposits offshore the Falkland plateau and the onshore exhumation history. In addition, cosmogenic dating on drainage routing patterns will constrain the onshore patterns further. Additional fission track studies can be used to assess the exhumation of the CFB by completing a transect.

Chapter 6 Erosion rates constrained by cosmogenic nuclides, in a large antecedent catchment, South Africa; does nature do the averaging?

6.1 Abstract

The ancient landscape of southern Africa preserves large-scale landforms despite its antiquity. Catchment wide denudation rates and point erosion rates were calculated using cosmogenic nuclides and are reported for trunk rivers and strath terraces of the understudied Gouritz catchment. The catchment wide denudation rates indicate low rates up to 11 mMa^{-1} and do not correlate with catchment properties such as slope, catchment area, relief or dissection. Using catchment wide denudation rates on terraces within the Seweweekspoort, there has been a maximum of 200m of incision during the Cenozoic of this small tributary river; by the start of the Cenozoic, there had been significant incision into the Cape Fold Belt. Average catchment denudation rates for catchments that drain a large proportion of the Cape Fold Belt are slightly lower than the trunk rivers that do not, and highlight the resistant nature of the mountain belt. The principal control on denudation cannot be elucidated and probably relates to the general quiescence of South Africa during the Cenozoic and the increasing aridity. Landscapes of different terrains are eroding at similar rates within the catchment and indicate that the Gouritz catchment is in steady-state over geomorphic timescales with nature averaging erosion rates between different terrains. Due to the overall long term stability of the catchment, Hack's landscape model ideas are represented in this catchment; with similar erosion rates in different terrains despite changes in geology and relief.

6.2 Introduction

Advancements in geochronology have allowed earth scientists to constrain landscape evolution more precisely. Cosmogenic analysis has become increasingly popular due to the range of settings that can be dated e.g., strath terraces (e.g., Burbank et al., 1996b; Leland et al., 1998; Pratt-Sitaula et al., 2004; Schaller et al., 2005), glacial moraines (e.g., Phillips et al., 1997; Owen et al., 2005; Barrows et al., 2007; Ballantyne, 2012) and catchment wide denudation rates (e.g., von Blanckenburg, 2005; Vanacker et al., 2007; Delunel et al., 2014). Traditionally, whole catchment erosion rates are collected from sediment trapping or sediment gauging data (Meade, 1988), however, these data are only available over short time-scales (<100 years, Tomkins et al., 2006). Cosmogenic nuclide dating allows a longer term assessment

of denudation rates, which can bridge the gap between geomorphic data collection and longer-term apatite fission track data (Matmon et al., 2003; Vance et al., 2003; Binnie et al., 2006). Catchment wide denudation studies have been undertaken in a range of settings from slowly eroding deserts (e.g., Bierman and Caffee, 2001; Clapp et al., 2002), passive margin settings (e.g., Von Blanckenburg et al., 2004; Vanacker et al., 2007) to tectonic settings with rapid erosion (e.g., Vance et al., 2003, Safran et al., 2005; Derrieux et al., 2014). The application of cosmogenic analysis has been used to question; 1) magnitude, frequency concepts and the role of extreme events (e.g., Tomkins et al., 2007); 2) the buffering capabilities of catchments (e.g., Wittman et al., 2010, Covault et al., 2013) and 3) the influence of morphometrics on erosion, especially in mountainous regions (e.g., Palumbo et al., 2010). Furthermore, cosmogenic analysis can help constrain the relative importance of climate or tectonics (e.g., Bierman et al., 2001; Riebe et al., 2001; von Blanckenburg, 2006, Vanacker et al., 2007; DiBiase et al., 2010; Bellin et al., 2014), which is fundamental in landscape development studies. Cosmogenic data can help constrain and validate landscape models (e.g., Derrieux et al., 2014) and has recently been applied to assess the impact of human activities on erosion rates (e.g., Brown et al., 1998; Hewawasam et al., 2003; Ferrier et al., 2005).

Catchment average denudation has the advantage of incorporating data from a range of geomorphic units and processes e.g., hillslope erosion, landslides, bedrock erosion (von Blanckenburg, 2005) and incorporates both physical and chemical (e.g., weathering) processes, which are integrated over long time scales (10^2-10^5 yrs; Vanacker et al., 2007; Delunel et al., 2014). The ‘let nature do the averaging’ rule encapsulated by von Blanckenburg (2005) is inherent in the application of catchment wide denudation, and argues that the isotopic output of the catchment will be equal to the input, and that the fluvial systems will naturally incorporate grains supplied at different rates and from different source areas. This method assumes the catchment is in isotopic steady state, and that the river sediment is well mixed and sediment storage in the catchment is minimal (von Blanckenburg, 2005; Binnie et al., 2006). However, studies have found that in some situations, such as in catchments with high rates of landsliding, nature does not do the averaging (e.g., Delunel et al., 2014) and that mixing does not occur (e.g., Wittmann et al., 2011). Catchment average denudation has not yet been applied to large-scale ancient catchments in South Africa. Ancient settings e.g., South Africa (Du Toit, 1954; King, 1953) are often related to Gondwana landscapes (Fairbridge, 1968) and incorporate large portions of the Earth (e.g., King 1956a,b; Ollier 1991; Ollier and Pain, 2000, Twidale 2007a, b;

Peulvast and Bétard, 2015). Analysing such landscapes can offer important insights into the assumptions associated with catchment average denudation due to the long time periods associated with their formation.

Geochronological studies applied to southern Africa have shown a substantial decrease in erosion rates from the Cretaceous (up to 175 mMa^{-1}, Gallagher and Brown, 1999; Cockburn et al., 2000; Brown et al., 2002; Tinker et al., 2008b; Kounov et al., 2009 and; Flowers and Schoene, 2010) to the present day (up to 60mMa^{-1}, Fleming et al., 1999; Cockburn et al., 2000; Bierman and Caffee, 2001; van der Wateren and Dunai, 2001; Kounov et al., 2007; Codilean et al., 2008; Dirks et al., 2012; Decker et al., 2011; Erlanger et al., 2012; Chadwick et al., 2013; Decker et al., 2013; Scharf et al., 2013; Bierman et al., 2014; Kounov et al., 2015). However, there is a lack of data from the Western Cape, with small-scale catchments in the Cape Fold Belt (Scharf et al., 2013) and some pediment surfaces and associated drainages analysed (e.g., Bierman et al., 2014; Kounov et al., 2015). Catchment average denudation has not yet been attempted for large-scale catchments such as the Gouritz catchment. The main transverse drainage of South Africa are discordant, with incised meanders and gorges common (Rogers, 1903), however the rates of catchment erosion and timing of incision into the Cape Fold Belt has not been assessed in detail (e.g., Scharf et al., 2013; Green et al., 2016). Ages of formation of the gorges that dissect the Cape Fold Belt are also contentious and range from Cretaceous (Taljaard, 1948, 1949; Lenz, 1957; Tinker et al., 2008a) to Cenozoic (Davis, 1906; Taljaard, 1948, 1949; Green et al., 2016). Further constraints on catchment development and timing of the incision into mountains can be obtained from point erosion data of strath terraces (Schaller et al., 2005).

The aim of this paper is to assess denudation rates reported from river sediment by using *in situ* cosmogenic analysis and to understand variation between the main trunk rivers of Gouritz catchment. This data will be used to assess the assumptions of catchment average denudation. Further, point erosion data using multiple strath terraces of the Cape Fold Belt, will be integrated into the analysis to provide a long term erosion perspective and to ascertain the erosional history related to gorge formation and associated drainage development of the Gouritz catchment.

6.3 Regional settings

The Gouritz catchment, Western Cape Province, South Africa (Figure 6.1) is one of several antecedent systems that drains the Great Escarpment. The Gouritz system is discordant to the underlying Cape Fold Belt (CFB), where superimposition has formed deeply incised meanders (up to 1 km in depth; Rogers, 1903) and gorges in the resistant CFB. The catchment has been affected by the Mesozoic break-up of Gondwana and the resulting large-scale exhumation of the Permian-Triassic Cape Fold Belt (Tankard et al. 2009; Flint et al. 2011) and Karoo infill in the Cretaceous (Tinker et al. 2008a). The development and retreat of the Great Escarpment (Fleming et al., 1999; Cockburn et al., 2000; Brown et al., 2002; Moore and Blenkinsop, 2006) has affected the headwaters of the catchment. Based on published geochronology (Fleming et al., 1999; Brown et al., 2002) and numerical modelling (van der Beek, 2002), the escarpment has had a limited retreat (~29 km; Brown et al., 2002).

The Gouritz catchment has an area of 6.45×10^4 km^2, and is composed of six main tributaries, which are bedrock or bedrock-alluvial in nature; the Traka, Touws, Buffels, Olifants, Dwyka and Gamka Rivers (Figure 6.1). Physiographically, the catchment can be split into the following components; escarpment, central Karoo, Cape Fold Belt and coastal (Chapter 8, Figure 6.2). There is no sediment transport data available for the catchment, however the bedforms in the ephemeral river indicate that boulders to sand-grade material is transported as bedload.

The Cretaceous period of South Africa (and the development of the major drainage network, Chapter 5) was humid and hot (Dingle et al., 1983; Partridge and Maud, 2000), and since then there has been a trend towards a more arid environment (Bakker and Mercer, 1986). The current climate of the system is semi-arid with mean annual precipitation of 262 mm (CSIR, 2007). The region has a clear split between summer and winter rainfall regimes, with late summer to winter rainfall in the Great Escarpment and central Karoo region, winter rainfall in the western CFB, late summer to winter rainfall in the southern CFB, and summer and winter rainfall in the coastal areas (CSIR, 2007). The lower part of the catchment in the coastal region has a Mediterranean-type climate (Midgley et al., 2003). Orographic rainfall over the CFB provides much of the discharge (Midgley et al., 2003), with the other main source being intense thunderstorms that usually form on the escarpment and move south over the central Karoo. Smaller tributaries in the upper reaches of many of the larger trunk rivers are ephemeral however south of the CFB, trunk rivers are perennial.

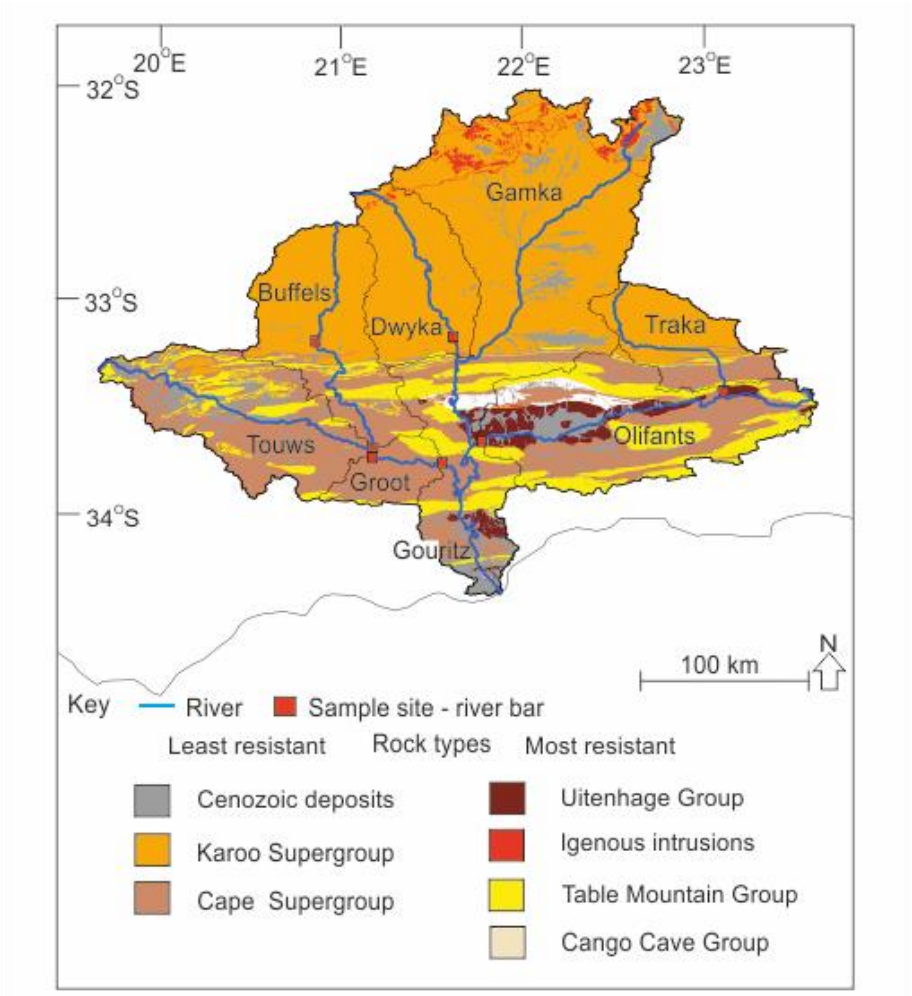

Figure 6.1 *– The trunk rivers and subcatchments of the Gouritz catchment where catchment wide denudation samples were taken from river bars. Simplified geology of the catchment with the key rock types.*

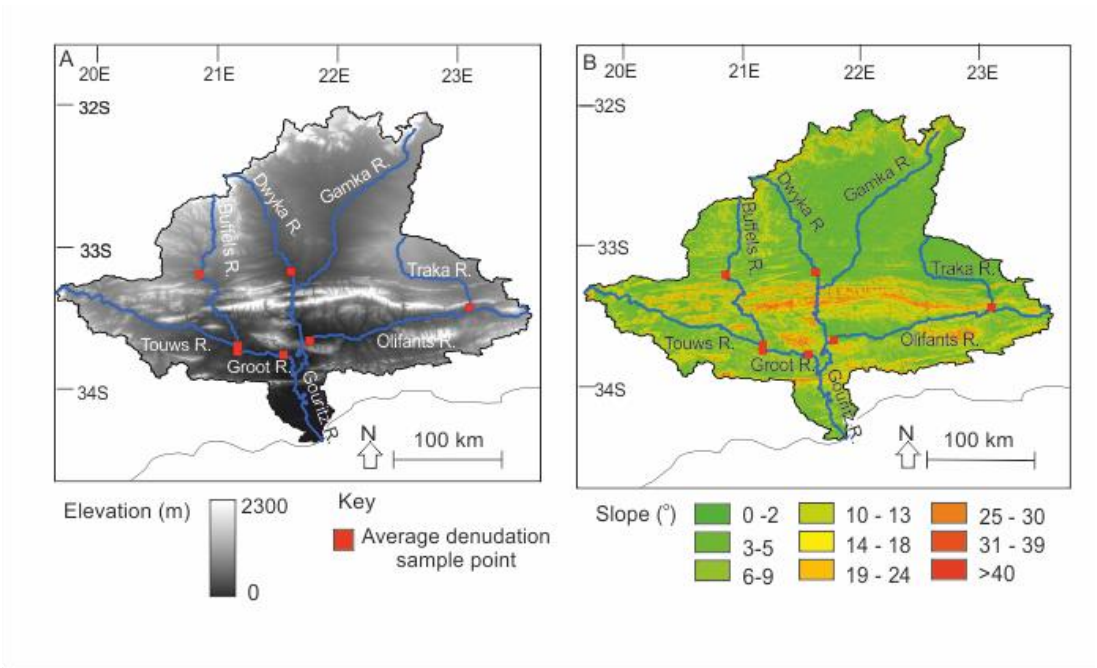

Figure 6.2 *– Gouritz catchment and trunk rivers, with A) terrain and B) slope.*

The geology of the catchment is dominated by lithologies of the Cape and Karoo supergroups. The Cape Supergroup has been metamorphosed to a lower greenschist facies (Frimmel et al., 2001), and is composed of sandstone and mudstones. Resistant quartzites form the backbone of the geomorphic expression of the Cape Fold Belt, in which the E-W folds decrease in amplitude towards the north (Paton, 2006; Spikings et al., 2015). The Karoo Supergroup is composed of various amounts of mudstones and sandstones, and represents a transition from deep marine to fully fluvial succession (e.g., Flint et al., 2011). The bedrock of the Gouritz catchment includes various inliers such as Cango Cave Group, composed of limestones, mudstones and arenites, Jurassic dolerite intrusions, which are dominantly towards the north of the catchment, and granitic plutons in the coastal areas. Mesozoic sediments are composed of conglomeratic and sandy units. Chapter 8 shows lithological variation and associated resistance has a dominant control on catchment morphometrics such as hypsometry and stream length gradient.

The catchment is dominated by large-scale reactivated extensional faults within the Cape Fold Belt e.g., Cango and Worcester Faults (Paton and Underhill 2004, Paton et al., 2006, Paton 2006). The Swartberg and Langeberg ranges are two large anticlines within the catchment. The Gouritz catchment is currently tectonically quiescent, with a lack of fault scarps, low seismicity (Bierman et al., 2014), and low rates of sediment supply (Kounov et al., 2007; Scharf et al., 2013). However, the tectonic history of the area is contentious (Burke, 1996; Gallagher and Brown, 1999; Brown et al., 2002; Tinker et al., 2008a; Kounov et al., 2009; Decker et al., 2013) with recent uplift argued for 30 Ma (Burke, 1996; Green et al., 2015) and a major Pleistocene phase of uplift of 100 – 900 m Partridge and Maud (1987).

6.3.1 Sample locations

The samples were taken from the Touws, Traka, Olifants, Groot and Dwyka rivers. The trunk river catchment areas range in size from 4362 – 18,500 km^2 (Tables 6.1, 6.2; Figure 6.3). Strath terraces were also analysed in the Seweweekspoort and Gamakaskloof (Figure 6.3; Table 6.1), which are two of several fluvial breaches of the Cape Fold Belt (Figure 6.3). The Seweweekspoort River used to have a larger catchment area but has undergone stream capture (Chapter 8). Several accessible strath terraces were analysed at various heights within the Seweweekspoort (Figure 6.4).

Table 6.1 *– Sample information for the river (catchment wide denudation) and strath terrace samples.*

Nr	Sample ID	Sample type	name	Latitude (D.D)	Longitude (D.D)	Elevation (m)	Topographic shielding
1	SA_RGO_RTR	River	Traka River	-33.1892	22.87538	879	0.990
2	SA_RGO_RGR	River	Groot River	-33.3934	20.75262	819	0.990
3	SA_RGO_RTO	River	Touws River	-33.5369	20.45742	803	0.990
4	SA_RGO_RDW	River	Dwyka River	-32.8921	21.39987	712	0.990
5	SA_RGO_RBU	River	Buffels River	-33.1367	20.93503	923	0.990
6	SA_RGO_ROL	River	Olifants River	-33.4674	22.66461	798	0.990
7	SA_SS_SURF7	Bedrock surface	Seweweekspoort	-33.2480	21.24242	801	0.850
8	SA_SS_SURF6	Bedrock surface	Seweweekspoort	-33.2480	21.24242	799	
9	SA_SS_SURF5	Bedrock surface	Seweweekspoort	-33.2480	21.24251	799	
10	SA_SS_SURF4	Bedrock surface	Seweweekspoort	-33.2480	21.24254	800	
11	SA_SS_SURF8	Bedrock surface	Seweweekspoort	-33.2585	21.24476	640	

12	SA_SS_SURF10	Bedrock surface	Seweweekspoort	-33.2499	21.23802	768
13	SA_SS_SURF9	Bedrock surface	Seweweekspoort	-33.2585	21.24411	680
14	SA_SS_SURF11	Bedrock surface	Seweweekspoort	-33.2500	21.23832	720
15	SA-SS_SURF3	Bedrock surface	Seweweekspoort	-33.2518	21.40356	929
16	SA-SS_SURF2	Bedrock surface	Seweweekspoort	-33.2518	21.40343	930
17	SA-SS_SURF1	Bedrock surface	Seweweekspoort	-33.2518	21.40327	931

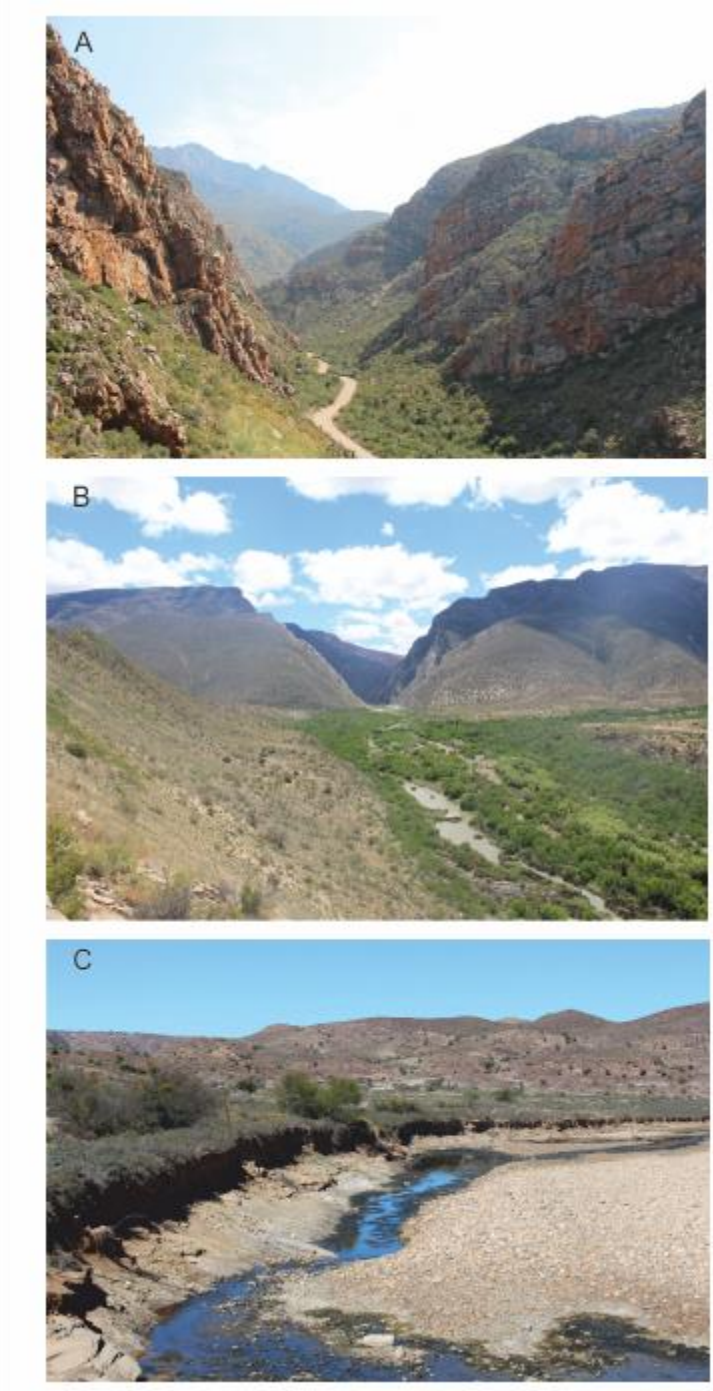

Figure 6.3 *– Cape Fold Belt gorges; A) Seweweekspoort and; B) Gamkaskloof; C) example catchment wide denudation sample site, the Touws River.*

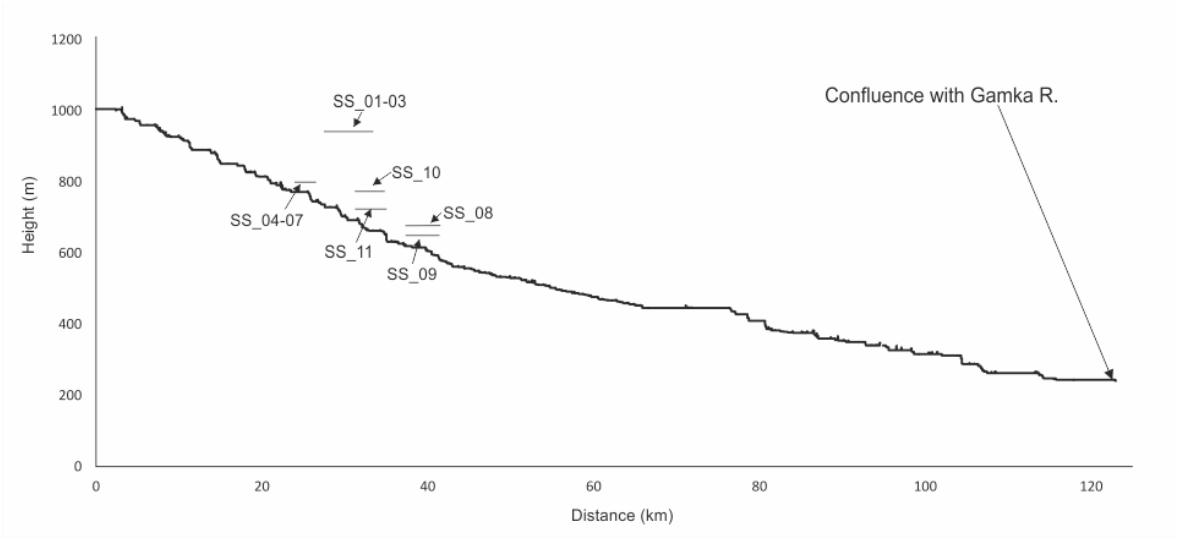

Figure 6.4 *– Long profile of Seweweekspoort and the location of the strath terraces.*

6.4 Method

6.4.1 Cosmogenic dating

The samples were collected from large trunk rivers of the Gouritz catchment to assess catchment average denudation (Figure 6.3) rates, further strath terraces were analysed within the Seweweekspoort using catchment average denudation rates(Tables 6.2, 6.3; Figure 6.4). The river samples were then sieved and the 250 to 500 µm grain size extracted. The ^{10}Be was extracted from purified sand using standard methods described in von Blanckenburg et al. (1996, 2004). The ^{10}Be/^{9}Be ratios were measured in BeO targets with accelerator mass spectrometry at ETH Zürich (Kubik and Christl, 2010). The samples were normalised to the ETH in-house secondary standard S2007N. Between 154 and 157 µg of ^{9}Be carrier was added to each sample, which was used to calculate the percentage of ^{10}Be present in the sample. The calculated ^{10}Be concentrations and analytical errors are shown in Tables 6.2 and 6.3. Uncertainties are propagated from AMS counting statistics and the 39% error on the blank sample. The CRONUS calculator (Balco et al., 2008) was then used, with the calculated ^{10}Be concentrations to calculate the erosion rates (reported using the Dunai, 2001 scheme). The catchment average shielding value was used for the river samples following the method of Norton and Vanacker (2009).

6.4.2 ArcGIS

Catchment topography from a digital elevation model (DEM) based on ASTER (30m) data was reprojected into WGS 1984 world Mercator coordinates. Catchments were delineated using the hydrology toolbox in ArcGIS 10.1. Following Abdelkareem et al. (2012) and Ghosh et al. (2015) a con value of 3000 was used to delineate stream networks. The individual subcatchments related to the catchment wide denudation

samples were delineated and area, relief (Eq. 6.1), dissection (Eq. 6.2) and slope extracted. Stratigraphic unit, rock type and structural geological data sets were obtained digitally from the Council of Geoscience, at a scale of 1:250,000. The stratigraphic units were simplified into key groups and Supergroups (Figure 6.1).

$$Relief = maximum\ elevation - minimum\ elevation \quad \text{Eq.6.1}$$

$$Dissection = mean\ elevation - minimum\ elevation \quad \text{Eq.6.2}$$

6.5 Results

The catchment wide denudation rates range from 3.10 to 11.90 mMa^{-1}, however most of the trunk rivers have rates below 5.00 mMa-1, except the Dwyka River which has the highest rates of 11.90 mMa^{-1} (Tables 6.1, 6.2). The catchment wide denudation rates appears to be independent of catchment properties as they do not correlate (R^2 value <0.25) with catchment morphometric parameters such as area, relief, dissection or mean slope (Figure 6.5).

Using the strath terrace data, and the average denudation rate of 6.40mMa^{-1}, incision time to the present day river of the small tributary ranges from Late Cenozoic for the highest samples to Pliocene for some of the lowest samples (Figure 6.4 and 6.6). The terraces are a maximum of 210 above the current day river (Figure 6.4). The data indicates that prior to the Cenozoic, significant incision had occurred within these tributary rivers.

Table 6.2 *– Cosmogenic averaged denudation data and subcatchment morphometrics including area, slope, dissection and relief.*

Nr	Sample	10Be concentration	Error 10Be conc	Denudation rate (mMa-1)	Denudation rate error (1S)	Area (km2)	Mean slope (°)	Relief (m)	Dissection (m)
1	SA_RGO_RTR	1.144E+06	1.217E+04	3.49	0.004	4362	2.92	1298	301.34
2	SA_RGO_RGR	1.023E+06	1.100E+04	3.78	0.005	18499	5.68	2083	646.33
3	SA_RGO_RTO	1.221E+06	1.296E+04	3.06	0.004	8471	5.56	2010	559.17
4	SA_RGO_RDW	3.268E+05	5.531E+03	11.89	0.021	5845	3.62	1453	360.42
5	SA_RGO_RBU	9.962E+05	1.075E+04	4.22	0.005	8008	5.65	1957	665.88
6	SA-RGO_ROL	1.087E+06	1.170E+04	3.47	0.004	15780	5.70	1934	597.32

Table 6.3 *– Information of strath terraces and time taken to incise to current day river.*

Nr	Strath name	10Be concentration	Error 10Be concentration	Deundation rate (mMa-1)	Denudation rate error (1S)	Height above current day river (m)	Time take to incise to current river location (Ma)	Time period
7	SA_SS_SURF7	2.637E+06	2.673E+04	3.60	0.001	210	58	Late Cenozoic
8	SA_SS_SURF6	4.074E+05	5.489E+03	3.60	0.014	209	58	Late Cenozoic
9	SA_SS_SURF5	2.748E+06	2.783E+04	3.60	0.001	208	57	Late Cenozoic
10	SA_SS_SURF4	9.524E+05	1.040E+04	3.60	0.005	78	21	Mid Cenozoic
11	SA_SS_SURF8	9.337E+05	1.024E+04	3.60	0.004	61	17	Mid Cenozoic
12	SA_SS_SURF10	1.252E+06	1.312E+04	3.60	0.003	41	11	Early Cenozoic
13	SA_SS_SURF9	1.323E+06	1.380E+04	3.60	0.003	40	11	Early Cenozoic
14	SA_SS_SURF11	5.293E+06	5.314E+04	3.60	0.001	39	11	Early Cenozoic

15	SA-SS_SURF3	1.041E+06	1.161E+04	3.60	0.005	39	11	Early Cenozoic
16	SA-SS_SURF2	5.460E+06	5.498E+04	3.60	0.016	30	8	Early Cenozoic
17	SA-SS_SURF1	2.834E+06	2.878E+04	3.60	0.002	21	6	Early Cenozoic
18	SA-DH_SURF3	1.966E+06	2.023E+04	3.60	0.002	90	25	Mid Cenozoic

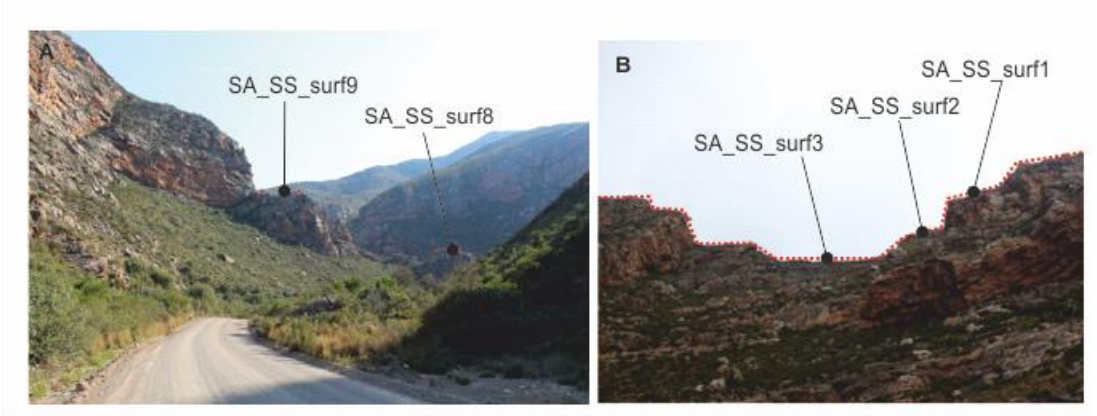

***Figure 6.6**– Example sample sites of the Seweweekspoort; A) samples SA_SS_surf8 and SA_SS_surf9 and; B) SA_SS_surf1, SA_SS_surf2 and SA_SS_surf3.*

6.6 Discussion

6.6.1 Spatial variation in denudation rates

The denudation rates of the Gouritz catchment are globally low (Portenga and Bierman, 2011) and are within the range of published data for southern Africa (Bierman and Caffee, 2001; Codilean et al., 2008; Chadwick et al., 2013; Scharf et al., 2013; Bierman et al., 2014). The variation in catchment wide denudation does not appear to be related to underlying geology in some trunk rivers; the Dwyka and Buffels river drain similar terrain (Escarpment and Central Karoo) with similar geology dominated by the Karoo Supergroup (Beaufort Group) and dolerite intrusions (Figure 6.1) but have denudation rates that vary by ~5mMa^{-1}.The higher rates of denudation in the Dwyka River could be related to the slightly steeper long profile (Figure 6.7, Chapter 8).However, stream gradient indexes are lower within the Dwyka River compared to the other trunk rivers that drain the escarpment (Buffels and Gamka rivers, Chapter 8). The Dwyka River also breaches the escarpment, and may therefore have a high frequency of flooding due to the formation of thunderstorms on the escarpment, which could explain the higher denudation rates. The catchments that contain a large portion of the resistant Cape Fold Belt have lower erosion rates than those dominated by the Karoo Supergroup lithologies and Great Escarpment / Central Karoo physiographic zones. The ‘alpine like’ Cape Fold Belt has been shown to have low denudation rates related to the resistance of the quarzitic lithologies (Scharf et al., 2013). The catchments in this study show similar denudation rates to Scharf et al. (2013) despite their larger areas. The strath terrace data corroborate the denudation rates in the Cape Fold Belt (Table 6.3).

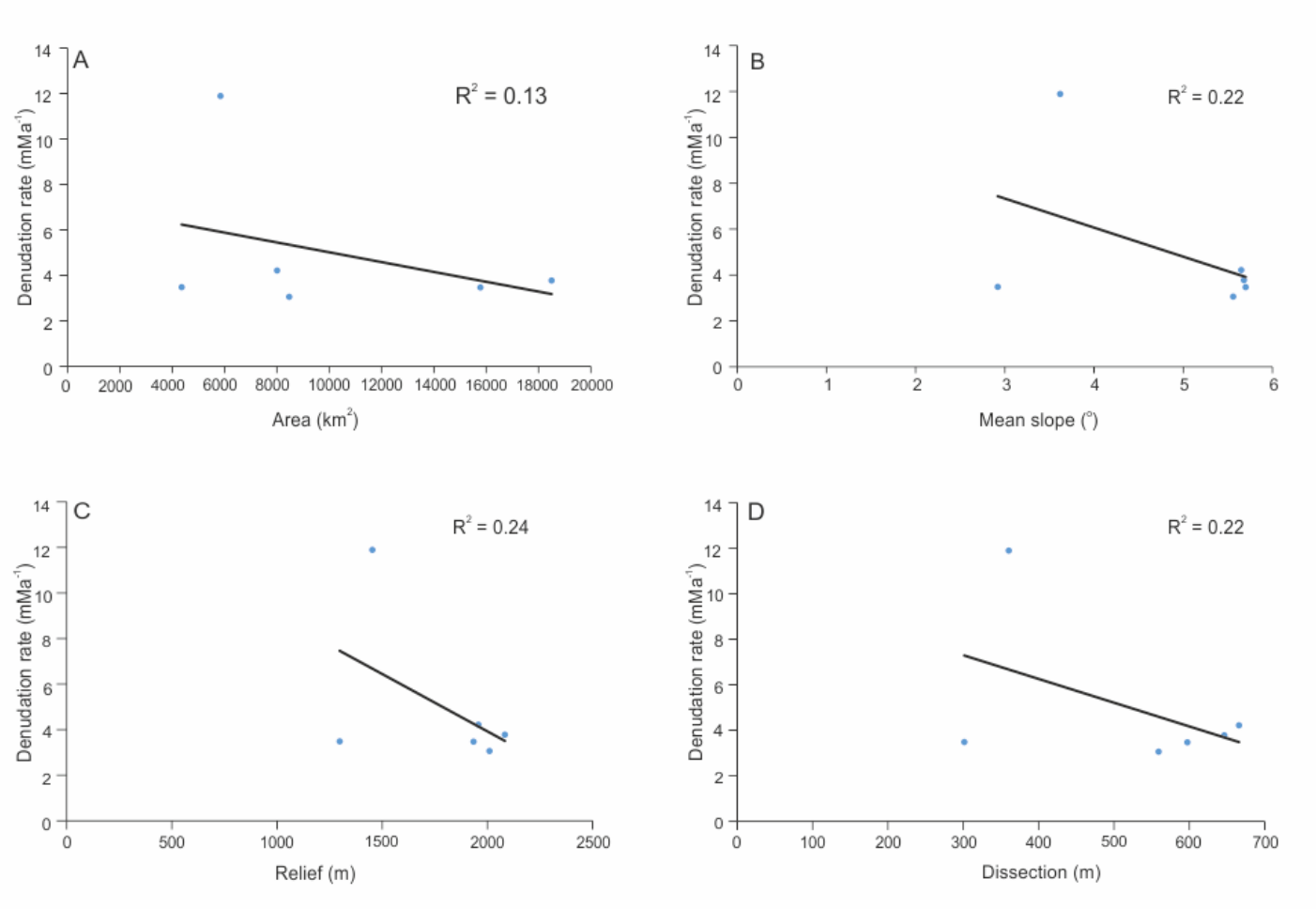

Figure 6.5 *– Correlation between catchment properties and catchment wide denudation rate; A) area; B) mean slope; C) relief and; D) dissection.*

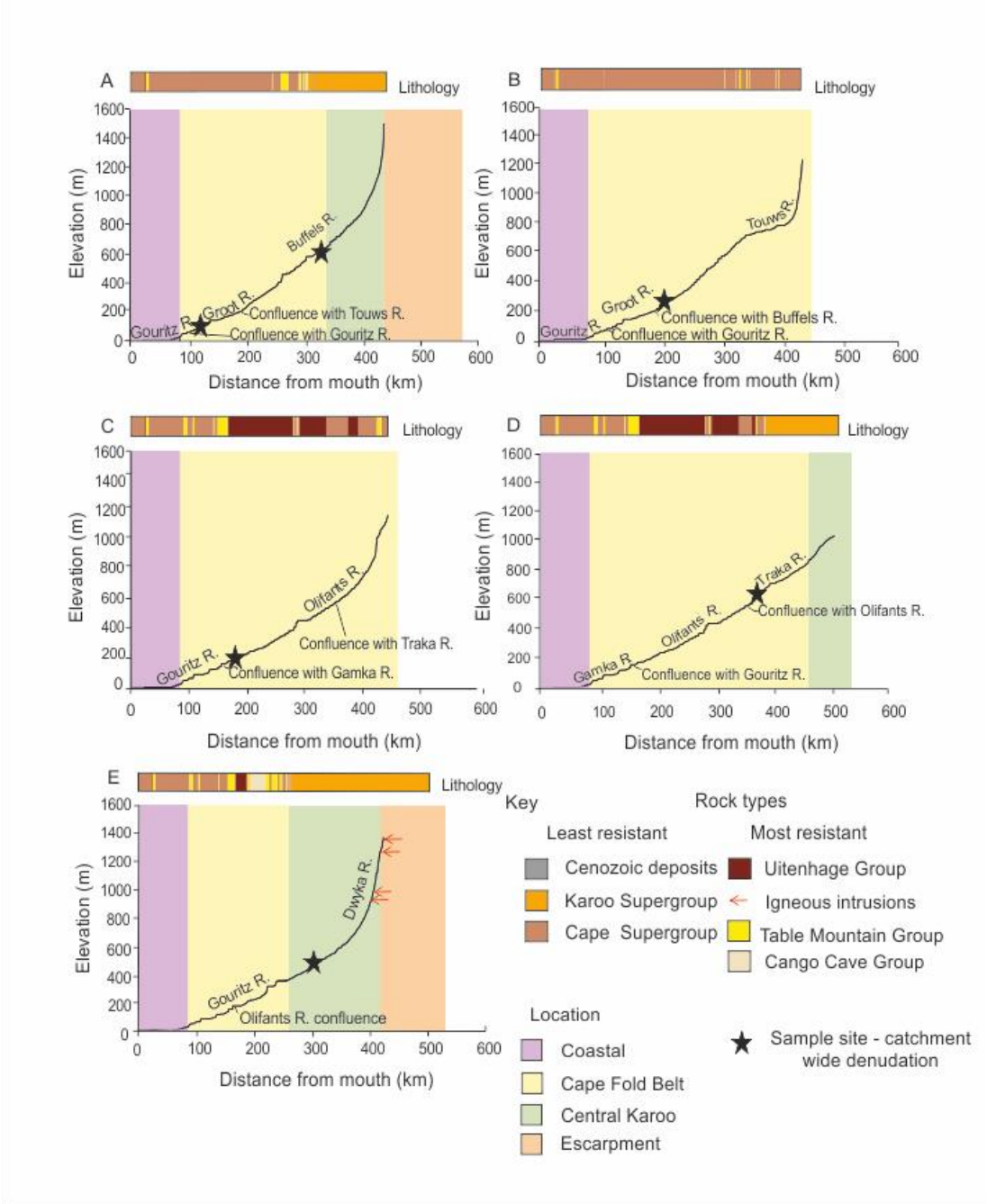

Figure 6.7 *– Long profiles of the sampled trunk rivers; A) Buffels River; B) Touws River; C) Olifants River; D) Traka River; E) Dwyka river showing the sampling sites and underlying lithology within the physiographic regions.*

6.6.2 Influence of catchment morphometrics

Gilbert (1877) argued that 'erosion is most rapid where slope is steepest', whilst Ahnert (1970) reported a linear relationship between erosion rates and mean relief for mid-latitude drainages. Denudation rates have been shown to correlate with slope, and other morphometric indices (e.g., relief; Summerfield and Hulton, 1994; Palumbo et al., 2010; Derrieux et al., 2014; Scherler et al., 2014), however this not the case for

the Gouritz catchment (Figure 6.3; e.g., Schmidt and Montgomery, 1995; Roering et al., 2001; Montgomery and Brandon, 2002). This indicates that denudation rates are no longer dependent on catchment properties, and that the system has decoupled from catchment morphometrics such as slope, with denudation rates dependent on external factors, such as tectonic uplift (Burbank et al., 1996; Densmore et al., 1998; Roering et al., 2001; Montgomery and Brandon, 2002). Slope decoupling has been reported from many tectonic settings (e.g., Burbank et al., 1996b; Montgomery et al., 2001; Roering et al., 2001), however South Africa is quiescent and the limiting factor of landscape evolution could be climate related (e.g., Decker et al., 2013). Further, Montgomery and Brandon (2002) stated that Ahnert's (1970) relationship 'appears to work well in tectonically inactive, low erosion rate landscapes' (pg. 485); however this is not the case for the Gouritz.

The similar results of incision rates between different morphometric zones and terrain, underlying geology and subcatchment morphometric indices of the Gouritz catchment indicates that nature averages the denudational input from different locations in this ancient setting in the majority of the trunk rivers, which are well mixed (von Blanckenburg, 2005). The Dwyka River is an outlier; in this trunk river the sediment does not appear to be well mixed as shown by the variation in denudation rates between this river and the other trunk rivers of the catchment. The lack of mixing could be related to a 'recent' event such as increased erosion due to flash flooding, which are common (Stear, 1985; Damm and Hagedorn, 2010) or due to human activity (e.g., Vanacker et al., 2007).

However, overall the different terrains are eroding at similar rates (Figure 6.2), and support Hack's theory (1960) that if boundary conditions remain constant, the whole landscape will be eroded at a similar rate. Steady-state landscapes or those in equilibrium with regards to erosion and uplift (See Chapter 2) are characterised by the following equations:

$$E = KA^m S^n \qquad \text{Eq. 6.3}$$

Where, *E is erosion, which in a steady state equals uplift*, *S* is channel gradient, *A* is drainage area, and *K* is an erosional efficiency factor related to lithology, climate, channel geometry and potentially sediment supply (Whipple and Tucker, 1999).

The equation above indicates that in a steady-state landscape there will be an inverse relationship between drainage area and slope. Additionally, catchment

morphometrics will not scale with denudation rates (*cf*. relief; Summerfield and Hulton, 1994; Palumbo et al., 2010; Derrieux et al., 2014; Scherler et al., 2014). Figure 6.5 shows a lack of correlation between morphometric indices and denudation rate and highlights the steady-state nature of this catchment. Of particular note are Figures 6.5a and 6.5c where denudation rates are similar despite the large variation in catchment size and relief. The assumption of steady-state is supported by the lack of geological control on the catchment as shown by the similar rates of denudation between different terrains.

Furthermore, the cosmogenic data reported here broadly agree with AFTT data and offshore sedimentation rates, whereby Cenozoic erosion rates are 10-15 mMa^{-1} (Tinker et al., 2008a). The similarity of erosion rates between different landforms and over geomorphic timescales (10^4-10^5 yrs) as shown by the similarity between cosmogenic data (10^2-10^6 yrs) and fission track (10^6-10^8 yrs) data coupled with the lack of correlation between slope and denudation rates indicates that the southern African landscape is in steady-state (Bierman and Caffee, 2001; Codilean et al., 2008).

6.6.3 Age of gorge formation

The data from the Seweweekspoort cannot be used to date when stream capture occurred (Chapter 8). The incision age data (Table 6.3) show that there was incision of the Cape Fold Belt in the Cenozoic and most likely incision started much earlier (pre-Cretaceous). The pulse of geomorphic activity was related to the rifting of Gondwana (e.g., Gilchrist et al., 1994; de Wit et al., 2000; Hattingh, 2008; Chapter 5). During the Cenozoic, the Seweweekspoort palaeoriver was a maximum of 200 m above the present day river; by this time at least 800m of incision had occurred. Green et al. (2016) argued for a second pulse of uplift related to the Swartberg Mountain range around ~30Ma, which could explain the erosion rates during the mid-Cenozoic. However, by this time the rivers had already incised a substantial volume of material. The uplift relates to the final stage of landscape development in the region (e.g., dissection of the pediments, Chapter 7) and not the initiation and integration of the drainage net (*c.f.* Green et al., 2016)

6.6.4 Landscape models

The data from this study and similarity of erosion rates across southern South Africa (Fleming et al., 1999; Cockburn et al., 2000; Bierman and Caffee, 2001; van der Wateren and Dunai, 2001; Kounov et al., 2007; Codilean et al., 2008; Dirks et al.,

2012; Decker et al., 2011; Erlanger et al., 2012; Chadwick et al., 2013; Decker et al., 2013; Scharf et al., 2013; Bierman et al., 2014; Kounov et al., 2015) indicate that low erosion rates are a regional feature, most likely related to relative tectonic stability that has prevailed during the Cenozoic (Kounov et al., 2007; Scharf et al., 2013; Bierman et al., 2014). Furthermore, increasing aridity during the Cenozoic (Bakker and Mercer, 1986) will compound low erosion rates. In landscapes with erosion rates <5mMa^{-1} weathering is argued to have a dominant control on rates of landscape evolution rather than fluvial processes (e.g., Decker et al., 2013; Scharf et al. 2013). The low erosion rates show that the principal topography of the Gouritz catchment is Mesozoic in age (e.g., Partridge, 1998; Brown et al., 2000; Brown et al., 2002; Doucouré and de Wit 2003; de Wit 2007; Tinker et al., 2008a; Kounov et al., 2015). The ancient setting of southern Africa, is a low erosion setting, and highlights that steep topography does not always indicate geomorphic activity. The erosion rates are independent of catchment properties and are now decoupled, related to the tectonic quiescence and increasing aridity. The system is now sediment limited with weathering now controlling the rate of landscape evolution (Decker et al., 2013; Scharf et al., 2013).

The Cenozoic uplift history of southern Africa is contentious, and has been argued to have uplifted at ~30 Ma (Burke, 1996; Green et al., 2016), ~20 Ma (Partridge and Maud, 1987, 2000) with a major Pliocene uplift of 100 – 900m at 5 – 3 Ma (Partridge and Maud, 1987, 2000). The catchment averaged denudation rates or strath terrace point erosion rates do not corroborate the recent uplift proposed by Partridge and Maud (1987, 2000). Incision into the Cape Fold Belt could have been aided by the proposed uplift of 30 or 20 Ma. However, by this stage a large amount of material had been removed, with the Seweweekspoort River a maximum of 200 m above its current day position. Within the main fluvial breach of the Gouritz Catchment at Gamkaskloof by the Gamka River, the majority of incision had occurred by the Cretaceous, with relatively small amounts of incision compared to the Seweweekspoort in the Cenozoic.

6.7 Conclusion

Catchment wide denudation rates in the Gouritz system are low and are decoupled from catchment morphometrics. External factors, such as climate and tectonic activity, now control the rate of landscape denudation. In low denudation settings such as this, physical and chemical weathering is the rate limiting process. The incision into the Cape Fold Belt had started by the Cretaceous and most likely much earlier, with low amounts of erosion experienced during the Cenozoic (up to 200m), and that

the drainage net was in place during the Cretaceous. The low reported denudation rates from this study also indicate that the principal topography of the Gouritz catchment is Mesozoic in age. Erosion rates are similar in the Gouritz catchment apart from the Dwyka River irrespective of lithology, slope, dissection, relief or catchment area. The catchment is now in geomorphic steady state, with similar denudation rates between different terrains over long time scales. The Gouritz catchment highlights that steep topography does not always mean geomorphic activity, and that in ancient settings, nature does do the averaging within river sediment sampling within the majority of the trunk rivers. The long periods of time permit the efficient mixing of sediment from different sources and terrains, and low denudation rates are aided by increasing aridity and tectonic quiescence of southern South Africa.

Chapter 7 Constraining the timing of pediment formation and dissection in the Western Cape, South Africa: implications for long-term landscape evolution

7.1 Abstract

Pediment surfaces are a widespread feature of the South African landscape and have long been regarded as ancient landforms. Cosmogenic nuclide data from four pediment surfaces in the Gouritz catchment, Western Cape are reported, including boulder surface samples and a depth profile through a colluvial pediment deposit. The results indicate low surface lowering rates (0.33 to 1.00 m Ma^{-1}) and *minimum* exposure ages of 0.55 – 1.31 Ma. Duricrusts have developed in the pediments and are preserved in some locations, which represent an internal geomorphic threshold limiting denudation and indicate at least 1 Ma of geomorphic stability following pediment formation. The pediments and the neighbouring Cape Fold Belt are deeply dissected by small order streams, forming up to 280 m deep river valleys in the resistant fold belt. Using the stratigraphic and geomorphic framework, the minimum age of pediment formation is considered to be Miocene. Several pediments grade above the present trunk rivers of the Gouritz catchment, and locally the pediments have deflected small incising rivers, which suggests that river incision occurred during the formation of the pediment surfaces. Integrating various strands of evidence indicates that the pediments are long-lived features. Caution should be taken when interpreting cosmogenic nuclide ages from pediments in ancient landscapes.

7.2 Introduction

Recent advancements in geochronology allow establishing erosion rates and exposure ages of landforms and place more precise constraints on landscape evolution. Knowing erosion rates and landform ages is essential for linking the evolution of drainage systems to downstream aggradation processes (e.g., Gallagher and Brown, 1999; Chappell et al., 2006; Tinker et al., 2008a; Wittmann et al., 2009; Sømme et al., 2011), constraining surface uplift and tectonic processes (e.g., Brook et al., 1995; Burbank et al., 1996; Granger et al., 1997; Jackson et al., 2002; Wittmann et al., 2007; Bellin et al., 2014; Vanacker et al., 2015), and palaeo-climate reconstructions (Margerison et al., 2005; Dunai et al., 2005; Owen et al., 2005; Willenbring and Blackenburg, 2010). Reconstructing ancient landforms and landscape development is challenging due to lower preservation and increasing signal overprinting forming a landscape palimpsest (e.g. Chorley et al., 1984; Bloom,

2002; Bishop, 2007; Jerolmack and Paola, 2010; Chapter 8). However, ancient landscapes and landforms cover a large portion of the globe (e.g., (1) Australia – e.g., Ollier, 1991, Ollier and Pain, 2000, Twidale, 2007 a,b; (2) southern South Africa – e.g., Du Toit, 1954, King 1956a, (3) South America – e.g. King, 1956b, Carignano et al., 1999, Demoulin et al., 2005, Panario et al., 2014, Peulvast and Bétard, 2015; (4) Asia – e.g., Gorelov et al., 1970, Gunnell et al., 2007, Vanacker et al., 2007; and (5) Europe – e.g., Lidmar-Bergström, 1988, Bessin et al., 2015) and offer important insights into long-term Earth surface dynamics.

Southern Africa's geomorphology has long intrigued Earth Scientists (Rogers, 1903; Davis, 1906; King, 1949, 1948, 1953; Dixey, 1944). Fundamental questions related to long-term landscape development remain unanswered, such as the mechanisms and timing of surface uplift (Gallagher and Brown, 1999, Brown et al., 2002, Tinker et al., 2008b, Kouvnov et al., 2009, Decker et al., 2013) and the chronological framework of the main phases of landscape development (Du Toit, 1937, 1954; King, 1951; Burke, 1996; Partridge, 1998; Brown et al., 2002; Doucouré and de Wit, 2003; de Wit, 2007; Kounov et al., 2015). In-situ produced cosmogenic nuclides can offer key information to unravel these questions and have been applied to ancient landforms within southern Africa (Fleming et al. 1999; Cockburn et al., 2000; Bierman and Caffee, 2001; van der Wateren and Dunai, 2001; Kounov et al., 2007; Codilean et al., 2008; Dirks et al., 2010; Decker et al., 2011; Erlanger et al., 2012; Chadwick et al., 2013; Decker et al., 2013). However, the area south of the Great Escarpment remains poorly studied (e.g., Scharf et al., 2013; Bierman et al., 2014; Kounov et al., 2015).

Currently, four different categories of landscape evolution models exist that address the evolution of pediments and surrounding mountain belts (Dohrenward and Parsons, 2009): (1) range front retreat where channelised fluvial processes dominate (e.g., Gilbert, 1877; Paige, 1912; Howard 1942); (2) range front retreat where diffuse hillslope processes dominate (e.g., Lawson, 1915; Rich; 1935; Kesel, 1977; Bourne and Twidale, 2007; Dauteuil et al., 2015); (3) range front retreat with valley development, which integrates varying spatial and temporal dominance of fluvial and diffusive erosion processes (e.g., Bryan, 1922; Sharp, 1940) and; (4) range denudation due to channelised stream flow dominated by catchment development (e.g., Lustig, 1969; Parsons and Abrahams, 1984). Model types 1 and 2 acknowledge the occurrence of diffusive and channelised erosion processes, respectively, but do not argue for their dominance in the formation process (Gilbert, 1877; Rich, 1935; Howard, 1942). Model 3 integrates fluvial and diffusive erosion processes, and their relative importance depends on the geomorphic setting (Bryan, 1922; Sharp, 1940)

with dominance of diffusive processes in regions with resistant lithologies, ephemeral streams and a low mountain mass. Model 4 is associated with the broader issues associated with mountain denudation and does not require parallel retreat of the mountain front to form the pediment surfaces (Lustig, 1969; Parsons and Abrahams, 1984). Pediments or erosional surfaces have been investigated in South Africa since the 1950s (King, 1953; King 1963; Partridge and Maud, 1987), and indicate denudation rates that are an order of magnitude lower than those in other landforms within southern Africa (van der Wateran and Dunai, 2001; Bierman et al., 2014; Kounov et al., 2015). The pediment surfaces are referred to as being Early Tertiary to Jurassic in age (King, 1963). Therefore, there remains a significant difference between the published *minimum* exposure ages based on in-situ produced cosmogenic nuclides and stated ages of the pediments.

In this paper, we present new isotopic data from pediment landforms in southern South Africa. The main objective of the paper is to constrain landscape development using in-situ produced ^{10}Be dating and to establish denudation rates and landform exposure ages. We assess the cosmogenic data within a wider geomorphic, and geologic framework in order to test the performance of cosmogenic dating in a geomorphic setting with low denudation rates.

7.3 Regional settings

7.3.1 Geological setting

South Africa is dominated by strata of the Cape and Karoo Supergroups (Figure 7.1), which are composed of various groups of sandstone, mudstone and shale. The Cape Supergroup has been metamorphosed, with quartzites common and forming the backbone of the exhumed Cape Fold Belt (CFB) (Tinker et al., 2008b; Scharf et al., 2013). The Cape and Karoo Supergroup has been intensively folded, with the E-W trending folds decreasing in amplitude towards the north (Paton, 2006; Spikings et al., 2015). The mechanisms of regional uplift since the Mesozoic, related to the anomalous height of southern Africa, are contentious; with landscape evolution either associated to mantle plumes (Nyblade and Robinson, 1994, Ebinger and Sleep, 1998) or to plate tectonics, with uplift along flexures (Moore et al., 2009) and epeirogenic uplift (Brown et al., 1990). Furthermore, the occurrence (e.g., Brown et al., 2002; van der Beek et al., 2002) and timing of Cenozoic uplift is disputed; Burke (1996) proposed the most recent uplift phase occurring ~30 Ma ago due to a thermal anomaly, whereas Partridge and Maud (1987) argued for a later phase of uplift around 18 Ma, with 200 m of uplift within the Western Cape. Partridge and Maud (1987) also argued for an even more recent phase of uplift at 2.5 Ma.

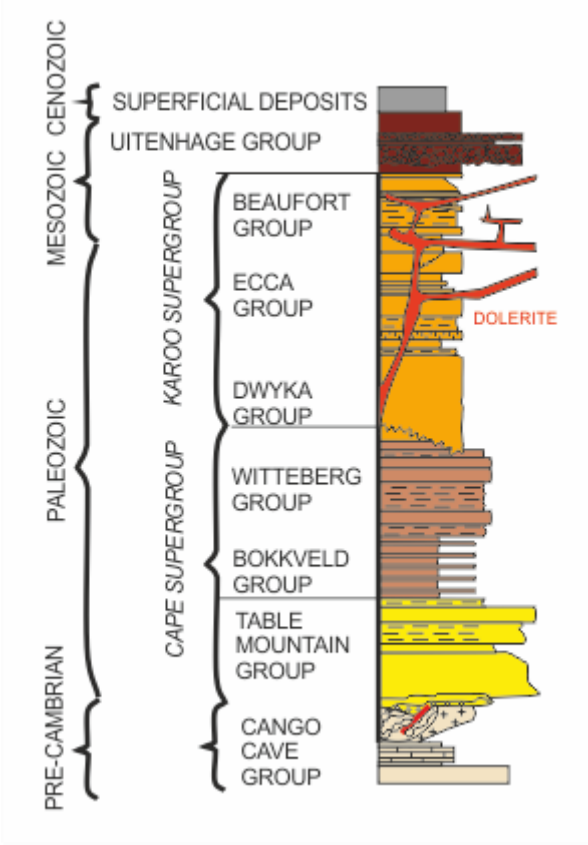

Figure 7.1 *– Stratigraphic chart showing the major lithostratigraphic units of South Africa.*

Figure 7.2 gives an overview of the geochronological studies in southern Africa that used either apatite fission track thermochronology (AFTT) to document landscape denudation from the Cretaceous to modern day, or in-situ produced cosmogenic radionuclides (^{26}Al, ^{10}Be, ^{3}He, ^{21}Ne) to date landforms. During the Mesozoic, the rifting of Gondwana initiated large-scale denudation across southern Africa, with up to 7 km of lithology removed (Tinker et al., 2008b). AFTT (Figure 7.1) indicates high rates of denudation, with respect to the present day rates (up to 175 m Ma^{-1}, Tinker et al., 2008b), towards the end of the Lower Cretaceous (100 Ma – 80 Ma) that decreased to up to 95 m Ma^{-1} by the late Cretaceous (90 Ma – 70 Ma; Brown et al., 2002). Denudation rates decreased to < 15 m Ma^{-1} by the Paleocene (65 Ma; Flowers and Schoene, 2010), and to 5 m Ma^{-1} by the late Eocene (36 Ma; Cockburn et al., 2000). Cosmogenic studies support a decrease in erosion rates since the Cenozoic (Figure 7.1; Fleming et al., 1999; Cockburn et al., 2000; Bierman and Caffee, 2001; van der Wateren and Dunai, 2001; Kounov et al., 2007; Codilean et al., 2008; Dirks et al., 2012; Decker et al., 2011; Erlanger et al., 2012; Chadwick et al., 2013; Decker et al., 2013; Scharf et al., 2013; Bierman et al., 2014; Kounov et al., 2015). With exception

of a retreat rate of 62.3 m Ma^{-1} for escarpment face retreat (Fleming et al. 1999), the majority of landforms are eroding very slowly, with mean denudation rates ranging between 9.4 m Ma^{-1} for the escarpment faces to 0.85 m Ma^{-1} for pediments (Figure 7.2). Southern South Africa is currently tectonically quiescent with only minor Quaternary-active faults (Bierman et al., 2014) and low denudation and sediment production rates (Kounov et al., 2007; Scharf et al. 2013). *Minimum* exposure ages for pediments range from 0.29 +/- 0.02 (Bierman et al., 2014) to 5.18 +/- 0.18 Ma (Van der Wateran and Dunai, 2001) with a mean *minimum* exposure age of 1.87 Ma (Pleistocene, van der Wateran and Dunai, 2001; Bierman et al., 2014; Kounov et al., 2015).

The climate of southern South Africa has gradually moved towards conditions that are more arid since the Cretaceous (Partridge, 1997; van Niekerk et al., 1999). At the end of the Cretaceous, there was an abrupt change from humid/tropical to arid conditions (Partridge and Maud, 2000) as shown by silcrete formation and saline soils (Partridge and Maud, 1987). Although there is an overall aridification trend, several authors have argued that wetter phases occurred from 65 – 30 Ma (Burke, 1996). Or that the arid phase started as late as 18 Ma (Partridge and Maud, 1987). The present day climate of the Western Cape is primarily semi-arid (Dean et al., 1995), while the coastal region has a Mediterranean type climate (Midgley et al., 2003).

7.3.2 Sample sites

The sampling sites are located within the large antecedent Gouritz catchment (Figure 7.3), where morphometric analysis has identified the presence of flat surfaces or pediments that carry a thin sedimentary cover (<1m) (Chapter 8). The pediments grade away from the CFB into adjacent alluvial plains, and samples were collected from pediments on the northern flank of the Swartberg and Witteberg Mountains (CFB) around Laingsburg and Prince Albert (Figure 7.3A). Samples were taken from five deeply dissected pediments ranging in surface area between < 1 to 20 km^2 and display slope angles below 10°, with the majority of the slopes below 4° (Figure 7.4).

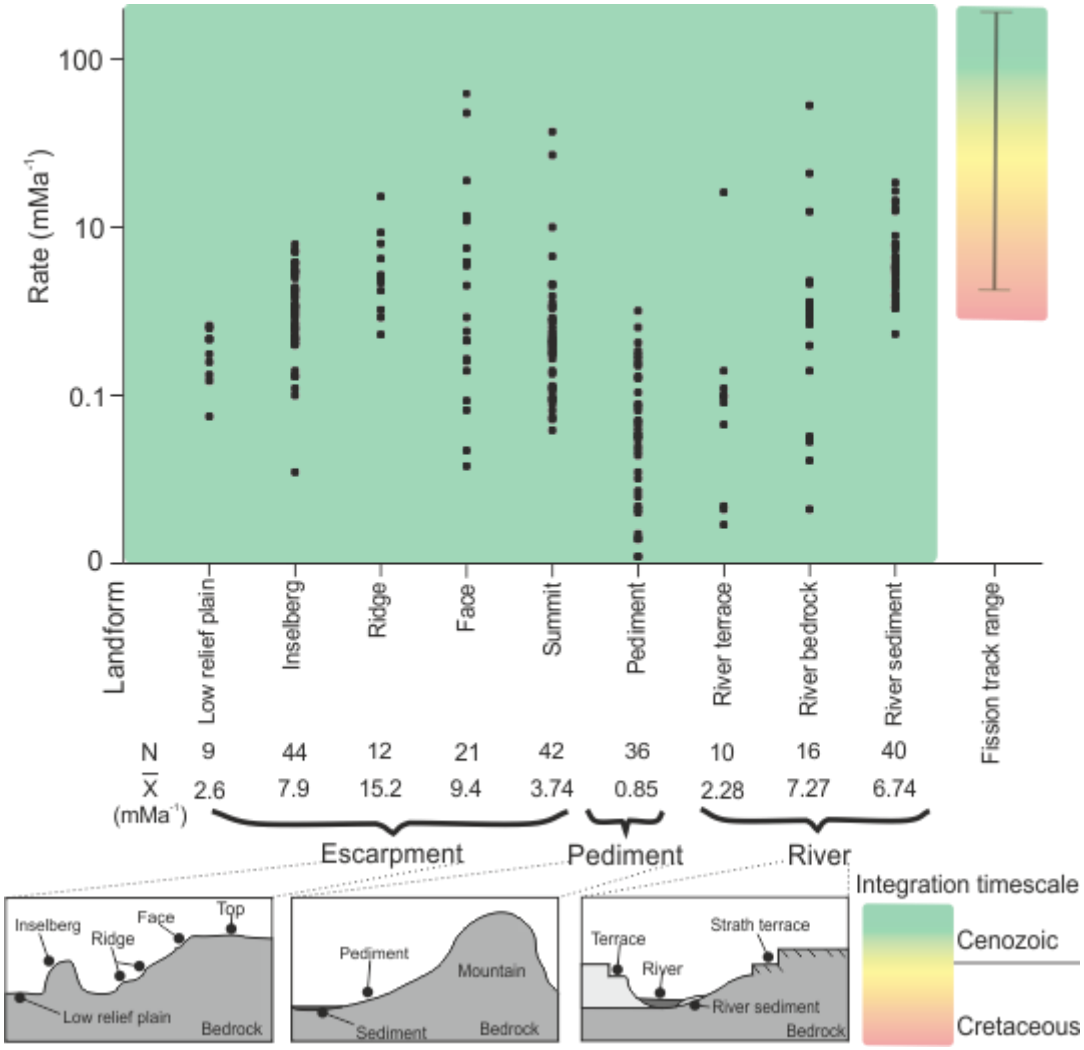

Figure 7.2 *– Semi-log plot of published erosion rates using cosmogenic data (using ^{10}Be, ^{26}Al, ^{21}Ne and ^{3}He) from southern Africa, for escarpment, pediment and river landforms. Apatite fission track data is also shown to indicate the longer-term erosion rates in the Cretaceous. Cosmogenic data is from the following sources; Flemming et al. 1999; Cockburn et al. 2000; Bierman and Caffee, 2001; van der Wateran and Dunai, 2001; Kounov et al. 2007; Codilean et al. 2008; Dirks et al. 2012; Decker et al. 2011; Erlanger et al. 2012; Chadwick et al. 2013; Decker et al. 2013; Scharf et al. 2013; Bierman et al. 2014 and; Kounov et al. 2015, Apatite fission track from; Gallagher and Brown, 1999; Cockburn et al. 2000; Brown et al. 2002; Tinker et al. 2008b; Kounov et al. 2009 and; Flowers and Schoene, 2010. The colour ramp indicates the period for which the data is scaled over, the cosmogenic data relates to the Cenozoic, whereas the fission track data range incorporates the Cenozoic to the Cretaceous.*

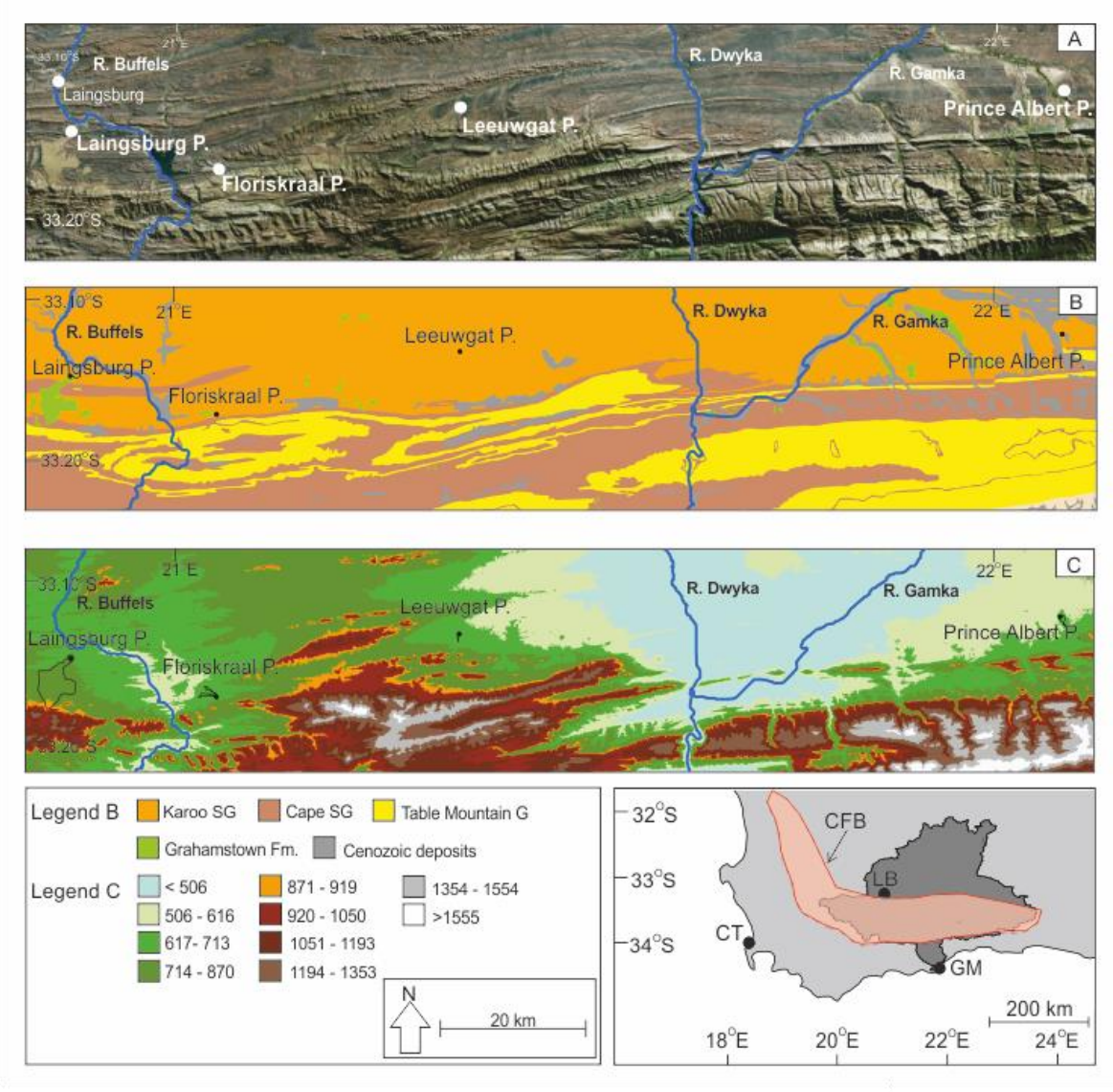

Figure 7.3 *– A) Pediment locations, the inset shows the location of the Gouritz catchment within South Africa, where CT – Cape Town, LB – Laingsburg; GM – Gouritzmond and the red polygon is the location of the Cape Fold Belt (CFB); B) underlying geology below the pediments and; C) pediment elevations as shown by elevation bins categorised by natural breaks in the elevation data.*

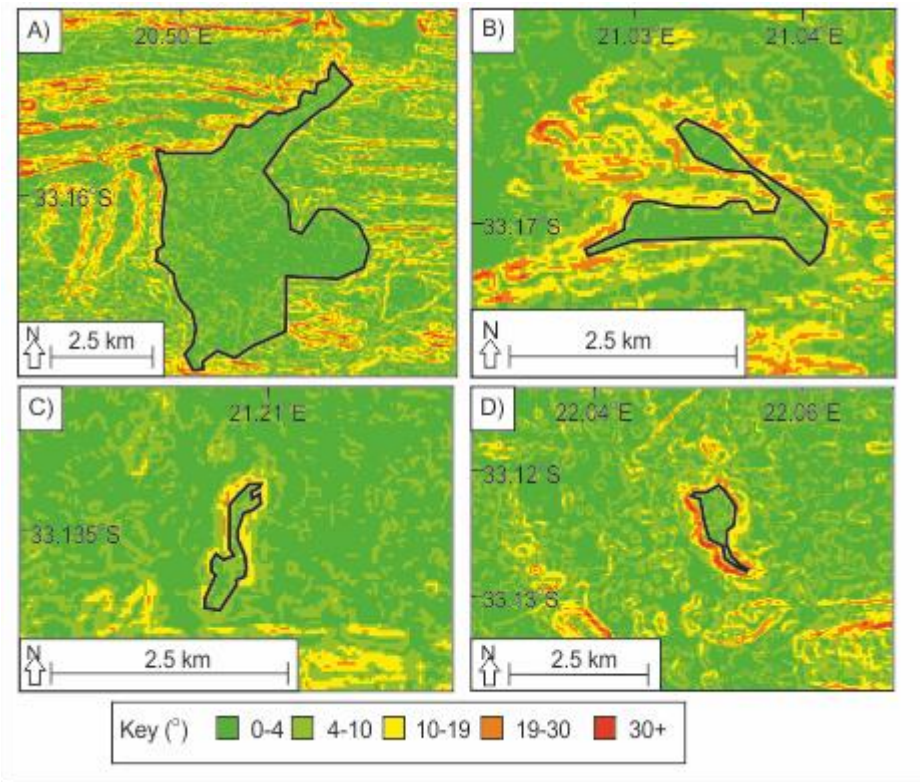

Figure 7.4 *– Pediment slope data; A) Laingsburg; B) Floriskraal; C) Leeuwgat and; D) Prince Albert.*

The pediments are composed of unconsolidated, poorly-sorted gravel to boulder material in a matrix of sand (Figure 7.5) underlain by truncated folded rocks of the Karoo Supergroup (Figure 7.3B). Some of the pediments are capped by silcrete, calcrete or ferricrete (Helgren and Butzer, 1977; Summerfield, 1983; Marker and Holmes, 1999; Partridge, 1999; Partridge and Maud, 2000; Marker et al., 2002). The silcrete is assigned to the Grahamstown Formation (Figure 7.3b); however, ferricrete is dominant on the Laingsburg pediment. The Grahamstown Formation has little age control ranging from Cretaceous to Cenozoic (Mountain, 1980; Summerfield, 1983) due to the lack of formal identification of the silcretes. Electron spin resonance ages for two caps in the Little Karoo were dated at 7.3 and 9.4 Ma (Hagedorn, 1988).

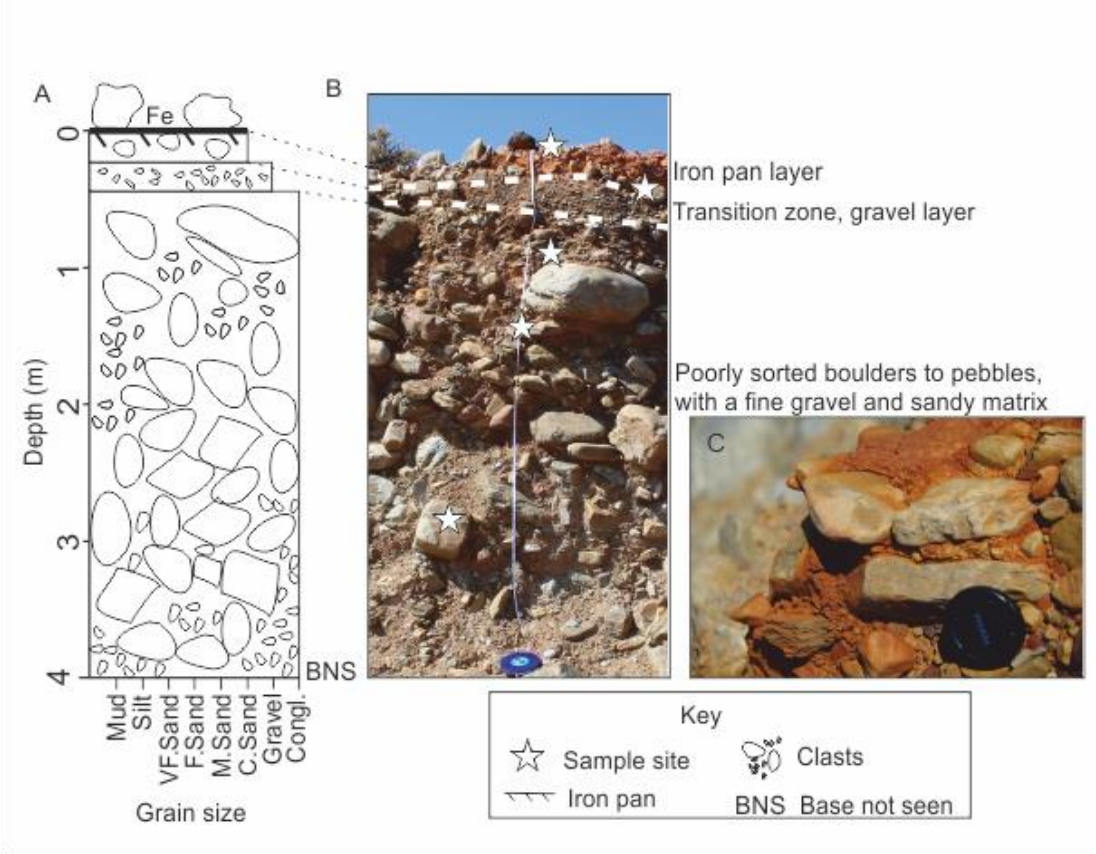

Figure 7.5 *– A) Sedimentary log of the Laingsburg pediment showing the unsorted boulders (dominantly quartzite) to gravel size material; B) photograph of the pediment and where the depth profile clasts were taken and; C) Iron-rich paleosol layer.*

7.4 Methodology

7.4.1 Cosmogenic radionuclide dating

Cosmogenic nuclide-derived denudation rates were determined by using in-situ produced ^{10}Be concentration in quartz grains, crushed from Cape Supergroup quarzitic boulders sampled at the surface or in a depth profile (Figure 7.6). Five pediment surfaces were investigated by sampling large boulders having a >1m diameter along the longest axis. For the depth profile in the pediment surface, quarzitic clasts (>25 cm diameter) were taken at the following depths (cm) below ground level: 0, 30, 85, 150, 255.

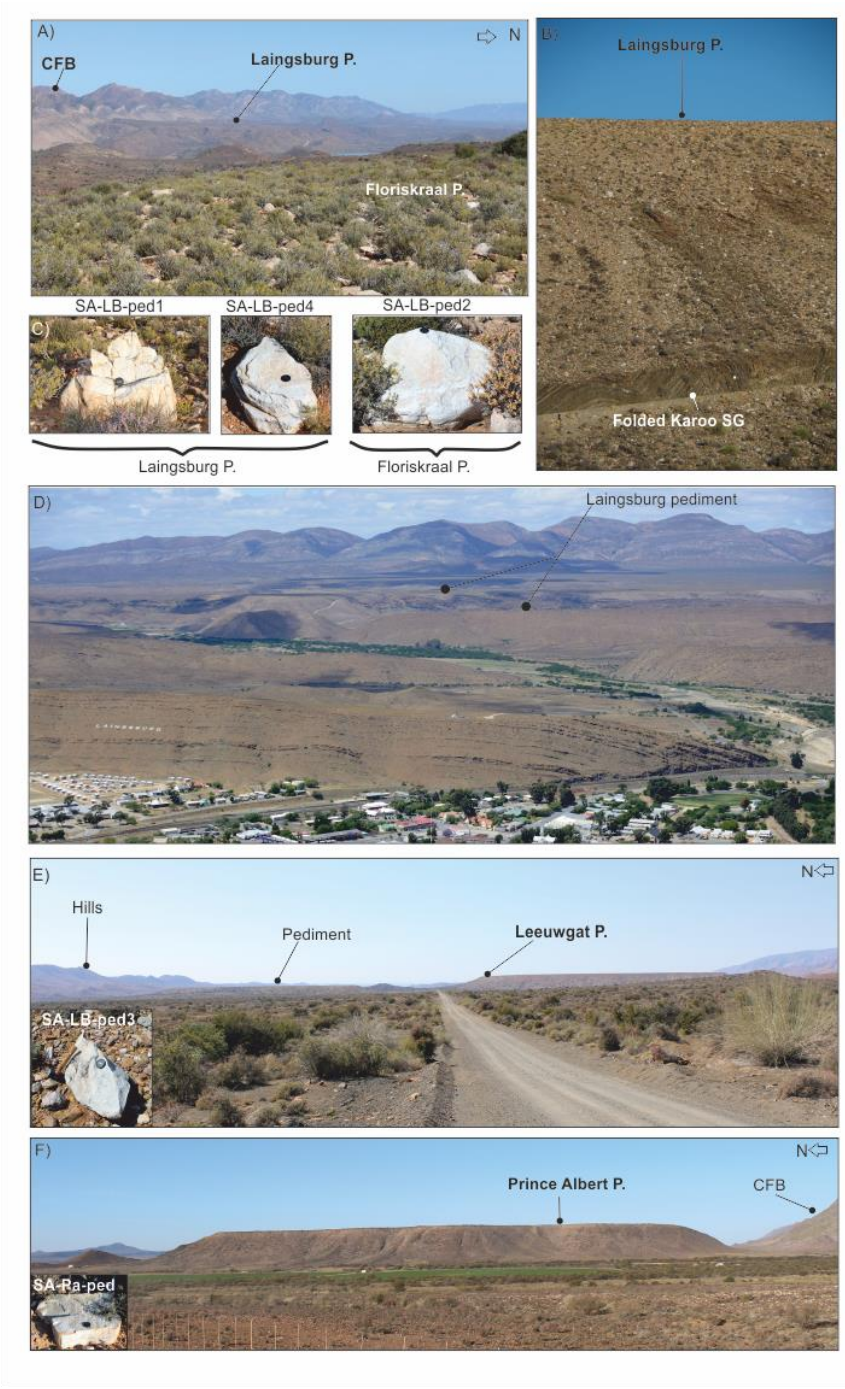

Figure 7.6 *– Sample sites; A) Laingsburg pediment from the Floriskraal pediment; B) Laingsburg pediment and contact with underlying folded Karoo Supergroup (SG) strata; C) Boulder samples from Laingsburg and Floriskraal pediments; D) large scale picture of the Laingsburg pediment E) Leeuwgat pediment and boulder sample (inset); F) Prince Albert and boulder sample (inset). The figure also shows the dissection of the pediments by small river catchments and how decoupled the Floriskraal and Prince Albert pediments are from the Cape Fold Belt.*

The samples were crushed, sieved and the 250 to 500 µm grain size extracted. The ^{10}Be was extracted from purified sand using standard methods described in von Blanckenburg et al. (1996, 2004). The ^{10}Be/^{9}Be ratios were measured in BeO targets with accelerator mass spectrometry at ETH Zürich (Kubik and Christl, 2010). The samples were normalised to the ETH in-house secondary standard S2007N. Between 154 and 157 µg of ^{9}Be carrier was added to each sample, which was used to calculate the percentage of ^{10}Be present in the sample. The calculated ^{10}Be concentrations and analytical errors are shown in Table 7.1. Uncertainties are propagated from AMS counting statistics and the 32% error on the blank sample. The CRONUS calculator (Balco et al. 2008) was employed to calculate denudation rates and exposure ages from the ^{10}Be concentrations (reported using the Dunai, 2001 scheme). For the exposure ages, an assumption of no erosion (0 m Ma^{-1}) was used (Bierman et al., 2014) and an erosion rate of 0.03m Ma^{-1}, to assess variation between exposure ages using different but realistic erosion rates.

Table 7.1 *– Information on the samples from the pediments used for cosmogenic nuclides study. All samples are taken from quartzite boulders, that were sampled either on the surface of the pediment or at depth.*

Nr	Sample ID	Sample type	Name	Latitude, D.D	Longitude, D.D	Elevation (m)	Topographic Shielding
1	SA-PA_ped	Surface	Prince Albert	-33.203	22.082	703	1.00
2	SA-LB_ped1	Surface	Laingsburg	-33.246	20.872	764	1.00
3	SA-LB_ped2	Surface	Floriskraal	-33.285	21.050	706	1.00
4	SA-LB_ped3	Surface	Leeuwgat	-33.221	21.347	691	1.00
5	SA-LB_ped4	Surface	Laingsburg	-33.261	20.854	791	1.00
6	SA-LB_DP0	Depth (0cm)	Laingsburg	-33.256	20.851	779	0.99
7	SA-LB_DP30	Depth (30cm)	Laingsburg	-33.256	20.851	776	0.99
8	SA-LB_DP85	Depth (85cm)	Laingsburg	-33.256	20.851	776	0.99
9	SA-LB_DP150	Depth (150cm)	Laingsburg	-33.256	20.851	776	0.99
10	SA-LB_DP255	Depth (255cm)	Laingsburg	-33.256	20.851	776	0.99

The depth profile (Table 7.2) was solved numerically following the method of Braucher et al. (2003, Eq. 7.1), whereby the concentration at a given depth is composed of two components: (1) the post-depositional concentration and (2) inherited concentration. The pre-inherited concentration is taken from the lowest sample in the depth profile

(2.55 m). The depth profile is then solved numerically, based on a chi-squared model fitting between the observed (Table 7.2) and simulated ^{10}Be depth profiles. As the depth profile is from a deposit, the shielding factor used for the CRONUS (Balco et al. 2008) calculator must incorporate the shielding for the whole catchment, which was calculated using Arc-GIS using the method of Norton and Vanacker (2009). The density of the depth profile material was taken as 1.6 g cm^{-3} following Kounov et al. (2015).

$$N(z,t) = \frac{P(z)}{\lambda+\frac{E}{z*}} e^{-(z_0-Et)/z*}\left(1-e^{-(\lambda+\frac{E}{z}*)t}\right) + N_{inh}e^{-\lambda t} \qquad \text{Eq.7.1}$$

where P(z) is the rate of production, λ is the decay constant (ln 2 /$t_{1/2}$), z_0 is the initial shielding depth, and E is the post-depositional erosion rate (cm/yr) of the top of the terrace.

Table 7.2 *– Depth profile sample information.*

Nr	Sample ID	Latitude, D.D	Longitude, D.D	10Be concentration, x10^6 at/g$_{qtz}$	Error on 10Be Concentration atoms/g X10^{6}at/g$_{qtz}$
6	SA-LB_DP0	-33.25555	20.85115	5.460	0.055
7	SA-LB_DP30	-33.25551	20.85088	1.196	0.013
8	SA-LB_DP85	-33.25551	20.85088	0.893	0.010
9	SA-LB_DP150	-33.25551	20.85088	0.376	0.006
10	SA-LB_DP255	-33.25551	20.85088	0.133	0.005

7.4.2 Morphometric analysis

Aster 30m data was used to create a DEM of the study area in ArcGIS 10.1. The DEM was re-projected into WGS 1984 world Mercator co-coordinates and filled using the hydrology toolbox. The drainage was extracted with an upstream contributing area of 3.35 km^2 delineating streams, which shows both ephemeral and perennial streams (e.g., Abadelkaarem et al., 2012; Ghosh et al., 2014). The pediments are now deeply dissected. To reconstruct the previous grading from the mountain front for each pediment a graded surface was built in ArcGIS (Figure 7.7). The surface was created using the normal profiles observed on other pediments globally. The uncertainties associated with this are mainly related to the deflation the surface has had post-formation; therefore the remnant features may have had higher elevations and the reconstruction using the current level may miss material. Deflation is a slow process

and would have affected the pediments in South Africa. This surface was then placed into ArcScene 10.1, with the difference between the reconstructed surface and the current pediment level (using the DEM) providing a volume of material missing post-pediment formation. This volume was converted to lithological thickness using the method of Aguilar et al. (2011). The minimum eroded volume was also calculated for the small subcatchments that back the pediment surfaces in the CFB. The watershed of each subcatchment was delineated and used to cap the current catchment basin. The difference was then calculated between the two surfaces and the volume difference calculated. The calculated volumes and corresponding lithological thicknesses were then compared to published data. The method used to extract the minimum eroded volume may represent an underestimation, as the watershed and interfluve areas would have been lowered due to erosion (Bellin et al., 2014; Brocklehurst and Whipple, 2002).

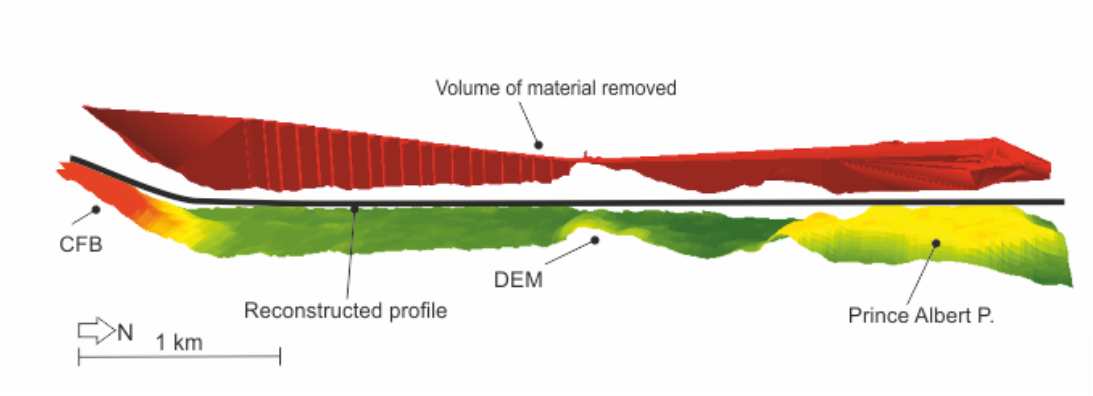

Figure 7.7 *– Example cross section of the Prince Albert pediment showing the method used in ArcGIS for the volume of material removed around the pediment surface.*

7.5 Results

7.5.1 Pediment composition

The contact with the underlying bedrock (e.g., Dwyka) is erosional and undulating, it is not a smooth planation contact. The pediments are composed of poorly sorted boulders to pebbles, with a fine gravel to sandy matrix. The clasts are predominantly quartzites (Table Mountain); however smaller clasts of Dwyka lithologies are present. Towards the top of the profile there is a small transition zone of gravel, which is capped by an iron crust (Figure 7.5). There is no indication of fluvial activity (i.e. imbrication). There is no grading or sediment clast size variation throughout the profile, and the boulders range from sub-rounded to sub-angular.

7.5.2 Cosmogenic nuclides

The surface lowering rates (Table 7.3) calculated for the boulders sampled on the pediment surface show very low rates, which range from 0.33 – 1.00 m Ma^{-1}. The Laingsburg pediment has higher rates of surface lowering closer to the CFB, with denudation rates decreasing towards the proximal part of the pediment as shown by the boulder samples.

The Prince Albert pediment has the highest rate of surface lowering (1.00 m Ma^{-1}), which is an order of magnitude higher than the average surface lowering rate of the other studied pediments. The minimum exposure ages assuming no erosion (Table 7.3) indicate the pediments are long-lived, with minimum ages between 0.55 to 1.31 Ma (Pleistocene) calculated. The Prince Albert pediment has the youngest *minimum* exposure age of 0.55 Ma, the Laingsburg pediment has variable ages from 0.81 to 1.08 Ma. Assuming erosion rates of 0.3 m Ma^{-1} the pediment minimum exposure ages range from 0.64 to 2.93 Ma (Table 7.3).

The depth profile (Figure 7.8; Table 7.2) indicates surface lowering rates of 4 m Ma^{-1} (χ^2 -0.007), which is an order of magnitude higher than the Laingsburg boulder pediment data. The data also shows that surface deflation has occurred on the pediment surface, as the higher data point does not follow the same trajectory as the lower samples. The depth profile indicates an exposure age of 1 Ma, which is close to the exposure ages shown by the Laingsburg pediment boulder samples.

7.5.3 Elevations and grading of pediment

Figure 7.3B shows the pediment heights as classified by the Jenks natural break scheme (De Smith and Goodchild, 2007). The pediments at Laingsburg and Floriskraal have elevations within the same class (714 – 870 m), and the Leeuwgat and Prince Albert share the same elevation class (617 - 713m). The Laingsburg pediment appears to have an aspect of slope that grades not only away from the CFB but towards the modern Buffels River location, which abuts the northern limit of the pediment (Figure 7.9).

Table 7.3 *- Analytical results from the cosmogenic radionuclide ^{10}Be analysis of the quartz samples. The reported ^{10}Be concentrations (1 S.D.) are corrected for a blank ratio of 1.01 ± 0.33 × 10^{-14}.*

Nr	Sample ID	Name	10Be concentration, x10^6 at/g_{qtz}	Error on 10Be Concentration atoms/g X10^6at/g_{qtz}	10Be Erosion rate, mMa^{-1}	Erosion rate uncertainty (1s)	No erosion (0 mMa-1)		Erosion rate 0.03mMa-1)	
							Exposure age (Ma)	Exposure age uncertainty (Ma)	Exposure age (Ma)	Exposure age uncertainty (Ma)
1	SA-PA_ped	Prince Albert	2.834	0.029	1.000	0.001	0.546	0.005	0.642	0.005
2	SA-LB_ped1	Laingsburg	5.199	0.052	0.435	0.001	1.078	0.008	1.739	0.008
3	SA-LB_ped2	Floriskraal	5.148	0.052	0.408	0.001	1.132	0.009	1.926	0.009
4	SA-LB_ped3	Leeuwgat	5.641	0.057	0.337	0.001	1.308	0.010	2.929	0.009
5	SA-LB_ped4	Laingsburg	4.252	0.043	0.622	0.001	0.811	0.007	1.081	0.007

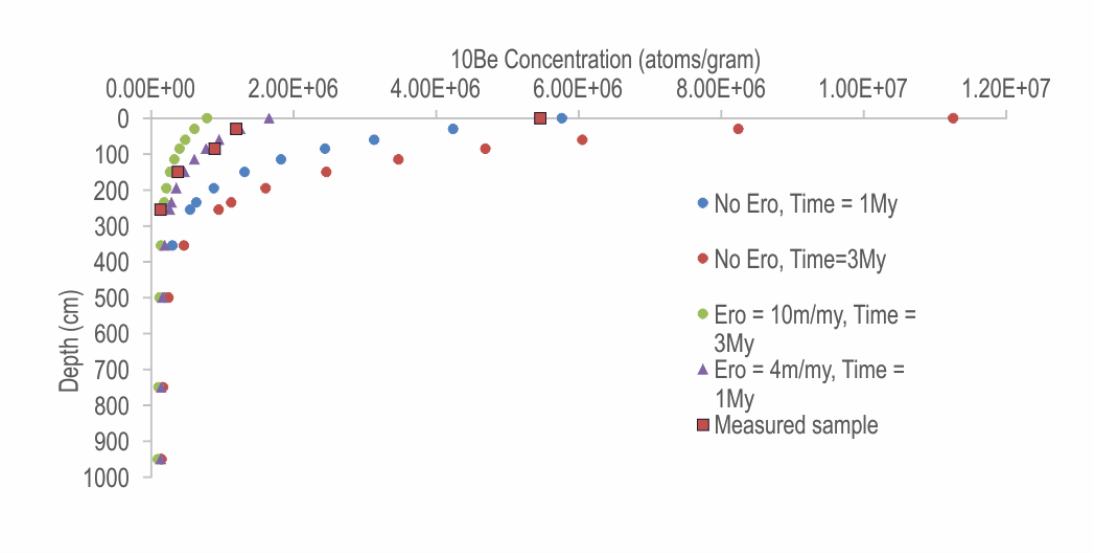

Figure 7.8 *– Depth profile results of the Laingsburg pediment.*

This relationship is less clear on the Floriskraal pediment, which is to the east of the Buffels River. The pediment at Leeuwgat, which sits between two folds of the CFB, has no large trunk river nearby (~30 km from Dwyka River) and simply grades away from the CFB (Figure 7.10A). The Prince Albert pediment grades to the Gamka River, although it is not as clear as in Laingsburg, the Prince Albert pediment is currently ~16 km from the Gamka River (Figure 7.10B). The fact that the pediments grade towards the present day trunk rivers but above their present day elevation indicates that they were active during the formation of the pediments and is discussed later.

7.5.4 Dissecting river planform

The dissecting river planforms are shown in Figure 7.11. Critical points, which were found objectively, are highlighted that relate to sections where the rivers (i) have been deflected by the pediment surface, or (ii) have anomalous changes in orientation. Overall the low order rivers (<4) that have dissected the pediments are strongly influenced by the folding within the CFB (Chapter 8). This is especially seen within the rivers that have dissected the Laingsburg pediment (Figure 7.11), where the linear river planform alligns with the axis of a syncline. Where the rivers breach the folds it appears that the presence of the pediments have deflected the river planforms; this relationship can also been seen at Floriskraal and Prince Albert pediments (Figure 7.11).

7.5.5 Volume of material removed

Table 7.4 shows the volume of material missing due to dissection of the pediment post formation. Converting this to an equivalent lithological thickness (Aguilar et al.,

2011), an average of 42.33 m has been eroded around the large Laingsburg pediment (Figure 7.9). The Prince Albert pediment has had the most dissection, with an average lithological thickness of 141.43 m removed. Leeuwgat has had the least amount of dissection, with 17.25 m eroded.

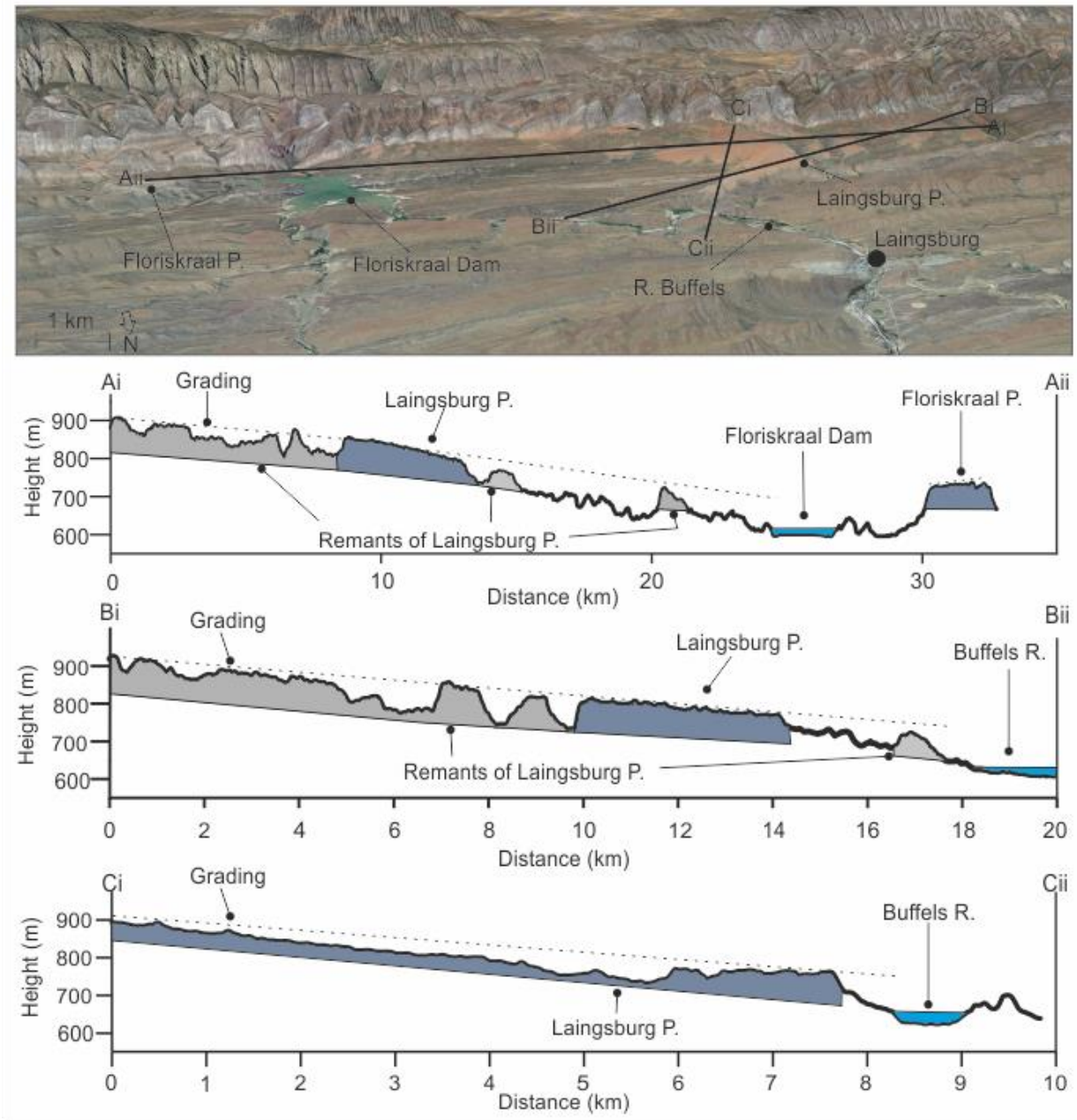

Figure 7.9 *– Grading of the Laingsburg pediment and related cross sections, which grade not only away from the Cape Fold Belt but towards the Buffels River.*

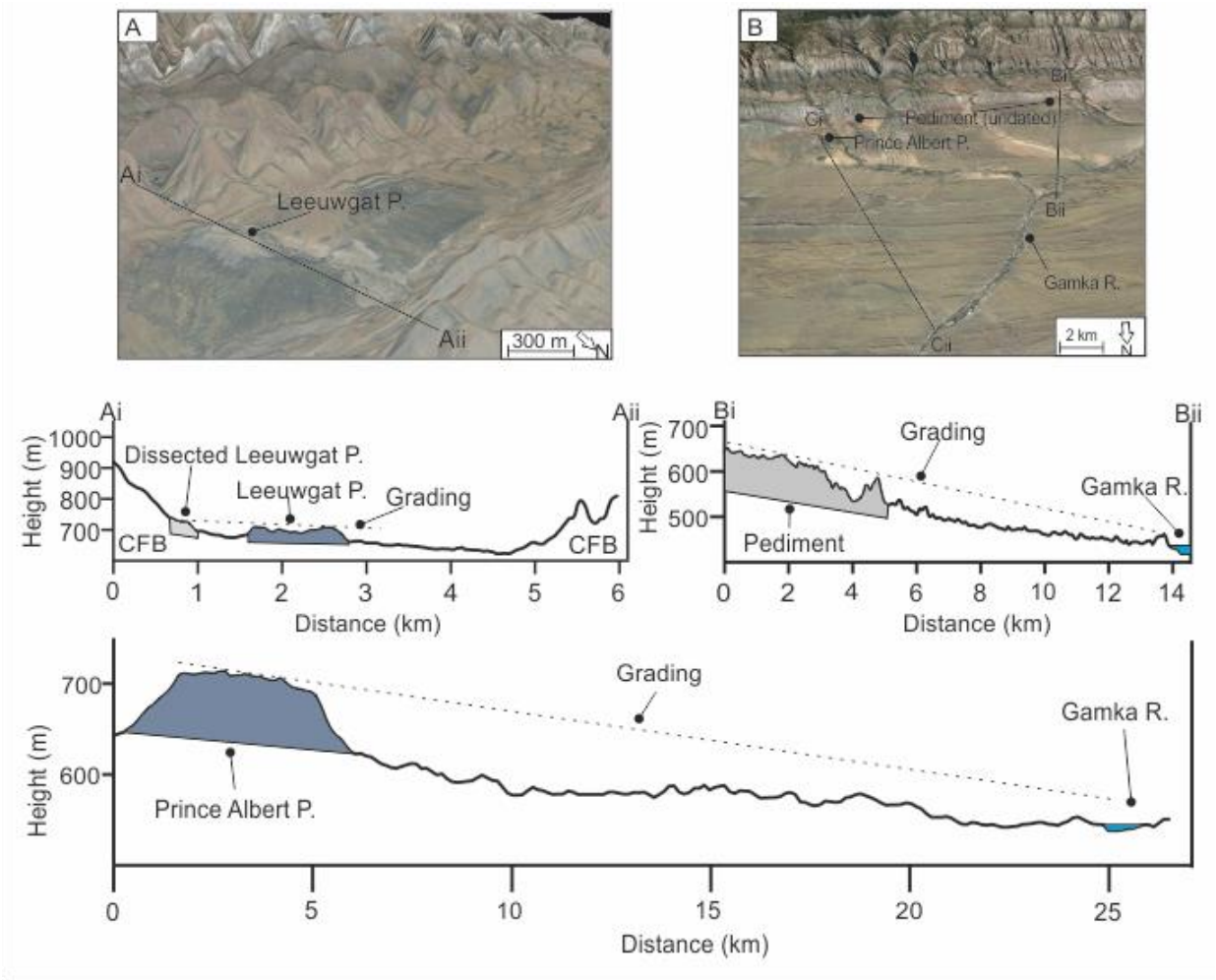

Figure 7.10 *– Grading of the A) Leeuwgat, which grades away from the Cape Fold Belt and B) Prince Albert pediment, which grades towards the Gamka River.*

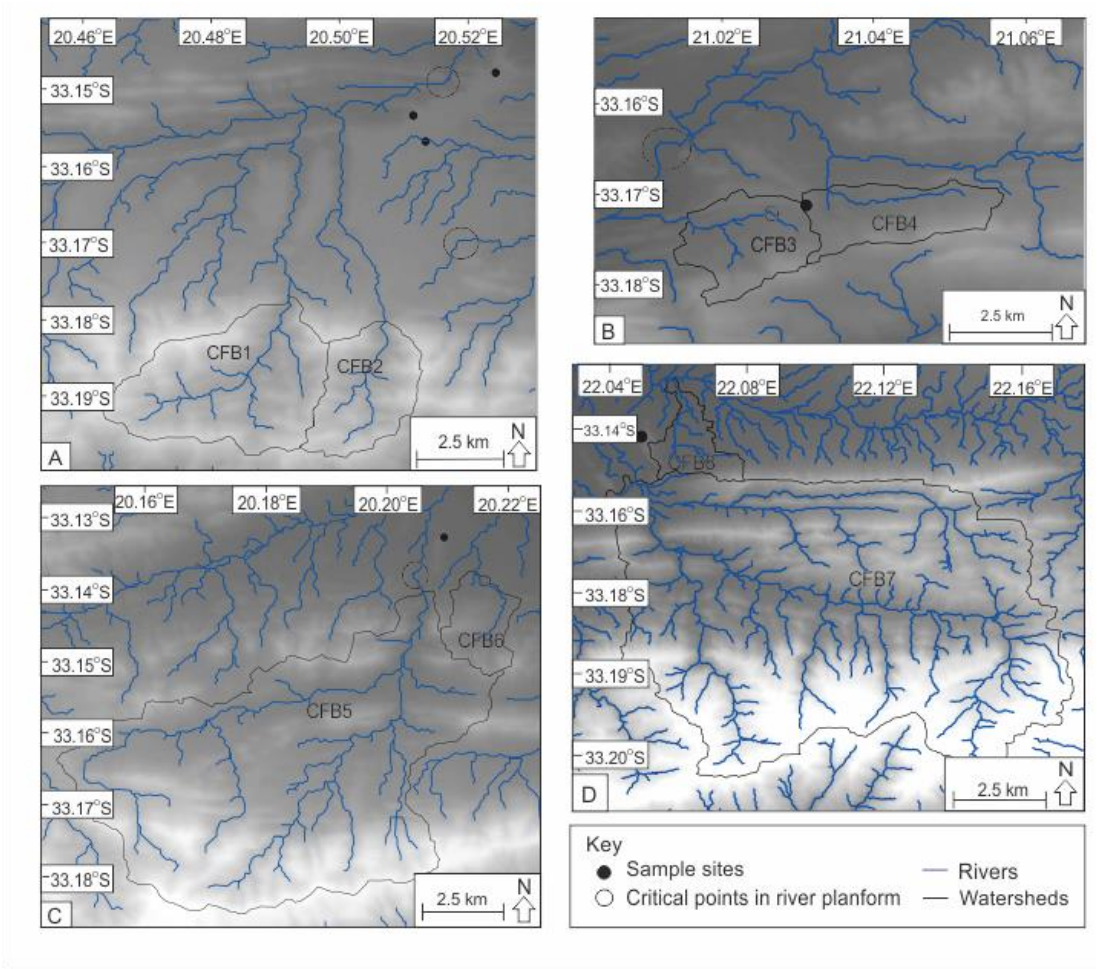

Figure 7.11 *– Planforms of the dissecting rivers and Cape Fold Belt subcatchments; A) Laingsburg; B) Floriskraal; C) Leeuwgat and; D) Prince Albert. The circles highlight critical points related to deflection of the river planforms by the Cape Fold Belt or the pediment.*

Table 7.4 *– Volume of material removed around the pediment, the equivalent rock thickness and the time taken for incision using the published data shown in Figure 7.2.*

Location	Volume of material removed (km^3)	Equivalent average rock thickness (m)	Time for incision (Ma)
Laingsburg	0.154	141.43	7.80
Floriskraal	3.240	42.33	8.15
Leeuwgat	0.169	44.27	3.18
Prince Albert	0.012	17.25	26.04

Table 7.5 shows the volume of material removed from the subcatchments in the CFB, which have dissected the pediments. The subcatchments range in area from 4.9 – 310 km^2, and the volume of material removed ranges from 0.11 - 89 km^3, which is the equivalent of 21- 286 m of lithological thickness. The pediments that have decoupled further from their CFB source have larger dissecting catchments associated with them. For example the Laingsburg pediment, which is backed by the CFB, has an average sub-catchment areas of 14.37 km^2, whereas the Prince Albert pediment is located ~ 2 km from the CFB and has an average sub-catchment area of 161.83 km^2.

Table 7.5 *– Volume of material removed from the Cape Fold Belt subcatchments, the equivalent rock thickness and time taken for incision using published data shown in Figure 7.2.*

Location	Catchment	Area (km^2)	Volume of material removed (km^3)	Equivalent average rock thickness (m)	Time for incision (Ma)
Laingsburg	CFB 1	19.79	2.86	144.39	26.59
	CFB 2	8.96	0.85	95.55	17.41
Floriskraal	CFB 3	6.21	0.28	45.31	8.35
	CFB 4	6.02	0.20	33.59	6.19
Leeuwgat	CFB 5	73.80	7.55	102.25	18.83
	CFB 6	4.91	0.11	21.64	3.98
Prince Albert	CFB 7	310.75	89.01	286.44	52.75
	CFB 8	12.92	0.23	17.79	3.28

7.6 Discussion

7.6.1 Pediment formation and characteristics

The pediments are underlain by folded strata of the Karoo and Cape Supergroups (sandstone, mudstone and shales), and backed by the resistant CFB quartzites (Figure 7.3b). It has been argued that pediments form on all lithology types, however the more extensive pediments can be found on the least resistant material (Dohrenward and Parsons, 2009). There is no systematic variation in pediment characteristics that can be related to the underlying geology (Figure 7.3b).

The pediments have formed by diffusive processes, dominated by slope processes, causing the gradual retreat of the Cape Fold Belt and coeval formation of colluvial material and soil, including an iron pan (Figure 7.12). There is no evidence in the colluvial sediment of fluvial activity, such as clast imbrication, bedforms or channel-

forms (Figure 7.5; *cf*. e.g., Gilbert, 1877; Sharp, 1940; Lustig, 1969). The iron pan layer is now at the surface of the pediment due to the removal of overlying material by surface deflation, as shown by the cosmogenic data from the depth profile (Figures 7.8, 7.12). The pediments grade towards but above large trunk rivers of the Gouritz catchment (Figures 7.9, 7.10), indicating that large transverse systems were active before pediment planation and colluvial build-up. The trunk rivers were also active during pediment formation, however they were probably less so; as shown by the build up of material. This suggests that at the time of pediment formation there was deposition of the colluvial material adjacent to large-scale sediment bypass, and erosional formation of the pediment surfaces. The trunk rivers represent an upper limit to the extent of the pediments and they should be regarded as individual landforms and not as an extensive 'surface' (*cf.* King, 1948, 1953, 1955; Partridge and Maud, 1987).

The distribution of the dissected pediments suggest these are remnants of much more extensive features (Figure 7.10). There has been a shift in the dominance of slope processes to fluvial processes as evidenced by the dissection by smaller subcatchments and the decoupling of the pediments from the CFB sediment source area. The dissecting river planform has primarily been controlled by tectonic folds. However, the pediments have also controlled the landscape evolution by deflecting the rivers, allowing the surfaces to be preserved. It appears that the structural integrity of the pediment is not continuous across the entire pediment, and stronger areas have been able to deflect dissecting rivers (Figure 7.11). This could be a function of the sedimentology (Figure 7.5) of the pediment, the calibre of material and the extent of packing, or the presence and thicknesses of the duricrust layer. Deflection of rivers has been shown to cause the formation of epigenetic gorges (Ouitmet et al., 2008). The pediments sit above the current level of erosion and are fossilised landforms that represent a store of sediment that is only subject to weathering and deflation, with hillslope processes supplying sediment to the nearby fluvial channels.

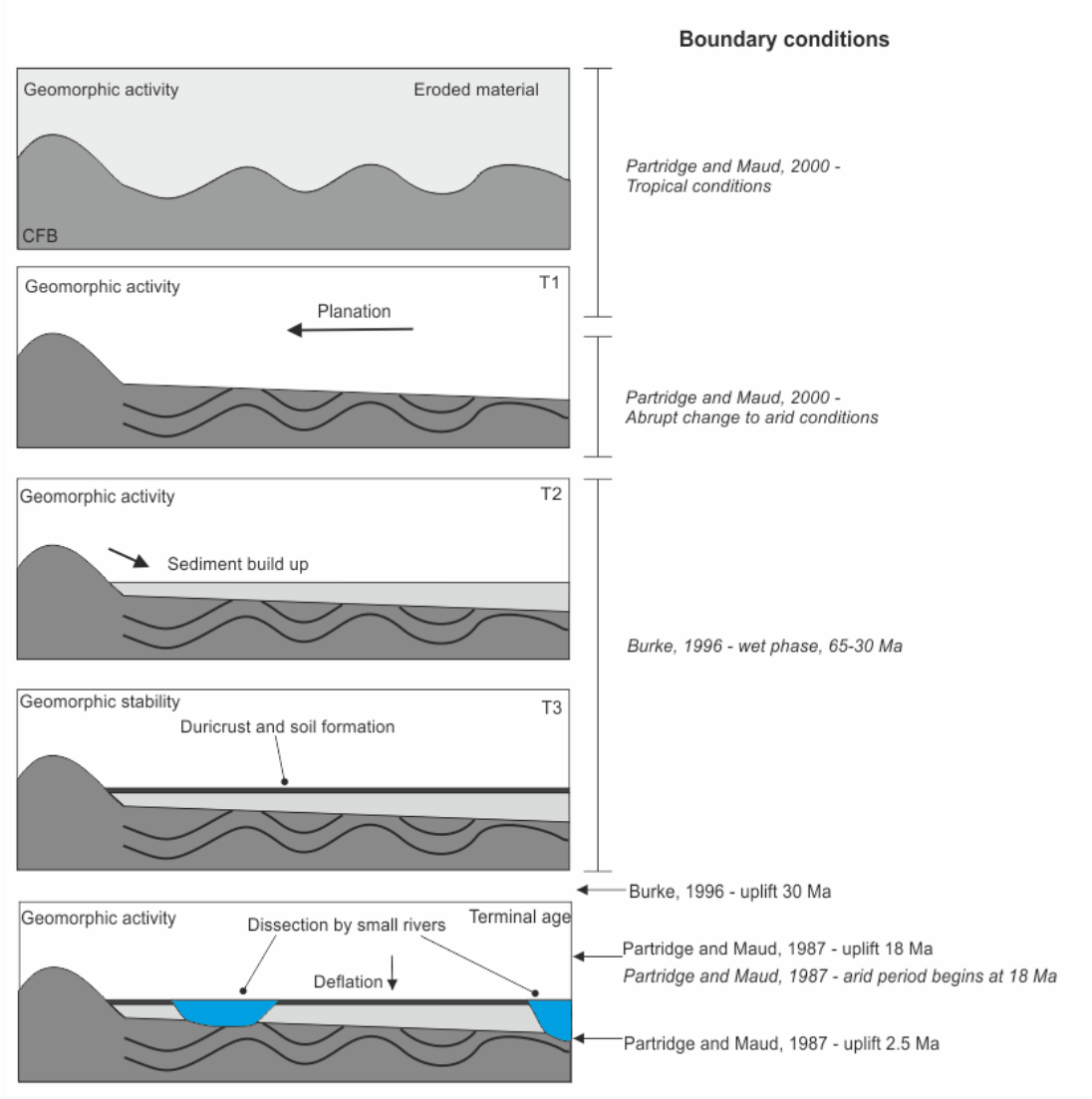

Figure 7.12 *- Sequence of events forming the pediments; in which the folded Karoo Supergroup Strata was planned, hillslope processes caused the build-up of sediment, soil formation and duricrust formation. The pediments were then dissected and fluvial processes dominate. The contentious boundary conditions are shown on the right, climatic change (italics) and tectonic conditions.*

7.6.2 Geomorphic, tectonic, climatic and stratigraphic considerations

The cosmogenic data presented in Table 7.3 and Figure 7.8 is within the range of data presented in Figure 7.2 (van der Wateran and Dunai, 2001; Bierman et al., 2014; Kounov et al., 2015). There is no systematic spatial variation in surface lowering rates between the pediments that can be correlated to pediment size, or variations in geology. The Prince Albert pediment is the most isolated from the CFB, with no duricrust present (Figure 7.3a), which could indicate why the surface lowering rates are the highest in this location. Further, the pediment surfaces only remain fossilised as long as the duricrust remains, when removed denudation rates will increase (but will likely still remain low compared to other landforms, Figure 7.2) and therefore the

duricrusts represent an intrinsic geomorphological threshold. Nonetheless, the minimum exposure ages of Pleistocene are dubious given the need for an intervening period of exceptional erosion rates to rectify the present day landscape configuration and do not help further constrain the landscape development of the Western Cape. The local and regional geomorphic and stratigraphic information was integrated to further understand the pediment development.

1) Volume of material missing and known erosion rates

The volume of material removed during the dissection of the surrounding pediments equates to a lithological thickness of 42 – 141 m (Table 7.4). Given the published surrounding denudation rates (Figure 7.2), denudation is constrained to 3 - 26 Ma, and so the pediments must be at least this age. However, as shown by the pediments causing the deflection of surrounding rivers (Figure 7.11), denudation of the pediment material could have taken longer as the resistance of the pediment is higher than the surrounding bedrock in some locations. The denudation of the subcatchments within the CFB that back the pediments (Figure 7.11, Table 7.5), indicates that a minimum of age of 17- 27 Ma for the Laingsburg pediment, 6 - 8 Ma for Floriskraal, 4 - 19 Ma for Leeuwgat and 3 – 53 Ma for Prince Albert based on the average denudation rate of published river data (Figure 7.2). The CFB subcatchment denudation ages represent the *minimum* ages of the dissecting rivers reaching the CFB after dissecting the pediment surfaces. Using the largest subcatchments, which represent the absolute *minimum* age of the pediments and the time taken to dissect the pediments, indicates that the Laingsburg pediment is a minimum age of 35 Ma; Floriskraal 16 Ma; Leeuwgat 22 Ma and; Prince Albert 79 Ma representing the cessation of pediment formation and the start of dissection assuming all the processes occurred at the same rate during the development; these ages therefore represent a crude estimate of age given the available information. The geomorphic evidence therefore indicates *minimum* ages that are an order of magnitude higher than the cosmogenic data. Previous works have classified pediment surfaces within height brackets (e.g., King, 1953), however in this study there is no correlation between pediment elevation and their geomorphic *minimum* ages.

2) Duricrust development

Duricrusts are found on many of the studied pediments (Summerfield, 1983; Marker et al., 2002). The pediments studied no longer have the overlying sediment preserved, and have been lowered to the iron pan layer, which is well-developed in the Laingsburg pediment (Figure 7.5). The depth profile indicates that some deflation has occurred (Figure 7.8), which has exposed the iron pan (laterites). The iron pan could have formed by leaching from surrounding lithologies and clasts or by lateral movement due to groundwater change (Widdowson, 2007). The formation of iron pans occurs on low relief surfaces that have been stable for at least a million years (Al-Subbary et al., 1998). Since the Cenozoic South Africa has been relatively quiescent (e.g., Bierman et al., 2014). Additionally, a favourable climate of high annual rainfall, high humidity and high mean annual temperature is required (Widdowson, 2007). Higher concentrations of carbon dioxide are also associated with the formation of laterites (and iron pans), greenhouse episodes have occurred in the late Cretaceous and Late Palaeocene to Early Eocene, leading to world-wide extensive weathering (Bardossy, 1981; Valeton, 1983).

The breakdown of minerals to form laterites involves many steps (Widdowson, 2007), however the time taken to form laterites is still poorly constrained. Laterite formation in coastal southern South Africa have been argued to be late Pliocene in age (Marker and Holmes, 1999) and to have continued into the late Pleistocene (Marker and Holmes, 2005), being a component of the Quaternary development of the Southern Cape (Marker et al., 2002). However, the Mediterranean climate of the coastal areas does not extend inland to the study location. Given the past climate and tectonic events, the iron pans were probably formed during the Late Cretaceous greenhouse episode, which is compounded by the constrained dissection rates of the pediment surfaces (e.g., Dauteuil et al., 2015); the iron pan had to form pre-dissection. The formation of duricrusts and iron pans would have occurred coevally with pediment formation, and would have extended post-pediment formation (Helgren and Butzer, 1977; Widdowson, 2007). The presence of iron pans indicates a period of geomorphic stability of at least 1 Ma, and probably much longer, prior to the dissection of the pediments.

7.6.3 Sequence of events

Pediment formation requires mountain range retreat, which causes the underlying lithological strata to be truncated (Figure 7.12). The *minimum* exposure ages calculated by cosmogenic nuclide dating do show the remarkable stability of the

pediments, which is related both to lithology (duricrust cappings, iron pans, resistant quartzite boulders; e.g., Scharf et al., 2013) and structure of the CFB deflecting incising rivers. Overall, however, the *minimum* exposure ages calculated using ^{10}Be for the pediments do not help constrain landscape development further. It is important to integrate geomorphologic and stratigraphic knowledge when reporting cosmogenic nuclide results, especially in an ancient setting with low denudation where the nuclide concentrations may be in saturation.

During the Cretaceous the Cape Fold Belt was exhumed (Figure 7.12; Tinker et al. 2008a, Tankard et al. 2009). During this time, the folded strata was planned by hillslope processes (e.g., Rich, 1935; Bourne and Twidale, 1998), coevally depositing colluvial material and forming soils (Figure 7.12); this was aided by the humid climate and greenhouse conditions of the Cretaceous causing deep weathering (Bardossy, 1981; Valeton, 1983). Tectonic stability allowed the formation of iron pans and duricrusts, which are now exposed at the surface of the pediments due to surface deflation and the removal of overbank material (Figure 7.12). The initial planation and colluvial build up had to have occurred pre-Miocene as shown by the dissection data (Tables 7.4, 7.5), however we posit the surfaces would have formed much earlier due to the very slow processes associated with pediment formation (e.g., Lustig, 1969; Dohrenwend and Parsons, 2009). By the mid-Miocene, dissection of the pediments and backing Cape Fold Belt occurred with the extension of small subcatchments. This latter stage of landscape development has decoupled the pediments from the CFB sediment source, and essentially fossilised the landform (Table 7.3).

7.6.4 Implications for landscape development

The large-scale dissection of the pediments requires a geomorphic pulse of activity. The *minimum* geomorphic ages reported here roughly correlate to the proposed uplift of 30 Ma (Burke, 1996), 18 Ma (Partridge and Maud, 1987) and 2.5 Ma (Partridge and Maud, 1987), and could indicate that the pediments were dissected due to different pulses of uplift. Nonetheless, this time period also corresponds to variation in climate, including periods of humidity reported to have ended at 30 Ma (Burke, 1996) or 18 Ma (Burke, 1996). It is not possible to distinguish the main driver of dissection (Figure 7.12), and tectonic signatures are not identified within the Gouritz catchment morphometry (Chapter 8).

The grading of the pediments indicates the main trunk rivers were active before the pediments, at least by the Miocene and probably established within the Cretaceous, when large scale exhumation occurred within South Africa (*cf.* Green et al., 2016).

The individual grading of the pediment surfaces indicates that the pediments cannot be taken as a singular surface (King, 1953) as the pediments are relatively local features that react to surrounding tectonic and geomorphological settings. The surface lowering rates of the pediments indicate a period of low activity as documented by other researchers (Figure 7.2, Fleming et al., 1999; Cockburn et al., 2000; Bierman and Caffee, 2001; van der Wateran and Dunai, 2001; Kounov et al., 2007; Codilean et al., 2008; Dirks et al., 2012; Decker et al., 2011; Erlanger et al., 2012; Chadwick et al., 2013; Decker et al., 2013; Scharf et al., 2013; Bierman et al., 2014; Kounov et al., 2015). There has been a drastic reduction in denudation rates since the Cretaceous as shown by apatite fission track and cosmogenic nuclide studies (Figure 7.2). The data reported in this study are some of the lowest in the world (Portenga and Bierman, 2011). Surface lowering is not consistent across landforms within southern South Africa. Rivers are dissecting at a faster rate (Scharf et al., 2013; Kounuv et al., 2015) than the pediment surfaces (this study, van der Wateran and Dunai, 2001; Bierman et al., 2014; Kounov et al., 2015), which indicates that relief is developing at a slow rate, as also argued by Bierman et al. (2014 reported) from the Eastern Cape. The offshore depositional record (Tinker et al. 2008a) mirrors the reduction in denudation rates with peaks in the Cenozoic most likely related to the rejuvenation of the landscape during dissected the pediments in this study (e.g., Hirsch et al., 2010; Dalton et al., 2015; Sonibare et al., 2015). These increases in offshore sediment flux are minor in comparison to rates in the Cretaceous.

7.7 Conclusion

In conclusion, large-scale erosional surfaces characterise the ancient landscape of southern South Africa. Cosmogenic nuclide dating using ^{10}Be of four pediment surfaces in the Western Cape (0.33 to 1.00 m Ma^{-1}), and a depth profile indicate low surface lowering rates and *minimum* exposure ages from the Early Pleistocene. Due to isotope concentrations close to saturation the *minimum* exposure ages do not aid in further constraining the landscape development of the study area. We contend that cosmogenic nuclide results must not be viewed in isolation and should be assessed together with surrounding geomorphologic and stratigraphic conditions. The pediments studied must be at least Miocene in age, and probably much older (i.e. Cretaceous) based on the volumes of post-pediment dissection, published erosion rates, the presence of duricrusts and the current understanding of tectonic and climatic variation. The duricrusts represent an internal geomorphic threshold which limits the rate of denudation. The dissection of the pediments has been largely

controlled by the structure of the Cape Fold Belt, with the initial geomorphic pulse of incision most likely related to tectonic uplift or climate change. The presence of the pediments has deflected dissecting rivers in some locations and controlled landscape evolution of the surrounding rivers. The pediments grade to individual base levels (trunk rivers), and although locally extensive, they are not a regional feature representing one single surface.

The pediments in southern South Africa are lowering at very low rates and are now decoupled from the surrounding rivers. Therefore, they are a fossilised landform that represents a store of sediment. The persistence of the pediments is due to the resistant duricrust capping and quarzitic boulders, but also due to the structural control of the Cape Fold Belt and pediments, deflecting dissecting rivers.

Chapter 8 Testing the applicability of morphometric characterisation in discordant catchments to ancient landscapes: a case study from southern Africa

8. 1 Abstract

The ancient landscapes south of the Great Escarpment in southern Africa preserve large-scale geomorphological features despite their antiquity. This study applies and evaluates morphometric indices (such as hypsometry, long profile analysis, stream gradient index, and linear / areal catchment characteristics) to the Gouritz catchment, a large discordant catchment in the Western Cape. Spatial variation of morphometric indices were assessed across catchment (trunk rivers) and subcatchment scales. The hypsometric curve of the catchment is sinusoidal, and a range of curve profiles are evident at subcatchment scale. Hypsometric integrals do not correlate to catchment properties such as area, circularity, relief, and dissection; and stream length gradients do not follow expected patterns, with the highest values seen in the mid-catchment areas. Rock type variation is interpreted to be the key control on morphometric indices within the Gouritz catchment, especially hypsometry and stream length gradient. External controls, such as tectonics and climate, were likely diminished because of the long duration of catchment development in this location. While morphometric indices can be a useful procedure in the evaluation of landscape evolution, this study shows that care must be taken in the application of morphometric indices to constrain tectonic or climatic variation in ancient landscapes because of inherited tectonic structures and signal shredding. More widely, we consider that ancient landscapes offer a valuable insight into long-term environmental change, but refinements to geomorphometric approaches are needed.

8.2 Introduction

The physiography of South Africa has received much attention owing to its distinctive topography and ancient setting, but the timing and processes involved in landscape evolution remain contentious in several respects. Major river networks within southern South Africa have evolved since the Mesozoic breakup of Gondwana (Moore and Blenkinsop, 2002; Hattingh, 2008), and their development has been synchronous with large-scale (6-7 km) exhumation of the southern African continental crust (Tinker et al., 2008a). However, the tectonic uplift history of southern Africa is poorly constrained, especially the causes and magnitude of uplift (Gallagher and Brown, 1999; Brown et al., 2002; Tinker et al., 2008a; Kounov et al., 2009; Decker et al.,

2013). Previous macroscale geomorphological research in southern South Africa has focussed on the formation of the Great Escarpment (e.g., King, 1953; Partridge and Maud, 1987; Brown et al., 2002), and the development of the Orange River (e.g., Dingle and Hendey, 1984). Furthermore, the timing of the main phase of landscape development in South Africa has been argued to be either Cenozoic (Du Toit, 1937, 1954; King, 1951; Burke, 1996) or Mesozoic (Partridge, 1998; Brown et al., 2002; Doucouré and de Wit, 2003; de Wit, 2007).

Long-lived ancient landscapes (Bishop, 2007) have been argued for many 'Gondwana landscapes' (Fairbridge, 1968) related to large parts of the planet, including cratonic areas and passive continental margins, such as Australia (e.g., Ollier, 1991; Ollier and Pain, 2000; Twidale, 2007a,b), southern South Africa (e.g., Du Toit, 1954; King, 1956a), and South America (e.g., King, 1956b; Carignano et al., 1999; Demoulin et al., 2005; Panario et al., 2014; Peulvast and Bétard, 2015). Long-lived landforms and surfaces have also been argued to form parts of Russia (Gorelov et al., 1970), India (Gunnell et al., 2007), Sweden (Lidmar-Bergström, 1988), and western France (Bessin et al., 2015). Ancient landscapes have the potential to offer insights into the temporal variation of controls such as tectonic uplift or climate. However, deciphering these factors is problematic within ancient catchments because the imprint of certain forcing factors on catchment morphology may no longer be present owing to long-term erosion. The loss of forcing signals can also be seen with regards to sediment transport, which mediates landscape response (Jerolmack and Paola, 2010). The catchments draining southward from the Great Escarpment in the Western Cape have been subject to cosmogenic (Scharf et al*.,* 2013) and apatite fission track analyses (Tinker et al., 2008a) to determine rates of fluvial erosion and exhumation, respectively; but these data have not been through a detailed geomorphological assessment (Rogers, 1903; Partridge and Maud, 1987). Fundamental morphometric analyses of South African drainage basins have yet to be attempted, although this approach has the potential to yield insights into the long-term landscape evolution as shown by the Walcott and Summerfield (2008) hypsometry study in the Eastern Cape.

Geomorphometry employs a range of morphometric indices to help characterise the history of a drainage basin (Horton, 1932; Miller, 1953; Schumm, 1956; Chorley, 1957; Strahler, 1964). Morphometric indices include river network analysis, hypsometry, and analysis of the stream profile. River networks are used to infer the tectonic and climatic history of a region (e.g., Montgomery et al., 2001; Walcott and Summerfield, 2008; Antón et al., 2014), as river form is closely linked to these

extrinsic factors. However, river networks are also governed by intrinsic factors such as network reorganisation through stream capture (Davis, 1889), bedrock geology (Tinkler and Wohl, 1998; Duvall et al., 2004), and sediment flux (Richards, 1982; Sklar and Dietrich, 2001). Many studies of morphometric indices relate to tectonically active areas (e.g., Snyder et al., 2000; Zhang et al., 2013; Antón et al., 2014; Ghosh et al., 2014). However, these indices are rarely applied to tectonically quiescent areas or ancient landscapes. An example of a morphometric approach to ancient landscape development is by Walcott and Summerfield (2008) who assessed the variation in hypsometric integral within catchments draining the Drakensberg mountain range in eastern South Africa. They argued that variation in hypsometric integral within streams of order 5 or less is because of differences in bedrock type resistance as well as moderate crustal displacement, whereas the larger stream orders (>6) are independent of rock type or tectonic control.

In this study, we test if morphometric indices can offer further insight into the history of the understudied ancient landscapes of southern South Africa, which have undergone reorganisation because of the exhumation of the resistant Cape Fold Belt and retreat of the Great Escarpment. Therefore, inherited structures are expected to play an important role in landscape evolution of the Gouritz catchment. We aim to address the following objectives: (i) to extract morphometric indices for an antecedent and tectonically quiescent drainage basin, the Gouritz Catchment; (ii) to document spatial variation in morphometric indices within the main tributaries; (iii) to test the prevailing conceptual models in the literature of external (e.g., Montgomery et al., 2001; Keller and Pinter, 2002; Manjoro, 2015) and internal controls (e.g., Tooth et al., 2004; Walcott and Summerfield, 2008; Jansen et al., 2010) on geomorphometry and landscape evolution; and (iv) to assess the broader suitability of morphometric indices for characterisation of ancient landscapes.

8.3 The Gouritz catchment

The Gouritz catchment is located within the Western Cape Province of South Africa (Figure 8.1) and is one of several antecedent systems draining from the Great Escarpment that cut across the west-east trending Cape Fold Belt (CFB) mountains to the Atlantic and Indian Oceans. Antecedence in the Western Cape is shown by the large-scale discordance of the main trunk rivers (Rogers, 1903), which completely dissect the resistant CFB and have deeply incised meanders into quartzites (up to 1 km in depth). The main catchment evolutionary events include the breakup of Gondwana in the Mesozoic (Summerfield, 1991; Goudie, 2005) and the large-scale incision in the Cretaceous resulting in the exhumation of the CFB (Tinker et al.,

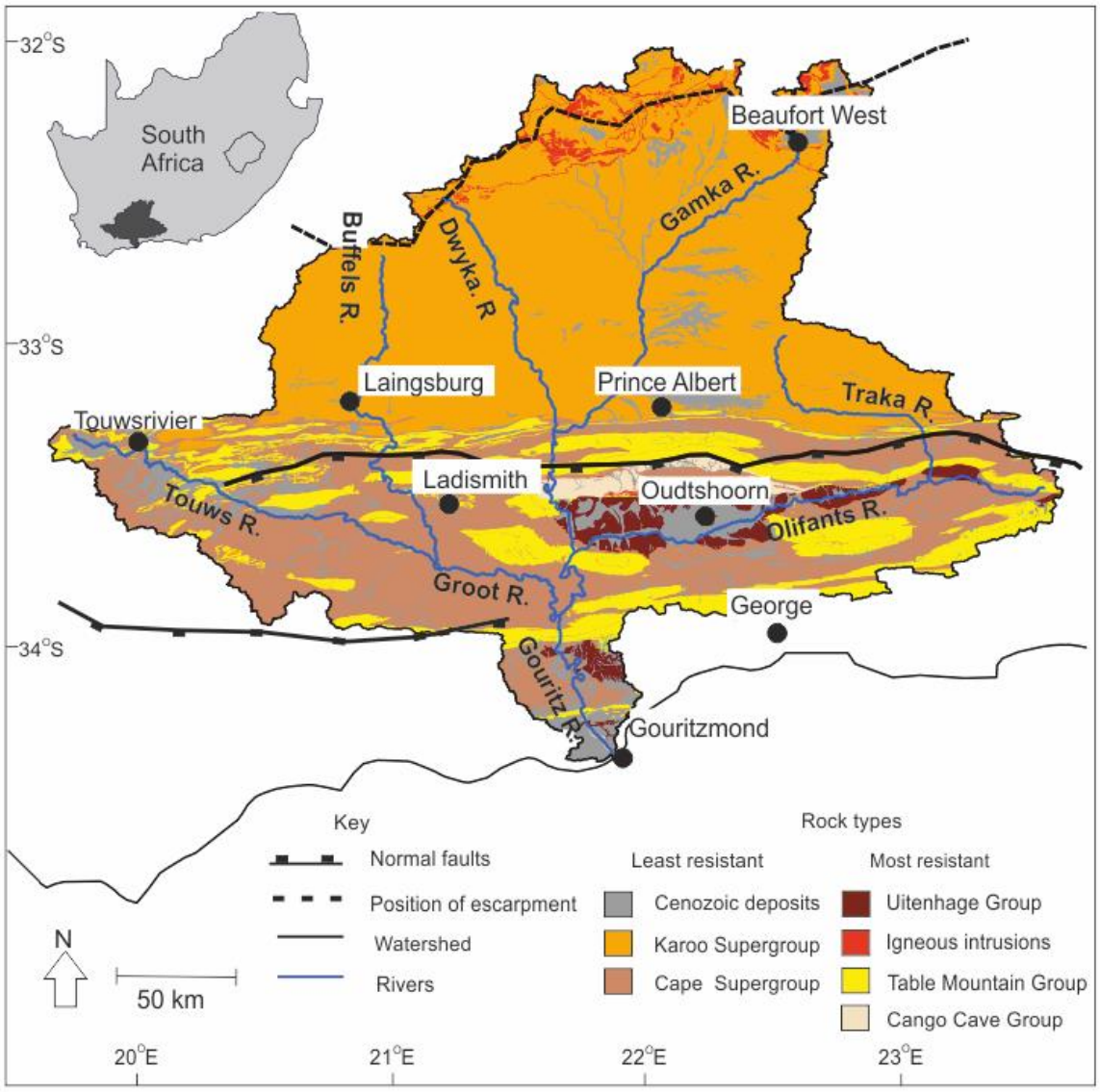

Figure 8.1 *- The location of the Gouritz catchment in southern South Africa and the six major tributaries and major extension faults. A simplified geological map is also shown highlighting the main rock types.*

2008a) and the Karoo basin-fill. As such, the retreat and development of the Great Escarpment (Fleming et al., 1999; Cockburn et al., 2000; Brown et al., 2002; Moore and Blenkinsop, 2006) has an important control on catchment evolution and stream capture of the Orange River catchment. King's (e.g., King, 1963, 1972) view of the escarpment forming at the coastline and retreating uniformally since the breakup of Gondwana has been disproved by numerical models (e.g., Gilchrist and Summerfield, 1990; van der Beek et al., 2002) and dating techniques (e.g., Fleming et al., 1999; Brown et al., 2002). On the basis of apatite fission track data, researchers have proposed that the Great Escarpment has retreated a *maximum* of 29 km to its current

position since the Cretaceous (Brown et al., 2002), which would have affected the headwaters of the Gouritz catchment.

The Gouritz catchment has an area of 6.45 x 10^4 km^2 and a stream order of 7 (Strahler, 1957). The basin is composed of six main tributaries: the Traka, Touws, Buffels, Olifants, Dwyka, and Gamka rivers (Figure 8.1). The source regions for many of the main tributaries are hillslopes to the south of the Great Escarpment, with the Gouritz system reaching the ocean at Gouritzmond (Figure 8.1). The majority of the rivers are bedrock or mixed bedrock-alluvial in nature, with common steep-sided valleys and bedrock-confined gorges.

The Great Escarpment separates an interior plateau of low relief and high elevation from a coastal region of high relief and low average elevation (Fleming et al., 1999; Tinker et al., 2008b; Moore et al., 2009). The Gouritz catchment also contains a segment of the exhumed CFB, which is a compressional mountain range that formed in the late Permian and Triassic (Tankard et al., 2009; Flint et al., 2011). Physiographically, and based on variation in elevation and landscape morphology, the drainage basin can be divided into the following units: escarpment, central Karoo, Cape Fold Belt, and coastal (Figure 8.2A). The application of Hammond's topographic analysis (Figure 8.2B) to the Gouritz catchment reveals that the area is dominated by (i) plains that usually carry a thin (<1 m) sedimentary cover, which decreases toward the north, and that include dissected pediment surfaces; and (ii) mountains where bedrock crops out in the CFB and escarpment regions with a thin regolith, if present.

The present day climate of the Gouritz catchment is primarily semiarid (Dean et al., 1995) with mean annual precipitation of 262 mm (CSIR, 2007). The region has a clear split between summer and winter rainfall regimes, with late summer to winter rainfall in the Great Escarpment and central Karoo region, winter rainfall in the western CFB, late summer to winter rainfall in the southern CFB, and summer and winter rainfall in the coastal areas (CSIR, 2007).

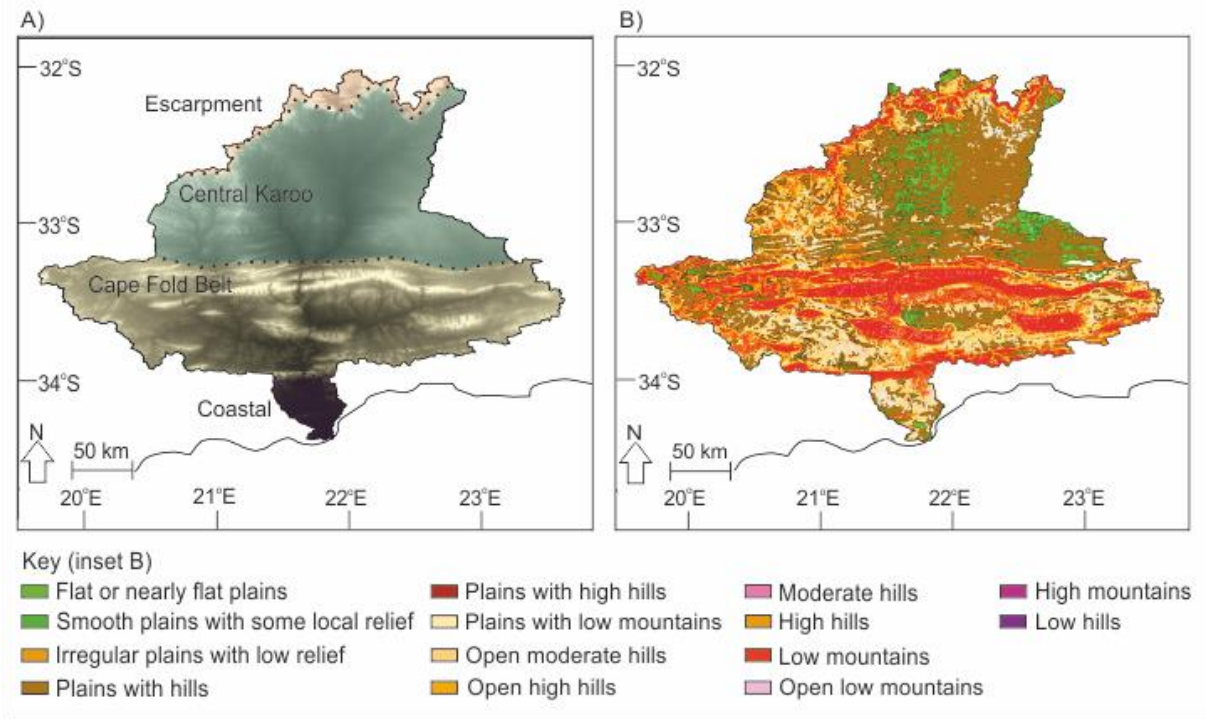

Figure 8.2 *- A) Topography variation within the Gouritz catchment showing the main physiographic regions; B) Hammond's landform classification map indicating the catchment is dominated by plains and mountains.*

The lower part of the catchment in the coastal region has a Mediterranean-type climate (Midgley et al., 2003). Orographic rainfall over the CFB provides much of the discharge (Midgley et al., 2003), with the other main source being intense thunderstorms that usually form on the escarpment and move south over the central Karoo. Smaller tributaries in the upper reaches of many of the larger trunk rivers are ephemeral. South of the CFB, trunk rivers are perennial with the main tributaries transporting boulders to sand-grade material as bedload, although no sediment transport data is available. The climatic history of southern South Africa is poorly constrained. Since the Cretaceous (and the development of the major drainage systems), we see a general trend toward a more arid environment (Bakker and Mercer, 1986), with variation in intensity in the winter or summer rainfall regime (Bar-Matthews et al., 2010) as well as the fire regime (Seydack et al., 2007).

The substrate of Gouritz catchment is predominantly Palaeozoic rocks of the Cape and Karoo Supergroups, composed of various mudstone and sandstone units (Figure 8.1). Small inliers of the Kansa Group (conglomerate, shale, mudstone) are found in the CFB. Resistant lithologies (Figure 8.3) within the Gouritz catchment include the Precambrian Cango Cave Group, which comprises metasediments (limestones, arenites, mudrocks), the Table Mountain Group quartzites, and Jurassic dolerite intrusions dominantly toward the north and granite plutons in coastal areas of the

catchment (Figure 8.1). The Mesozoic Uitenhage Group comprised mainly of conglomeratic and sandy units represents the youngest resistant rock type within the basin.

The structural geology of the drainage basin is dominated by large-scale (~11 km wavelength; Tankard et al., 2009) E-W trending folds that decrease in amplitude toward the north (Paton, 2006, Spikings et al., 2015). The folds formed along the southwestern margin of Gondwana during Paleozoic-Mesozoic convergence (e.g., Tankard et al., 2009). The Gouritz catchment contains two large anticlines, the Swartberg and Langeberg (CFB), which are cut by large Mesozoic normal faults (Paton, 2006), the Swartberg and Worcester faults, respectively (Figure 8.1).

The Gouritz catchment is currently tectonically quiescent, with a lack of fault scarps, low seismicity (Bierman et al., 2014), and low rates of sediment supply (Kounov et al., 2007; Scharf et al., 2013). The tectonic history of the area is contentious (Gallagher and Brown, 1999; Brown et al., 2002; Tinker et al., 2008a; Kounov et al., 2009; Decker et al., 2013). Researchers have debated about the events causing the large-scale denudation in the Cretaceous, with ideas often related to plume activity in the Early Cretaceous (Moore et al., 2009). Burke (1996) proposed that the most recent uplift occurred around 30 Ma ago because of a thermal anomaly, whereas Partridge and Maud (1987) argued for a later period of activity in the Miocene (~250 m uplift) and again in the Quaternary (900 m uplift). The large-scale exhumation across southern South Africa could still be driving eperiogenic uplift (Tinker et al., 2008a).

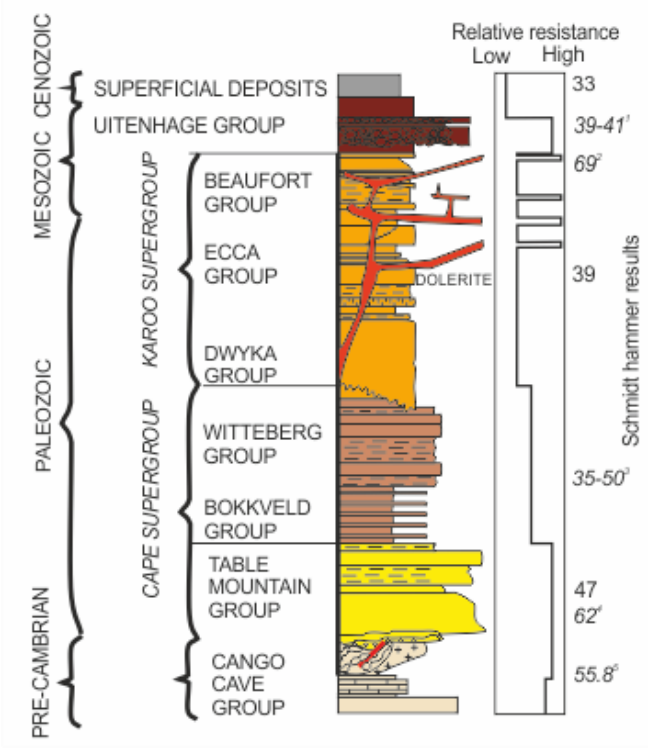

Figure 8.3 *- Relative resistance of rock types within the Gouritz catchment. Quartzite (Table Mountain Group) and dolerites are the most resistant rock types. The values indicate Schmidt hammer results from the study area, italicised numbers are from published studies of the same rock type (1 – Özbek, 2009; 2 – Dardis and Beckedahl 1991; 3 – Goudie, 2006; 4 – Shelton, 2015; 5 - Goudie et al., 1990).*

8.4 Methodology

Catchment topography from a digital elevation model (DEM) based on ASTER (30 m) data, was reprojected into WGS 1984 world Mercator coordinates. Catchment boundaries were extracted using the default hydrology toolbox in ArcGIS 10.1, in which the DEM was manually filled in order to remove any holes within the DEM to allow for flow path extraction. Following Abedlkareem et al. (2012) and Ghosh et al. (2014), a minimum upstream drainage area threshold of 3.35 km^2 was used to delineate the drainage network, showing perennial and ephemeral rivers. Stratigraphic unit, rock type, and structural geological data sets were obtained digitally from the Council of Geoscience, at a scale of 1:250,000.

8.4.1 Drainage characterisation and landforms

Zernitz (1932) laid the foundation of drainage pattern analyses, argued that structure and slope determine the spatial arrangement of rivers, and determined six river patterns (dendritic, trellis, rectangular, radial, annular, and parallel). A more refined classification was provided by Howard (1967) with additional subclassifications, which included subdendritic, pinnate, anastomotic, and distributary. Drainage patterns are

fundamental in determining structural change at a local and regional scale (Hills, 1963) with analyses used primarily in tectonic settings (e.g., Gupta, 1997; Friend et al., 2009).

The drainage pattern of the Gouritz Catchment was assessed and assigned drainage categories in order to assess controls on the catchment (Zernitz, 1932) at a regional scale (Knighton, 1998). The impact of tectonic structures is shown by the dominance of trellis or parallel patterns. Tectonic structure has been shown to be important in catchments draining the western domain of the CFB (Manjoro, 2015): 49% of the catchment area of the Gouritz drains the southern domain of the CFB.

8.4.2 Morphometric indices

8.4.2.1 Long profile

Long profiles of the main trunk rivers were extracted using ArcGIS by digitising the stream network with 10-m vertical spacing along the stream. Assessing long profiles of rivers allows quantitative analysis of fluvial incision and lithological controls (Hack, 1973). The analysis of long profiles can highlight knickpoints, which are the principal method of channel lowering within bedrock channels (Whipple, 2004). In this study, long profiles were further quantified using the stream gradient index (Hack, 1973), which would be expected to be approximately constant along a graded long profile in a homogenous lithology. Deviations from the average value were therefore assumed to be caused by forcing factors (Antón et al., 2014) such as tectonics (Keller and Pinter, 2002), lithology (Hack, 1973), or migrating knickpoints (Bishop et al., 2005).

8.4.2.2. Stream gradient index

Long profile geometry was used to assess the level of grading within a river by employing the stream gradient index (SL; Hack, 1973) and was calculated as

$$SL = (\Delta H/\Delta Lr)\Delta Lsc \qquad \text{Eq. 8.1}$$

where ***ΔH*** is change in altitude, ***ΔLr*** is length of the reach, and ***ΔLsc*** is the horizontal flow path length from the watershed divide to the midpoint of the reach. The stream length gradient was calculated in 50-m reaches for the main trunk rivers, the data were then normalised (to a value between zero and one, using the range of values collected from all trunk rivers) to allow comparison between the trunk rivers.

8.4.2.3 Morphometric indices

Morphometric indices permit the quantitative assessment of, and comparison between, landscapes and can highlight anomalies along the river network. Linear measurements such as stream order, stream length, and bifurcation ratio (Horton,

1945) were extracted using ArcGIS. Areal measurements such as basin area, drainage density (Horton, 1945), and circularity (the ratio of the perimeter of the basin to the perimeter of a circle with the same area) were also extracted. Drainage density was extracted for the entire catchment and also for the main rock types within the catchment (Figure 8.1) in order to assess the impact of different bedrock resistances to the drainage pattern.

8.4.2.4 Hypsometry

Hypsometry describes the area distribution of elevation within a catchment. Strahler (1952) defined the hypsometric integral (HI) as the differences in sinuosity of curve form and the proportionate area below the curve. Strahler (1952) argued that catchments where HI > 0.6 are in disequilibrium (youth) and the catchment shows rapid slope transformation as the drainage system expands, and where HI is between 0.4 and 0.6 catchments are in equilibrium (mature). Below 0.4 the catchments are argued to be in a monadnock phase (old age; Strahler, 1952). More recently hypsometry has been used for a wide range of applications, including the evolution of landscapes (Hancock and Willgoose, 2001), the effect of climate (Montgomery et al., 2001), and the influence of tectonics on catchments (Ohmori, 1993). Hypsometric curves have been used to decipher the forcing factors in catchments (Strahler, 1952; Montgomery et al., 2001; Walcott and Summerfield, 2008). However, the influence of drainage basin properties such as area, circularity, relief, and dissection on the HI has received mixed results, with researchers arguing for correlation (Hurtrez et al., 1999; Chen et al., 2003) and no correlation (Walcott and Summerfield, 2008). Strahler (1952) argued that catchments try to maintain a convex or sinusoidal curve, with erosion of the transitory concave monadnock phase returning the curve to a sinusoidal curve.

In this study, hypsometric data (hypsometric integral (Eq. 8.2) and curve) were extracted by an ArcGIS tool (Hypsometric Tools by Davis, 2010) for the whole catchment and then western-draining subcatchments. The western-draining catchments are defined as those that drain the western part of the Gouritz catchment, delineated at the confluence with the main trunk river (Gamka River). These subcatchments were chosen to investigate the variation in hypsometric integral and curve shape with respect to the location of the catchment and the stream order. Only analysing the western-draining subcatchments is justified because the Gouritz catchment is nearly symmetrical (Figure 8.1) and because the geology is broadly similar in the western and eastern portions of the catchment (Figure 8.1). Hypsometric

integrals were then compared to basin properties including circularity, area, relief (Eq. 8.3), dissection (Eq. 8.4), and key rock types and geological structure.

$$H.I. = \frac{mean\ elevation - minimum\ elevation}{maximum\ elevation - minimum\ elevation} \quad \text{Eq. 8.2}$$

$$Relief = maximum\ elevation - minimum\ elevation \quad \text{Eq. 8.3}$$

$$Dissection = mean\ elevation - minimum\ elevation \quad \text{Eq. 8.4}$$

8.5 Results

8.5.1 Catchment characteristics

Overall, the Gouritz catchment exhibits a dendritic drainage pattern (Figure 8.1), but spatial variation is seen within the subcatchments in different physiographic regions. Dendritic patterns are present within the central Karoo and escarpment regions, where the Karoo Supergroup crops out, which is an area dominated by irregular plains with low relief (Figure 8.2B). Within the CFB, trellis drainage patterns are found (Figure 8.4A). The coastal region is dominated by small dendritic catchments (Figure 8.4A).

The Gouritz catchment is a stream order 7 catchment (Strahler, 1952) and has a drainage density of 0.454 km/km^2. Drainage density is lowest on quartzite bedrock, the most resistant rock type (Figure 8.3), and is the highest on the more easily eroded Karoo Supergroup sandstones and mudstones (Table 8.1). Physiographically, the CFB- and escarpment-draining subcatchments have the greatest variation in elevation. The CFB is dominated by streams of a lower order which drain the majority of the slopes, with the high order (>4) streams cutting straight through the mountain chain. The lower order streams (<3) are normally straight with meandering dominating in stream order >4 (Figure 8.4). Deeply incised meander bends are found in some of the main trunk rivers that cut across the CFB, e.g. Gamka-Gouritz River. Several rivers show right angles in their courses and evidence of beheading (Figures 8B, C) and are remnants of stream capture sites, of which many are expected in such a long-lived catchment. The mean bifurcation ratio of the catchment is 3.39; however, variation within individual stream orders is seen, with a range from 2 to 6 (Table 8.2).

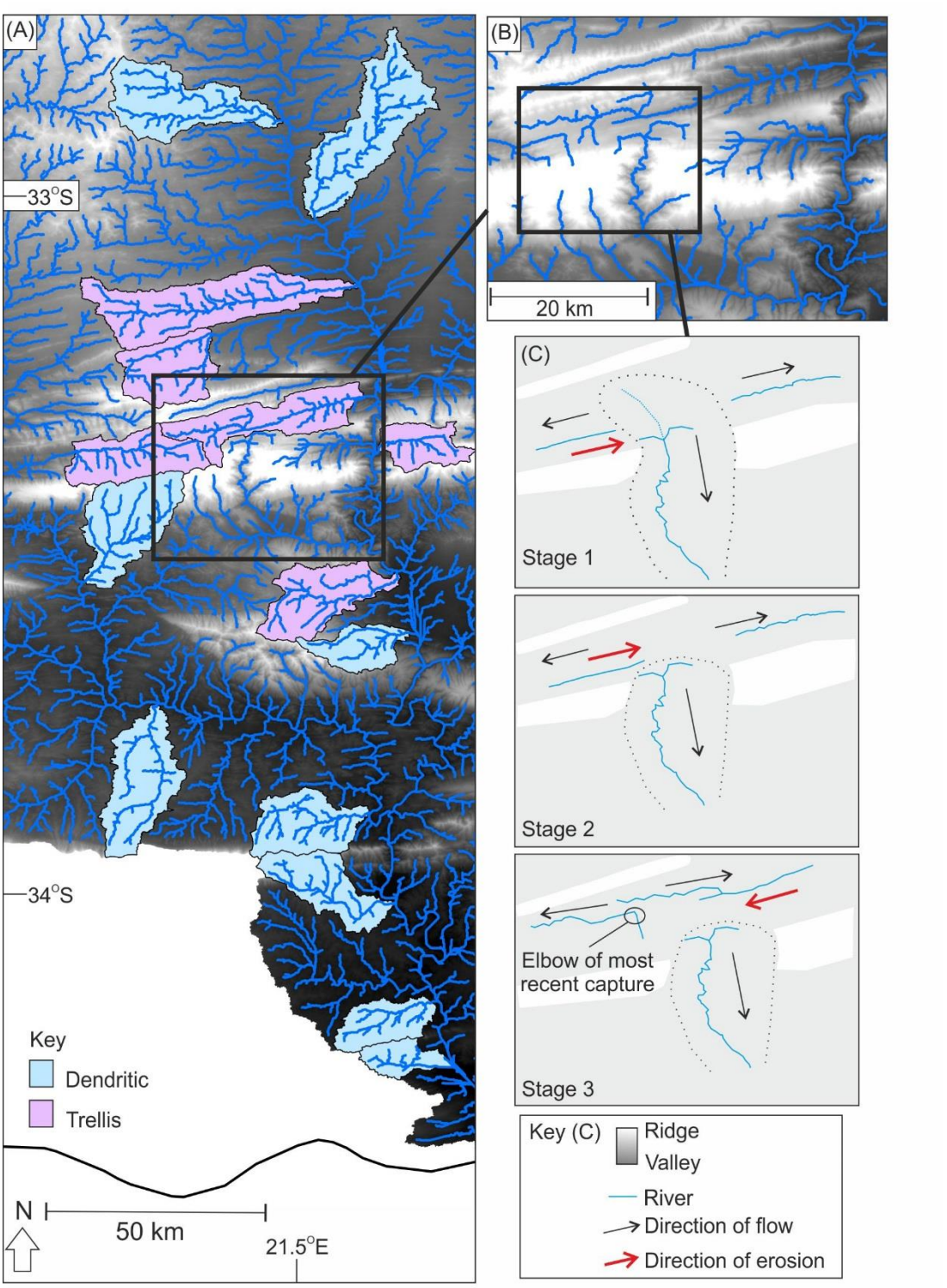

Figure 8.4 *- A) Drainage pattern of the Cape Fold Belt and Coastal physiographic region, showing stream order 3 streams categorised by shape. See Figure 8.1 for location. B) and (C) show evidence of stream capture and linear streams confined by folding.*

Table 8.1 - Variation in drainage density for the main lithological groups of the Gouritz catchment.

Lithology	Drainage density (km/km^2)
Igneous intrusions	0.28
Quartzites	0.23
Cango Cave group	0.37
Uitenhage group	0.35
Karoo Supergroup	0.44
Cape Supergroup	0.37

Table 8.2 *- Linear aspects of the Gouritz catchment*

Stream order	Stream number	Average stream length (km)	Bifurcation ratio
1	2811	5.36	3.45
2	814	9.29	3.86
3	211	17.51	3.91
4	54	30.01	6.00
5	9	117.77	4.50
6	2	52.44	2.00
7	1	355.96	
Mean			3.39

8.5.2 Morphometric indices

8.5.2.1 Long profiles

The long profiles of the main tributaries of the Gouritz catchment show a lack of single-graded form. Overall, the long profiles are concave in the headwater regions and fairly straight in the CFB (Figure 8.5). Concave long profiles are mainly found in the physiographic regions of the Great Escarpment and central Karoo regions but are also found in the transverse Olifants and Traka rivers whose headwaters form in the Cape Fold Belt (Figure 8.5). Knickpoints are present along the long profiles (Figure 8.5), which in some cases relate to artificially dammed lakes. These dams were

preferentially sited at the upstream side of narrow canyons, with the knickpoints corresponding to lithostratigraphic boundaries between quartzite and other Cape Supergroup rock types or the Uitenhage Group. Dolerite intrusions (Dwyka and

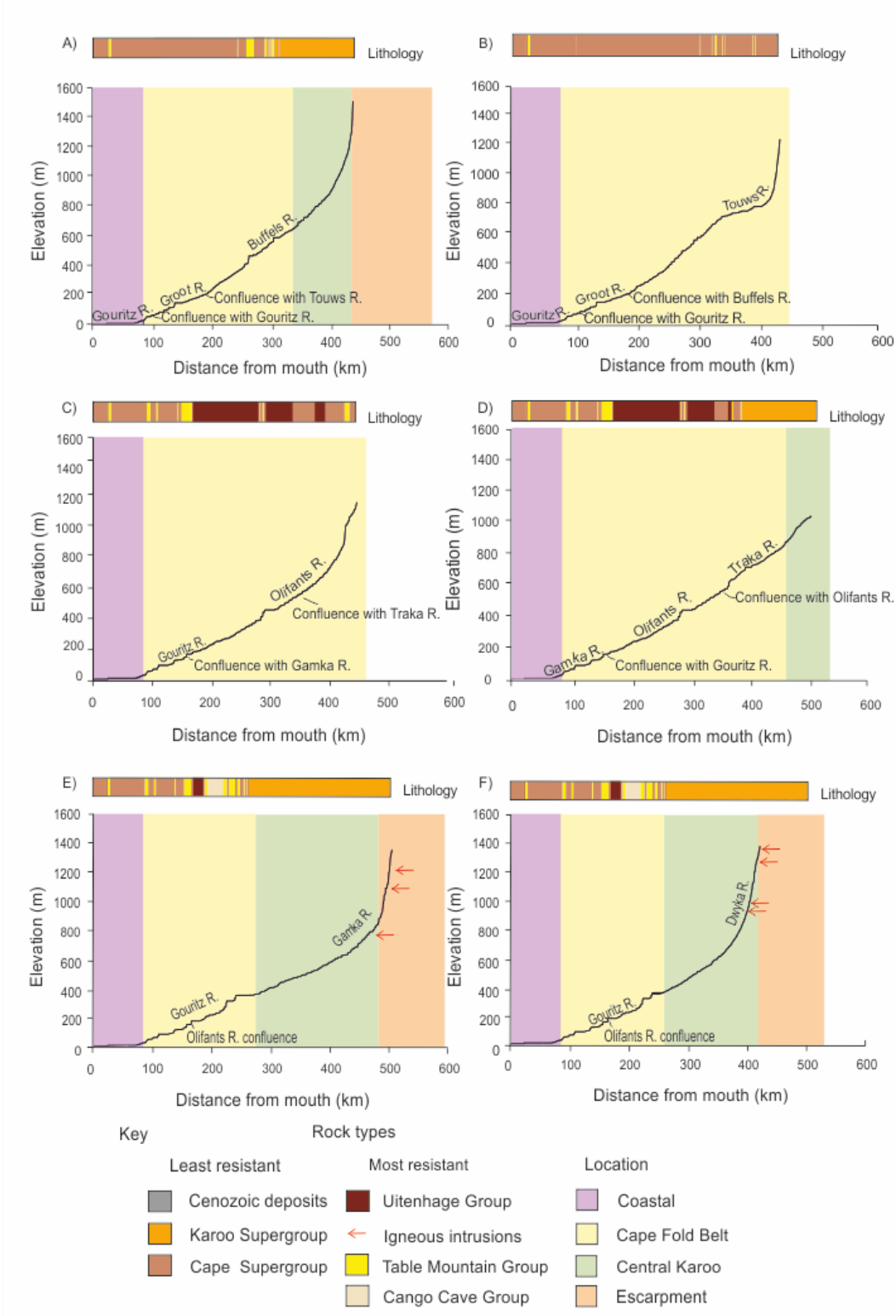

Figure 8.5 - *Long profiles of the Gouritz catchment and main tributaries: A) Buffels River, B) Touws River, C) Olifants River, D) Traka River, E) Gamka River and F) Dwyka River.*

Gamka rivers) do not always exhibit knickpoints. A detailed study of the Swartberg mountains indicates that in the smaller mountain-draining catchments (stream order <3) knickpoints are prevalent and commonly are tied to lithostratigraphic boundaries involving quartzite (Figures 8.3, 8.6).

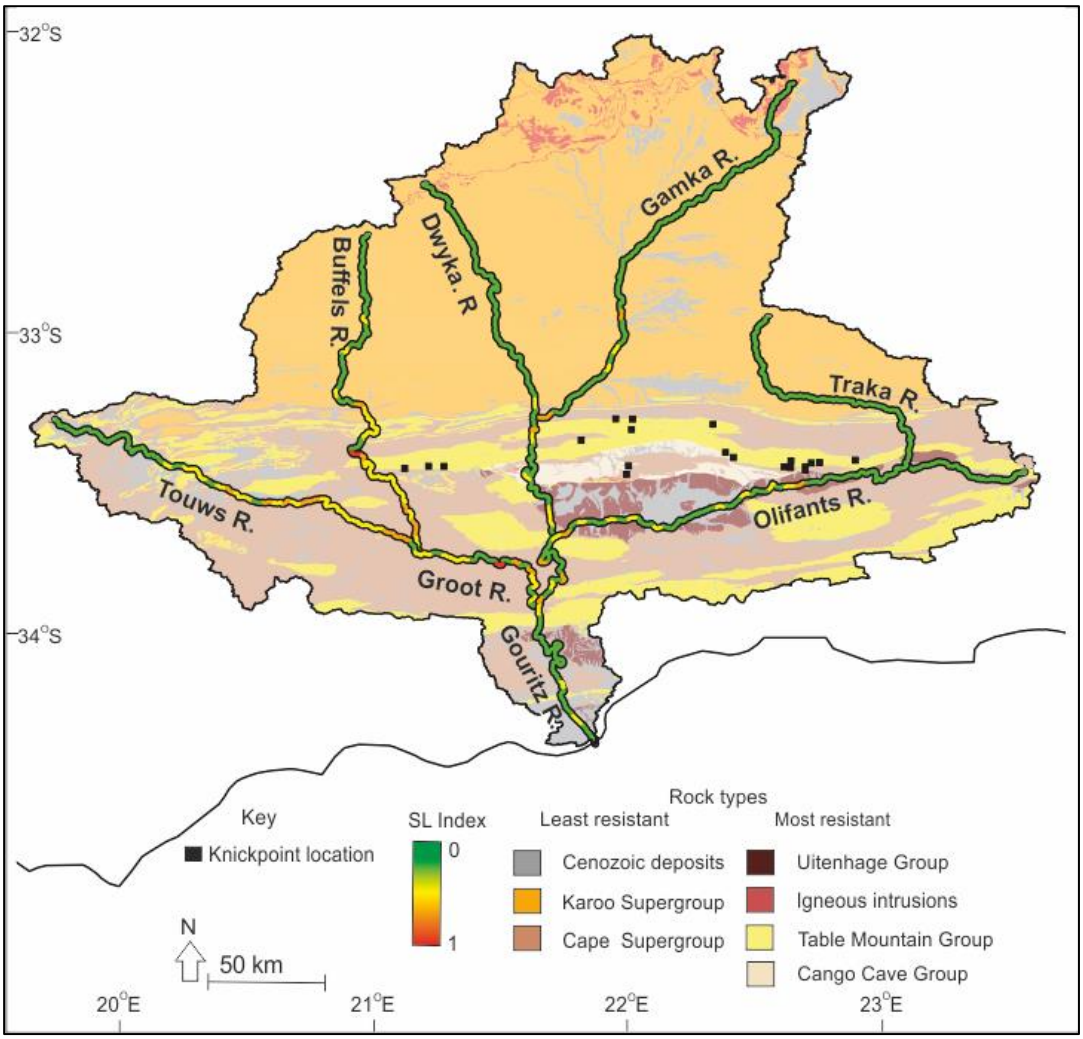

Figure 8.6 *- Normalised stream length gradient and the relationship to simplified geology within the Gouritz catchment. The locations of knickpoints within the smaller catchments of the Swartberg range are also shown.*

8.5.2.2 Stream gradient index

Figure 8.6 shows the variation of stream gradient indices within the Gouritz catchment. The data were normalised with a value of 1 indicating high stream gradients; a full range of SL are seen within the catchment. The headwaters of all the trunk rivers have low SL, with values below 0.2, which is exceptionally low and shows an increase downstream. The rivers that cross the central Karoo (Buffels, Gamka, and Dwyka rivers) show gradients between 0 and 0.4. This area is characterised by flat plains and is dominated by the relatively easily eroded Karoo Supergroup rock

types. The CFB, which all the main trunk rivers either run parallel to or transverse (Figure 8.1), shows the highest variation in SL, with values between 0.2 and 1. The CFB is dominated by the Cape Supergroup, with resistant quartzites and metamorphosed sandstones as well as the resistant Uitenhage Group and Cango Cave Group rock types. Stream gradient indices then decrease in the coastal region with the SL of the majority of reaches below 0.2, where the Cape Supergroup outcrops are dominated by mudstones. Stream gradient is unaffected by large-scale faults (mapped at 1:25,000).

8.5.2.3 Hypsometry

The hypsometric integral of the Gouritz catchment is 0.34, and the hypsometric curve for the catchment is sinusoidal (Figure 8.7). The overall drainage basin has a circularity of 0.16, which indicates the drainage basin shape is highly irregular. In order to understand how hypsometry varies throughout the drainage basin, the western-draining catchments of the main trunk river (Gamka River) were assessed in detail.

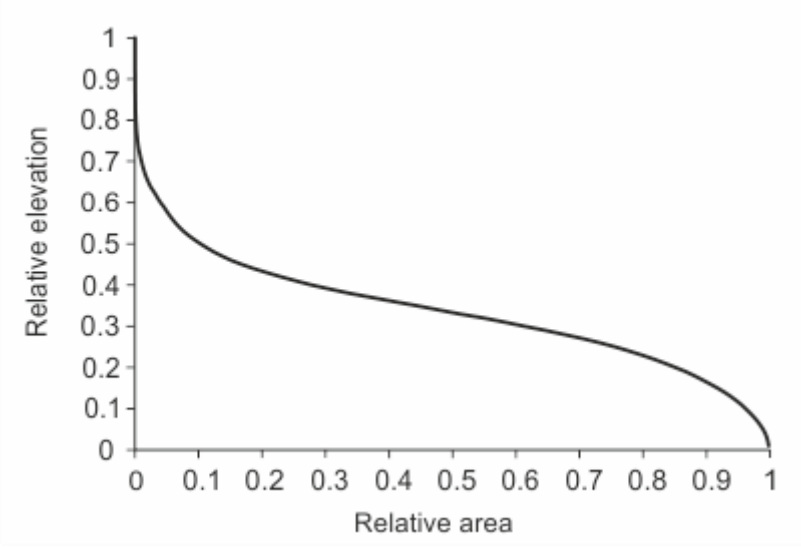

Figure 8.7 *- The sinusoidal hypsometric curve of the Gouritz catchment.*

Western-draining catchments range in stream order from 1 to 6 and have a mean basin area of 728.10 km^2 (ranging from 4.37 to 19,054.91 km^2). In Figure 8.8, hypsometric integrals are plotted against catchment characteristics. The R^2 value shows no correlation between the hypsometric integral and each variable: hypsometric integral and circularity = 0.0053, hypsometric integral and area = 0.0872, hypsometric integral and dissection = 0.0321, and hypsometric integral and relief = 0.1761. The hypsometric integral, therefore, appears to be independent of catchment factors. The hypsometric integral on average decreases with increasing stream order

(Table 8.3). The central Karoo catchments have the highest mean hypsometric integral, and the coastal catchments the lowest (Table 8.4).

Some patterns between stream order and geomorphological location are apparent. Catchment area increases with stream order, with larger basins having lower hypsometric integrals (Figure 8.8A). Higher order streams (>4) on average have a lower circularity and data is less scattered than lower order streams (<3; Figure 8.8B).

Table 8.3 *- Variation in hypsometric integral in the western-draining catchments with stream order.*

Stream order	N	Highest hypsometric integral	Lowest hypsometric integral	Mean	Range	Standard deviation
1	18	0.53	0.32	0.43	0.21	0.62
2	13	0.69	0.27	0.43	0.42	0.11
3	13	0.51	0.23	0.38	0.27	0.75
4	3	0.38	0.18	0.30	0.20	0.10
5	1			0.24		
6	2			0.30		

Table 8.4 - *Variation in hypsometric integral with catchment location.*

Location	**N**	**Highest hypsometric integral**	**Lowest hypsometric integral**	**Mean**	**Range**	**Standard deviation**
Coastal	7	0.69	0.19	0.35	0.50	0.17
Cape Fold Belt	14	0.56	0.30	0.41	0.26	0.07
Central Karoo	28	0.53	0.25	0.41	0.28	0.07

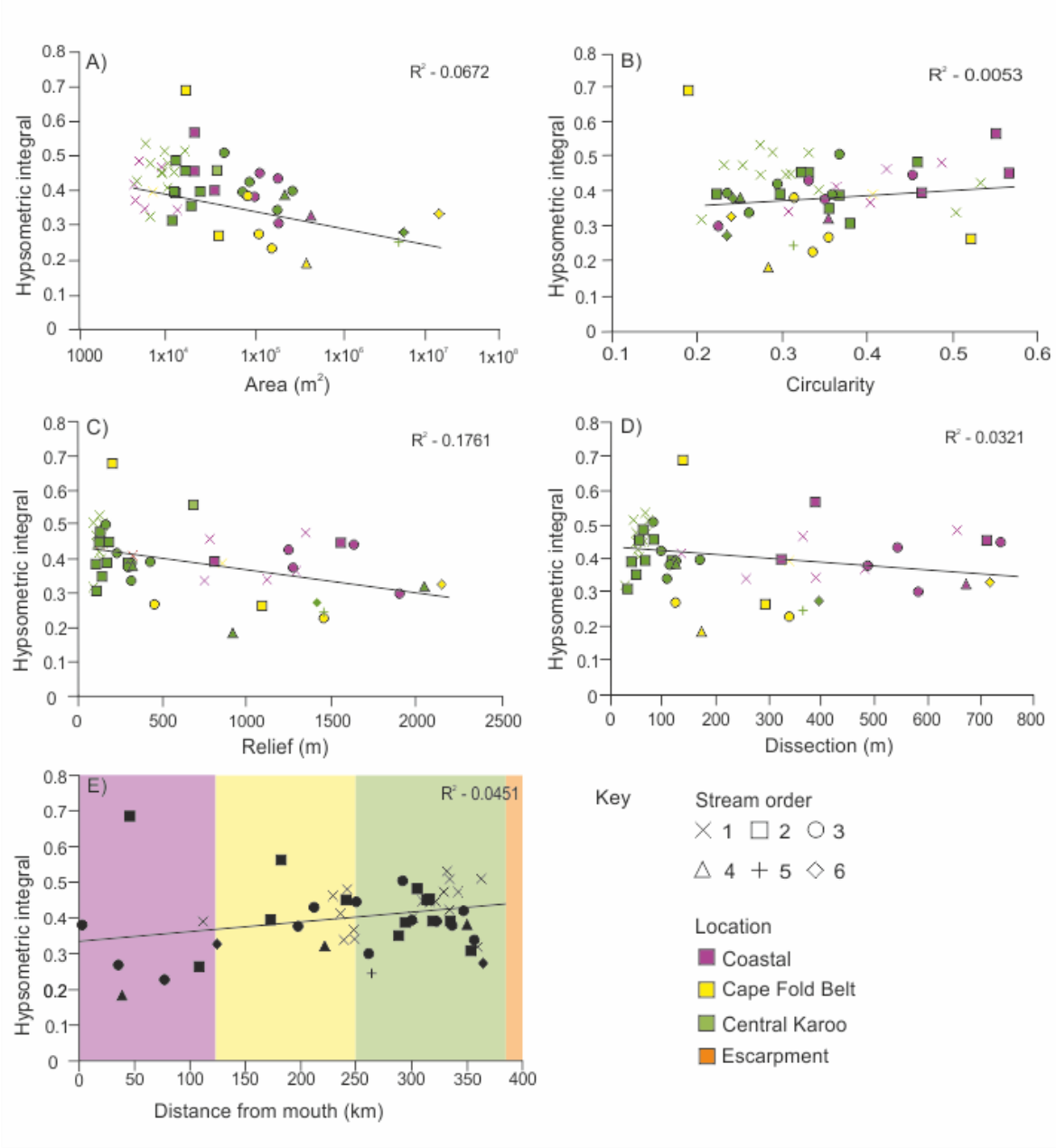

Figure 8.8 *- Relationship between location, catchment properties, and hypsometric integral: A) area, B) circularity, C) relief, D) dissection, and E) distance from mouth of Gouritz River. The R^2 values indicate no correlation between catchment properties and hypsometric integral.*

The lower circularity value of higher stream order catchments relates to a more complicated drainage network and watershed shape. Lower order streams (<3) have a wider range of dissection and relief (Figures 8C, D); this seems to be a function of location with many of these streams draining the CFB. The central Karoo catchments are more homogenous and less scattered, with low levels of dissection and relief, and the area is characterised by large flat areas (Figure 8.2B). The escarpment represents the headwaters of many of the central Karoo catchments, and only represents a small proportion of the total catchment area. Hypsometric integrals do not correlate with the distance of the catchment from the river mouth (Figure 8.8E; R^2 = 0.05). Figure 8.8E also shows how the range of integrals decreases toward the escarpment, whilst the drainage density increases (i.e., density of data points increases).

Hypsometric curves: The hypsometric curves from subcatchments within the Gouritz catchment can be classified as sinusoidal, straight, concave, and convex (Figure 8.9A). Overall, the Gouritz catchment has a sinusoidal curve (Figure 8.7), whereas at subcatchment scale, the majority of curves are concave (Figure 8.9A). The concave curves can be seen in a range of stream orders (stream order 1 to 6), whereas the convex, straight, and sinusoidal catchments are associated with the lower stream orders (<3) (Figure 8.9). No systematic variation in the curve shape is seen toward the escarpment (Figure 8.9B) or within each geomorphological region.

Curve shapes were quantified to assess whether the observed variation could be attributed to internal or external catchment controls. Figure 8.8C shows the percentage area of the catchment that lies below half the maximum elevation within the western-draining catchments. The more dissected a basin is, the higher the area of the catchment below the maximum value within the basin. The coastal catchments are

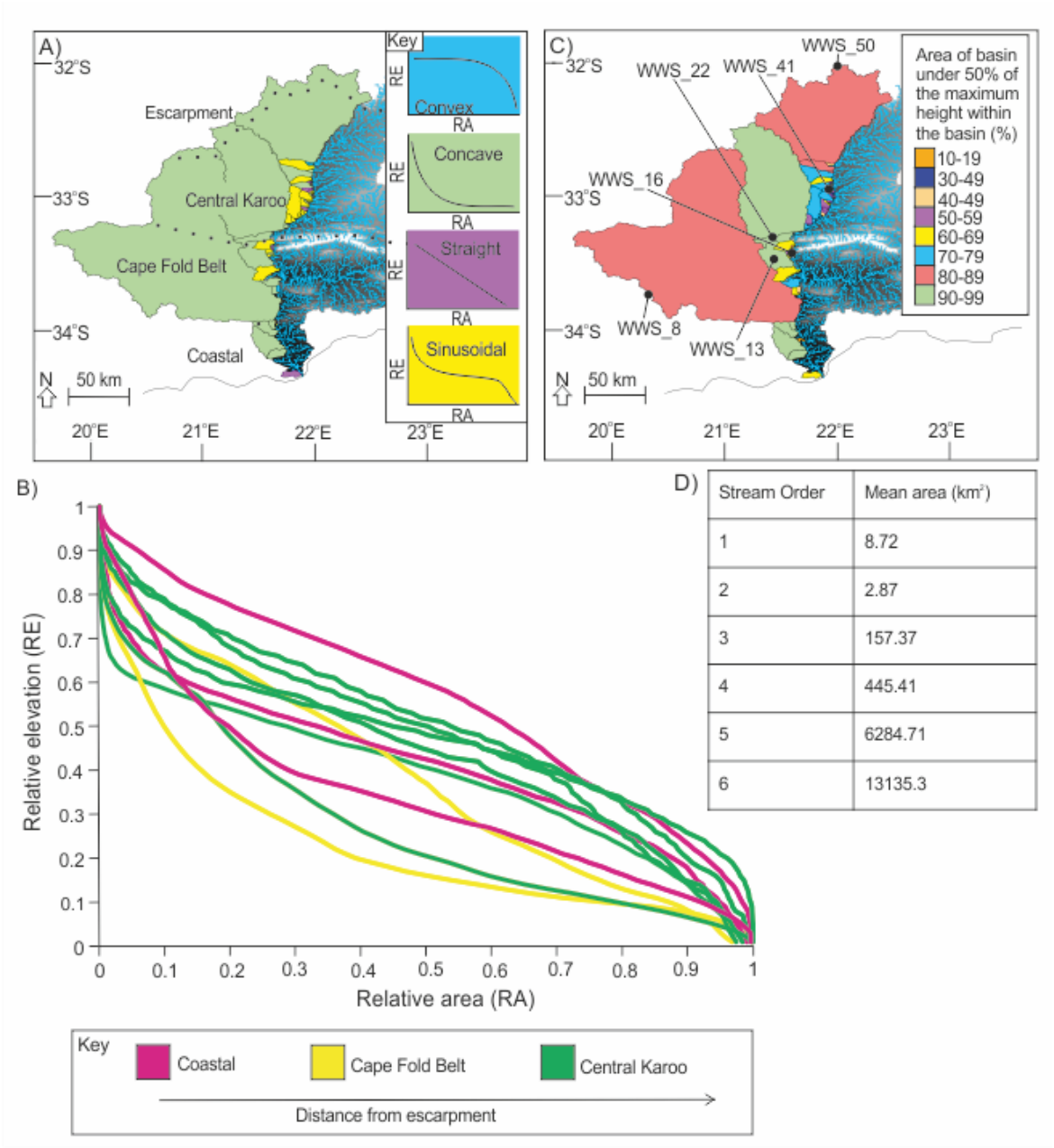

Stream Order	Mean area (km²)
1	8.72
2	2.87
3	157.37
4	445.41
5	6284.71
6	13135.3

Figure 8.9 - *A) Distribution of 'type' curves (straight, convex, concave, and sinusoidal) where RA is relative area and RE is relative elevation; B) variation in curve shape toward the escarpment. Data extracted from every fifth catchment: C) area of catchments below 50% of the maximum elevation within the basin; D) the average lengths of stream order 1 to 6 streams draining the Western Cape.*

highly dissected, with the majority of catchments having >90% of area lower than 50% of the maximum height. The CFB has similar levels of dissection where many catchments have >80% of area lower than 50% of the maximum height. Dissection also increases toward the escarpment where, on average, the lowest percentage of area below 50% of the maximum height is within the central Karoo catchments, where average elevation is high and slope angles are low.

Figure 8.10 shows the influence of rock type on hypsometric curves of stream order 1 to 6 streams. The presence of resistant rock types (Figure 8.3), such as the Cango Cave Group and igneous intrusions at the higher elevations of the catchment, allows elevation to be preserved causing a disturbance of the hypsometric curve. The hypsometric curve in these locations has a lower slope than the catchments without resistant rock types, with a higher proportion of area preserved in the higher elevations (e.g. Figures 8.10A, E). Hypsometric curve slope also decreases when resistant rock types are found at lower elevations (e.g. igneous intrusions, Uitenhage, and Cango Cave groups; Figure 8.10D). At the lower elevations of catchments the influence of resistant rock types decreases, e.g. below 50% of the maximum elevation, especially in the larger catchments. The presence of quartzite does not impact the curve shape significantly (Figures 8.10C, D). Curve shape variation within catchments dominated by the Karoo Supergroup cannot be attributed to different rock types, although the lithostratigraphic groups within the Karoo Supergroup have different proportions of mudstone and sandstone (Figure 8.10B). Some catchments have a large change in slope at the lower elevations (Figures 8.10D, F), which does not correspond to a change in the proportions of rock type.

8.6 Discussion

When assessing the dominant controls on the development of an ancient landscape, uncertainty remains in the timing and effects of external forcing factors; and the long timescales involved mean that external signals can be overprinted. Nonetheless, the Gouritz catchment is an ideal test of a morphometric approach to considering the dominant controls on the evolution of long-lived drainage basins.

8.6.1 Impact of bedrock type

The impact of bedrock type is seen in the hypsometric curves, where the high relief of some subcatchments is related to the resistant dolerite intrusions and Cango Cave Group bedrock (Figures 8.3, 8.10A, E). The deviation in curves dominated by the Cape (including quartzites) and Karoo supergroups cannot be related to rock type, and the resistance of the units appears to be fairly similar (Figure 8.3). However, parameters such as bed thickness, bed orientation (strike and dip), and the extent of jointing – which have not been taken into account in this study – also impacts the resistance of bedrock to erosion (Walcott and Summerfield, 2008).

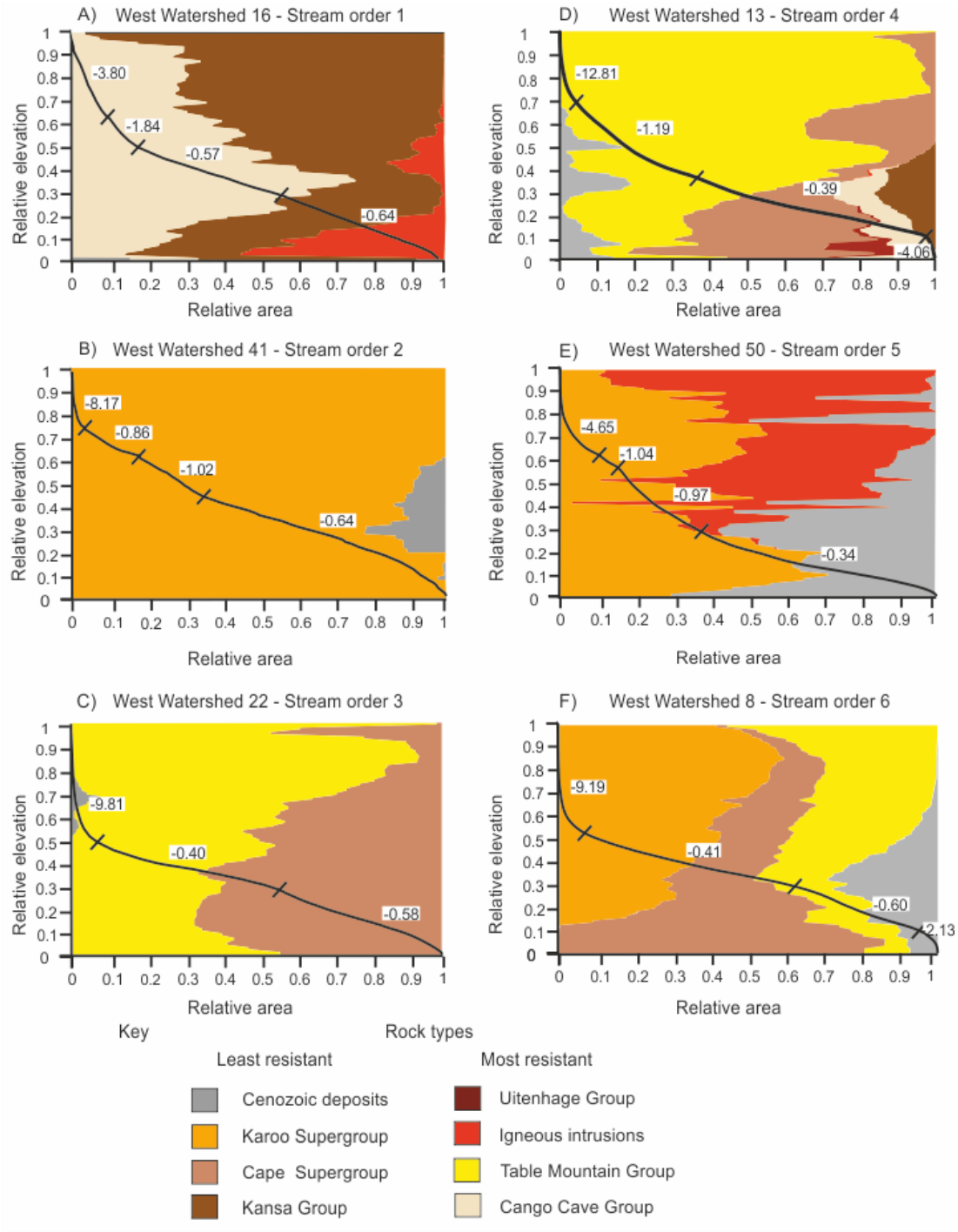

Figure 8.10 *- Hypsometric curves and lithostratigraphic units for stream order 1-6 (A-F) catchments draining the western side of the Gouritz catchment. Inflection points in the curve are highlighted. The numbers indicate the gradient of each section, delineated by a change in curve shape.*

Cape Supergroup rocks have also been metamorphosed, which can cause rocks of different compositions to have more similar resistance to erosion (Zernitz, 1935).

The level of dissection within catchments as shown by the hypsometric curves can also be attributed to variation in bedrock type; many of the coastal catchments are underlain by mudstones (Bokkeveld Group, Cape Supergroup), which are more easily eroded (Figure 8.3), resulting in a concave curve. The CFB-draining subcatchments are dominated by resistant metamorphosed bedrock, associated with lower rates of erosion (Scharf et al., 2013) and, therefore, a longer duration of evolution resulting in sinusoidal or straight curves (Figures 8.9A, B). In the CFB area, the catchments are lower order streams (<3), and the impact of bedrock type appears to be more dominant (Figure 8.4A). The wide range in circularity values in the CFB-draining subcatchments also indicates a larger structural and lithological control within these mountainous catchments (Figure 8.8A).

The impact of bedrock type appears to be stream-order dependent; knickpoints are pinned to contacts between rock types of different resistance within the subcatchments (Figure 8.6). The large trunk rivers do not show this relationship as such pronounced changes in stream profile, which could be a function of temporal development; however, the profiles are straighter in the CFB area because of the high rock resistance (Figures 8.3, 8.5). Bedrock type also impacts on drainage densities. The Karoo Supergroup rocks have the highest drainage densities (Table 8.1), and these rocks have been less affected by burial metamorphism. The more resistant rocks have lower drainage densities owing to the time taken for incision and the formation of a drainage network. Dolerite has been shown to play a key role in catchment development within South Africa (Tooth et al., 2004). In the upper Gouritz catchment, where dolerite is dominantly found, low stream gradients are present and the impact differs from Tooth et al. (2004) as the dolerite intrusions are not always represented as knickpoints along the long profile (Figure 8.5). This could be because of the limited thickness of the dolerite intrusions in the Gouritz catchment in comparison to those exhumed in the South African Highveld (Tooth et al., 2004).

Quartzite has been argued to be the most dominant rock type on catchment dynamics (Jansen et al., 2010); however, in this study the presence of quartzites does not always vary morphometric indices. Typically, high SLs are located in the upper reaches of catchments (Antón et al., 2014); however, this is not the case for the Gouritz catchment (Figure 8.6). The highest values are seen within the CFB, with low values at headwater regions. The highest values of SL are not always associated with

the rivers crossing quarzitic lithologies, but mainly with the Uitenhage Group. When assessing the major trunk streams at reach level, quartzite does not have strong control. This is because the main trunk rivers breach the quartzite in only seven locations (Figure 8.6), where deeply dissected gorges have formed resulting in high gradients and meandering in these locations. The majority of the river courses transverse other rock types such as the resistant Cango Cave Group, where high stream gradients and meanders are present (Figure 8.6). The large degree of variation in stream length gradient within the Cape Supergroup rock types could be explained by the variation of bed thickness, bedding orientation, and jointing, as well as the degree of metamorphism.

8.6.2 Impact of inherited tectonic structures

The impact of tectonic structures within the Gouritz catchment is primarily exhibited in the drainage pattern of the lower order streams (order 2 and 3; Figure 8.4A). Bifurcation ratios above 5 normally indicate a structural control (Strahler, 1957). However, in the case of the large trunk rivers of the Gouritz catchment (stream order 4 and 6), the higher stream orders dissect the CFB and are not directed or deflected by the E-W trending structures; this discordance supports their interpretation as antecedent systems (Rogers, 1903). Additional evidence of antecedence is shown by the combination of high gradients and meander forms into resistant lithologies within the CFB (Figure 8.3). The CFB folds have the greatest control on subcatchments; this is especially evident in a stream order 2 river in Figure 8.4B that has a linear planform and stream order 3 rivers in Figure 8.4A. The strong structural control within the catchment with regards to bifurcation ratio is, therefore, the antecedence of the major tributaries (Rogers, 1903), which explains the higher bifurcation ratios in stream order 4 and 6 streams.

Across the catchment, the CFB represents a large proportion of elevation resulting in the plateau in the hypsometric curve (Figure 8.7). The CFB has low rates of erosion, with the resistant rock types allowing the post-orogenic feature to persist (Scharf et al., 2013). Additional preservation of elevation is caused by the widespread presence of fossilised plains, pediments (Kounov et al., 2015), and presence of the Great Escarpment (Figure 8.2B). Exceptionally low SL in the ephemeral headwaters indicates the importance of the flat top nature of the Great Escarpment (Figure 8.2B). South Africa formed a central part of Gondwana and was a super-elevated continent (Patridge and Maud, 1987; Rust and Summerfield, 1990); during rifting in the Mesozoic, reorganisation of seaward-draining catchments such as the Gouritz occurred. The headwaters of the Gouritz incised the escarpment face and now drain

a portion of the flat area on the escarpment inherited from the breakup of Gondwana. The concave nature of the headwaters shown in the long profiles (Figure 8.5) indicates the large change in elevation between the flat top of the Great Escarpment and the central Karoo, which sits ~700 m below the escarpment.

Large-scale extensional faults (Figure 8.1) do not appear to have an important control within the catchments, either within the hypsometric curves or the morphometric indices. However, the rock types within the catchment, especially the CFB, are pervasively jointed and faulted, and therefore, must be an important control at a small scale (Manjoro, 2014).

8.6.3 Large-scale forcing factors

Variation in morphometric indices (circularity, SL, and hypsometry) indicate that the Gouritz catchment has had a complicated development history (Figure 8.11). Commonly, hypsometric curves are used to elucidate large-scale forcing factors in catchments (Montgomery et al., 2001). The sinusoidal shape of the Gouritz catchment (Figure 8.9) is often related to rejuvenation (Ohmori, 1993). The uplift in South Africa is contentious (Gallagher and Brown, 1999; Brown et al., 2002; Tinker et al., 2008a; Kounov et al., 2009; Decker et al., 2013), however Walcott and Summerfield (2008) argued that if tectonic activity did occur within South Africa, it was either at a low rate or a long time ago because the hypsometry of the catchments are concave-up with low integral values, and the tectonic pulse is no longer expressed physiographically (Figure 8.11). Summerfield (1991) related sinusoidal curves extracted from rivers in South Africa to coastal upwarp. The lower curve portion of the Gouritz catchment is not underlain by resistant lithologies, and the sinuous nature at these low elevations could be related to coastal upwarp. Strahler (1952) argued that fluvial equilibrium is shown by hypsometric integrals between 0.4 and 0.6. However, this is not always the case, as shown by this study, and caution is needed in the application of hypsometric integrals.

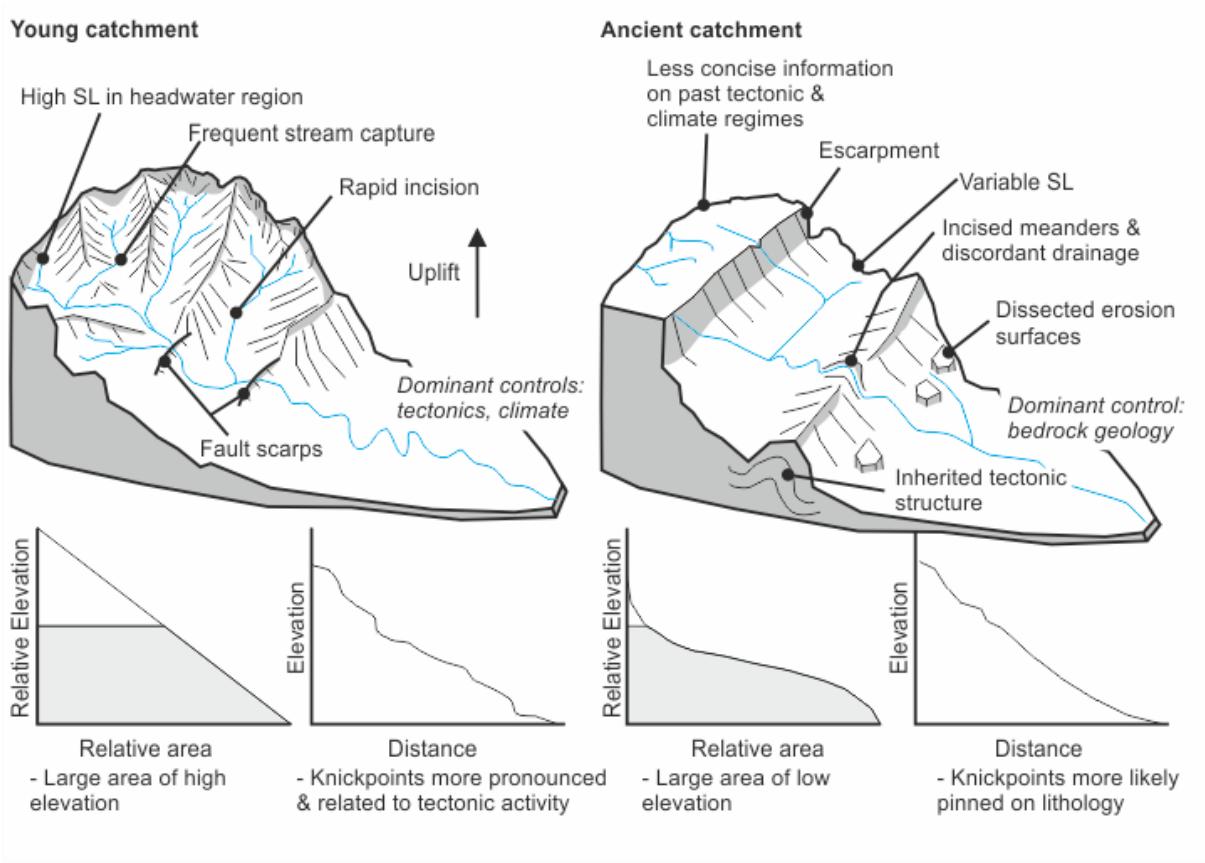

Figure 8.11 *- Synthesis diagram showing the differences between young and ancient catchments and the impact on morphometric indices. Within young landscapes, recent tectonic activity is represented as knickpoints and straight hypsometric curves. However, in ancient catchments this signal is diminished, resulting in pinned knickpoints on lithological divides, sinusoidal curves, and composite effects of multiple factors that make it hard to distinguish dominant controls.*

In the western-draining catchments, many of the hypsometric curves are convex, with variation in shape occuring in adjacent catchments. This suggests that either different forcing factors are affecting the catchments or they are reacting to the same forcing factors in different ways. Within smaller subcatchments, stream capture has been shown to cause rejuvenation and can occur as an allogenic process (Prince et al., 2011). Stream capture can explain the variation in some of the subcatchments; however, it is not sufficient to explain such large-scale processes for the entire drainage basin.

Hurtrez et al. (1999) and Chen et al. (2003) proposed that the hypsometry of catchments correlates to catchment properties. However, the lack of correlation between the hypsometric integral and catchment properties in this study does not support these findings but does support those by Walcott and Summerfield (2008) who also worked in ancient settings. When assessing variation in the western-draining catchments, the hypsometric integral values generally decrease toward the

escarpment but show large variation. Regardless of stream order or location, correlation between catchment properties and the hypsometric integral is poor, which was also identified by Walcott and Summerfield (2008). Variation is larger between smaller subcatchments (<4), which is attributed to the smaller subcatchments having had less time to develop or to structural/rock type control having a larger influence on the smaller basins.

8.6.4 Implications and application of morphometric indices to ancient settings

The Gouritz catchment has had a long history of development since the Mesozoic breakup of Gondwana and the concomitant Cretaceous exhumation of southern South Africa. When assessing morphometric indices, this history needs to be understood, especially as large catchments like the Gouritz do not evolve in a uniform manner (Grimaud et al., 2014) as indicated by the variation in trunk river morphometric indices.

The long-lived nature of ancient catchments causes morphometric indices to record the composite effects of multiple factors. This is seen within the hypsometric curve of the Gouritz catchment whereby the middle portion appears to record rock type controls related to inherited structure (Figure 8.7) and the lower portion tectonic impacts. Over long timescales, signals can be lost, overprinted, or truncated (Figure 8.11), which can also be recorded in the sedimentary history of basins (Jerolmack and Paola, 2010; Covault et al., 2013; Romans et al., 2015). The large-scale tectonic event of Gondwana rifting and the debated tectonic uplift history of the catchment since rifting cannot directly be related to morphometric indices in this study (e.g., Walcott and Summerfield, 2008). This is because of the long time for the catchment to respond to and erode the resulting geomorphological impression of the tectonic pulse, coupled with overprinting of other signals (both internal and external; Allen, 2008) and the poorly constrained history of the Gouritz catchment. This is complicated by the lack of understanding of the timescale at which tectonic or climatic factors affect catchments after their initiation and of the response time within the catchment (e.g. Allen, 2008). Overall, the prevailing theories of tectonic and climatic impacts on landscape development cannot be tested properly using morphometric indices in this ancient landscape. The Gouritz catchment has preserved drainage structures (*sensu* Hack, 1960) because of the relatively constant climate since the end of the Cretaceous and lack of tectonic activity. The current planform of the Gouritz is closely linked to rock type, as shown by the hypsometric curves, with steep relief, knickpoints, and high SL in the CFB and subdued relief in the less resistant Karoo Supergroup rock types. Nonetheless, a range of controls will have shaped the Gouritz catchment.

However, bedrock geology within these ancient catchments is judged to be the dominant control on the morphometrics as it is the longest lived *relatively* constant boundary condition in comparison to tectonic or climatic change (Figure 8.11).

8.7 Conclusion

Morphometric indices, including stream length gradient and hypsometric integrals, were extracted from the tectonically quiescent Gouritz catchment and confirm that the catchment has had a complicated extended geomorphological history. This is expected for a catchment that has developed since the Jurassic break-up of Gondwana and large-scale exhumation from the Cretaceous onward. Nonetheless with a combined geological-geomorphological approach and analysis across different spatial scales, we are able to decipher that at a catchment scale, indices such as hypsometry are affected by resistant rock types, whereby resistant units preserve topography at a subcatchment and catchment scale. The influence of rock type is scale dependent on river channel long profiles and is more prevalent in catchments of stream orders <4; knickpoints are pinned on boundaries between quartzites and less resistant rock types. Within the larger trunk rivers, stream length gradient is mainly affected by the Uitenhage Group with low values experienced in the upper reaches of the catchment. The trunk rivers dissect the CFB because of their antecedence. Contacts between quartzite and less resistant rock types in these locations are not shown as knickpoints or the highest stream length gradient values, indicating a long duration of development. Control by inherited tectonic structures in this study is therefore mainly seen within smaller subcatchments that drain the CFB as shown by the range in circularity values and within the long profiles of the rivers that cross the CFB

Hypsometric curve shape is normally related to external variation in climate or tectonics; however, the sinusoidal hypsometric curve of the Gouritz catchment can be attributed to elevation preservation owing to resistant lithologies and to the preservation of pediments because of low erosion rates. Tectonic influence caused by mantle plumes would cause systematic variation in indices, which is not seen as shown by the lack of correlation between catchment location or stream order. However, large scale differential uplift related to exhumation in the Cretaceous and coastal upwarp because of Mesozoic rifting could still be impacting catchment development, but these controls are hard to distinguish. Within smaller subcatchments, variation in hypsometric curve can be attributed to stream capture in some locations.

Overall, morphometric indices allow a first-order characterisation of ancient landscapes and highlight the importance of resistant lithologies. In long-lived catchments, the influence of tectonic activity cannot clearly be ascribed to variation in morphometric indices and appear to be subdued and shredded by the impact of resistant rock types. Caution must therefore be taken when comparing morphometric indices within different tectonic regimes and with different durations of development. Future work should investigate how morphometric indices vary over time in such tectonically quiescent and/or ancient regions and examine how long a tectonic or climatic pulse can be preserved within different environments.

Chapter 9 Discussion

The aim of the research was to investigate the long-term landscape evolution of southern South Africa, an ancient landscape, through integration of traditional and novel techniques (Figures 9.1, 9.2). This thesis set out to address a series of research questions outlined in Chapter 1. The objective of this chapter is to address the initial research questions posed and present a summary of the main findings (Chapter 1).

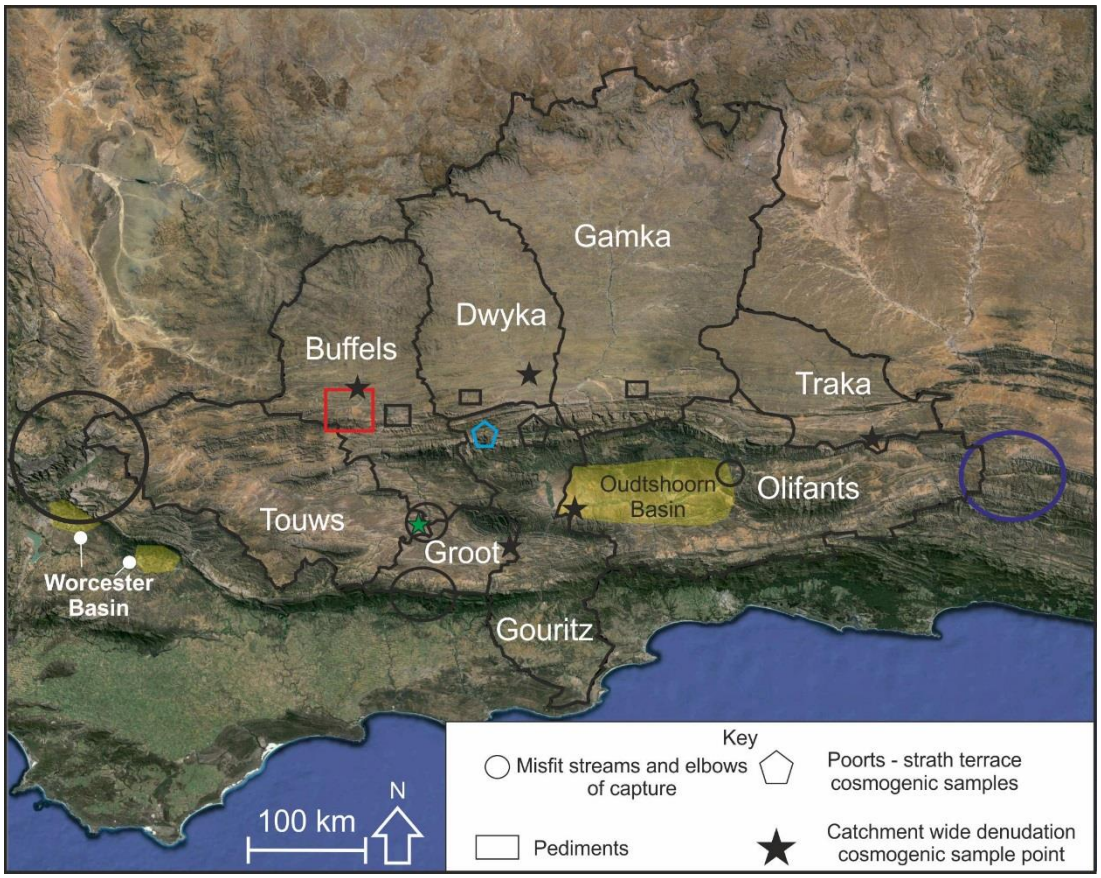

Figure 9.1 *– Synthesis of main study location; the Gouritz catchment and Mesozoic sedimentary basins, with the sub catchments sampled for cosmogenic catchment wide average denudation (stars), location of strath terrace cosmogenic samples (pentagon), pediment cosmogenic samples (rectangle) and evidence of drainage reorganisation (circles). The coloured symbols correspond to specific examples in Figure 9.2.*

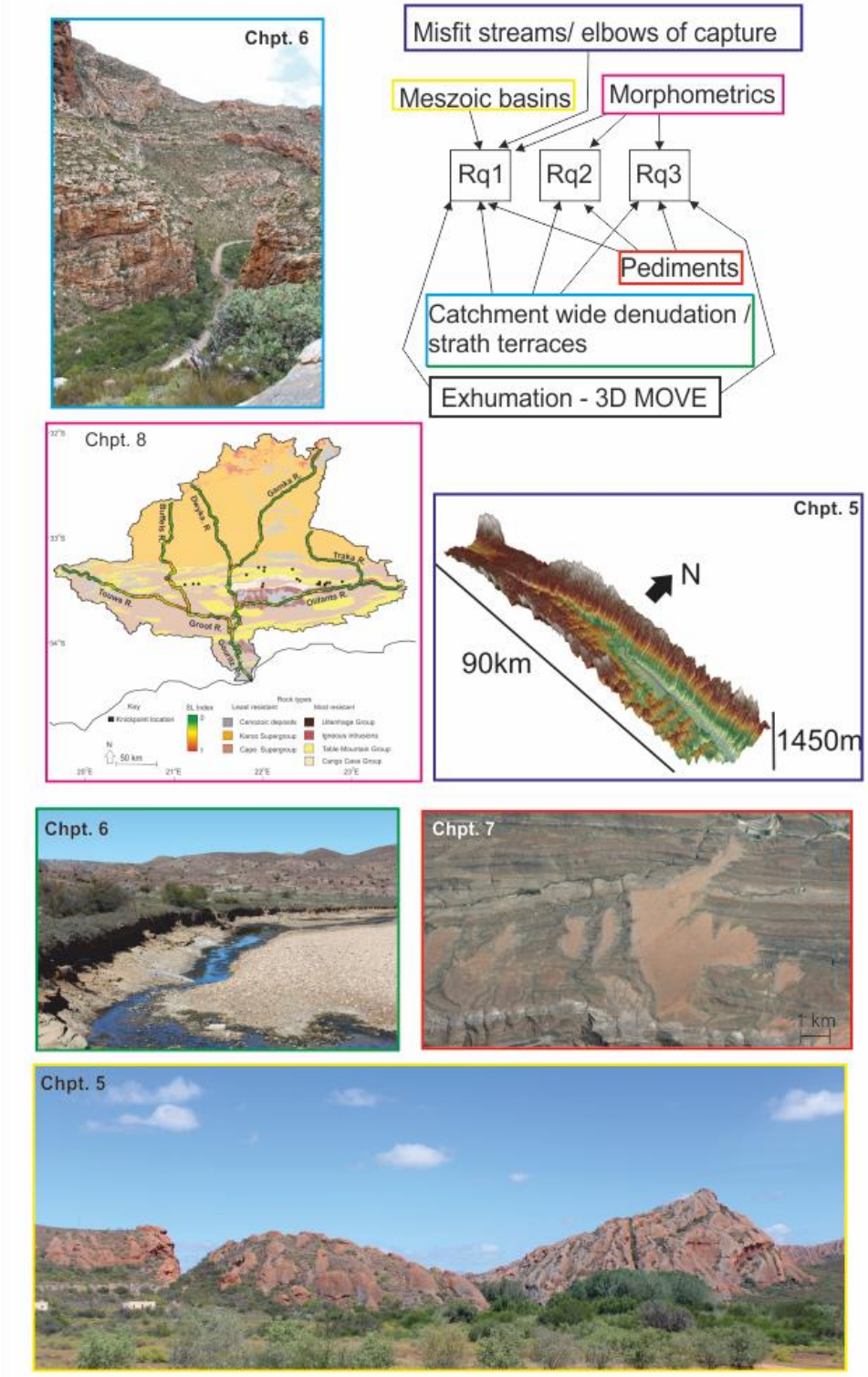

Figure 9.2 *– Synthesis of research questions and chapters including examples of cosmogenic sampling sites (strath terraces, catchment wide denudation river bar and pediment); Mesozoic sedimentary basin and Enon Conglomerate, misfit streams (drainage reorganisation) and catchment morphometrics. The coloured boxes refer to the location of coloured symbols on Figure 9.1.*

9.1 Drainage reconstruction and wider implications

Question 1: How can reconstructing drainage development help constrain source-to-sink concepts and rift basin facies models within South Africa?

Previous workers have shown large-scale exhumation during the Cretaceous (e.g., Brown, 1990; Tinker et al. 2008a) based on AFTT work with up to 7 km removed. The fission track studies are limited by inconsistencies in the geothermal gradient used to extract exhumation rates, and the limited coverage of the data sets (Figure 9.3), as well as a lack of knowledge of the active drainage systems. In Chapter 5, the absolute maximum thicknesses of lithologies that could have been removed from the Western Cape was calculated using 3D MOVE. Maximum thicknesses were constrained employing several assumptions (Chapter 5), with an absolute maximum value of 2.52 $x10^6$ km^3 (equivalent lithological thickness of ~11 km) removed; this is an order of magnitude larger than the values reported by Tinker et al. 2008a. When constraining the exhumation to the southern draining system (delineated by the location of the Great Escarpment e.g., Brown et al., 2002), this value is 7.81 $x10^5$ km^3 (equivalent to ~3.5 km of lithological thickness). There is a mismatch of onshore denudation volumes and offshore accumulation volumes, with a maximum of 5.13$x10^5$ km^3 of material 'missing' offshore during the Cretaceous (Chapter 5, Tinker et al., 2008b).

The depositional record of large-scale exhumation is seen within the remnant fills of several small Mesozoic extension basins onshore in the Western Cape (McLachlan and McMillian, 1976; Green et al., 2016; Chapter 5). The age of the studied conglomerate is contentious, but has been argued to be Jurassic-Cretaceous in age. The deposits indicate the presence of river systems (Hattingh, 2008) as shown by the clasts sizes and levels of roundness.

By constraining the provenance of the clasts, the position of palaeo-drainages can be reconstructed. The Oudtshoorn Basin deposits are sourced from the footwall; the Cape Fold Belt. In Worcester, the provenance of the clasts no longer crop out in the area, smaller clasts sizes, higher levels of clast roundness and abundance of sandy layers indicate reasonable transport distances. There is variation in the depth of exhumation between the Worcester and Oudtshoorn basins. During subsidence and infill of the Worcester Basin, the Witteberg quartzites were still buried, whereas in the Oudtshoorn Basin there had been exhumation down to the older Table Mountain stratigraphy. The absence of Beaufort or Drakensberg clasts in the Worcester Basin suggest either absence in the drainage basins at the time, or the lower resistance of the units and breakdown into fine material/ matrix.

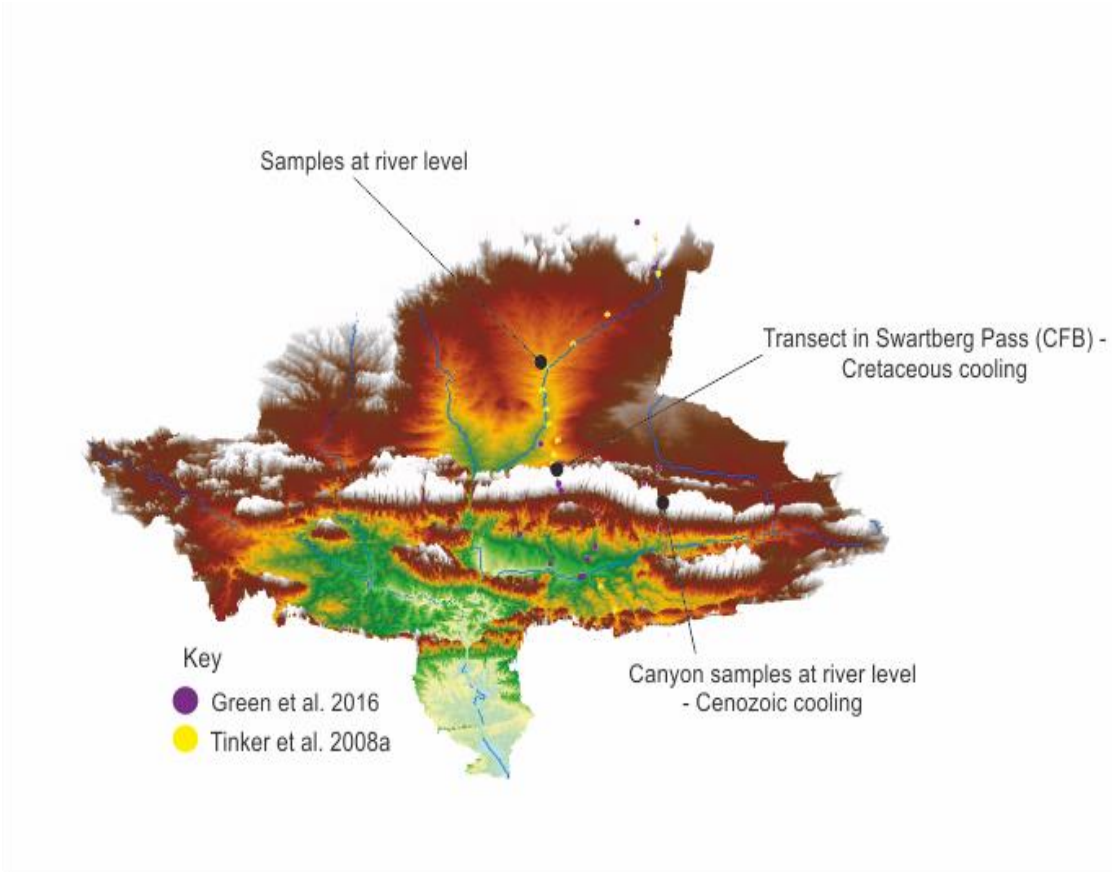

Figure 9.3 *– Limited coverage of apatite fission track study locations of Tinker et al. (2008a) and Green et al. (2016). Tinker's work indicates a Cretaceous age of the drainage net, whereas Greens CFB transect indicates a Cretaceous age and the canyon samples a Cenozoic age of the drainage net.*

The provenance data was integrated within a wide geomorphic and structural framework, in order to assess the likely routing of the sediment. The overall drainage of the trunk-rivers of Gouritz system are discordant with the underlying geology. In order for this to occur the rivers had to have a component of vertical incision during drainage evolution. During the rifting of Gondwana and initiation of the large-scale exhumation and drainage redevelopment (e.g., Gilchrist et al., 1994), it is argued that rapid drainage reorganisation occurred. Highly active transverse systems eroded headward, with a component of vertical incision, forming the incised meanders and poorts within the Cape Fold Belt). This led to capture of axial drainage systems that had developed following the structural grain of the Cape Fold Belt. This re-organisation is interpreted to have transported the majority of sediment towards the southward, rather than eastward as previously argued (*cf.* Lock et al. 1975). Evidence for superimposition of the Gouritz system on the underlying strata include the deeply incised meander bends and morphometric analysis. The trunk rivers are only slightly

modified by the fold belt, with straightening of the long profile (Chapter 8). Strath terrace data and catchment wide denudation rates, extrapolated from Gamkaskloof, indicates crudely that the Gamka River was in place by the Early Cretaceous, whilst strath terrace data of the Seweweekspoort also indicates incision into the fold belt started at least by the Cretaceous (Chapters 5, 6). This indicates that large-scale deposition in the Outdshoorn Basin and sediment bypass in the Gamka River was occurring within < 1km of each other. The transverse river systems were much more active than the parallel drainages as indicated by the lack of Uitenhage Group deposits within the Gamka River, which could also be a function of the high stream powers associated with bedrock rivers and lack of accommodation.

Some evidence of drainage re-organisation is still evident within the Gouritz catchment, most likely due to the slow Cenozoic erosion rates (Chapters 6, 7; Figures 9.1, 9.2). Elbows of capture, misfit streams and barbed confluences all indicate a complex history of evolution of the Gouritz catchment. Structural reconstructions by Paton (2006) have shown pre-rift strata caused drainage divides within the Olifants River.

Within ancient settings, the reconstruction of previous drainage patterns can become difficult due to the impact of erosion, and the corresponding lack of deposits/ evidence related to drainage evolution. However, by integrating sedimentology and geomorphology with crude estimates using cosmogenic analysis; it is evidenced that the Gouritz system is *ancient*, and has been in place since the Cretaceous (e.g., Rogers, 1903; King, 1951; Tinker et al. 2008a, *c.f.* Green et al., 2016). The age is compounded by the fact that the pediments of the Gouritz catchment grade into the location of the main trunk rivers (Chapter 7) and the variation in morphometric indices (Chapter 8). With this knowledge, the potential sink of the missing sediment can be speculated.

Where is the 'missing' sediment?

At the time of formation of the Mesozoic basins and the large-scale Cretaceous exhumation, the final stages of the break-up of Gondwana was occurring (Adie, 1952; Richard et al., 1996; Fish, 2005). The Falkland Plateau was in a rotated position east of South Africa (Adie, 1952) and moving westward along the south side of the Falkland-Agulhus transform fault. It is highly likely that the large-scale deposits of the Falkland Basins (e.g., Sea Lion complex; Bunt, 2015; Williams, 2015) are from the large-scale exhumation of South Africa (MacDonald et al. 2003). Previous workers have argued that the Falklands form the missing SE corner of the Karoo Basins (Adie,

1952; Trewin et al. 2000) and that there is a similarity between the stratigraphy of the Falkland Plateau basins and offshore Mesozoic basins of South Africa (Martin et al., 1981; McMillian et al., 1997). Constraining the length of the Cretaceous Gouritz River by using the Cretaceous location of the Great Escarpment, which is the regional drainage divide and Sømmes et al.'s (2009) analysis of correlation between trunk river length and fan length, indicates fan lengths of 400 km if point sourced (Sømme et al., 2009), which would have bypassed the shelf width.

Source-to-sink and sediment budgets

This study has shown that drainage basin 'source' areas can be thousands of kilometres from the present day sedimentary basin 'sink', and that tectonic reconstructions should be integrated into source-to-sink studies. Tectonic reconstructions have rarely been applied to source to sink studies (e.g., Crouch, 1979; Sharman et al., 2015) however they are especially important in divergent and/or strike slip/transform situations and passive margins where the distance between source and sinks distance will increase over geologic time, such as the Atlantic Ocean, and the Californian Borderlands. Data presented have has shown that there is a mismatch within the sediment budget of the Gouritz catchment. Reconstructing the cross sections of southern South Africa and the maximum amount of material missing highlighted a mismatch of the sediment budget, which allowed the investigation of where the sink could be. Commonly, within sediment budget studies, pediments are overlooked and represent a store of sediment within the Gouritz catchment that formed during the mid-Cenozoic, and most likely much older. However, if the pediments were formed in the Cretaceous, the small volume of sediment cannot account for the mismatch of the onshore and offshore budget of the Gouritz catchment (Chapter 5). The remnant pediment currently only represent a small store of sediment and they are predominantly erosional features.

Rift basin facies models

Previous rift basin facies models (Chapter 2) have not included large-scale transverse systems. Large-scale transverse systems are not only fundamental to the development of the Western Cape, but can be found globally e.g., Cordilleran foreland basin, Utah (Szwarc et al., 2014). The previous models have suggested that the parallel (axial) drainages are the most important, with regards to basin development and sediment transport; with small-scale transverse rivers draining mountains and supplying sediment. This is not always the case, as shown by this study, in which the large-scale transverse rivers are acting as zones of bypass (as shown by the lack of

sediments) – efficiently routing material offshore during periods of large-scale deposition <1 km away. This might be due to the evolution of the rift fault segments, which are reactivated thrust faults, and started long (Paton et al. 2006), with little relay zone development.

9.2 Denudational history

Question 2: What is the spatial and temporal variation in denudation across southern South Africa and the Gouritz Catchment?

Previous workers have shown large-scale exhumation occurred in the Cretaceous within southern South Africa (e.g., Brown et al., 1990; Tinker et al., 2008a). By reconstructing the pre-exhumation lithological thickness using 3DMOVE, volumes of 8.87 $x10^5$ km^3 (4 km lithological thickness) to 2.52 $x10^6$ km^3 material (11 km lithological thickness) have been removed over the western Cape (Chapter 5). Constraining the lithological thicknesses removed during the Cretaceous, exhumation rates of 50 - 143 mMa^{-1} have been calculated. These rates are within the range of published AFFT (Tinker et al., 2008) and lithological thickness removed with the metamorphic facies range of the Cape Fold Belt (Frimmel et al., 2001).

Published cosmogenic data (Fleming et al. 1999; Cockburn et al., 2000; Bierman and Caffee, 2001; van der Wateren and Dunai, 2001; Kounov et al., 2007; Codilean et al., 2008; Dirks et al., 2010; Decker et al., 2011; Erlanger et al., 2012; Chadwick et al., 2013; Decker et al., 2013) and data from pediments, rivers and strath terraces of the Gouritz catchment (Chapters 6, 7), suggest large-scale reduction in incision rates since the Cretaceous. Reduction in incision rates over the Cenozoic, and crude age estimates of channel incision in Gamkaskloof and Swartberg (Chapter 6), suggest that the principal topography and drainage net integration occurred within the Mesozoic. Further evidence that the trunk rivers were in place during the Mesozoic include the deeply incised meanders into resistant quartzites (Chapter 8) and the grading of the pediment surfaces (Chapter 7).

The low incision rates are related to the general trend towards aridity (Partridge, 1997; van Niekerk et al., 1999) and overall reduction in geodynamic activity in southern Africa during the Cenozoic (Tinker et al., 2008b; Bierman et al., 2014), coupled with the exhumation of resistant lithologies (Scharf et al., 2013). Locally, however, erosion is important as shown by the dissection of the pediment surfaces and a second phase of landscape development related to uplift and climatic boundaries (Chapter 7).

There is spatial variation in erosion rates between different landscape elements of the Gouritz catchment, although the data generally indicate globally low incision rates (Portenga and Bierman, 2011). The pediments are lowering at rates from 0.33 to 1m Ma^{-1}, whereas the rivers have denudation rates from 3.06 to 11.89m Ma^{-1}. This suggests relief is growing, albeit very slowly in the Gouritz catchment. The catchment wide denudation rates indicate that the trunk rivers are denuded at similar rates, apart from the Dwyka River. The high rates associated with the Dwyka River could be related to the slightly steeper gradient than the other trunk rivers, or a higher frequency of flash flooding in this location due its proximity and breaching of the escarpment where frequent thunderstorms form resulting in flooding.

The main bedrock geology control is related to the resistant Table Mountain quartzites. Incision rates into the Cape Fold Belt, denudation of the pediment surfaces which have abundant quarzitic boulders, and the sub-catchments that drain the Cape Fold Belt region, have lower denudation rates than the catchments that drain the Karoo Supergroup lithologies. The resistant nature of the exhumed Cape Fold Belt has been argued to be a principal reason for the persistence of the mountain belt with the Western Cape (Scharf et al., 2013) and the data presented in this thesis supports this interpretation. Within the Karoo Supergroup, erosion rates by lithology vary between the Dwyka and Buffels rivers, which drain similar geology (Beaufort Group) and terrain. Therefore, the variation in denudation rates are not related to lithology in this location but to other factors such as the magnitude of flood events.

The catchment wide denudation rates do not correlate with catchment properties such as slope, area, dissection or relief and indicate that denudation rates are decoupled from catchment properties. Denudation rates are now dependent on external factors such as tectonics or climate (Burbank et al., 1996; Densmore et al., 1998; Roering et al., 2001; Montgomery and Brandon, 2002) and the catchment appears to be in steady state.

9.2.1 Landscape evolution timeframe

The initial trigger of change from long-term deposition and sediment accummulation (e.g., Karoo Basin; Flint et al., 2011) to incision, and formation of the principal topography, occurred due uplift related to rifting of Gondwana. This caused the formation of small transverse systems (e.g., Gilchrist et al., 1994) that eventually captured the axial drainage systems of the pre-Cretaceous (Figures 9.4). After the rifting of Gondwana, the axial and transverse drainages were rapidly integrated as

shown by the highly active river systems, high denudation rates, incised meanders and the increased deposition offshore (Chapters 5, 8). The drainage net had to be at least partially integrated at the time of the exhumation of the Cape Fold Belt as the river planforms are superimposed on the resistant quartzite (e.g., confluence of the Olifants and Gamka rivers and incised meanders in the Swartberg mountain range; Chapter 2. During the integration of the drainage net, reactivation of faults within the fold belt led to the development of half-graben basins and onshore deposition of the Uitenhage group (Chapter 5). Exhumation of the Swartberg mountain range, which backs the Oudtshoorn Basin, was deeper than the Worcester Basin. This could be a function of the larger transverse systems in the Gouritz catchment than the Breede catchment. During the exhumation process, only the largest rivers could keep pace, as shown by the morphometric indices (Chapter 8) of the Gouritz catchment. The large transverse trunk rivers simply dissect the fold belt largely unaffected by underlying geology except for straightening of the long profiles, whereas the small order streams are trellised and have a large structural control due to the fold belt. This indicates that the small order streams are younger than the trunk rivers. Additional evidence of the younger age of the smaller streams is shown by the pediments. No small order streams were present during their formation as they were locally extensive, only the large trunk rivers were present as shown by the pediment grading. Initiation of the smaller order streams occurred in the mid-Cenozoic, which caused the dissection of the pediment surfaces (Chapter 7). The mid-Cenozoic boundary coincides with uplift (e.g., Burke, 1996; Green et al., 2016) and climate change (Partridge, 1997; Séranne, 1999; Linder, 2007), and the potential trigger of the new phase of incision cannot be discriminated. The smaller order streams are therefore Cenozoic in age, whereas the large trunk rivers were formed in the Mesozoic (Figures 9.4).

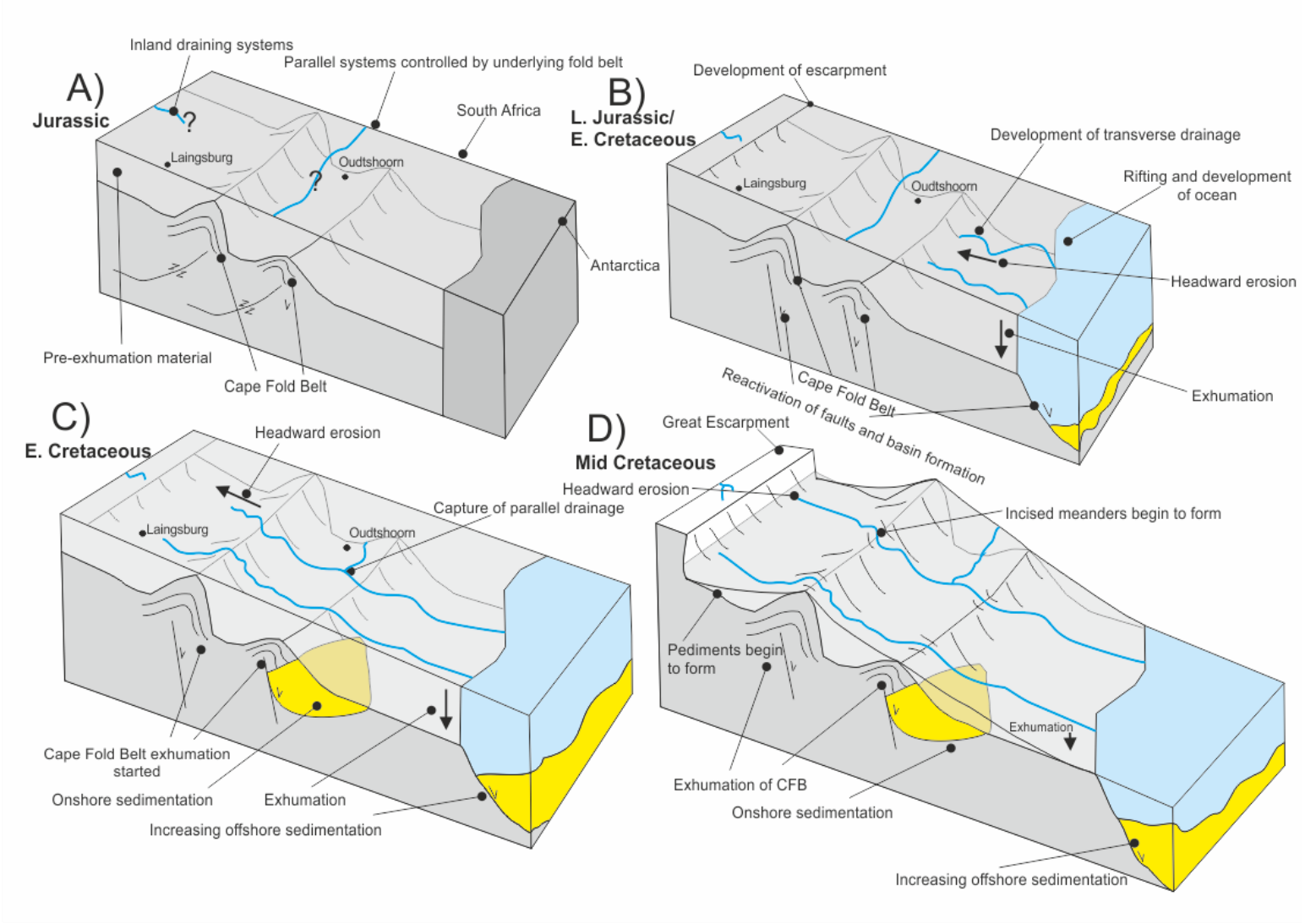
A)
Jurassic
Inland draining systems
Parallel systems controlled by underlying fold belt
South Africa
Laingsburg
Oudtshoorn
Antarctica
Pre-exhumation material
Cape Fold Belt
B)
L. Jurassic/
E. Cretaceous
Development of escarpment
Development of transverse drainage
Rifting and development of ocean
Laingsburg
Oudtshoorn
Headward erosion
Exhumation
Cape Fold Belt
Reactivation of faults and basin formation
C)
E. Cretaceous
Headward erosion
Capture of parallel drainage
Laingsburg
Oudtshoorn
Cape Fold Belt exhumation started
Onshore sedimentation
Exhumation
Increasing offshore sedimentation
D)
Mid Cretaceous
Great Escarpment
Headward erosion
Incised meanders begin to form
Pediments begin to form
Exhumation
Exhumation of CFB
Onshore sedimentation
Increasing offshore sedimentation

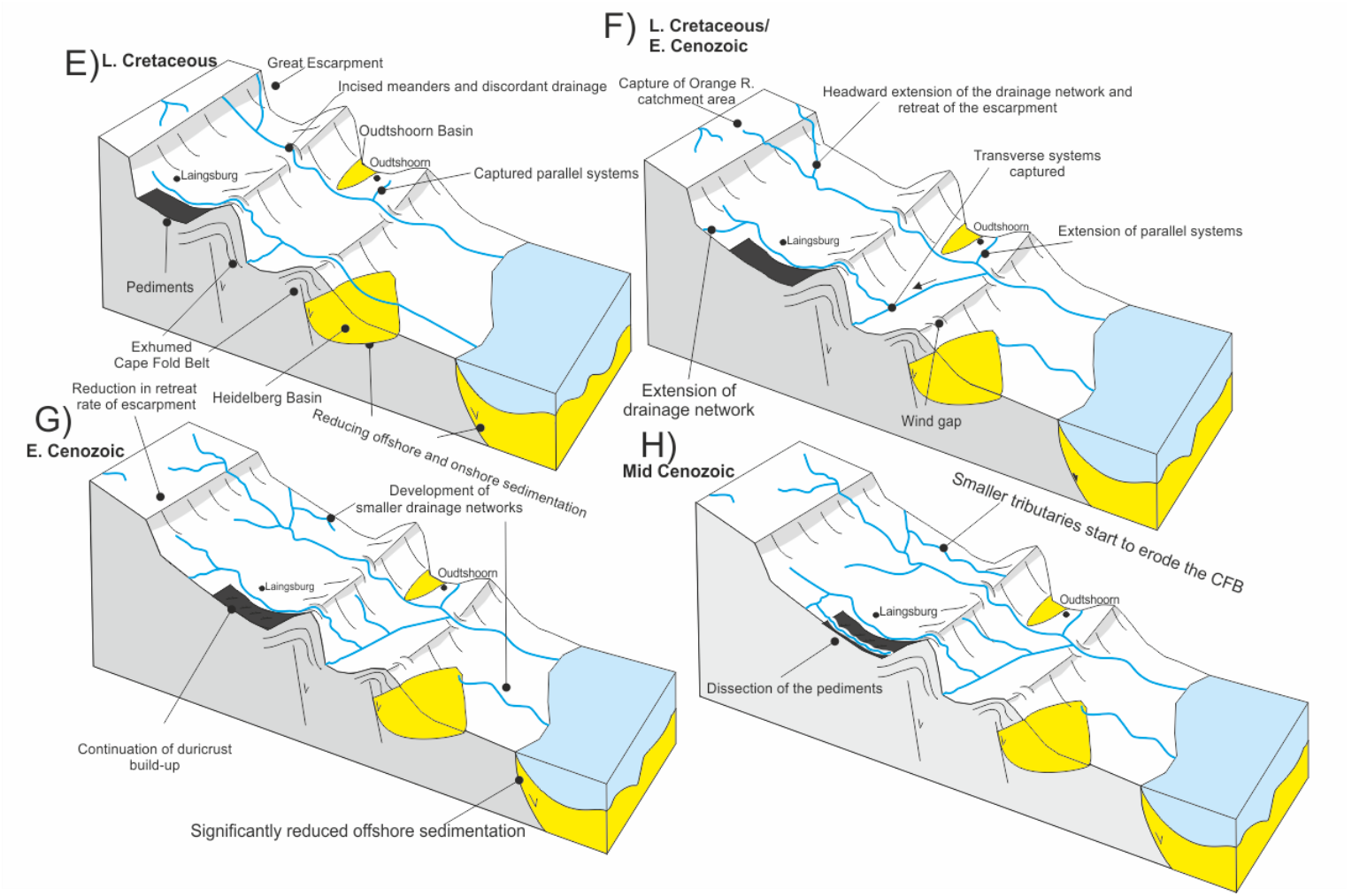

Figure 9.4 *– Synthesis diagram of catchment evolution, rough timings of evolution shown in bold.. The diagrams show the evolution from pre-rifting (early Mesozoic; A) to the present day (H).*

A major geomorphic landform of the Gouritz catchment are pediments (Figures 9.4), which are revealed as a key component of Hammond's landscape analysis (Chapter 8). Cosmogenic ages of the pediment surfaces in the Gouritz catchment indicate that they are long-lived features with little or no geomorphic activity since the Pleistocene. Integrating additional geomorphic and stratigraphic information (Chapter 7) has shown the pediments are at least mid-Cenozoic in age and most likely much older; as shown by the dissection of the pediments, the incision of small sub-catchments into the backing fold belt and the formation of duricrusts. The pediments were formed during the exhumation of the Cape Fold Belt in the Late Cretaceous, dissected during the mid-Cenozoic and are now an essentially fossilised landform above the level of erosion (Figures 9.4).

The landscape of South Africa is now only slowly eroding, and a large proportion of denudation can be related to weathering (e.g., Decker et al., 2013) as shown by the catchment denudation values which are $<5 mMa^{-1}$ (Scharf et al., 2013), with the rivers completing work during flooding. Climate has become increasingly important over the evolution of the catchment, with a dominant tectonic control during the Mesozoic, forming the principal topography. Increasing aridity, and decreasing denudation rates, has allowed weathering to be the current rate limiting factor of landscape evolution in the sediment-limited Gouritz catchment (e.g., Decker et al., 2013). As well as the dominant control, there has been variation in process dominance during the drainage evolution. During the Mesozoic exhumation, fluvial processes dominated. However, by the time of formation of the pediments hillslope processes and later, soil development dominated. During the second phase of landscape development and pediment dissection, fluvial processes once again dominated. However, due to decreasing denudation rates and the increasing importance of weathering during the later part of the Cenozoic, hillslope processes are once again dominant and limit the transport of sediment to the river systems.

9.2.2 Landscape evolution concepts and the age of southern Africa

The uplift history of southern South Africa is contentious (Section 3.3). After a single discrete uplift event, knickpoints are predicted to be at similar elevations within the catchment related to the pulse of uplift (e.g. Roberts and White, 2010). For example, if the Robert and White (2010) Cenozoic uplift model was recorded in the Gouritz catchment, knickpoints at similar elevations would be able to be assigned to this uplift following the equations in Section 2.2. However, Roberts and White (2010) model has many assumptions (Section 3.1.2) such as variation in controls such as climate, discharge and lithology are not taken into account.

The morphometric analysis of the catchment (Chapter 8) indicated that this is not the case. Knickpoints within the Gouritz Catchment are not at similar elevations, and further, are pinned on resistant lithologies. This indicates, that either the Gouritz catchment responded quicker than the catchments analysed by Robert and White (2010) and the wave of incision has passed through the catchment; that uplift did not occur or; that the uplift did not pass a threshold of geomorphological response; alternatively the uplift experienced in the Gouritz catchment could be much older. Given the slow rates of incision recorded within the catchment and regionally (e.g., Fleming et al., 1999; Cockburn et al., 2000; Bierman and Caffee, 2001; van der Wateran and Dunai, 2001; Kounov et al., 2007; Codilean et al., 2008; Dirks et al., 2010; Decker et al., 2011; Erlanger et al., 2012; Chadwick et al., 2013; Decker et al., 2013; Scharf et al., 2013; Bierman et al., 2014; Kounov et al., 2015), it is unlikely that a wave of incision from Cenozoic uplift would have quickly dissipated through the catchment. The knickpoints experienced within the trunk streams of the Gouritz catchment (Chapter 8) could have been caused by previous uplift, and were subsequently pinned on resistant lithologies. It is plausible that the recorded Cenozoic uplift in the catchments studied by Roberts and White (2010) did not affect the Gouritz catchment trunk rivers, or was at a different time. Cenozoic uplift is not recorded by AFTA within the Gouritz catchment (Gilchrist et al., 1994; Gallagher and Brown, 1999; Cockburn et al., 2000; Brown et al., 2002; Tinker et al., 2008a; Kounov et al., 2009; Flowers and Schoene, 2010), however this could be a threshold issue related to the large drainage areas of the main trunk rivers. Green et al. (2016) argued for significant Cenozoic uplift of the Swartberg Range. This local uplift affected the smaller draining trunk rivers, and could relate the numerous knickpoints seen within the lower order streams that drain the fold belt (Chapter 8).

Green et al. (2016) also argued that the river systems of the Gouritz system are Cenozoic in age, the data presented in this thesis does not support this entirely. As shown by the antecedence of the main trunk rivers (Chapter 5 and 8), the grading of the pediments into the main trunk rivers (Chapter 7) and the cosmogenic data (Chapter 6 and 7), it is evident the trunk rivers are ancient, and at least Cretaceous in age. However, the smaller order streams are not ancient, and it is likely that the uplift Green et al. (2016) recorded caused the initiation of these smaller order streams and the dissection of the pediments and backing CFB near the Swartberg Range; nonetheless these knickpoints are not at similar elevations and are dependent on lithological variation. Nonetheless, the data presented in this thesis indicates a Mesozoic age of the principle topography and main drainage network of

the Gouritz Catchment (e.g., Tinker et al., 2008a; Kounov et al., 2009). This indicates that the knickpoints in the trunk rivers of the Gouritz catchment are much older than the Cenozoic uplift modelled by Roberts and White (2010), and are now controlled by lithological variation and are therefore at different heights within the landscape (Chapter 8).

9.3 Geomorphological techniques and concepts

Question 3: How can advancements in geomorphic techniques and concepts help constrain landscape development in ancient settings?

A range of established (Chapters 6, 7) and novel techniques have been used in this project (Chapter 5 – MOVE, misfit stream analysis; Chapter 6 – pediment reconstruction) in order to try and constrain landscape development, which has been greatly assisted by the development of remote sensing data collection and GIS (Figures 9.1, 9.2).

9.3.1 Morphometric analysis

Chapter 8 focused on the application of commonly used morphometric indices to the Gouritz catchment. Morphometric studies have rarely been applied to ancient settings, with a focus on active settings to try and delineate the influence of climate or tectonic activity. Within the Gouritz catchment, tectonic influence could not be delineated as a primary control, i.e., large-scale Mesozoic rifting is no longer seen within the river morphometric indices. However, the lower part of the hypsometric curve could be related to recent coastal uplift (Chapter 8). The morphometric indices variation within the catchment can be related to inherited structures and there appears to be a dominant lithological control. Overall, morphometric indices work well in ancient settings, and are able to give a first order assessment of the catchment; however the variation of indices over time need to be reassessed, and the commonly used reasons behind variations in morphometric indices critically assessed with ancient settings (Chapter 10).

9.3.2 Minimum eroded volumes

Misfit streams within bedrock settings have not been quantitatively assessed within the literature, but are fundamental when assessing long-term landscape development. Minimum eroded volumes have been extracted for several subcatchments in the Gouritz catchment and surrounding area (Chapters 5, 7). Minimum eroded volumes have helped identify misfit streams, and delineate previous drainage courses of the Gouritz and Breede catchments (Chapter 5). Whilst relating minimum eroded volumes to published cosmogenic erosion rates has helped place

age constraints on the pediments within the catchment (Chapter 7). Calculating the minimum eroded volume and relating the volume removed to published cosmogenic rates is an efficient way to assess landscape evolution remotely; especially as the resolution of DEMs are improving.

9.3.3 Pediment reconstruction

Reconstructing the palaeosurfaces of the multiple pediments within southern South Africa had not been undertaken previously. The technique highlighted in Chapter 4 and used in Chapter 7, has been fundamental in benchmarking the cosmogenic nuclide data. By calculating the volume of material removed by reconstructing the palaeosurface (Section 7.3.2), the evolution of the pediment surfaces were able to be relatively dated. By integrating desktop based analysis of geomorphic indicators with cosmogenic data the landscape evolution of the Gouritz catchment has been delineated.

9.3.4 Cosmogenic analysis

Cosmogenic analysis was successful in southern South Africa, due to the high quartz content of basement lithologies. Cosmogenic analysis has been successfully used for a variety of landforms including river sediment (Chapter 6) and pediment surfaces (Chapter 7). The data indicate very low erosion rates within South Africa. However, the reported exposure ages of the pediments (Chapter 7) did not help to constrain landscape development further. The exposure ages are an order of magnitude less than the age of pediment development. The *minimum* exposure ages do indicate remarkable stability within the catchment, but do not aid constraining landscape development and need to be benchmarked on geomorphologic and stratigraphic information.

9.3.5 Geomorphic concepts

Sadler effect

One concept of sedimentology is that of Sadler (1981) who showed that rates of accumulation (and therefore denudation) appear to decrease with increasing time measurement interval due to hiatuses, non-preservation and the unsteady nature of sediment deposition; which causes an apparent increase in accumulation rates (/denudation rates) in recent times. However, the Gouritz catchment does not fit this trend; there has been a long-term reduction in denudation rates (Chapters 5, 6, 7) since the start of the Cenozoic and related sediment accumulation (e.g., Tinker et al., 2008b). The Cretaceous (up to 184 mMa^{-1}) was characterised by high denudation

rates in comparison to the present day, although the Cretaceous rates were not globally high compared to present day active settings (Portenga and Bierman, 2011). The rates have decreased substantially in the Cenozoic (up to 15 mMa^{-1}) due to increasing aridity and tectonic quiescence, the catchment is now essentially 'fossilised' with low rates of activity and sediment accumulation.

Averaging by nature

The concept of 'let nature do the averaging' (Chapter 6) related to the integration of cosmogenic nuclide concentration from a range of sources in fluvial sediment is fundamental to calculating catchment wide denudation rates (von Blanckenburg, 2005), and appears to hold true within the Gouritz catchment (c.f. Wittmann et al., 2011; Delunel et al., 2014). The catchment wide denudation rates are similar in multiple trunk rivers regardless of catchment morphometrics or lithology and over different terrains.

Dominant controls

The morphometric analysis highlighted the dominant influence of bedrock lithology on catchment dynamics (Chapter 8). Incision rates into the Cape Fold Belt are low (Chapter 6). There is slight variation between catchments dominated by Cape Supergroup lithologies over Karoo Supergroup lithologies with regards to catchment denudation rates (Chapter 6). However, the overall similarity of catchment denudation rates (Chapter 6) indicate that terrains of different geology are lowering at similar rates (*sensu* Hack, 1960) and the lack of correlation between catchment properties and morphometric indices indicate the system has decoupled with allogenic factors becoming dominant. Within settings of low denudation, weathering is argued to be the rate limiting factor (Scharf et al., 2013), and this is the case for the Gouritz. The relative importance of tectonic activity has decreased since the Mesozoic and formation of the drainage net. Whilst there has been variation in the dominance of fluvial and hillslope processes, with hillslope processes and weathering now limiting the sediment supply to the drainage system.

Landscape models

King's (1953, 1967) landscape model has been disputed by numerical modelling and geochronology (e.g., Fleming et al., 1999; van der Beek et al., 2002; Brown et al., 2002; Kounov et al., 2007). Chapter 7 highlighted that the pediment surfaces should be taken as individual landforms that cannot be correlated over large areas, as shown

by the individual grading of the pediments to large-scale trunk rivers. Furthermore, the minimum exposure ages integrated with geomorphic and stratigraphic evidence (Chapter 7) highlights that the ages of the pediments do not correlate with the elevation of the pediment surfaces, which King used as an assumption to correlate the pediment surfaces (King, 1953, 1967).

Hack's (1960) landscape evolution theories (Chapter 2) appear to hold true within the Gouritz catchment as shown by the morphometric indices (Chapter 8) and catchment wide denudation rates (Chapter 6). The catchment has been in long-term geomorphic steady state (Chapter 6), in which the denudation rates between different lithologies are similar. This is aided by the relative quiescence of South Africa since the Cenozoic and the increasing aridity (Bakker and Mercer, 1968). Nonetheless, if climate or the tectonic regime changes, Hacks landscape evolution theories will no longer hold true, and the catchment will react (Summerfield, 1991). The Gouritz catchment appears to be in geomorphic steady-state and there is the long term integration of denudation rates as shown by cosmogenic data (Chapters 6, 7) and apatite fission track data (e.g., Tinker et al., 2008a).

Chapter 10 Conclusions

The overall aim of this study was to investigate the long-term drainage evolution of the Western Cape, with a specific emphasis on the Gouritz catchment. This was achieved by addressing three key research questions (Chapter 1). The study of ancient settings is often overlooked, but this study has highlighted the importance of understanding such landscapes that are found on many continents. By reconstructing long-term drainage evolution through integrating modern techniques such as GIS and cosmogenic isotope dating with established sedimentological and geomorphic principles the landscape evolution of the Western Cape has been delineated for the first time. The main transverse river systems have been in place since the Cretaceous (*c.f.* Green et al., 2016), and acted as a large-scale zone of sediment bypass during the formation of the onshore Mesozoic basins in which there was large scale deposition (*c.f*. Leeder and Gawthorpe, 1987). There is a large mismatch between the volume of onshore denudation and offshore sediment accumulation (Chapter 5), and the reconstructed catchment drainage, integrated with tectonic plate reconstructions, indicates that much of the 'missing' sediment could be around the Falklands Plateau. This configuration separates the source from the sink by 6000 km. Cosmogenic dating of geomorphic landforms (e.g., pediments, strath terraces, catchment averaged denudation) has shown a major long-term decrease in erosion rates since the Cretaceous (Chapters 6, 7). The low Cenozoic denudation rates indicate that the principal topography of southern Africa is Mesozoic in age. The catchment-wide denudation rates indicate that the nature does average the erosion rates of different sources and that the catchment is currently in geomorphic steady-state. The spatial variability in denudation rates cannot be related to catchment morphometrics or lithology in the case of the Dwyka River, however the Cape Supergroup lithologies are denuding at lower rates. The pediments are now essentially fossilised landforms within the catchment that have evolved since the Cretaceous with phases of increased geomorphic activity (Chapter 7). The application of modern techniques (Chapters 4 – 8) helped to constrain the evolution of the Gouritz Catchment. However, caution is needed when applying cosmogenic dating due to the influence of *minimum* exposure ages; to concisely date landforms the cosmogenic data must be benchmarked on geomorphic and stratigraphic information.

10.1 Landscape evolution

Integrating the research questions and techniques has allowed the development of the Gouritz catchment to be delineated. During the Cretaceous there was large-scale exhumation of southern South Africa with a maximum of 2.52 $x10^6$ km^3 material removed (Chapter 5). The main trunk river systems were active in the Cretaceous (Chapter 5) as shown by the deeply incised river courses in resistant lithologies of the Cape Fold Belt; with large scale sediment bypass within 1km of significant sedimentation of the Enon conglomerate in the onshore Mesozoic basins. Incision of the fold belt has been dated to have started in the Cretaceous or earlier using calculated denudation rates of strath terraces by cosmogenic nuclides and catchment wide denudation rates (Chapter 6). Further evidence of the ancient nature of the trunk rivers is provided by the grading of the pediment surfaces (Chapter 7) and the morphometric indices of the trunk rivers (Chapter 8). The trunk rivers dissect the fold belt with minimal impact on the indices apart from a slight straightening of the long profile. The *ancient* nature of the trunk river indicates that sediment was routed to the south, and accreted to the Falkland Plateau. Prior to the exhumation of the Cape Fold Belt large scale re-organisation of the trunk rivers occurred, and during this time the pediments began to form (Chapter 7). The pediments are net erosional features, but were able to build up large amounts of hillslope material and develop ferricrete, most likely during the humid intense weathering of the Cretaceous. During the Cenozoic the climate became increasingly arid, with decreasing tectonic activity and denudation rates (Chapter 6, 7). However, a pulse of geomorphic activity occurred in the mid-Cenozoic; which could be related to tectonic uplift or climate change (e.g., Burke, 1996; Partridge, 1997), which allowed the initiation of smaller draining rivers, which dissected the pediment surfaces and backing Cape Fold Belt. The smaller order rivers have morphometric indices that are influenced by the structure of the fold belt (Chapter 8). The Cenozoic evolution of the Gouritz catchment has resulted in geomorphic steady state, in which the denudation rates have become decoupled from catchment properties. The major control on landscape evolution is now weathering in this sediment limited setting.

10.2 Study limitations

This study aimed to provide a first assessment of the drainage systems of the Western Cape. However, the work is limited by the lack of published data on long-term climate and tectonic change of southern Africa. There remains considerable contention between different theories of uplift and this makes it difficult to assign

definitively landforms and landscape change to specific boundary condition changes. Further, the lack of long-term climate data compounds this, as the start of the arid conditions remains poorly constrained.

The work is also limited by the lack of understanding of ancient settings, the morphometric analysis completed in this thesis is the first of its kind, and there are no other in-depth studies for comparison. Further, the variation in morphometric indices over time is not known and research has focused on high erosion rates in 'young' and dynamic settings.

Due to the ancient setting of the study area, the planform changes over time have been eroded, and only small sections of evidence remain, which in some cases can be speculative. However, this is a problem common to research of ancient settings, and the work in this thesis has quantified evidence of drainage evolution such as misfit streams and pediment reconstruction. In the future, additional evidence, such as high level gravels in wind gaps, could be integrated to strengthen the arguments presented.

The study is also limited by the lack of offshore data integrated within the data chapters, although much of this remains confidential. The erosion rates calculated could be tied into offshore deposits offshore South Africa and Falkland Islands to place further benchmarks on onshore drainage development. The provenance of sediment within chapter 5 is limited by the lack of geochemical analysis, if more data was available, a more in depth investigation of the conglomerate matrix could have occurred. Further, offshore cores could be correlated to onshore geological variation.

10. 3 Further work

The Western Cape draining catchments remain understudied, and the techniques used in this study could be applied to, and developed in other antecedent catchments such as the Olifants catchment, South Africa (Chapter 3). The techniques applied in this thesis could also be used to assess antecedent catchments in other ancient settings such as Australia and other 'Gondwanan landscapes'.

Research Question 1

In order to assess the sink of the missing sediment from South Africa, the provenance of the offshore sands of the Falkland Plateau Basin should be assessed. Provenance studies will help delineate the source area and seismic data should be integrated to assess the relationship between sediment packages. The matrix of the Enon

conglomerate should be assessed to ascertain if the Beaufort and Drakensberg lithologies are a component. The stream captures of the Gouritz catchment should be studied in greater detail, with the high level terrace gravels analysed. Furthermore, the exhumation history of the Cape Fold Belt should be constrained further to help date the ages of the bedrock gorges more precisely; by collecting apatite fission track samples from higher elevations of the Cape Fold Belt. Facies models and facies variation should also be assessed in locations where large scale transverse systems occur that are coeval with axial drainages.

Future research questions could include:

1. Is there a provenance match between the sediment offshore the Falkland Islands and the South African bedrock, and if so is there a reverse stratigraphy present?
2. Did the Falkland Islands undergo a similar landscape evolution to South Africa in the late Mesozoic?
3. What are the sedimentological deposits and facies variations associated with transverse systems that dominate the axial systems?

Research Question 2

The cosmogenic technique should be developed further in ancient landscapes and as the technique improves the age limits of the method should extend. In order to help constrain the pediment ages further, the ferricretes should be dated. Additional sedimentological assessment of the pediments will help constrain formation mechanisms further. Catchment wide denudation river samples should be dated for the smaller subcatchments to constrain landscape evolution in different physiographic regions.

Future research questions could include:

1. What are the age of ferricretes found within the pediment surfaces?
2. What is the sedimentological variation throughout the pediment from proximal to distal facies?
3. How does catchment wide denudation rate vary between smaller sub-catchments dominated by specific geological groups and physiographic locations?

Research Question 3

Whilst geomorphic concepts have been successfully applied to the Gouritz catchment, the variation of the morphometric indices over time need to be assessed. By using landscape evolution models the forcing factors and resulting impact on morphometric indices can be extracted at certain time intervals. Additional work is needed on applying commonly used geomorphic analysis techniques to ancient settings.

Future research questions could include:

1. How do morphometric indices vary over time, with specific changes in tectonics and climate?
2. What would be the topographic expression of the competing theories of tectonic and climatic evolutions of South Africa?
3. How can misfit channels in bedrock settings be best quantified?
4. How can cosmogenic dating be extended to settings with low erosion rates?

Reference list

Abdelkareem, M., El-Baz, F., 2015. Evidence of drainage reversal in the NE Sahara revealed by space-borne remote sensing data. Journal of African Earth Sciences, 110, 245-257.

Abdelkareem, M., Ghoneim, E., El-Baz, F., Askalany, M., 2012. New insight on paleoriver development in the Nile basin of the eastern Sahara. Journal of African Earth Sciences, 62, 35-40.

Adams, S., Titus, R., Pietersen, K., Tredoux, G., Harris, C., 2001. Hydrochemical characteristics of aquifers near Sutherland in the Western Karoo, South Africa. Journal of Hydrology, 241, 91-103.

Adie, R.J., 1952. The position of the Falkland Islands in a reconstruction of Gondwanaland. Geological Magazine, 89, 401-410.

Agassiz, L. 1840. Etudes sur les glaciers: Privately published, Neuchˆatel.

Aguilar, G., Riquelme, R., Martinod, J., Darrozes, J., Maire, E., 2011. Variability in erosion rates related to the state of landscape transience in the semi-arid Chilean Andes. Earth Surface Processes and Landforms, 36, 1736-1748.

Ahnert. F., 1970. Functional relationships between denudation, relief, and uplift in large mid-latitude drainage basins, American Journal of Science, 268, 243–263.

Allen, P. A., 2008. Time scales of tectonic landscapes and their sediment routing systems. In: Gallagher, K., Jones, S.J., Wainwright, J. (Eds.), Landscape Evolution: Denudation, Climate and Tectonics over Different Time and Space Scales, Geological Society of London, Special Publication, 296, pp. 7-28.

Allen, P.A., Densmore, A.L., 2000. Sediment flux from an uplifting fault block. Basin Research, 12, 367-380.

Alvarez-Marrón, J., Hetzel, R., Niedermann, S., Menéndez, R., Marquínez, J., 2008. Origin, structure and exposure history of a wave-cut platform more than 1 Ma in age at the coast of northern Spain: A multiple cosmogenic nuclide approach. Geomorphology, 93, 316-334.

Anders, M.D., Pederson, J.L., Rittenour, T.M., Sharp, W.D., Gosse, J.C., Karlstrom, K.E., Crossey, L.J., Goble, R.J., Stockli, L., Yang, G., 2005. Pleistocene geomorphology and geochronology of eastern Grand Canyon: linkages of landscape components during climate changes. Quaternary Science Reviews, 24, 2428-2448.

Anderson, R.S., 1994. Evolution of the Santa Cruz Mountains, California,

through tectonic growth and geomorphic decay. *Journal of Geophysical Research: Solid Earth*, *99*(B10), 0161-20179.

Antón, L., De Vicente, G., Muñoz-Martín, A., Stokes, M., 2014. Using river long profiles and geomorphic indices to evaluate the geomorphological signature of continental scale drainage capture, Duero basin (NW Iberia). Geomorphology, 206, 250-261.

Attal, M., Cowie, P.A., Whittaker, A.C., Hobley, D., Tucker, G.E.,Roberts, G.P., 2011. Testing fluvial erosion models using the transient response of bedrock rivers to tectonic forcing in the Apennines, Italy. *Journal of Geophysical Research: Earth Surface*, *116*(F2).

Babault, J., Van Den Driessche, J., Teixell, A., 2012. Longitudinal to transverse drainage network evolution in the High Atlas (Morocco): The role of tectonics. Tectonics, 31, TC4020.

Bakker, E. M. V. Z., Mercer, J. H., 1986. Major late Cainozoic climatic events and palaeoenvironmental changes in Africa viewed in a world wide context. Palaeogeography, Palaeoclimatology, Palaeoecology. 56, 217-235.

Balco, G., Stone, J.O., Lifton, N.A., Dunai, T.J., 2008. A complete and easily accessible means of calculating surface exposure ages or erosion rates from 10 Be and 26 Al measurements. Quaternary geochronology, 3, 174-195.

Ballantyne C., 2012. Chronology of glaciation and deglaciation during the Loch Lomond (Younger Dryas) Stade in the Scottish Highlands: implications of recalibrated 10Be exposure ages. Boreas, 41, 513-526.

Bardossy, G., 1981. Paleoenvironments of laterites and lateritic bauxites – effect of global tectonism on bauxite formation. In: International Seminar on Lateritisation Processes (Trivandrum, India). Rotterdam: Balkema, pp. 284–297.

Bar-Matthews, M., Marean, C. W., Jacobs, Z., Karkanas, P., Fisher, E. C., Herries, A. I., Brown, K., Williams, H. M., Bernatchez, J., Ayalon, A., Nilssen, P. J., 2010. A high resolution and continuous isotopic speleothem record of paleoclimate and paleoenvironment from 90 to 53 ka from Pinnacle Point on the south coast of South Africa. Quaternary Science Review, 29, 2131-2145.

Barrows, T., Lehman, S., Fifield, L., De Deckker, P., 2007. Absence of Cooling in New Zealand and the Adjacent Ocean During the Younger Dryas Chronozone. Science 318, 86-89

Beaumont, C., Kooi, H., Willett S., 2000. Coupled tectonic-surface process models

with applications to rifted margins and collisional orogens. In Summerfield, M.A. (ed.), Geomorphology and Global Tectonics, Wiley, Chichester, pp. 29–55.

Bellin, N., Vanacker, V., Kubik, P.W., 2014. Denudation rates and tectonic geomorphology of the Spanish Betic Cordillera. Earth and Planetary Science Letters, 390, 19-30.

Belmont, P., Gran, K.B., Schottler, S.P., Wilcock, P.R., Day, S.S., Jennings, C., Lauer, J.W., Viparelli, E., Willenbring, J.K., Engstrom, D.R., Parker, G., 2011. Large shift in source of fine sediment in the Upper Mississippi River. Environmental science & technology, 45, 8804-8810.

Belton, D.X., Brown, R.W., Kohn, B.P., Fink, D., Farley, K. A., 2004. Quantitative resolution of the debate over antiquity of the central Australian landscape: implications for the tectonic and geomorphic stability of cratonic interiors. Earth and Planetary Science Letters, 219, 21–34.

Ben-Avraham, Z., Hartnady, C. J. H., Malan, J. A., 1993. Early tectonic extension between the Agulhas Bank and the Falkland Plateau due to the rotation of the Lafonia microplate. Earth and Planetary Science Letters, 117, 43-58.

Ben-Avraham, Z., Hartnady, C. J. H., Kitchin, K. A., 1997. Structure and tectonics of the Agulhas-Falkland fracture zone. Tectonophysics, 282, 83-98.

Bessin, P., Guillocheau, F., Robin, C., Schrötter, J. M., Bauer, H., 2015. Planation surfaces of the Armorican Massif (western France): Denudation chronology of a Mesozoic land surface twice exhumed in response to relative crustal movements between Iberia and Eurasia. Geomorphology, 233, 75-91.

Bierman, P. R., 1994. Using in situ produced cosmogenic isotopes to estimate rates of landscape evolution: A review from the geomorphic perspective. Journal of Geophysical Research: Solid Earth, 99, B7, 13885-13896.

Bierman, P.R., Caffee, M., 2001. Slow rates of rock surface erosion and sediment production across the Namib Desert and escarpment, southern Africa. American Journal of Science, 301, 326-358.

Bierman, P. R., Coppersmith, R., Hanson, K., Neveling, J., Portenga, E. W., Rood, D. H., 2014. A cosmogenic view of erosion, relief generation, and the age of faulting in southern Africa. GSA Today, 24, 4-11.

Bierman, P. R., Nichols, K. K., Matmon, A., Enzel, Y., Larsen, J., and Finkel, R., 2007. 10-Be shows that Namibian drainage basins are slowly, steadily and uniformly eroding: Quaternary International, 167–168, 33.

Bierman, P. R., Reusser, L. J., Nichols, K. K., Matmon, A., Rood, D., 2009,

Where is the sediment coming from and where is it going - A 10Be examination of the northern Queensland escarpment, Australia, 2009 Portland GSA Annual Meeting: Portland, Or.

Bierman, P., Turner, J., 1995. 10 Be and 26 Al evidence for exceptionally low rates of Australian bedrock erosion and the likely existence of pre-Pleistocene landscapes. Quaternary Research, 44, 378-382.

Binnie, S.A., Phillips, W.M., Summerfield, M.A., Fifield, L.K., 2006. Sediment mixing and basin-wide cosmogenic nuclide analysis in rapidly eroding mountainous environments. Quaternary Geochronology, 1, 4-14.

Bishop, P., 1985. Southeast Australian late Mesozoic and Cenozoic denudation rates: a test for late Tertiary increases in continental denudation. Geology, 13, 479-482.

Bishop, P., 1988. The eastern highlands of Australia: the evolution of an intraplate highland belt. Progress in Physical Geography, 12, 159-182.

Bishop, P., 1995. Drainage rearrangement by river capture, beheading and diversion. Progress in Physical Geography, 19, 449-473.

Bishop, P., 2007. Long-term landscape evolution: linking tectonics and surface processes. Earth Surfaces Processes and Landforms, 32, 329-365.

Bishop, P., Goldrick, G., 1998. Eastern Australia, in Summerfield, M.A. (ed.) Global Tectonics and Geomorphology, John Wiley, New York.

Bishop, P., Goldrick, G., 2010. Lithology and the evolution of bedrock rivers in post-orogenic settings: constraints from the high-elevation passive continental margin of SE Australia. Geological Society, London, Special Publications, 346, 267-287.

Bishop, P., Hoey, T. B., Jansen, J. D., Artza, I. L., 2005. Knickpoint recession rate and catchment area: the case of uplifted rivers in Eastern Scotland. Earth Surfaces Processes and Landforms, 30, 767-778.

Bloom, A.L., 2002. Teaching about relict, no-analog landscapes. Geomorphology, 47, 303-311.

Blum, M.D., Roberts, H.H., 2009. Drowning of the Mississippi Delta due to insufficient sediment supply and global sea-level rise. Nature Geoscience, 2, 488-491.

Blum, M.D., Törnqvist, T.E., 2000. Fluvial responses to climate and sea-level change: a review and look forward. Sedimentology, 47, 2-48.

Blumberg, D.G., Neta, T., Margalit, N., Lazar, M., Freilikher, V., 2004. Mapping exposed and buried drainage systems using remote sensing in the Negev Desert, Israel. Geomorphology, 61, 239-250.

Bonnet, S., 2009. Shrinking and splitting of drainage basins in orogenic landscapes from the migration of the main drainage divide. Nature Geoscience, 2, 766-771.

Bookhagen, B., Fleitmann, D., Nishiizumi, K., Strecker, M.R., Thiede, R.C., 2006. Holocene monsoonal dynamics and fluvial terrace formation in the northwest Himalaya, India. Geology, 34, 01-604.

Borraccini, F., De Donatis, M., Di Bucci, D. and Mazzoli, S., 2002. 3D model of the active extensional fault system of the high Agri River valley, Southern Apennines, Italy. Journal of Virtual Explorer, 6, 1-6.

Bourne, J.A., Twidale, C.R., 1998. Pediments and alluvial fans: genesis and relationships in the western piedmot of the Flinders Ranges, South Australia. Australian Journal of Earth Sciences, 45, 123–135.

Bracciali, L., Najman, Y., Parrish, R.R., Akhter, S.H., Millar, I., 2015. The Brahmaputra tale of tectonics and erosion: Early Miocene river capture in the Eastern Himalaya. Earth and Planetary Science Letters, 415, 25-37.

Braucher, R., Brown, E.T., Bourlès, D.L., Colin, F., 2003. In situ produced 10 Be measurements at great depths: implications for production rates by fast muons. Earth and Planetary Science Letters, 211, 251-258.

Braun J., Sambridge M., 1997. Modelling landscape evolution of geological time scales: a new method based on irregular spatial discretization. Basin Research, 9, 27–52.

Breeze, P.S., Drake, N.A., Groucutt, H.S., Parton, A., Jennings, R.P., White, T.S., Clark-Balzan, L., Shipton, C., Scerri, E.M., Stimpson, C.M., Crassard, R., 2015. Remote sensing and GIS techniques for reconstructing Arabian palaeohydrology and identifying archaeological sites. Quaternary International, 382, 98-119.

Brocklehurst, S.H., Whipple, K.X., 2002. Glacial erosion and relief production in the Eastern Sierra Nevada, California. Geomorphology, 42, 1–24.

Brook, E.J., Brown, E.T., Kurz, M.D., Ackert, R.P., Raisbeck, G.M., Yiou, F., 1995. Constraints on age, erosion, and uplift of Neogene glacial deposits in the Transantarctic Mountains determined from in situ cosmogenic 10Be and 26Al. Geology, 23, 1063-1066.

Brook, E., Kurz, M., Ackert, R., Denton, G., Brown, E., Raisbeck, G., Yiou F., 1993. Chronology of Taylor Glacier Advances in Arena Valley, Antarctica, Using in Situ Cosmogenic 3He and 10Be. Quaternary Research, 39, 11-23.

Brink, G. J., Keenan, J. H. G., 1993. Deposition of Fourth-Order, Post-Rift

Sequences and Sequence Sets, Lower Cretaceous (Lower Valanginian to Lower Aptian), Pletmos Basin, Southern Offshore, South Africa: Chapter 3: Recent Applications of Siliciclastic Sequence Stratigraphy, pp. 43 - 69.

Broquet, C.A.M., 1992. The sedimentary record of the Cape Supergroup: A review. In. Inversion tectonics of the Cape Fold Belt, Karoo and Cretaceous basins of southern Africa. (eds.: de Wit, M.J. and Ransome, I.G.D.) A.A. Balkema, Rotterdam. pp. 159-183.

Brown, E.T., Stallard, R.F., Larsen, M.C., Bourlès, D.L., Raisbeck, G.M., Yiou, F., 1998. Determination of predevelopment denudation rates of an agricultural watershed (Cayaguas River, Puerto Rico) using in-situ-produced 10 Be in river-borne quartz. Earth and Planetary Science Letters, 160, 723-728.

Brown, L. F., (Ed.) 1995. Sequence Stratigraphy in Offshore South African Divergent Basins: An Atlas on Exploration for Cretaceous Lowstand Traps by Soekor (Pty) Ltd, AAPG Studies in Geology 41 (No. 41). AAPG.

Brown, R.W., Rust, D.J., Summerfield, M.A., Gleadow, A.J., De Wit, M.C., 1990. An Early Cretaceous phase of accelerated erosion on the south-western margin of Africa: Evidence from apatite fission track analysis and the offshore sedimentary record. International Journal of Radiation Applications and Instrumentation. Part D. Nuclear Tracks and Radiation Measurements, 17, 339-350.

Brown, R.W., Gallagher, K., Gleadow, A.J.W., Summerfield, M.A., 2000. Morphotectonic evolution of the South Atlantic margins of Africa and South America. In: Summerfield, M.A. (Ed.), Geomorphology and Global Tectonics. John Wiley and Sons Ltd., 255–284.

Brown, R.W., Summerfield, M.A., Gleadow, A.J.W., 2002. Denudation history along a transect across the Drakensberg Escarpment of southern Africa derived from apatite fission track thermochronology. Journal of Geophysical Research, 107, 1-18.

Brunt, R.L., Hodgson, D.M., Flint, S.S., Pringle, J.K., Di Celma, C., Prélat, A., Grecula, M., 2013. Confined to unconfined: anatomy of a base of slope succession, Karoo Basin, South Africa. Marine and Petroleum Geology, 41, 206-221.

Bryan, K., 1922. Erosion and sedimentation in the Papago country, Arizona. U.S Geological Survey Bulletin, 730, 19–90.

Bunt, R.J., 2015. The use of seismic attributes for fan and reservoir definition in the Sea Lion Field, North Falkland Basin. Petroleum Geoscience, 21, 137-149.

Burbank, D. W., Anderson, R. S., 2011. Tectonic geomorphology. Wiley-Blackwell, USA, 274 pp.

Burbank, D., Meigs, A., Brozović, N., 1996a. Interactions of growing folds and coeval depositional systems. Basin Research, 8, 199-223.

Burbank, D.W., Leland, J., Fielding, E., Anderson, R.S., Brozovic, N., Reid, M.R., Duncan, C., 1996b. Bedrock incision, rock uplift and threshold hillslopes in the northwestern Himalayas. Nature, 379, 505-510.

Burke, K., 1996. The African plate. South African Journal of Geology, 99, 341-409.

Busk, H. G., 1929, Earth flexures. Cambridge Univ. Press (reprinted, 1957, by William Trussell) 106 pp.

Carignano, C., Cioccale, M., Rabassa, J., 1999. Landscape antiquity of the Central Eastern Sierras Pampeanas (Argentina): Geomorphological evolution since Gondwanic times. Zietrich fur Geomorphology, Supplement Band 118, 245–268.

Catuneanu, O., Hancox, P.J. and Rubidge, B.S., 1998. Reciprocal flexural behaviour and contrasting stratigraphies: a new basin development model for the Karoo retroarc foreland system, South Africa. Basin Research, 10, 417-439.

Catuneanu, O., Wopfner, H., Eriksson, P. G., Cairncross, B., Rubidge, B. S., Smith, R. M. H., Hancox, P. J., 2005. The Karoo basins of south-central Africa. Journal of African Earth Sciences, 43, 211-253.

Cawood, P.A., Hawkesworth, C.J., Dhuime, B., 2012. Detrital zircon record and tectonic setting. Geology, 40, 875-878.

Chadwick, O.A., Roering, J.J., Heimsath, A.M., Levick, S.R., Asner, G.P., Khomo, L., 2013. Shaping post-orogenic landscapes by climate and chemical weathering. Geology, 41, 1171-1174.

Chappell, J., Zheng, H., Fifield, K., 2006. Yangtse River sediments and erosion rates from source to sink traced with cosmogenic 10 Be: Sediments from major rivers. Palaeogeography, Palaeoclimatology, Palaeoecology, 241, 79-94.

Chen, Y.C., Sung, Q., Cheng, K.Y., 2003. Along-strike variations of morphotectonic features in the Western Foothills of Taiwan: tectonic implications based on stream-gradient and hypsometric analysis. Geomorphology, 56, 109-137.

Chorley, R. J., 1957. Climate and morphometry. Journal of Geology, 65, 628-638.

Clapp, E. M., Bierman, P. R., Schick, A. P., Lekach, J., Enzel, Y., Caffee, M., 2000, Sediment yield exceeds sediment production in arid region drainage basins: Geology, 28, 995-998.

Clapp, E.M., Bierman, P.R., Caffee, M., 2002. Using 10 Be and 26 Al to determine sediment generation rates and identify sediment source areas in an arid region drainage basin. Geomorphology, 45, 89-104.

Clapperton, C.M., 1968. Channels formed by the superimposition of glacial meltwater streams, with special reference to the East Cheviot Hills, North-East England. Geografiska Annaler. Series A. Physical Geography, 1, 207-220.

Clarke, J.I., 1966. Morphometry from Maps. In, Dury, D. H. (ed.) Essays in geomorphology. Heinemann, London, pp. 235 – 274.

Clift, P.D., Blusztajn, J., Nguyen, A.D., 2006. Large-scale drainage capture and surface uplift in eastern Tibet–SW China before 24 Ma inferred from sediments of the Hanoi Basin, Vietnam. Geophysical Research Letters, 33, L19403.

Cockburn, H. A. P., Brown, R. W., Summerfield, M. A., Seidl, M. A., 2000. Quantifying passive margin denudation and landscape development using a combined fission-track thermochronology and cosmogenic isotope analysis approach. Earth and Planetary Science Letters, 179, 429-435.

Cockburn H, Summerfield M. 2004. Geomorphological applications of cosmogenic isotope analysis. Progress in Physical Geography, 28, 1-42

Codilean, A., Bishop, P., Hoey, T.B., 2006. Surface process models and the links between tectonics and topography. Progress in Physical Geography, 30, 307–333.

Codilean, A.T., Bishop, P., Stuart, F.M., Hoey, T.B., Fabel, D., Freeman, S.P., 2008. Single-grain cosmogenic 21Ne concentrations in fluvial sediments reveal spatially variable erosion rates. Geology, 36, 159-162.

Cooke, R.U., 1970. Morphometric analysis of pediments and associated landforms in the western Mohave Desert, California. American Journal of Science, 269, 26-38.

Cooke, R.U., Mason, P., 1973. Desert Knolls pediment and associated landforms in the Mojave Desert, California. Revue de geomorphologie dynamique, 20, 71-8.

Coughlin, T.J., O'Sullivan, P.B., Kohn, B.P. and Holcombe, R.J., 1998. Apatite fission-track thermochronology of the Sierras Pampeanas, central western Argentina: Implications for the mechanism of plateau uplift in the Andes. Geology, 26, 999-1002.

Coulthard TJ. 2001. Landscape evolution models: a software review. Hydrological Processes, 15, 165–173.

Coutand, I., Carrapa, B., Deeken, A., Schmitt, A.K., Sobel, E.R., Strecker, M.R., 2006. Propagation of orographic barriers along an active range front: Insights from sandstone petrography and detrital apatite fission-track thermochronology in the intramontane Angastaco basin, NW Argentina. Basin Research, 18, 1-26.

Covault, J. A., Craddock, W. H., Romans, B. W., Fildani, A., Gosai, M., 2013. Spatial and temporal variations in landscape evolution: Historic and longer-term sediment flux through global catchments. Journal of Geology, 121, 35-56.

Coward, M.P., 1983. Thrust tectonics, thin skinned or thick skinned, and the continuation of thrusts to deep in the crust. Journal of Structural Geology, 5, 113-123.

Cox, K.G., 1989. The role of mantle plumes in the development of continental drainage patterns. Nature, 342, 873-877.

Crickmay CH., 1975. The hypothesis of unequal activity. In Melhorn, W.N., Flemal, R.C. (eds) Theories of Landform Development, State University of New York Press: Binghamton, NY; 103–109.

Crosby, B.T., Whipple, K.X., 2006. Knickpoint initiation and distribution within fluvial networks: 236 waterfalls in the Waipaoa River, North Island, New Zealand. Geomorphology, 82,16-38.

Croissant, T., Braun, J., 2014. Constraining the stream power law: a novel approach combining a landscape evolution model and an inversion method. Earth Surface Dynamics, 2, 155.

CSIR., 2007. State of Rivers Report. Rivers of the Gouritz Water Management area 2007. Available - http://www.csir.co.za/rhp/state_of_rivers/WCape/gouritz07.pdf

Cuartero, A., Felicísimo, A.M., Ariza, F.J., 2004. Accuracy of DEM generation from TERRA-ASTER stereo data. International Archives of Photogrammetry and Remote Sensing, 35, 559-563.

Dalton, T.J.S., Paton, D.A., Needham, T., Hodgson, N., 2015. Temporal and spatial evolution of deepwater fold thrust belts: Implications for quantifying strain imbalance. Interpretation, 3, pp.SAA59-SAA70.

Dardis, G.F., Beckedahl, H.R., 1991. The role of rock properties in the development of bedrock-incised rills and gullies: examples from southern Africa. Geojournal, 23, 35-40.

Darvill, C.M., 2013. Cosmogenic nuclide analysis. Geomorphological Techniques, Chapter 4, Section 2.10. British Society of Geomorphology.

Damm, B., Hagedorn, J., 2010. Holocene floodplain formation in the southern Cape region, South Africa. Geomorphology, 122, 13-222.

Da Silva, L.C., Gresse, P.G., Scheepers, R., McNaughton, N.J., Hartmann, L.A., Fletcher, I., 2000. Ub- Pb SHRIMP and Sm- Nd age constraints on the timing and sources of the Pan-African Cape Granite Suite, South Africa. Journal of African Earth Sciences, 30, 795-815.

Dauteuil, O., Bessin, P., Guillocheau, F., 2015. Topographic growth around the Orange River valley, southern Africa: A Cenozoic record of crustal deformation and climatic change. Geomorphology, 233, 5-19.

Davis, J., 2010. Hypsometric Tools. Available – http://arcscripts.esri.com/details.asp?dbid=16830

Davis, W. M., 1889. The rivers and valleys of Pennsylvania. National Geographical Magazine, 1, 183-253.

Davis, W.M., 1899. The geographical cycle. Geography Journal, 14, 481–504.

Davis, W.M., 1906. Observations in South Africa. Geological Society of America Bulletin, 17, 377-450.

Davis, W.M., 1930. Rock floors in arid and humid climates. Journal of Geology, 38, 136–158.

Dean, W. R. J., Hoffinan, M. T., Meadows, M. E., Milton, S. J., 1995. Desertification in the semi-arid Karoo, South Africa: review and reassessment. Journal of Arid Environments, 30, 247-264.

Decker, J.E., Niedermann, S., de Wit, M.J., 2011. Soil erosion rates in South Africa compared with cosmogenic 3He-based rates of soil production. South African Journal of Geology, 114, 475-488.

Decker, J. E., Niedermann, S., de Wit, M. J., 2013. Climatically influenced denudation rates of the southern African plateau: Clues to solving a geomorphic paradox. Geomorphology, 190, 48-60.

Delunel, R., Beek, P.A., Bourlès, D.L., Carcaillet, J., Schlunegger, F., 2014. Transient sediment supply in a high-altitude Alpine environment evidenced through a 10Be budget of the Etages catchment (French Western Alps). Earth Surface Processes and Landforms, 39, 890-899.

Demoulin, A., Zárate, M., Rabassa J., 2005. Long-term landscape development: a perspective from the southern Buenos Aires ranges of east central Argentina. Journal of South American Earth Sciences. 19, 193–204.

Densmore, A.L., Ellis, M.A., Anderson, R.S., 1998. Landsliding and the evolution of normal-fault-bounded mountains. Journal of Geophysical Research, 103, 15203-15219.

Derrieux, F., Siame, L.L., Bourlès, D.L., Chen, R.F., Braucher, R., Léanni, L., Lee, J.C., Chu, H.T., Byrne, T.B., 2014. How fast is the denudation of the Taiwan mountain belt? Perspectives from in situ cosmogenic 10 Be. Journal of Asian Earth Sciences, 88, 230-245.

Desilets, D., Zreda, M., Prabu, T., 2006. Extended scaling factors for in situ cosmogenic nuclides: New measurements at low latitude. Earth and Planetary Science Letters, 246, 265- 276.

De Smith, M.J., Goodchild, M.F., Longley, P., 2007. Geospatial analysis: a comprehensive guide to principles, techniques and software tools. Troubador Publishing Ltd, pp 389.

de Wit, M., 1999. Post-Gondwana drainage and the development of diamond placers in western South Africa. Economic Geology, 94, 721-740.

de Wit, M., 2007. The Kalahari Epeirogeny and climate change: differentiating cause and effect from core to space. South African Journal of Geology, 110, 367-392.

de Wit, M., Marshall, T., Partridge, T., 2000. Fluvial deposits and drainage evolution. In, Patridge, T., Maud, R., (Eds.) The Cenozoic of Southern Africa, Oxford monographs on geology and geophysics no. 40: NY

DeVecchio, D. E., Heermance, R. V., Fuchs, M., Owen, L. A., 2012. Climate-controlled landscape evolution in the Western Transverse Ranges, California: Insights from Quaternary geochronology of the Saugus Formation and strath terrace flights. Lithosphere, 4, 110-130.

De Villiers, J., Jansen, H., Mulder, M.P., 1964. Die geologie van die gebied tussen Worcester en Hermanus. Explanation Sheets 3319C (Worcester), 3419A (Caledon), part of 3318D (Stellenbosch) and 3418B (Somerset West), Geology Survey of South Africa, 69.

DiBiase, R.A., Whipple, K.X., Heimsath, A.M., Ouimet, W.B., 2010. Landscape form and millennial erosion rates in the San Gabriel Mountains, CA. Earth and Planetary Science Letters, 289, 134-144.

Dingle, R.V., 1973. Mesozoic paleogeography of the Southern Cape, South Africa. Palaeogeography, palaeooclimatology, palaeoecology, 13, 203-213.

Dingle, R. V., Hendry, Q. B., 1984. Late Mesozoic and Tertiary sediment supply to the eastern Cape Basin (SE Atlantic) and palaeo-drainage systems in southwestern Africa. Marine Geology, 56, 13-26.

Dingle, R. V., Scrutton, R. A., 1974. Continental breakup and the development of post-Paleozoic sedimentary basins around southern Africa. Geological Society of America Bulletin, 85, 1467-1474.

Dingle, R. V., Siesser, W. G., Newton, A. R., 1983. Mesozoic and Tertiary geology of southern Africa. Rotterdam: Balkema. 375 pp.

Dirks, P.H., Kibii, J.M., Kuhn, B.F., Steininger, C., Churchill, S.E., Kramers, J.D., Pickering, R., Farber, D.L., Mériaux, A.S., Herries, A.I., King, G.C., 2010. Geological setting and age of Australopithecus sediba from southern Africa. Science, 328, pp. 205-208.

Divins, D.L., 2003. Total Sediment Thickness of the World's Oceans & Marginal Seas, NOAA National Geophysical Data Center, Boulder, CO.

Dixey, F., 1944. African landscape. Geographical Review, 34, 457-465.

Dohrenwend, J.C., Parsons, A.J., 2009. Pediments in arid environments. In, Parsons, A.J., Abrahams, A.D., (eds.) Geomorphology of desert environments. Springer Netherlands. pp. 377-411.

Douglass, J., Meek, N., Dorn, R.I., Schmeeckle, M.W., 2009. A criteria-based methodology for determining the mechanism of transverse drainage development, with application to the southwestern United States. Geological Society of America Bulletin, 121, 586-598.

Doucouré, C.M., de Wit, M.J., 2003. Old inherited origin for the present near bimodal topography of Africa. Journal of African Earth Sciences, 36, 371–388.

Dunai, T., 2001. Influence of secular variation of the geomagnetic field on production rates of in situ produced cosmogenic nuclides. Earth and Planetary Science Letters, 193, 197-212

Dunai, T., 2010. Cosmogenic Nuclides: Principles, concepts and applications in the earth surface sciences. Cambridge University Press, Cambridge.

Dunai, T., López, G.A.G., Juez-Larré, J., 2005. Oligocene–Miocene age of aridity in the Atacama Desert revealed by exposure dating of erosion-sensitive landforms. Geology, 33, 321-324.

Duncan, R. A., Hooper, P. R., Rehacek, J., Marsh, J. S., Duncan, A. R., 1997. The timing and duration of the Karoo igneous event, southern Gondwana. Journal of Geophysical Research: Solid Earth, 102, 18127-18138.

Du Toit, A.L., 1933. Crustal movements as a factor in the geographical evolution of South Africa. South African Geographraphical Journal, 16, 1–33.

Du Toit, A., 1937. Our Wandering Continents. Oliver and Boyd, U.K, 366 pp.

Du Toit, A., 1954. The Geology of South Africa, 3rd edn. Oliver and Boyd, U.K. 539 pp.

Dury, G.H., 1958. Tests of a general theory of misfit streams. Transactions and Papers Institute of British Geographers, 25, 105-118.

Dury, G. H., 1960. Misfit streams: problems in interpretation, discharge, and distribution. Geographical Review, 50, 219-242.

Du Preez, J. W., 1944. Lithology, structure and mode of deposition of the Cretaceous deposits in the Oudtshoorn area. Annale van die Uniwersiteit van Stellenbosch, 22, 209-237.

Duxbury, J., 2009, Erosion rates in and around Shenandoah National Park, VA, determined using analysis of cosmogenic 10Be. PhD thesis, University of Vermont, 134 pp.

Duvall, A., Kirby, E., Burbank, D., 2004. Tectonic and lithologic controls on bedrock channel profiles and processes in coastal California. Journal of Geophysical Research: Earth Surface, 109, 1-18.

Ebinger, C.J., Sleep, N.H., 1998. Cenozoic magmatism throughout east Africa resulting from impact of a single plume. Nature, 395, 788-791.

Ehlers, T.A., Farley, K.A., 2003. Apatite (U–Th)/He thermochronometry: methods and applications to problems in tectonic and surface processes. Earth and Planetary Science Letters, 206, 1–14.

Einsele, G., Ratschbacher, L., Wetzel, A., 1996. The Himalaya-Bengal Fan denudation-accumulation system during the past 20ma. Journal of Geology, 104, 163-184.

England, P., Molnar, P., 1990. Surface uplift, uplift of rocks, and exhumation of rocks. Geology, 18, 1173-1177.

Erlanger, E.D., Granger, D.E., Gibbon, R.J., 2012. Rock uplift rates in South Africa from isochron burial dating of fluvial and marine terraces. Geology, 40, 1019-1022.

Fairbridge, R.W., 1968. The encyclopedia of geomorphology. Reinhold Book Corporation, New York, 1295 pp.

Farrimond, P., Green, A., Williams, L.S., 2015. Petroleum geochemistry of the Sea Lion Field, North Falkland Basin. Petroleum Geoscience, 21, 125-135.

Ferrier, K.L., Kirchner, J.W. and Finkel, R.C., 2005. Erosion rates over millennial and decadal timescales at Caspar Creek and Redwood Creek, northern California Coast Ranges. Earth Surface Processes and Landforms, 30, 1025-1038.

Finnegan, N.J., Roe, G., Montgomery, D.R., Hallet, B., 2005. Controls on the

channel width of rivers: Implications for modeling fluvial incision of bedrock. Geology, 33, 229-232.

Fish, P., 2005. East Falkland basins reveal important exploration potential, Oil and Gas Journal, 103, 34-40.

Fitzgerald, P.G., Stump, E., 1997. Cretaceous and Cenozoic episodic denudation of the Transantarctic Mountains, Antarctica: new constraints from apatite fission track thermochronology in the Scott Glacier region. Journal of Geophysical Research: Solid Earth, 102, 7747-7765.

Fleming, A., Summerfield, M. A., Stone, J. O., Fifield, L. K., Cresswell, R. G., 1999. Denudation rates for the southern Drakensberg escarpment, SE Africa, derived from in-situ-produced cosmogenic ^{36}Cl: initial results. Journal of the Geological Society, 156, 209-212.

Flowers, R.M., Schoene, B., 2010. (U-Th)/He thermochronometry constraints on unroofing of the eastern Kaapvaal craton and significance for uplift of the southern African Plateau. Geology, 38, 827-830.

Flint, S. S., Hodgson, D. M., Sprague, A. R., Brunt, R. L., Van der Merwe, W. C., Figueiredo, J., Prélat., A, Box, D., Di Celma., C., Kavanagh, J. P., 2011. Depositional architecture and sequence stratigraphy of the Karoo basin floor to shelf edge succession, Laingsburg depocentre, South Africa. Marine Petroleum Geology, 28, 658-674.

Fouché, J., Bate, K. J., Van der Merwe, R., 1992. Plate tectonic setting of the Mesozoic Basins, southern offshore, South Africa: A review. Inversion tectonics of the Cape Fold Belt, Karoo and cretaceous basins of Southern Africa, pp. 27-32.

Friend, P. F., Jones, N. E., Vincent, S. J., 2009. Drainage evolution in active mountain belts: extrapolation backwards from present-day Himalayan river patterns. In: Smith, N.D., Rogers, J. (Eds). Fluvial Sedimentology VI, Blackwell Publishing Ltd., Oxford, UK, pp. 305-313.

Frimmel, H. E., Fölling, P. G., Diamond, R., 2001. Metamorphism of the Permo-Triassic Cape Fold Belt and its basement, South Africa. Mineralogy and Petrology, 73, 325-346.

Fordham, A.M., North, C.P., Hartley, A.J., Archer, S.G., Warwick, G.L., 2010. Dominance of lateral over axial sedimentary fill in dryland rift basins. Petroleum Geoscience, 16, 299-304.

Frostick, L.E., Reid, I., 1987. Tectonic control of desert sediments in rift basins

ancient and modern. Geological Society, London, Special Publications, 35, 53-68.

Gallagher, K., Brown, R., Johnson, C., 1998. Fission track analysis and its applications to geological problems. Annual Review of Earth and Planetary Science, 26, 519-572.

Gallagher, K., Brown, R., 1999. Denudation and uplift at passive margins: the record on the Atlantic Margin of southern Africa. Philosophical Transactions of the Royal Society of London A: Mathematical, Physical and Engineering Sciences, 357, 835-859.

Galloway, W.E., Ganey-Curry, P.E., Li, X., Buffler, R.T., 2000. Cenozoic depositional history of the Gulf of Mexico Basin. AAPG Bulletin, 84, 1743-1774.

Gasse, F., Chalié, F., Vincens, A., Williams, M.A., Williamson, D., 2008. Climatic patterns in equatorial and southern Africa from 30,000 to 10,000 years ago reconstructed from terrestrial and near-shore proxy data. Quaternary Science Reviews, 27, 2316-2340.

Gawthorpe, R.L., Leeder, M.R., 2000. Tectono-sedimentary evolution of active extensional basins. Basin Research, 12, 195-218.

George, A.D., Marshallsea, S.J., Wyrwoll, K.H., Jie, C., Yanchou, L., 2001. Miocene cooling in the northern Qilian Shan, northeastern margin of the Tibetan Plateau, revealed by apatite fission-track and vitrinite-reflectance analysis. Geology, 29, 939-942.

Ghosh, P., Sinha, S. and Misra, A., 2015. Morphometric properties of the trans-Himalayan river catchments: Clues towards a relative chronology of orogen-wide drainage integration. Geomorphology, 233, 127-141.

Gilbert, G.K. 1877. Report on the geology of the Henry Mountains.US Geographical and Geological Survey of the Rocky Mountain Region. Washington, DC: U.S. Department of the Interior.

Gilchrist, A.R., Summerfield, M.A., 1990. Differential denudation and flexural isostacy in formation of rift-margin upwarps. Nature, 346, 739-742.

Gilchrist, A.R. and Summerfield, M.A., 1991. Denudation, isostasy and landscape evolution. Earth Surface Processes and Landforms, 16, 555-562.

Gilchrist, A. R., Kooi, H., Beaumont, C., 1994. Post-Gondwana geomorphic evolution of southwestern Africa: Implications for the controls on landscape development from observations and numerical experiments. Journal of Geophysical Research: Solid Earth, 99, 12211-12228.

Gleadow, A.J.W., Brown, R.W., 2000. Fission-track thermochronology and the long-

term denudational response to tectonics. In, Summerfield, M.A., (ed.). Geomorphology and Global Tectonics, Wiley: Chichester; 57–75.

Gleadow, A.J.W., Duddy, I.R., Lovering, J.F., 1983. Fission track analysis: A new tool for the evaluation of thermal histories and hydrocarbon potential. Australian Petroleum Exploration Association Journal, 23, 93-102.

Gleadow, A.J.W., Duddy, I.R., Green, P.F., Lovering, J.F., 1986. Confined fission track lengths in apatite: a diagnostic tool for thermal history analysis. Contributions to Mineralogy and Petrology, 94, 405-415.

Goldhammer, R.K., Wickens, H., Bouma, A.H., Wach, G.D., 2000. Sequence stratigraphic architecture of the late Permian Tanqua submarine fan complex, Karoo basin, South Africa. Special publication -SEPM, 68, 165-172.

Goodbred, S.L., 2003. Response of the Ganges dispersal system to climate change: a source-to- sink view since the last interstade. Sedimentary Geology, 162, 83-104.

Goodbred, S.L., Kuehl, S.A., 1999. Holocene and modern sediment budgets for the Ganges-Brahmaputra river system: evidence for highstand dispersal to flood-plain, shelf, and deep- sea depocenters. Geology, 27, 559-562.

Gorelov, S.K., Drenev, N.V., Meschcheryakov, Y.A., Tikanov, N.A., Fridland, V.M., 1970. Planation surfaces of the USSR. Geomorphology, 1, 18–29.

Gosse, J. C., Phillips, F. M., 2001. Terrestrial in situ cosmogenic nuclides: theory and application. Quaternary Science Reviews, 20, 1475-1560.

Goudie, A. S., 2005. The drainage of Africa since the Cretaceous. Geomorphology, 67, 437-456.

Goudie, A.S., 2006. The Schmidt Hammer in geomorphological research. Progress in Physical Geography, 30, 703-718.

Goudie, A., Viles, H., Allison, R., Day, M., Livingstone, I., Bull, P., 1990. The geomorphology of the Napier Range, Western Australia. Transactions of the Institute of British Geographers, 15, 308-322.

Granger, D.E., Kirchner, J.W., Finkel, R.C., 1997. Quaternary downcutting rate of the New River, Virginia, measured from differential decay of cosmogenic 26Al and 10Be in cave-deposited alluvium. Geology, 25, 107-110.

Granger, D.E., Lifton, N., Willenbring, J., 2013. A cosmic trip: 25 years of cosmogenic nuclides in geology. Geological Society of America Bulletin, 125, 1379-1402.

Granjeon, D., Joseph, P., 1999. Concepts and applications of a 3-D multiple

lithology, diffusive model in stratigraphic modeling. In: Harbaugh, J. W., Watney, W. L. et al. (eds) Numerical Experiments in Stratigraphy: Recent Advances in Stratigraphic and Computer Simulations. Society for Sedimentary Geology, Special Publications, 62, 197–210.

Green, P.F., Duddy, I.R., Japsen, P., Bonow, J.M., Malan, J.A., 2016. Post-breakup burial and exhumation of the southern margin of Africa. Basin Research, doi: 10.1111/bre.12167.

Griffin, D.L., 2006. The late Neogene Sahabi rivers of the Sahara and their climatic and environmental implications for the Chad Basin. Journal of the Geological Society, 163, 905-921.

Griffiths, A., 2015. The reservoir characterization of the Sea Lion Field. Petroleum Geoscience, 21, 199-209.

Grimaud, J.L., Chardon, D., Beauvais, A., 2014. Very long-term incision dynamics of big rivers. Earth and Planetary Science Letters, 405, 74-84.

Grimmer, J.C., Jonckheere, R., Enkelmann, E., Ratschbacher, L., Hacker, B.R., Blythe, A.E., Wagner, G.A., Wu, Q., Liu, S., Dong, S., 2002. Cretaceous−Cenozoic history of the southern Tan-Lu fault zone: apatite fission-track and structural constraints from the Dabie Shan (eastern China). Tectonophysics, 359, 225-253.

Grosjean, A. S., Pittet, B., Gardien, V., Leloup, P. H., Mahéo, G., Barraza Garcia, J. 2015. Tectonic heritage in drainage pattern and dynamics: the case of the French South Alpine Foreland Basin (ca. 45–20 Ma). Basin Research, doi: 10.1111/bre.12134.

Gulliford, A.R., Flint, S.S., Hodgson, D.M., 2014. Testing applicability of models of distributive fluvial systems or trunk rivers in ephemeral systems: Reconstructing 3-D fluvial architecture in the Beaufort Group, South Africa. Journal of Sedimentary Research, 84, 1147-1169.

Gunnell, Y., Braucher, R., Bourles, D., André, G., 2007. Quantitative and qualitative insights into bedrock landform erosion on the South Indian craton using cosmogenic nuclides and apatite fission tracks. Geological Society of America Bulletin, 119, 576-585.

Gupta, S., 1997. Himalayan drainage patterns and the origin of fluvial megafans in the Ganges foreland basin. Geology, 25, 11-14.

Gupta, A.K., Sharma, J.R., Sreenivasan, G., Srivastava, K.S., 2004. New findings on the course of River Sarasvati. Journal of the Indian Society of Remote Sensing, 32, 1-24.

Gurnis, M., Mitrovica, J.X., Ritsema, J., van Heijst, H.J., 2000. Constraining mantle

density structure using geological evidence of surface uplift rates: The case of the African superplume. Geochemistry, Geophysics, Geosystems, 1, 1999GC000035.

Hack, J. T., 1960. Interpretation of erosional topography in humid temperate regions. American Journal of Science, 258-A, 80-97.

Hack, J. T., 1973. Stream-profile analysis and stream-gradient index. Journal of Research of the US Geological Survey, 1, 421-429.

Hagedorn, J., 1988, Silcretes in the Western Little Karoo and their relation to geomorphology and palaeoecology: Palaeoecology of Africa, 19, 371–375.

Hahn, D.G., Manabe, S., 1976. Role of Mountains in South Asian Monsoon Circulation-Reply. Journal of the Atmospheric Sciences, 33, 2258-2262.

Hall, M., 1976. Dendrochronology, rainfall and human adaptation in the Later Iron Age of Natal and Zululand. Southern African Humanities, 22, 693-703.

Halle, T.G., 1912. On the geological structure and history of the Falkland Islands. Bulletin of the Geological Institute of Upsala, 11, 115-229.

Hancock, G.S., Anderson, R.S., Whipple, K.X., 1998. Beyond power: Bedrock river incision process and form. In, Tinkler, K.J., Wohl, E (eds.) Rivers over rock: Fluvial processes in bedrock channels, 107, American Geophysical Union, pp.35-60.

Hancock, G., Willgoose, G., 2001. Use of a landscape simulator in the validation of the SIBERIA Catchment Evolution Model: Declining equilibrium landforms. Water Resources Research, 37, 1981-1992.

Hansma, J., Tohver, E., Schrank, C., Jourdan, F., Adams, D., 2015. The timing of the Cape Orogeny: New 40 Ar/39 Ar age constraints on deformation and cooling of the Cape Fold Belt, South Africa. Gondwana Research, 32, 122-137.

Hanson, E.K., Moore, J.M., Bordy, E.M., Marsh, J.S., Howarth, G., Robey, J.V.A., 2009. Cretaceous erosion in central South Africa: Evidence from upper-crustal xenoliths in kimberlite diatremes. South African Journal of Geology, 112, 125-140.

Harvey, A.M., Wells, S.G., 1987. Response of Quaternary fluvial systems to differential epeirogenic uplift: Aguas and Feos river systems, southeast Spain. Geology, 15, 689-693.

Hasbargen, L. E., Paola, C. 2000. Landscape instability in an experimental drainage basin. Geology, 28, 1067-1070.

Hattingh, J., 2008. Fluvial Systems and Landscape Evolution. In: Lewis, C. (Ed.). Geomorphology of the Eastern Cape, South Africa, NISC, pp. 21-42.

Haworth, R. J., Ollier, C. D., 1992. Continental rifting and drainage reversal: the Clarence River of eastern Australia. Earth Surface Processes and Landforms, 17, 387-397.

Hawthorne, J.B., 1975. Model of a kimberlite pipe. Physics and Chemistry of the Earth, 9, pp.1-15.

Hayakawa, Y., Matsukura, Y., 2003. Recession rates of waterfalls in Boso Peninsula, Japan, and a predictive equation. Earth Surface Processes and Landforms, 28, 675-684.

Heimsath, A., Chappel, J., Finkel, R. C., Fifield, K., Alimanovic, A., 2006, Escarpment Erosion and Landscape Evolution in Southeastern Australia: Special Papers-Geological Society of America, 398, 173.

Heimsath, A. M., Fink, D., Hancock, G. R., 2009, The 'humped' soil production function: eroding Arnhem Land, Australia: Earth Surface Processes and Landforms, 34, 1674-1684.

Hein, A., Hulton, N., Dunai, T., Schnabel, C., Kaplan, M., Naylor, M., Xu, S., 2009. Middle Pleistocene glaciation in Patagonia dated by cosmogenic-nuclide measurements on outwash gravels. Earth and Planetary Science Letters, 286, 184-197.

Helgren, D.M., Butzer, K.W., 1977. Paleosols of the southern Cape Coast, South Africa: implications for laterite definition, genesis, and age. Geographical review, 430-445.

Hewawasam, T., von Blackenburg, F., Schaller, M., Kubik, P., 2003, Increase of human over natural erosion rates in tropical highlands constrained by cosmogenic nuclides, Geology, 31, 7, 597-600.

Hills, E.S., 1963. Elements of Structural Geology. Methuen, London, 483 pp.

Hill, R.S., 1972. The geology of the northern Algoa basin, Port Elizabeth. MSc thesis (unpublished). University of Stellenbosch.

Hirano, A., Welch, R., Lang, H., 2003. Mapping from ASTER stereo image data: DEM validation and accuracy assessment. ISPRS Journal of Photogrammetry and Remote Sensing, 57, 356-370.

Hirsch, K.K., Scheck-Wenderoth, M., van Wees, J.D., Kuhlmann, G., Paton, D.A., 2010. Tectonic subsidence history and thermal evolution of the Orange Basin. Marine and Petroleum Geology, 27, 565-584.

Hlaing, K.T., Haruyama, S., Aye, M.M., 2008. Using GIS-based distributed soil loss modeling and morphometric analysis to prioritize watershed for soil conservation in Bago river basin of Lower Myanmar. Frontiers of Earth Science in China, 2, 465-478.

Hodgson, D.M., Flint, S.S., Hodgetts, D., Drinkwater, N.J., Johannessen, E.P., Luthi, S.M., 2006. Stratigraphic evolution of fine-grained submarine fan systems, Tanqua depocenter, Karoo Basin, South Africa. Journal of Sedimentary Research, 76, 20-40.

Hodge, R.A., Hoey, T.B., Sklar, L.S., 2011. Bed load transport in bedrock rivers: The role of sediment cover in grain entrainment, translation, and deposition. Journal of Geophysical Research: Earth Surface, 116(F4).

Hofstra, M., Hodgson, D.M., Peakall, J., Flint, S.S., 2015. Giant scour-fills in ancient channel-lobe transition zones: Formative processes and depositional architecture. Sedimentary Geology, 329, 98-114.

Holmgren, K., Karlén, W., Lauritzen, S.E., Lee-Thorp, J.A., Partridge, T.C., Piketh, S., Repinski, P., Stevenson, C., Svanered, O., Tyson, P.D., 1999. A 3000-year high-resolution stalagmitebased record of palaeoclimate for northeastern South Africa. The Holocene, 9, 295-309.

Horton, R. E., 1932. Drainage-basin characteristics. Transactions American Geophysical Union, 13, 350-361.

Horton, R. E., 1945. Erosional development of streams and their drainage basins; hydrophysical approach to quantitative morphology. Geological Society of American Bulletin, 56, 275-370.

House M, Wernicke BP, Farley KA. 1998. Dating topography of the Sierra Nevada, California, using apatite (U–Th)/He ages. Nature, 396, 66–69.

Hovius, N., 1996. Regular spacing of drainage outlets from linear mountain belts. Basin Research, 8, 29-44.

Howard, A.D. 1942. Pediment passes and the pediment problem. Journal of Geomorphology 5, 3–32, 95–136.

Howard, A. D., 1967. Drainage analysis in geologic interpretation: a summation. AAPG Bulletin, 51, 2246-2259.

Howard, A. D. 1994. A detachment-limited model of drainage basin evolution, Water Resources Research, 30, 2261–2285.

Howard, A. D., G. Kerby. 1983. Channel changes in badlands, Geology Society of American Bullentin, 94, 739–752.

Humphrey, N.F., Konrad, S.K., 2000. River incision or diversion in response to bedrock uplift. Geology, 28, 43-46.

Hurtrez, J. E., Sol, C., Lucazeau, F., 1999. Effect of drainage area on hypsometry from an analysis of small-scale drainage basins in the Siwalik Hills (Central Nepal). Earth Surface Processes and Landforms, 24, 799-808.

Hutton J.,1795. *The Theory of the Earth*. Creech, Edinburgh, 2 volumes.

Insel, N., Ehlers, T.A., Schaller, M., Barnes, J.B., Tawackoli, S., Poulsen, C.J., 2010. Spatial and temporal variability in denudation across the Bolivian Andes from multiple geochronometers. Geomorphology, 122, 65-77

Ivy-Ochs, S., Kober, F., 2008. Surface exposure dating with cosmogenic nuclides. Eiszeitalter und Gegenwart - Quaternary Science Journal, 57: 179-209.

Jackson, J., Ritz, J.F., Siame, L., Raisbeck, G., Yiou, F., Norris, R., Youngson, J., Bennett, E., 2002. Fault growth and landscape development rates in Otago, New Zealand, using in situ cosmogenic 10 Be.Earth and Planetary Science Letters, 195, 185-193.

Jacobsen, K., Lohmann, P., 2003. Segmented filtering of laser scanner DSMs. International Archives of Photogrammetry and Remote Sensing, 34(3/W13).

Jansen J.D., 2006. Flood magnitude-frequency and lithologic controls on bedrock river incision in post-orogenic terrain. Geomorphology, 82, 39–57.ott

Jansen, J. D., Codilean, A. T., Bishop, P., Hoey, T. B., 2010. Scale dependence of lithological control on topography: Bedrock channel geometry and catchment morphometry in western Scotland. Journal of Geology, 118, 223-246.

Jerolmack, D. J., Paola, C., 2010. Shredding of environmental signals by sediment transport. Geophysical Research Letters, 37, 1-5.

Johnson, M.R., 1991, Sandstone petrography, provenance and plate tectonic setting in Gondwana context of the southeastern Cape–Karoo Basin: South African Journal of Geology, 94, 137–154.

Johnson, S.D., Flint, S., Hinds, D., De Ville Wickens, H., 2001. Anatomy, geometry and sequence stratigraphy of basin floor to slope turbidite systems, Tanqua Karoo, South Africa. Sedimentology, 48, 987-1023.

Johnson, M.R. van Vuuren, C.J., Hegenberger, W.F., Rey, R., Shoko. U, 1996. Stratigraphy of the Karoo Supergroup in South Africa: an overview. Journal of African Earth Sciences, 23, 3-15.

Johnson, M.R., van Vuuren, C.J., Visser, J.N.J., Cole, D.I., Wickens, H.de V., Christie, A.D.M., Roberts, D.L., Brandl, G., 2006. Sedimentary rocks of the Karoo Supergroup. In: Johnson, M.R., Anhaeusser, C.R., Thomas, R.J. (Eds.), The Geology of South Africa, Geological Society of South Africa and Council for Geoscience, pp. 461–499.

Jourdan, F., Féraud, G., Bertrand, H., Kampunzu, A.B., Tshoso, G., Watkeys, M.K., Le Gall, B., 2005. Karoo large igneous province: Brevity, origin, and relation to mass extinction questioned by new 40Ar/39Ar age data. Geology, 33, 745-748.

Kale, V, Ely, L, Enzel, Y., Baker, V., 1994 Geomorphic and hydraulic aspects of monsoon floods on the Narmada and Tapi Rivers central India. Geomorphology, 10, 157-168.

Kamp, U., Owen, L.A., 2012. Polygenetic landscapes. In Owen, L.A., (ed.) Treatise of Geomorphology: Amsterdam, Netherlands, Elsevier.

Kaplan, M., Ackert, R., Singer, B., Douglass, D., Kurz, M., 2004. Cosmogenic nuclide chronology of millennial-scale glacial advances during O-isotope stage 2 in Patagonia. Geological Society of America Bulletin, 116, 308-321

Keller, E.A., Pinter, N., 2002. Active tectonics: Earthquakes, Uplift and Landscape-Second Edition. Prentice Hall, New Jersey, 362 pp.

Kesel, R.H., 1977. Some aspects of the geomorphology of inselbergs in central Arizona, USA. Zeitschrift fur Geomorphologie 21, 119–46.

Kim, W., Connell, S.D., Steel, E., Smith, G.A. and Paola, C., 2011. Mass-balance control on the interaction of axial and transverse channel systems. Geology, 39, 611-614.

King, L.C., 1942. South African scenery. A textbook of geomorphology. South African scenery. A textbook of geomorphology. 308 pp.

King, L. C., 1944. Geomorphology of the Natal Drakensberg. Transactions of the Geological Society of Southern Africa, 47, 255-282.

King, L.C., 1948. On the ages of African land-surfaces. Quarterly Journal of the Geological Society, 104, 439-459.

King, L., 1949. The pediment landform: some current problems. Geological Magazine, 86, 245-250.

King, L.C., 1951. South African Scenery. 2nd edn. Oliver and Boyd, U.K, pp. 379.

King, L. C., 1953. Canons of landscape evolution. Geol. Soc. Am. Bull. 64, 721-752.

King, L.C., 1955. Pediplanation and isostasy: an example from South Africa. Quarterly Journal of the Geological Society, 111, 353-359.

King, L.C., 1956a. A geomorphological comparison between Brazil and South Africa. Quarterly Journal of the Geological Society, 112, 445–474.

King, L.C., 1956b. A geomorfologia do Brasil oriental. Revista Brasileira de Geografia, 18,186–263.

King, L.C., 1963. South African Scenery. Oliver and Boyd, London, United Kingdom, 308 pp.

King, L.C., 1966. The origin of bornhardts: Zeitschrift fur Geomorphologie, 10, 97–98.

King, L.C., 1967. South African Scenery. Oliver and Boyd, Edinburgh, 3rd ed.

King, L.C., 1972. The Natal monocline: explaining the origin and scenery of Natal,

South Africa. Geology Department, University of Natal, South Africa, 113 pp.

King, R.C., Hodgson, D.M., Flint, S.S., Potts, G.J., Van Lente, B., 2009. Development of subaqueous belts as a control on the timing and distribution of deepwater sedimentation: an example from the southwest Karoo Basin, South Africa. In: Kneller, B.C., Martinsen, O.J., McCaffrey, W.D. (Eds.), 2009. External Controls on Deep-Water Depositional Systems: SEPM, Special Publication, 92, pp. 261-278.

Kirby, E., Whipple, K., 2001. Quantifying differential rock-uplift rates via stream profile analysis. Geology, 29, 415-418.

Knighton, D., 1998. Fluvial forms and processes: a new perspective. Routledge, 400 pp.

Kong, P., Na, C., Brown, R., Fabel, D., Freeman, S., Xiao, W., Wang, Y., 2011. Cosmogenic 10 Be and 26 Al dating of paleolake shorelines in Tibet. Journal of Asian Earth Sciences, 41, 263-273.

Kooi, H., Beaumont C., 1996. Large-scale geomorphology: classical concepts reconciled and integrated with contemporary ideas via a surface process model. Journal of Geophysical Research, 101, 3361–3386.

Kounov, A., Niedermann, S., De Wit, M. J., Viola, G., Andreoli, M., Erzinger, J., 2007. Present denudation rates at selected sections of the South African escarpment and the elevated continental interior based on cosmogenic ^{3}He and ^{21}Ne. South Africa Journal of Geology, 110, 235-248.

Kounov, A., Niedermann, S., de Wit, M.J., Viola, G., Andreoli, M., Erzinger, J., 2007. Present denudation rates at selected sections of the South African escarpment and the elevated continental interior based on cosmogenic 3He and 21Ne. South African Journal of Geology, 110, 235-248.

Kounov, A., Viola, G., De Wit, M., Andreoli, M. A. G., 2009. Denudation along the Atlantic passive margin: new insights from apatite fission-track analysis on the western coast of South Africa. In: Lisker, F., Ventura, B., Glasmacher, U.A., (eds.),Thermochronological Methods: From Palaeotemperature Constraints to Landscape Evolution Models, Geological Society of London, Special Publication, 324, 287-306.

Kounov, A., Niedermann, S., de Wit, M. J., Codilean, A. T., Viola, G., Andreoli, M., Christl, M., 2015. Cosmogenic ^{21}Ne and ^{10}Be reveal a more than 2 Ma Alluvial Fan Flanking the Cape Mountains, South Africa. South African Journal of Geology 118, 129-144.

Kubik, P.W., Christl, M., 2010. 10 Be and 26 Al measurements at the Zurich 6MV

Tandem AMS facility. Nuclear Instruments and Methods in Physics Research Section B: Beam Interactions with Materials and Atoms, 268, 880-883.

Lawson, A.C. 1915. The epigene profiles of the desert. University of California Department of Geology Bulletin, 9, 23–48.

Leeder, M.R., Gawthorpe, R.L., 1987. Sedimentary models for extensional tilt-block/half-graben basins. Geological Society, London, Special Publications, 28, 139-152.

Leland, J., Reid, M.R., Burbank, D.W., Finkel, R. and Caffee, M., 1998. Incision and differential bedrock uplift along the Indus River near Nanga Parbat, Pakistan Himalaya, from 10 Be and 26 Al exposure age dating of bedrock straths. Earth and Planetary Science Letters, 154, 93-107.

Lenz, C.J., 1957. The river evolution and the remnants of the Tertiary surfaces in the western Little Karoo. In Annals of the University of Stellenbosch: Series A, 33, 193-234.

Leoni, G., Barchiesi, F., Catallo, F., Dramis, F., Fubelli, G., Lucifora, S., Mattei, M., Pezzo, G., Puglisi, C., 2009. GIS methodology to assess landslide susceptibility: application to a river catchment of Central Italy. Journal of maps, 5, 87-93.

Liang, Y.H., Chung, S.L., Liu, D., Xu, Y., Wu, F.Y., Yang, J.H., Wang, Y., Lo, C.H., 2008. Detrital zircon evidence from Burma for reorganization of the eastern Himalayan river system. American Journal of Science, 308, 618-638.

Lidmar-Bergström, K., 1988. Exhumed cretaceous landforms in south Sweden. Zeitschrift fur Geomorphologie, Supplement Band 72, 21–40.

Lifton N, Bieber J, Clem J, Duldig M, Evenson P, Humble J, Pyle R. 2005. Addressing solar modulation and long-term uncertainties in scaling secondary cosmic rays for in situ cosmogenic nuclide applications. Earth and Planetary Science Letters, 239, 140-161.

Lithgow-Bertelloni, C., Silver, P.G., 1998. Dynamic topography, plate driving forces and the African superswell. Nature, 395, 269-272.

Lock, B.E., Shone, R., Coates, A. T., Hatton, C. J., 1975. Mesozoic Newark type sedimentation within the Cape Fold Belt of South Africa. Proceedings of the 9th International Congress of Sedimentology, Nice 1975, 2, 217-225.

López-Gamundí, O. R., Rossello, E. A., 1998. Basin fill evolution and paleotectonic patterns along the Samfrau geosyncline: the Sauce Grande basin–Ventana foldbelt (Argentina) and Karoo basin–Cape foldbelt (South Africa) revisited. Geologische Rundschau, 86, 819-834.

Lowman, L.E. and Barros, A.P., 2014. Investigating links between climate and orography in the central Andes: Coupling erosion and precipitation using a physical-statistical model. Journal of Geophysical Research: Earth Surface, 119, 1322-1353.

Ludwig, W. J., 1983, Geologic framework of the Falkland Plateau: Initial reports DSDP, Leg 71, Valparaiso to Santos, 1980, 1, 281–293.

Lustig, L.K., 1969. Trend surface analysis of the Basin and Range province, and some geomorphic implications. US Geological Survey Professional Paper 500-D.

Macdonald, D., Gomez-Perez, I., Franzese, J., Spalletti, L., Lawver, L., Gahagan, L., Dalziel, I., Thomas, C., Trewin, N., Hole, M. and Paton, D., 2003. Mesozoic break-up of SW Gondwana: implications for regional hydrocarbon potential of the southern South Atlantic. Marine and Petroleum Geology, 20, 287-308.

Macgregor, D.S., 2012. The development of the Nile drainage system: integration of onshore and offshore evidence. Petroleum Geoscience, 18, 417-431.

Manjoro, M., 2015. Structural control of fluvial drainage in the western domain of the Cape Fold Belt, South Africa. Journal of African Earth Sciences, 101, 350-359.

Margerison, H.R., Phillips, W.M., Stuart, F.M., Sugden, D.E., 2005. Cosmogenic 3 He concentrations in ancient flood deposits from the Coombs Hills, northern Dry Valleys, East Antarctica: interpreting exposure ages and erosion rates. Earth and Planetary Science Letters, 230, 163-175.

Marker, M.E., Holmes, P.J., 1999. Laterisation on limestones of the Tertiary Wankoe Formation and its relationship to the African Surface, southern Cape, South Africa. Catena, 38, 1-21.

Marker, M.E., Holmes, P.J., 2005. Landscape evolution and landscape sensitivity: the case of the southern Cape. South African Journal of Science, 101, 53-60.

Marker, M.E., McFarlane, M.J., Wormald, R.J., 2002. A laterite profile near Albertinia, Southern Cape, South Africa: its significance in the evolution of the African Surface. South African Journal of Geology, 105, 67-74.

Martin, A.K., 1987. Comparison of sedimentation rates in the Natal Valley, southwest Indian Ocean, with modern sediment yields in east coast rivers of Southern Africa. South African Journal of Science, 83, 716-724.

Martin, A. K., Hartnady, C. J., Goodlad, S. W., 1981. A revised fit of South America and south central Africa. Earth and Planetary Science Letters, 54, 293-305.

Martin, A. K., Hartnady, C. J. H., 1986. Plate tectonic development of the South West Indian Ocean: a revised reconstruction of East Antarctica and Africa. Journal of Geophysical Research: Solid Earth, 91, 4767-4786.

Martinsen, O.J., Sømme, T.O., Thurmond, J.B., Helland-Hansen, W. and Lunt, I., 2010, January. Source-to-sink systems on passive margins: theory and practice with an example from the Norwegian continental margin. Geological Society, London, Petroleum Geology Conference series, 7, 913-920.

Maske, S., 1957, A critical review of superimposed and antecedent rivers in southern Africa. In Annals of the University of Stellenbosch: Series A, 33, 1, 1-22.

Matmon, A., Bierman, P. and Enzel, Y., 2002. Pattern and tempo of great escarpment erosion. Geology, 30, 1135-1138.

Matmon, A. S., Bierman, P., Larsen, J., Southworth, S., Pavich, M., Finkel, R., Caffee, M., 2003, Erosion of an ancient mountain range, the Great Smoky Mountains, North Carolina and Tennessee: American Journal of Science, 303, 817-855.

Matthai, H.F., 1990. Floods. In, Wolman, M.G., Riggs, H.C., The Geology of North America: Vols. 0-1, Surface Water Hydrology, Geological Society of America, Boulder, pp. 97-120.

Maw, G., 1866. Notes on the comparative structure of surfaces produced by sub-aerial and marine denudation. Geological Magazine 3, 439–451.

McCauley, J.F., Breed, C.S., Schaber, G.G., McHugh, W.P., Issawi, B., Haynes, C.V., Grolier, M.J., Kilani, A.E., 1986. Paleodrainages of the Eastern Sahara-The Radar Rivers Revisited (SIR-A/B Implications for a Mid-Tertiary Trans-African Drainage System). IEEE Transactions on Geoscience and Remote Sensing, 4, 624-648.

McHugh, W.P., McCauley, J.F., Haynes, C.V., Breed, C.S., Schaber, G.G., 1988. Paleorivers and geoarchaeology in the southern Egyptian Sahara. Geoarchaeology, 3, 1-40.

McLachlan, I. R., McMillan, I. K., 1976. Review and stratigraphic significance of southern Cape Mesozoic palaeontology. Transactions of the Geology Society of South Africa, 79, 197-212.

McMillan, I. K., Brink, G. I., Broad, D. S., Maier, J. J., 1997. Late Mesozoic sedimentary basins off the south coast of South Africa. Sedimentary Basins of the World, 3, 319-376.

Meade, R.H., 1982. Sources, sinks, and storage of river sediment in the Atlantic drainage of the United States. The Journal of Geology, 90, 235-252.

Meade, R.H., 1988, Movement and storage of sediment in river systems, in Lerman, A., and Meybeck, M., eds., Physical and chemical weathering in geochemical cycles: Dordrecht, Netherlands, Kluwer Academic Publishers, p. 165–179.

Meade, R.H., Yuzyk, T. R., Day, T.J., 1990. Movement and storage of sediment in rivers of theUnited States and Canada. In, Wolman, M.G., Riggs, H.C., (eds.) The Geology of North America: Vols. 0-1, Surface Water Hydrology,. Geological Society of America, Boulder, pp. 255-280.

Metivier, F., Gaudemer, Y., 1999 Stability of output fluxes of large rivers in south and East Asia during the last 2 million years: implications on floodplain processes. Basin Research, 11, 293-303.

Meybeck, M., Laroche, L., Duerr, H.H., Syvitski, J.P.M., 2003. Global variability of daily total suspended solids and their fluxes in rivers. Global Planetary Change, 39, 65-93.

Midgley, G. F., Hannah, L., Millar, D., Thuiller, W., Booth, A., 2003. Developing regional and species-level assessments of climate change impacts on biodiversity in the Cape Floristic Region. Biological Conservation, 112, 87-97.

Milliman, J.D., Meade, R.H., 1983. World-wide delivery of river sediment to the oceans. Journal of Geology, 91, 1-21.

Milliman, J.D., Syvitski, J.P.M., 1992. Geomorphic tectonic control of sediment discharge to the ocean - the importance of small mountainous rivers. Journal of Geology, 100, 525-544.

Miller, J.R., 1991. The influence of bedrock geology on knickpoint development and channel-bed degradation along downcutting streams in south-central Indiana. The Journal of Geology, 591-605.

Miller, V.C., 1953. A Quantitative Geomorphic Study of Drainage Basin Characteristics in the Clinch Mountain Area. New York. Columbia University, Virginia and Tennessee, Project. NR, Technical Report, 389-402.

Mitchell, G., McDonald, A.T., 1995. Catchment characterization as a tool for upland water quality management. Journal of Environmental management, 44, 83-95.

Molnar, P., 2004. Late Cenozoic increase in accumulation rates of terrestrial sediment; how might climate change have affected erosion rates? Annual Review of Earth and Planetary Sciences, 32, 67-89.

Montgomery, D. R., Balco, G., Willett, S. D., 2001. Climate, tectonics, and the morphology of the Andes. Geology, 29, 579-582.

Montgomery, D.R., Brandon, M.T., 2002. Topographic controls on erosion rates in tectonically active mountain ranges. Earth and Planetary Science Letters, 201, 481-489.

Moore, G.T., 1969. Interaction of rivers and oceans; Pleistocene petroleum potential. AAPG Bulletin, 53, 2421-2430.

Moore, A.E., 1999. A reappraisal of epeirogenic flexure axes in southern Africa. South African Journal of Geology, 102, 363–376.

Moore, A., Blenkinsop, T., 2002. The role of mantle plumes in the development of continental-scale drainage patterns: the southern African example revisited. South African Journal of Geology, 105, 353-360.

Moore, A., Blenkinsop, T., 2006. Scarp retreat versus pinned drainage divide in the formation of the Drakensberg escarpment, southern Africa. South African Journal of Geology, 109, 599-610.

Moore, A., Blenkinsop, T., Cotterill, F. W., 2009. Southern African topography and erosion history: plumes or plate tectonics? Terra Nova, 21, 310-315.

Moore, A.E., Larkin, P.A., 2001. Drainage evolution in south-central Africa since the breakup of Gondwana. South African Journal of Geology, 104, 47-68.

Mountain, E.D., Grahamstown peneplain. Transactions of the Geological Society of South Africa, 83, 47-53.

NASA Reverb. 2015. http://reverb.echo.nasa.gov/reverb/

Nishiizumi, K., Kohl, C.P., Arnold, J.R., Klein, J., Fink, D., Middleton, R., 1991. Cosmic ray produced 10Be and 26Al in Antarctic rocks; exposure and erosion history. Earth and Planetary Science Letters, 104, 440–454.

Norton, K.P., Vanacker, V., 2009. Effects of terrain smoothing on topographic shielding correction factors for cosmogenic nuclide-derived estimates of basin-averaged denudation rates. Earth Surface Processes and Landforms, 34, 145-154.

Nyblade, A.A., Robinson, S.W., 1994. The African Superswell. Geophysical Research Letters, 21, 765-768.

Nyblade, A.A., Sleep, N.H., 2003. Long lasting epeirogenic uplift from mantle plumes and the origin of the Southern African Plateau. Geochemistry, Geophysics, Geosystems, 4, 1 - 29.

Oberlander, M., 1985. Origin of drainage transverse to structures in orogens. In, Ed. Morisawa, M., Hack, J.T., (eds.) Tectonic Geomorphology, Allen & Unwin, Boston. pp. 155-182.

Ohmori, H., 1993. Changes in the hypsometric curve through mountain building

resulting from concurrent tectonics and denudation. Geomorphology, 8, 263-277.

Ollier C., 1979. Evolutionary geomorphology of Australia and Papua-New Guinea. Transactions of the Institute of British Geographers, 4, 516–539.

Ollier, C., 1991. Ancient landscapes. Belhaven Press, London/New York, 233 pp.

Ollier CD, Gaunt GFM, Jurkowski I. 1988. The Kimberley plateau, Western Australia: a Precambrian erosion surface. Zeitschrift fur Geomorphologie 32, 239–246.

Ollier, C., Pain, C., 1996. Regolith, soils and landforms. John Wiley & Sons.

Ollier, C., Pain, C., 2000. The origin of mountains. Routledge, London/New York, 345 pp.

Ouimet, W.B., Whipple, K.X., Crosby, B.T., Johnson, J.P., Schildgen, T.F., 2008. Epigenetic gorges in fluvial landscapes. Earth Surface Processes and Landforms, 33, 1993-2009.

Owen, L.A., Finkel, R.C., Barnard, P.L., Haizhou, M., Asahi, K., Caffee, M.W., Derbyshire, E., 2005. Climatic and topographic controls on the style and timing of Late Quaternary glaciation throughout Tibet and the Himalaya defined by 10 Be cosmogenic radionuclide surface exposure dating. Quaternary Science Reviews, 24, 1391-1411.

Özbek, A., 2009. Variation of Schmidt hammer values with imbrication direction in clastic sedimentary rocks. International Journal of Rock Mechanics and Mining Sciences, 46, 548-554.

Paige, S., 1912. Rock-cut surfaces in the desert regions. Journal of Geology, 20, 442–50.

Palumbo, L., Hetzel, R., Tao, M., Li, X., 2010. Topographic and lithologic control on catchment-wide denudation rates derived from cosmogenic 10 Be in two mountain ranges at the margin of NE Tibet. Geomorphology, 117, 130-142.

Panario, D., Gutiérrez, O., Sánchez Bettucci, L., Peel, E., Oyhantçabal, P., Rabassa, J., 2014. Ancient landscapes of Uruguay. In: Rabassa, J., Ollier, C. (Eds.) Gondwana landscapes in southern South America, pp. 161–199.

Paola, C., 2000. Quantitative models of sedimentary basin filling. Sedimentology, 47, 121–178.

Parsons, A.J., Abrahams, A.D., 1984. Mountain mass denudation and piedmont formation in the Mojave and Sonoran Deserts. American Journal of Science, 284, 255–71.

Partridge, T.C., 1997. Cainozoic environmental change in southern Africa, with

special emphasis on the last 200 000 years. Progress in Physical Geography, 21, 3-22.

Partridge, T.C., 1998. Of diamonds, dinosaurs and diastrophism: 150 million years of landscape evolution in southern Africa. South African Journal of Geology, 101, 165–184.

Partridge, T.C., 1999. Evolution of Landscapes. In, Cowling, R.M., Richardson, D.M. Pierce, S.M., (eds.) Vegetation of southern Africa. Cambridge University Press, pp. 1-20.

Partridge, T.C., Dollar, E.S.J., Moolman, J., Dollar, L.H., 2010. The geomorphic provinces of South Africa, Lesotho and Swaziland: A physiographic subdivision for earth and environmental scientists. Transactions of the Royal Society of South Africa, 65, 1-47.

Partridge, T. C., Maud, R. R., 1987. Geomorphic evolution of southern Africa since the Mesozoic. South African Journal of Geology, 90, 179-208.

Partridge, T.C., Maud, R.R.M., 2000. Macro-scale geomorphic evolution of southern Africa. In Partridge, T.C., Maud, R.R.M., (eds.) The Cenozoic of southern Africa. Oxford University Press. pp. 418.

Paton, D. A., 2006. Influence of crustal heterogeneity on normal fault dimensions and evolution: southern South Africa extensional system. Journal of structural geology, 28, 868-886.

Paton, D., 2011. Post-Rift Deformation of the North East and South Atlantic Margins: Are “Passive Margins” Really Passive? In Busby, C., Azor, A., (eds.) Tectonics of Sedimentary Basins: Recent Advances, John Wiley & Sons, Ltd, Chichester, UK.

Paton, D.A., Macdonald, D.I., Underhill, J.R., 2006. Applicability of thin or thick skinned structural models in a region of multiple inversion episodes; southern South Africa. Journal of Structural Geology, 28, 1933-1947.

Paton, D.A., Underhill, J.R., 2004. Role of crustal anisotropy in modifying the structural and sedimentological evolution of extensional basins: the Gamtoos Basin, South Africa. Basin Research, 16, 339-359.

Pederson, J.L., Mackley, R.D. and Eddleman, J.L., 2002. Colorado Plateau uplift and erosion evaluated using GIS. GSA TODAY, 12, 4-10.

Penck, W., 1924. Die Morphologische Analyse (Morphological Analysis of Landforms), In, J. Engelhorn’s Nachfolger, Suttgart, 283 p. English translation by Czech, H., Boswell, K.C., London, 1953, St. Martin’s Press, New York, 429 pp.

Penck, W., 1953 Morphological analysis of land forms: a contribution to physical

geology. MacMillan and Company. 429 pp.

Peulvast, J. P., Bétard, F., 2015. A history of basin inversion, scarp retreat and shallow denudation: The Araripe basin as a keystone for understanding long-term landscape evolution in NE Brazil. Geomorphology, 233, 20-40.

Phillips, J.D., Lutz, J.D., 2008. Profile convexities in bedrock and alluvial streams. Geomorphology, 102,554-566.

Phillips, F.M., Zreda, M.G., Gosse, J.C., Klein, J., Evenson, E.B., Hall, R.D., Chadwick, O.A., Sharma, P., 1997. Cosmogenic 36Cl and 10Be ages of Quaternary glacial and fluvial deposits of the Wind River Range, Wyoming. Geological Society of America Bulletin, 109, 1453-1463.

Phillips F, Zreda M, Smith S, Elmore D, Kubik P, Sharma P. 1990. Cosmogenic Chlorine-36 Chronology for Glacial Deposits at Bloody Canyon, Eastern Sierra Nevada. Science, 248, 1529-1532

Pik, R., Marty, B., Hilton, D.R., 2006. How many mantle plumes in Africa? The geochemical point of view. Chemical Geology, 226, 100-114.

Playfair, J., 1802. Illustrations of the Huttonian theory of the earth (reprint): Urbana, University of Illinois Press, 528 pp.

Portenga, E.W., Bierman, P.R., 2011. Understanding Earth's eroding surface with 10 Be. GSA Today, 21, 4-10.

Pratt-Sitaula, B., Burbank, D.W., Heimsath, A., Ojha, T., 2004. Landscape disequilibrium on 1000–10,000 year scales Marsyandi River, Nepal, central Himalaya. Geomorphology, 58, 223-241.

Prélat, A., Hodgson, D.M., Flint, S.S., 2009. Evolution, architecture and hierarchy of distributary deep-water deposits: a high-resolution outcrop investigation from the Permian Karoo Basin, South Africa. Sedimentology, 56, 2132–2154

Prince, P. S., Spotila, J. A., Henika, W. S., 2011. Stream capture as driver of transient landscape evolution in a tectonically quiescent setting. Geology, 39, 823-826.

Quigley, M.C., Sandiford, M., Cupper, M.L., 2007. Distinguishing tectonic from climatic controls on range-front sedimentation. Basin Research, 19, 491-505.

Quigley, M., Sandiford, M., Fifield, K., and Alimanovic, A., 2007b, Bedrock erosion and relief production in the northern Flinders Ranges, Australia. Earth Surface Processes and Landforms, 32, 929-944.

Rabassa, J., 2010. Gondwana paleolandscapes: long-term landscape evolution, genesis, distribution and age. Geociências (São Paulo), 29, 541-570.

Ramasamy, S.M., Bakliwal, P.C., Verma, R.P., 1991. Remote sensing and river migration in Western India. Remote Sensing, 12, 2597-2609.

Ramsey, L.A., Walker, R.T., Jackson, J., 2008. Fold evolution and drainage development in the Zagros mountains of Fars province, SE Iran. Basin Research, 20, 23-48.

Rastall, R. H., 1911. The Geology of the Districts of Worcester, Robertson, and Ashton (Cape Colony). Quarterly Journal of the Geological Society, 67, 701-733.

Raymo, M. E., Ruddiman, W. F., 1992. Tectonic forcing of late Cenozoic climate. Nature, 359, 117-122.

Reiners PW, Ehlers T.A., (eds). 2005. Low-temperature thermochronology: techniques, interpretations, and applications. Reviews in Mineralogy and Geochemistry 58, 622 pp.

Repka, J.L., Anderson, R.S., Finkel, R.C., 1997. Cosmogenic dating of fluvial terraces, Fremont River, Utah. Earth and Planetary Science Letters, 152, 59-73.

Rich, J.L., 1935. Origin and evolution of rock fans and pediments. Bulletin of the Geological Society of America 46, 999–1024.

Richards, K., 1982. Rivers, Form and Processes in Alluvial channels. London: Methuen, 358 pp.

Richards, P.C., Gatliff, R.W., Quinn, M.F., Fannin, N.G.T., Williamson, J.P., 1996. The geological evolution of the Falkland Islands continental shelf. Geological Society, London, Special Publications, 108, 05-128.

Richards, P.C., Stone, P., Kimbell, G.S., McIntosh, W.C., Phillips, E.R., 2013. Mesozoic magmatism in the Falkland Islands (South Atlantic) and their offshore sedimentary basins. Journal of Petroleum Geology, 36, 61-73.

Riebe, C.S., Kirchner, J.W., Granger, D.E., Finkel, R.C., 2001. Strong tectonic and weak climatic control of long-term chemical weathering rates. Geology, 29, 511-514.

Rigassi, D. A., Dixon, G. E. 1972. Cretaceous of the Cape Province, Republic of South Africa. Ibadan University Conference on African Geology, 170, 513-527.

Ring, U., Brandon, M.T., Willett, S.D., Lister, G.S., 1999. Exhumation processes. Geological Society, London, Special Publications, 154, 1-27.

Roberts, G.G., White, N., 2010. Estimating uplift rate histories from river profiles using African examples. Journal of Geophysical Research: Solid Earth, 115(B2).

Roering, J.J., Kirchner, J.W., Sklar, L.S., Dietrich, W.E., 2001. Hillslope evolution

by nonlinear creep and landsliding An experimental study, Geology, 29, 143-146.

Rogers, C. A., 1903. The geological history of the Gouritz River system. Transactions of the South African Philosophical Society, 14, 375-384.

Romans, B. W., Castelltort, S., Covault, J. A., Fildani, A., Walsh, J. P., 2015. Environmental signal propagation in sedimentary systems across timescales. Earth-Science Review, DOI: 10.1016/j.earscirev.2015.07.012

Romans, B.W., Graham, S.A., 2013. A deep-time perspective of land-ocean linkages in the sedimentary record. Annual review of marine science, 5, 69-94.

Romans, B.W., Normark, W.R., McGann, M.M., Covault, J.A., Graham, S.A., 2009. Coarse-grained sediment delivery and distribution in the Holocene Santa Monica Basin, California: implications for evaluating source-to-sink flux at millennial time scales. Geological Society of America Bulletin, 121, 1394-1408.

Rosenbloom, N.A. and Anderson, R.S., 1994. Hillslope and channel evolution in a marine terraced landscape, Santa Cruz, California. Journal of Geophysical Research: Solid Earth, 99, 14013-14029.

Rouby, D., Bonnet, S., Guillocheau, F., Gallagher, K., Robin, C., Biancotto, F., Dauteuil, O. and Braun, J., 2009. Sediment supply to the Orange sedimentary system over the last 150My: An evaluation from sedimentation/denudation balance. Marine and Petroleum Geology, 26, 782-794.

Rowsell, D., De Swardt, A., 1976. Diagenesis in Cape and Karoo sediments, South Africa, and its bearing on their hydrocarbon potential. Transactions of the Geological Society of South Africa, 79, 81-145.

Rozendaal, A., Gresse, P.G., Scheepers, R., Le Roux, J.P., 1999. Neoproterozoic to early Cambrian crustal evolution of the Pan-African Saldania belt, South Africa. Precambrian research, 97, 303-323.

Rozman, D.J., 2000. AAPG Memoir 72/SEPM Special Publication No. 68, Chapter 24: Characterization of a Fine-Grained Outer Submarine Fan Deposit, Tanqua-Karoo Basin, South Africa.

Rust, D.J., Summerfield, M.A., 1990. Isopach and borehole data as indicators of rifted margin evolution in southwestern Africa. Marine Petroleum Geology, 7, 277-287.

Sadler, P.M., 1981. Sediment accumulation rates and the completeness of stratigraphic sections. The Journal of Geology, 89, 569-584.

Safran, E.B., Bierman, P.R., Aalto, R., Dunne, T., Whipple, K.X., Caffee, M., 2005. Erosion rates driven by channel network incision in the Bolivian Andes. Earth Surface Processes and Landforms, 30, 1007-1024.

Schaller, M., Hovius, N., Willett, S.D., Ivy-Ochs, S., Synal, H.A., Chen, M.C., 2005. Fluvial bedrock incision in the active mountain belt of Taiwan from in situ-produced cosmogenic nuclides. Earth Surface Processes and Landforms, 30, 955-971.

Schaller, M., Von Blanckenburg, F., Veldkamp, A., Tebbens, L.A., Hovius, N. and Kubik, P.W., 2002. A 30 000 yr record of erosion rates from cosmogenic 10 Be in Middle European river terraces. Earth and Planetary Science Letters, 204, 307-320.

Scharf, T. E., Codilean, A. T., de Wit, M., Jansen, J. D., Kubik, P., W. 2013. Strong rocks sustain ancient postorogenic topography in southern Africa. Geology 41, 331-334.

Scherler, D., Bookhagen, B., Strecker, M.R., 2014. Tectonic control on 10Be-derived erosion rates in the Garhwal Himalaya, India. Journal of Geophysical Research: Earth Surface, 119, 83-105.

Schlische, R.W., 1992. Structural and stratigraphic development of the Newark extensional basin, eastern North America: Evidence for the growth of the basin and its bounding structures. Geological Society of America Bulletin, 104, 1246-1263.

Schmidt, K.M., Montgomery, D.R., 1995, Limits to relief. Science, 270, 617-620.

Schumm, S. A., 1956. Evolution of drainage systems and slopes in badlands at Perth Amboy, New Jersey. Geological Society of America Bulletin, 67, 597-646.

Schumm, S.A., 1977. The fluvial system (Vol. 338). New York: Wiley

Scott, L., Woodborne, S., 2007. Vegetation history inferred from pollen in Late Quaternary faecal deposits (hyraceum) in the Cape winter-rain region and its bearing on past climates in South Africa. Quaternary Science Reviews, 26, 941-953.

Seidl M., Dietrich W.E., Kirchner J.W., 1994. Longitudinal profile development into bedrock: an analysis of Hawaiian channels. Journal of Geology, 102, 457–74.

Seidl M.A., Finkel R.C., Caffee M.W., Hudson G.B., Dietrich W.E., 1997. Cosmogenic isotope analyses applied to river longitudinal profile evolution: problems and interpretations. Earth Surface Processes and Landforms, 22, 195–209.

Seydack, A. H., Bekker, S. J., Marshall, A. H. 2007. Shrubland fire regime scenarios in the Swartberg Mountain Range, South Africa: Implications for fire management. International Journal of Wildland Fire, 16, 81-95.

Sharp, R.P. 1940. Geomorphology of the Ruby–East Humboldt Range, Nevada. Bulletin of the Geological Society of America, 51, 337–72.

Shelton, C. M., 2015. Rebound hardness results for raw material located near Pinnacle Point, South Africa and the implications thereof. Ma Thesis, The University of Texas, America.

Shone, R.W., 1978. A case for lateral gradation between the Kirkwood and Sundays River Formations, Algoa Basin. Transactions of Geology Society of South Africa, 81, 319- 326.

Shone, R. W., 2006. Onshore post-Karoo Mesozoic deposits. In: Johnson, M.R., Anhaeusser, C.R., Thomas, R.J. (Eds.) The geology of South Africa, pp. 541-552. Geological Society of South Africa, Marshalltown. pp. 541-552.

Shone, R. W., Booth, P. W. K., 2005. The Cape Basin, South Africa: A review. Journal of African Earth Sciences, 43, 196-210.

Simpson, G., 2004. Role of river incision in enhancing deformation. Geology, 32, 341-344.

Sklar, L. S., Dietrich, W. E., 2001. Sediment and rock strength controls on river incision into bedrock. Geology, 29, 1087-1090.

Sklar, L.S., Dietrich, W.E., 2004. A mechanistic model for river incision into bedrock by saltating bed load. Water Resources Research, 40.

Smith, R.M.H., 1986. Sedimentation and palaeoenvironments of Late Cretaceous crater-lake deposits in Bushmanland, South Africa. Sedimentology, 33, 369-386

Smith, R.M.H., 1987a, Morphology and depositional history of exhumed Permian point bars in the southwestern Karoo, South Africa: Journal of Sedimentary Petrology, 57, 19–29.

Smith, R.M.H., 1993, Sedimentology and ichnology of floodplain paleosurfaces in the Beaufort Group (Late Permian), Karoo sequence, South Africa: Palaios, 8, 339–357.

Snyder, N. P., Whipple, K. X., Tucker, G. E., Merritts, D. J., 2000. Landscape response to tectonic forcing: Digital elevation model analysis of stream profiles in the Mendocino triple junction region, northern California. Geological Society of America Bulletin, 112, 1250-1263.

Söhnge, P. G., 1934. The Worcester fault. Transactions of geology Society of South Africa, 37, 253-277.

Sømme, T.O., Helland-Hansen, W., Martinsen, O.J., Thurmond, J.B., 2009a. Relationships between morphological and sedimentological parameters in source-to-sink systems: a basis for predicting semi-quantitative characteristics in subsurface systems. Basin Research, 21, 361-387.

Sømme, T.O., Martinsen, O.J., Thurmond, J.B., 2009b. Reconstructing morphological and depositional characteristics in subsurface sedimentary systems: An example from the Maastrichtian–Danian Ormen Lange system, More Basin, Norwegian Sea. AAPG bulletin, 93, 1347-1377.

Sømme, T.O., Piper, D.J., Deptuck, M.E., Helland-Hansen, W., 2011. Linking onshore–offshore sediment dispersal in the Golo source-to-sink system (Corsica, France) during the Late Quaternary. Journal of Sedimentary Research, 81, 118-137.

Sonibare, W.A., Sippel, J., Scheck-Wenderoth, M. and Mikeš, D., 2015. Crust-scale 3D model of the Western Bredasdorp Basin (Southern South Africa): data-based insights from combined isostatic and 3D gravity modelling. Basin Research, 27, 125-151.

Spikings, A. L., Hodgson, D. M., Paton, D. A., Spychala, Y. T., 2015. Palinspastic restoration of an exhumed deep-water system: a workflow to improve paleogeographic reconstructions. Interpretation, 3, SAA71-SAA87 http://dx.doi.org/10.1190/INT-2015-0015.1

Spychala, Y.T., Hodgson, D.M., Flint, S.S., Mountney, N.P., 2015. Constraining the sedimentology and stratigraphy of submarine intraslope lobe deposits using exhumed examples from the Karoo Basin, South Africa. Sedimentary Geology, 322, 67-81.

Stanley, J.R., Flowers, R.M., Bell, D.R., 2013. Kimberlite (U-Th)/He dating links surface erosion with lithospheric heating, thinning, and metasomatism in the southern African Plateau. Geology, 41, 1243-1246.

Stankiewicz, J. and de Wit, M.J., 2006. A proposed drainage evolution model for Central Africa—Did the Congo flow east? Journal of African Earth Sciences, 44, 75-84.

Stankiewicz, J., Ryberg, T., Schulze, A., Lindeque, A., Weber, M. H., De Wit, M. J., 2007. Initial results from wide-angle seismic refraction lines in the southern Cape. South African Journal of Geology, 110, 407-418.

Stear, W.M., 1985. Comparison of the bedform distribution and dynamics of modern and ancient sandy ephemeral flood deposits in the southwestern Karoo region, South Africa. Sedimentary Geology, 45, 209-230.

Stewart AJ, Blake DH, Ollier C., 1986. Cambrian river terraces and ridgetops in

Central Australia: oldest persisting landforms? Science, 233, 758–761.

Stock, J.D., Montgomery, D.R., 1999. Geologic constraints on bedrock river incision using the stream power law. Journal of Geophysical Research B, 104, 4983-4993.

Stokes, M., Mather, A.E., 2003. Tectonic origin and evolution of a transverse drainage: the Rıo Almanzora, Betic Cordillera, Southeast Spain. Geomorphology, 50, 59-81.

Stokes, M., Mather, A.E., Belfoul, A., Farik, F., 2008. Active and passive tectonic controls for transverse drainage and river gorge development in a collisional mountain belt (Dades Gorges, High Atlas Mountains, Morocco). Geomorphology, 102, 2-20.

Stone, P., Kimbell, G.S., Richards, P.C., 2009. Rotation of the Falklands microplate reassessed after recognition of discrete Jurassic and Cretaceous dyke swarms. Petroleum Geoscience, 15, 279-287.

Strahler, A.N., 1950. Equilibrium theory of erosional slopes approached by frequency distribution analysis; part 1: American Journal of Science, 248, 673–696.

Strahler, A. N., 1952. Hypsometric (Area-Altitude) Analysis of Erosional Topography. Geological Society of America Bulletin, 63, 1117.

Strahler, A. N., 1957. Quantitative analysis of watershed geomorphology. Journal of Civil Engineering, 101, 1258-1262.

Strahler, A.N., 1964. Quantitative geomorphology of drainage basins and channel networks. In, Chow, V.T., (Ed.), Handbook of Applied Hydrology. McGraw Hill Book Company, New York, pp. 39-76.

Summerfield, M.A., 1983. Silcrete as a palaeoclimatic indicator: evidence from southern Africa. Palaeogeography, Palaeoclimatology, Palaeoecology, 41, 65-79.

Summerfield, M. A., 1991. Global geomorphology. Routledge, pp. 537.

Summerfield, M.A., 1996. Tectonics, geology and long-term landscape development. W. M. Adams et al, pp.1-17.

Summerfield, M.A., Hulton, N.J., 1994. Natural controls of fluvial denudation rate in major world drainage basins. Journal of Geophysical Research, 99, 13871–13883.

Summerfield, M.A., Stuart, F.M., Cockburn, H.A.P., Sugden, D.E., Dunai, T.,

Marchant, D.R., Denton, G.H., 1999a. Long-term rates of denudation in the Dry Valleys region of Transantarctic Mountains, southern Victoria Land, Antarctica: preliminary results based on in-situ-produced cosmogenic 21Ne. Geomorphology, 27, 113–129.

Summerfield, M.A., Sugden, D.E., Denton, G.H., Marchant, D.R., Cockburn, H.A.P., Stuart, F.M., 1999b. Cosmogenic isotope data support previous evidence of extremely low rates of denudation in the Dry Valleys region, southern Victoria Land, Antarctica. In, Smith, B.J., Whalley, W.B., Warke, P.A. (eds). Uplift, Erosion and Stability: Perspectives on Long-Term Landscape Development, Special Publication 162, Geological Society: London; 255–267.

Syvitski, J. P. M., Bahr, D. B. 2001. Numerical models of marine sediment transport and deposition. Computers and Geosciences, 27, 617–753.

Syvitski, J. P. M., Milliman, J. D., 2007. Geology, geography and humans battle for dominance over the delivery of fluvial sediment to the coastal ocean. Journal of Geology, 115, 1–19.

Syvitski, J. P. M., Peckham, S. D., Hilberman, R., Mulder, T., 2003. Predicting the terrestrial flux of sediment to the global ocean: a planetary perspective. Sedimentary Geology, 162, 5–24.

Szwarc, T. S., Johnson, C. L., Stright, L. E., McFarlane, C. M., 2015. Interactions between axial and transverse drainage systems in the Late Cretaceous Cordilleran foreland basin: Evidence from detrital zircons in the Straight Cliffs Formation, southern Utah, USA. Geological Society of America Bulletin, 127, 372-392.

Taljaard, M.S., 1948. On some concepts in geomorphology. The South African Geographer, 50, 5-16.

Taljaard, M.S., 1949. A glimpse of South Africa. The University Publishers and Booksellers (Pty) Ltd., Grahamstown, 226 pp.

Talling, P.J., Stewart, M.D., Stark, C.P., Gupta, S., Vincent, S.J., 1997 Regular spacing of drainage outlets from linear fault blocks. Basin Research, 9, 275-302.

Talma, A.S., Vogel, J.C., 1992. Late Quaternary paleotemperatures derived from a speleothem from Cango caves, Cape province, South Africa. Quaternary Research, 37, 203-213.

Tankard, A., Welsink, H., Aukes, P., Newton, R., Stettler, E., 2009. Tectonic evolution of the Cape and Karoo basins of South Africa. Marine Petroleum Geology, 26, 1379-1412.

Tanner, D.C., Behrmann, J.H., Dresmann, H., 2003. Three-dimensional retro-deformation of the Lechtal nappe, Northern Calcareous Alps. Journal of Structural Geology, 25, 737-748.

Tator, B.A., 1952. Pediment characteristics and terminology. Annals of the Association of American Geographers, 42, 295-317.

Thackeray, J.F., 1996. Ring width variation in a specimen of South African Podocarpus, circa 1350–1937 AD. Palaeoecology of Africa, 24, 233-240.

Thomas, M.F., 1974. Tropical geomorphology. NewYork: Wiley.

Thomson, K., 1999. Role of continental break-up, mantle plume development and fault reactivation in the evolution of the Gamtoos Basin, South Africa. Marine and petroleum geology, 16, 409-429.

Thornbury, W.C., 1954. Principles of Geomorphology. New York: Wiley and Sons, 618 p.

Thornbury, W.D., 1969 Principles of Geomorphology. New York: John Wiley and Sons, Inc

Tinker, J., 2005. Quantifying South African Uplift: using apatite fission track thermochronology and offshore sediment volumes to test the balance between denudation (onshore) and deposition (offshore) since Gondwana break-up. PhD thesis Cape Town University.

Tinker, J., De Wit, M., Brown, R., 2008a. Mesozoic exhumation of the southern Cape, South Africa, quantified using apatite fission track thermochronology. Tectonophysics, 455, 77-93.

Tinker, J., de Wit, M., Brown, R., 2008b. Linking source and sink: evaluating the balance between onshore erosion and offshore sediment accumulation since Gondwana break-up, South Africa. Tectonophysics 455, 94-103.

Tinkler, K., Wohl, E., 1998. A primer on bedrock channels. In: Tinkler, K.J., Wohl, E.E. (Eds.), Rivers over rock: Fluvial processes in bedrock channels, pp. 1-18.

Tomkins, K.M., Humphreys, G.S., Wilkinson, M.T., Fink, D., Hesse, P.P., Doerr, S.H., Shakesby, R.A., Wallbrink, P.J., Blake, W.H., 2007. Contemporary versus long-term denudation along a passive plate margin: the role of extreme events. Earth Surface Processes and Landforms, 32, 1013-1031.

Tooth, S., Brandt, D., Hancox, P. J., McCarthy, T. S., 2004. Geological controls on alluvial river behaviour: a comparative study of three rivers on the South African Highveld. Journal of African Earth Sciences, 38, 79-97.

Trauerstein, M., Norton, K.P., Preusser, F., Schlunegger, F., 2013. Climatic imprint

on landscape morphology in the western escarpment of the Andes. Geomorphology, 194, 76-83.

Trewin, N.H., 2000. The ichnogenus Undichna, with examples from the Permian of the Falkland Islands. Palaeontology, 43, 979-997.

Trewin, N.H., Macdonald, D.I.M., Thomas, C.G.C., 2002. Stratigraphy and sedimentology of the Permian of the Falkland Islands: lithostratigraphic and palaeoenvironmental links with South Africa. Journal of the Geological Society, 159, 5-19.

Tucker, G. E., Slingerland, R. 1996. Predicting sediment flux from fold and thrust belts, Basin Res., 8, 329– 349.

Tucker, G.E., Whipple, K.X., 2002. Topographic outcomes predicted by stream erosion models: Sensitivity analysis and intermodel comparison.Journal of Geophysical Research: Solid Earth, 107(B9).

Turowski, J.M., Hovius, N., Wilson, A., Horng, M.J., 2008. Hydraulic geometry, river sediment and the definition of bedrock channels. Geomorphology, 99, 26-38.

Twidale C. R., 1976. On the survival of palaeoforms. American Journal of Science 276: 77–94.

Twidale, C., 2004. River patterns and their meaning. Earth-Science Reviews, 67, 159-218.

Twidale, C. R., 2007a. Ancient Australian Landscapes. Rosenberg Pub Pty Limited, 144 pp.

Twidale, C.R., 2007b. Bornhardts and associated fracture patterns. Revista Asociación Geológica Argentina, 62, 139–153.

Twidale, C.R., Bourne, J.A., 1996. The development of the land surface. In, Davies, M., Twidale, C. R., Tyler, M.J., (eds) Natural History of the Flinders Ranges, Royal Society of South Australia, Adelaide, pp.46-62.

Twidale, C.R., Campbell, E.M., 1988. Ancient Australia. GeoJournal, 16, 339-354.

Twidale, C.R., Romani, J.V., 1994. On the multistage development of etch forms. Geomorphology, 11, 107-124.

Valeton, I., 1983. Palaeoenvironment of lateritic bauxites with vertical and lateral differentiation. In: Wilson, R.C.L., (ed.) Residual Deposits: Surface Related Weathering Processes and Materials. Special Publication 11, Geological Society of London, pp. 77–90.

Vanacker, V., von Blanckenburg, F., Hewawasam, T., Kubik, P.W., 2007.

Geomorphic development of the Sri Lanka Central Highlands. Earth and Planetary Science Letters, 253, 402-414.

Vanacker, V., von Blanckenburg, F., Govers, G., Molina, A., Campforts, B., Kubik, P.W., 2015. Transient river response, captured by channel steepness and its concavity. Geomorphology, 228, 234-243.

Vance, D., Bickle, M., Ivy-Ochs, S., Kubik, P.W., 2003. Erosion and exhumation in the Himalaya from cosmogenic isotope inventories of river sediments. Earth and Planetary Science Letters, 206, 273-288.

van der Beek P, Braun J, Lambeck K. 1999. Post-Palaeozoic uplift history of southeastern Australia revisited: results from a process-based model of landscape evolution. Australian Journal of Earth Sciences, 46, 157–172.

van der Beek, P., Summerfield, M.A., Braun, J., Brown, R.W. and Fleming, A., 2002. Modeling postbreakup landscape development and denudational history a cross the southeast African (Drakensberg Escarpment) margin. Journal of Geophysical Research: Solid Earth, 107(B12).

van der Wateren, F.M., Dunai, T.J., 2001. Late Neogene passive margin denudation history—cosmogenic isotope measurements from the central Namib desert. Global and Planetary Change, 30, 271-307.

Van der Werff, W., Johnson, S., 2003. High resolution stratigraphic analysis of a turbidite system, Tanqua Karoo Basin, South Africa. Marine and Petroleum Geology, 20, 45-69.

Van Lente, B., 2004, Chemostratigraphic trends and provenance of the Permian Tanqua and Laingsburg depocentres, southwestern Karoo basin, South Africa [Unpublished Ph.D. thesis]: University of Stellenbosch, 339 p

van Niekerk, H.S., Beukes, N.J., Gutzmer, J., 1999. Post-Gondwana pedogenic ferromanganese deposits, ancient soil profiles, African land surfaces and palaeoclimatic change on the Highveld of South Africa. Journal of African Earth Sciences, 29, 761-781.

Visser, J. N. J., 1984. A review of the Stormberg Group and Drakensberg volcanics in southern Africa. Palaeontologica Africana, 25, 5-27.

Visser, J.N.J., Van Niekerk, B.N., Van der Merwe, S.W., 1997. Sediment transport of the Late Palaeozoic glacial Dwyka Group in the southwestern Karoo Basin. South African Journal of Geology, 100, 223-236.

von Blanckenburg, F., 2005. The control mechanisms of erosion and weathering at basin scale from cosmogenic nuclides in river sediment. Earth and Planetary Science Letters, 237, 462-479.

von Blanckenburg, F., Belshaw, N., O'Nions, R., 1996. Separation of 9Be and cosmogenic 10Be from environmental materials and SIMS isotope dilution analysis. Chemical Geology 129, 93–99.

von Blanckenburg, F., Hewawasam, T., Kubik, P.W., 2004. Cosmogenic nuclide evidence for low weathering and denudation in the wet, tropical highlands of Sri Lanka. Journal of Geophysical Research: Earth Surface,109 (F3).

von Blanckenburg, F., Willenbring, J. K., 2014. Cosmogenic nuclides: Dates and rates of Earth-surface change. Elements, 10, 341-346.

Walcott, R. C., Summerfield, M. A., 2008. Scale dependence of hypsometric integrals: An analysis of southeast African basins. Geomorphology, 96, 174-186.

Warrick, J.A., Milliman, J.D., 2003. Hyperpycnal sediment discharge from semiarid southern California rivers: implications for coastal sediment budgets. Geology, 31, 781-784.

Westaway, R., Demir, T., Seyrek, A., Beck, A., 2006. Kinematics of active left-lateral faulting in SE Turkey from offset Pleistocene river gorges: improved constraint on the rate and history of relative motion between the Turkish and Arabian plates. Journal of the Geological Society, 163, 149-164.

Weissel J.K., Seidl M.A., 1998. Inland propagation of erosional escarpments and river profile evolution across the southeastern Australian passive continental margin. In, Tinkler, K.J., Wohl, E (eds.) Rivers over rock: Fluvial processes in bedrock channels, 107, American Geophysical Union, pp.189–206.

Whipple, K.X., 2001. Fluvial landscape response time: how plausible is steady-state denudation?. American Journal of Science, 301(4-5), pp.313-325.

Whipple, K.X., 2004. Bedrock rivers and the geomorphology of active orogens. Annu. Rev. Earth Planet. Sci., 32, pp.151-185.

Whipple, K.X., Hancock, G.S., Anderson, R.S., 2000. River incision into bedrock: Mechanics and relative efficacy of plucking, abrasion, and cavitation. Geological Society of America Bulletin, 112(3), pp.490-503.

Whipple, K.X., Tucker, G.E., 1999. Dynamics of the stream-power river incision model: Implications for height limits of mountain ranges, landscape response timescales, and research needs. Journal of Geophysical Research: Solid Earth, 104, p.17661-17674.

Whipple, K.X., Tucker, G.E., 2002. Implications of sediment-flux-dependent river incision models for landscape evolution. Journal of Geophysical Research: Solid Earth, 107(B2).

Whitchurch, A.L., Carter, A., Sinclair, H.D., Duller, R.A., Whittaker, A.C., Allen,

P.A., 2011. Sediment routing system evolution within a diachronously uplifting orogen: Insights from detrital zircon thermochronological analyses from the South-Central Pyrenees. American Journal of Science, 311, 442-482.

Whittaker, A.C., 2012. How do landscapes record tectonics and climate? Lithosphere, 4, 160-164.

Whittaker, A.C., Boulton, S.J., 2012. Tectonic and climatic controls on knickpoint retreat rates and landscape response times. Journal of Geophysical Research: Earth Surface, 117(F2).

Wickens, D.V.H., 1994. Basin floor fan building turbidites of the southwestern Karoo Basin, Permian Ecca Group, South Africa. University of Port Elizabeth.

Widdowson, M., 2007. Laterite and Ferricrete. In: Nash, David J. and McLaren, Sue J. (eds.) Geochemical Sediments and Landscapes. Oxford, UK: Wiley-Blackwell, pp. 46–94.

Wild, R., Flint, S.S., Hodgson, D.M., 2009. Stratigraphic evolution of the upper slope and shelf edge in the Karoo Basin, South Africa. Basin Research, 21, 502-527.

Willett, S.D., Brandon, M.T., 2002. On steady states in mountain belts. Geology, 30, 175-178.

Willett, S.D., Slingerland, R., Hovius, N., 2001. Uplift, shortening, and steady state topography in active mountain belts. American journal of Science, 301, 455-485.

Willenbring, J.K., von Blanckenburg, F., 2010. Long-term stability of global erosion rates and weathering during late-Cenozoic cooling. Nature, 465, 211-214.

Willgoose G. 2005. Mathematical modeling of whole landscape evolution. Annual Review of Earth and Planetary Sciences, 33, 443–459.

Williams, L.S., 2015. Sedimentology of the Lower Cretaceous reservoirs of the Sea Lion Field, North Falkland Basin. Petroleum Geoscience, 21, 183-198.

Wilson, A., Flint, S., Payenberg, T., Tohver, E., Lanci, L., 2014. Architectural styles and sedimentology of the fluvial lower Beaufort Group, Karoo Basin, South Africa. Journal of Sedimentary Research, 84, 326-348.

Winter, H. De la R. 1973. Geology of the Algoa Basin, South Africa. Sedimentary Basins of the African Coasts, Association of African Geology Survey, Paris, 2nd part (south and east coasts), 17-48.

Wittmann, H., von Blanckenburg, F., Guyot, J.L., Maurice, L., Kubik, P.W., 2009.

From source to sink: Preserving the cosmogenic 10 Be-derived denudation rate signal of the Bolivian Andes in sediment of the Beni and Mamoré foreland basins. Earth and Planetary Science Letters, 288, 463-474.

Wittmann, H., von Blanckenburg, F., Kruesmann, T., Norton, K.P., Kubik, P.W., 2007. Relation between rock uplift and denudation from cosmogenic nuclides in river sediment in the Central Alps of Switzerland. Journal of Geophysical Research: Earth Surface, 112(F4).

Wittmann, H., von Blanckenburg, F., Maurice, L., Guyot, J.L., Filizola, N., Kubik, P.W., 2010. Sediment production and delivery in the Amazon River basin quantified by in situ—produced cosmogenic nuclides and recent river loads. Geological Society of America Bulletin, pp.B30317-1.

Wobus, C.W., Crosby, B.T., Whipple, K.X., 2006, Hanging valleys in fluvial 63 systems; controls on occurrence and implications for landscape evolution: Journal of Geophysical Research, 111, (F2), 14.

Wobus, C.W., Tucker, G.E., Anderson, R.S., 2010. Does climate change create distinctive patterns of landscape incision? Journal of Geophysical Research: Earth Surface, 115(F4).

Wohl E.E., Greenbaum N, Schick A.P., Baker V.R., 1994. Controls on bedrock channel incision along Nahal Paran, Israel. Earth Surface Processes and Landforms, 19, 1–13.

Wolman,M.G., Miller, J.P., 1960. Magnitude and frequency of forces in geomorphic processes. Journal of Geology, 68, 54-74.

Yamaguchi, Y., Kahle, A.B., Tsu, H., Kawakami, T. and Pniel, M., 1998. Overview of advanced spaceborne thermal emission and reflection radiometer (ASTER). Geoscience and Remote Sensing, IEEE Transactions on, 36, 1062-1071.

Yamaguchi, Y., Tsu, H. and Fujisada, H., 1993, August. Scientific basis of ASTER instrument design. In Optical Engineering and Photonics in Aerospace Sensing (pp. 150-160). International Society for Optics and Photonics.

Yang, W., Jolivet, M., Dupont-Nivet, G., Guo, Z., Zhang, Z. and Wu, C., 2013. Source to sink relations between the Tian Shan and Junggar Basin (northwest China) from Late Palaeozoic to Quaternary: evidence from detrital U-Pb zircon geochronology. Basin Research, 25, 219-240.

Youssef, A.M., 2009. Mapping the mega paleodrainage basin using shuttle radar topography mission in Eastern Sahara and its impact on the new development projects in Southern Egypt. Geo-spatial Information Science,12, 182-190.

Young R.W., 1983. The tempo of geomorphological change: evidence from southeastern Australia. Journal of Geology, 91, 221–230.

Zernitz, E. R., 1932. Drainage patterns and their significance. Journal of Geology, 40, 498-521.

Zhang, P.Z., Molnar, P., Downs, W.R., 2001. Increased sedimentation rates and grain sizes 2-4 myr ago due to the influence of climate change on erosion rates. Nature, 410, 891-897.

Zhang, W., Oguchi, T., Hayakawa, Y. S., Peng, H., 2013. Morphometric analyses of Danxia landforms in relation to bedrock geology: a case of Mt. Danxia, Guangdong Province, China. Open Geology Journal, 7, 54-62.

Zhao, M., Dupont, L., Eglinton, G., Teece, M., 2003. n-Alkane and pollen reconstruction of terrestrial climate and vegetation for NW Africa over the last 160 kyr. Organic Geochemistry, 34, 131-143.

Zheng, D., Zhang, P.Z., Wan, J., Yuan, D., Li, C., Yin, G., Zhang, G., Wang, Z., Min, W., Chen, J., 2006. Rapid exhumation at~ 8 Ma on the Liupan Shan thrust wfault from apatite fission-track thermochronology: Implications for growth of the northeastern Tibetan Plateau margin. Earth and Planetary Science Letters, 248, pp.198-208.

Appendices

Appendix 1 – Rawcliffe, A., masters thesis

The volume of rock eroded from SW South Africa since the start of the Cretaceous

Adam F. Rawcliffe

School of Earth and Environment, University of Leeds, Leeds, LS2 9JT, UK

Abstract

The long term landscape evolution of South Africa's abnormal topography is not well known. Late Cretaceous-Early Tertiary denudation, due to uplift associated with the African superplume, is thought to be responsible for the majority of erosion. A better understanding of the evolution can be determined by quantifying the maximum volume removed from southern South Africa since the start of the Cretaceous. The southern offshore basins are of interest to industry, and with a better understanding of the volume and composition of the eroded sediment; assessment of reservoir quality can be improved. Several assumptions have been made to construct structural cross sections across a c. 140,000 km^2 area in SW South Africa, with the estimated maximum thickness of lithostratigraphic groups extrapolated above topography. These have been georeferenced into 3DMove, and a maximum surface fit between. The volume calculated, 1.56 x 10^6 km^3, is compared to previous studies and the implications of this study are discussed. This study calculates *the* maximum volume of eroded material; however it is an order of magnitude greater than the

material found in offshore basins and therefore suggests further research is required.

INTRODUCTION

Location

The study area is a c. 140,000 km^2 region of southwestern South Africa; spanning part of the Cape Fold Belt and Karoo Basin (Fig. 1). It encompasses the entire Breed, Gouritz and Southern Cape river systems, plus parts of the Olifants, South Western Cape and Gamtoos river systems.

Rationale

South Africa has abnormally high elevation considering it is surrounded by passive margins; it has an interior plateau of low relief and high elevation, separated by the Great Escarpment from the coastal region of high relief and low average elevation. By calculating the volume of sediment removed, this study aids in the analysis of the long term landscape evolution. Apatite Fission Track Analysis (AFTA) data indicates significant late Cretaceous-Early Tertiary denudation in the interior of western south Africa (Gallagher and Brown, 1999), which is suggested to be due to uplift associated with the initiation and growth of the African superplume (Al-Hajri et al., 2009). The majority of the sediment eroded from the study area is thought to have been transported into the southern offshore basins (Tinker et al., 2008a), known to be hydrocarbon reservoirs. Placer diamond deposits are also known to exist in the offshore area. This study provides an estimate of the eroded sediment volume along with the composition of the sediment. This will assist in determining better evaluations towards reservoir and resource quality, and the methods used provide an approach for similar assessments of comparable source to sink configurations across the globe; such as the Norwegian Margin and the Gulf of Mexico.

Previous Research

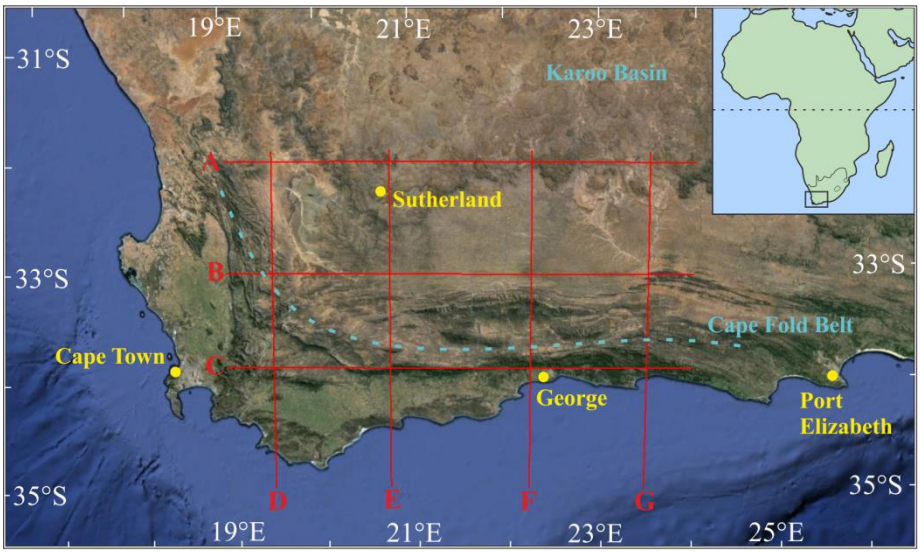

Figure 1. Map showing the location of the study area in SW South Africa (inset map). The grid (red lines) shows the locations of the section lines, discussed below, (**A**; 19°E, 32°05'S – 24°E,32°05'S, **B**; 19°E,33°05'S - 19°E, 33°05'S, **C**; 19°E, 33°55'S – 24°E,33°55'S, **D**; 19°30'E, 32°S – 19°30'E,35°S, **E**; 20°45'E, 32°S – 20°45'E,35°S, **F**; 22°15'E, 32°S – 22°15'E,35°S and **G**; 23°30'E, 32°S – 23°30'E,35°S). *Google Earth Image (2014)*.

There has been little previous research into the volume of eroded sediment from South Africa since the start of the Cretaceous. Tinker et al. (2008b) used AFTA in three boreholes to estimate 3.3-4.5 km thickness of stratigraphy eroded across the southern cape escarpment and coastal plain since the mid-late Cretaceous, and up to 7.5 km of stratigraphy including Early Cretaceous denudation. This was then compared with sediment accumulation in the southern offshore basins (Tinker et al., 2008a). The offshore accumulated volume, 268,500 km^3, equated to an onshore vertical elevation of only 860 m of eroded sediment; an order of magnitude lower than the 7.5 km estimated from AFTA. Tinker et al. (2008a) suggests that; the uncertainty of using only three boreholes; the removal of sediment by chemical weathering; and the 'loss' of sediment through offshore unconformities and sediment-bypass are the cause of the significant difference.

Aims

The aim of this study is to build on previous research and produce an estimate of a maximum value of the total volume removed from SW South Africa since the Cretaceous. Structural cross-sections establish a maximum elevation surface to the stratigraphy prior to landscape denudation, and a volume between this and present day topography can then be calculated.

METHODS

Literature Review

Before the maximum volume of eroded sediment can be calculated the stratigraphic configuration prior to denudation needs to be considered. Lithostratigraphic groups within the study area need to be established, along with their stratigraphic thicknesses (Table 1). This can then be used to aid the construction of structural cross-sections showing the maximum upper surface of the stratigraphy. The oldest groups known to have been eroded are the Table Mountain Group and the Precambrian Malmesbury Group. Above these are the Bokkeveld, Witteberg, Dwyka, Ecca, Beaufort, Stormberg and Drakensberg Groups.

Group	**Thickness (m)**	**Reference**
Drakensberg	1,400	(Catuneanu et al., 2005)
Stormberg	1,400	(Johnson, 1976)
Beaufort	3,000	(Adams et al., 2001)
Ecca	1,800	(Adams et al., 2001)
Dwyka	1,300	(Rowsell and De Swardt, 1976)
Witteberg	2,000	Ros March 03
Bokkeveld	2,000	1:250,000 Map Data
Table Mountain	2,500	(Shone and Booth, 2005)

A bias towards the maximum thicknesses in southeastern South Africa is used to select the preferred thicknesses, discussed below, of these groups: Table Mountain Group; 2,500 m based on the sum of the individual formation values suggested by Shone and Booth (2005) from the Western Cape region. Bokkeveld Group; 2,000 m based on interpretations of map data within the study area. Witteberg Group; 2,000 m based on cross-sections (KING, 2005, KING et al., 2009) in the Swartberg region. Dwyka Group; 1,300 m based on borehole data from the Western and Central Cape (Rowsell and De Swardt, 1976). Ecca Group; 1,800 m based on values from Sutherland (Adams et al., 2001) and borehole data (Rowsell and De Swardt, 1976). Beaufort Group; 3,000 m based on values from Sutherland (Adams et al., 2001). Stormberg Group; 1,400 m based on map data within the study area and values from the Eastern Cape (Johnson, 1976). Drakensberg Group; 1,400 m based on values from the Karoo Foredeep (Catuneanu et al., 2005).

These values sum to a total of c. 13 km of sediment above the Table Mountain Group which is consistent with the 12 km suggested by Johnson (1976), and the 10 km diagenesis depth of the Table Mountain Group (Rowsell and De Swardt, 1976).

Cross Section Construction

Published 1:250,000 geological map sheets from the Council for Geosciences span the study area (3218 Clanwilliam, 3220 Sutherland, 3222 Beaufort West, 3319 Worcester, 3320 Ladismith, 3322 Oudtshoorn and 3420 Riversdale). These provide the initial surface geology data used to construct basic structural cross sections, and further constrain group thicknesses. The calculated thicknesses (Table 1) of the stratigraphic groups are used with the Arc method (Busk, 1929) of cross section construction (Fig. 2) to assist in the extrapolation of the seven cross-sections; three E-W and four N-S, **A**, **B**, **C**, **D**, **E**, **F** and **G** respectively (Fig. 1).

Calculations in 3DMove

A mean elevation of present day topography was calculated using the 'summary statistics' tool in ArcGIS, the raster data of the Digital Elevation Model (DEM). The average elevation across the study area is 587.4 m, based on 196187508 data points from the ASTER (30 m) DEM. This value can be put into Midland Valley 3DMove software to create a lower bounding surface representing the current level of erosion.

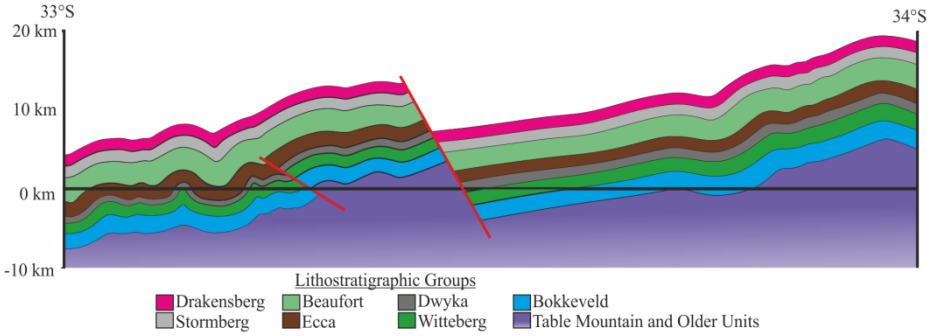

Figure 2. Showing part of cross section **F** between 33°S and 34°S. Cross section constructed from map sheets and thickness values from Table 1 using the Arc method (Busk, 1929). The top surface is the maximum extent of the lithologies prior to erosion.

Using 3DMove, the seven structural cross sections can be georeferenced to create an interactive 3D version (Fig. 3) of the grid depicted in Figure 1. The maximum upper surface can be digitised as horizons, with slight modifications being made to align the upper surface at cross section intersections. By adding additional tie-lines between structural features, faults and folds can be correlated between cross sections allowing for a more accurate surface representation. Using the 'create surface from horizon' tool in 3DMove an upper surface over the top of the maximum horizon lines can be generated to represent the maximum vertical extent of sediment prior to erosion. Several construction methods are available however the 'ordinary kriging' tool provides the best-fit surface for the dataset discussed. Once upper and lower bounding horizons, maximum vertical extent and mean present day topography respectively, have been created; the 'volume between horizons' tool in 3DMove can be used to determine the total volume of eroded sediment. This is

calculated by fitting multiple cubes between the surfaces. Decreasing the cube size means a more accurate value can be determined.

ASSUMPTIONS

Several assumptions need to be made in order to calculate a maximum value of the total volume removed from SW South Africa since the Cretaceous. This study focuses on the total eroded volume since the start of the Cretaceous and therefore Cretaceous and younger aged deposits have not been included in the total volume. It has been assumed that these younger deposits, especially the exposure of Cretaceous Enon Formation near Oudtshoorn, are derived from eroded sediment of the pre-Cretaceous lithostratigraphic groups being studied; and therefore these can be ignored and excluded when constructing cross sections.

There are poor constraints on the lateral extent of the Stormberg group and Jurassic aged Drakensberg flood basalts. Both of these are only exposed in the Eastern Cape region however there is no conclusive evidence of a boundary that would have prevented these units being laterally extensive across the Western Cape to the study area. Dolerite dykes and sills of Jurassic-age are common across large parts of the study area that may have fed Drakensberg flood basalts. As the aim of this study is to provide a maximum value of the total volume removed, it is assumed that these lithostratigraphic groups have also been eroded.

Due to the large 1:250,000 scale that the study uses, it is not practical to construct the structural cross sections on true scale topography. Therefore the mean elevation across the study area was instead used as the baseline for the cross sections.

Several faults are found across the study area and the offset along them has an

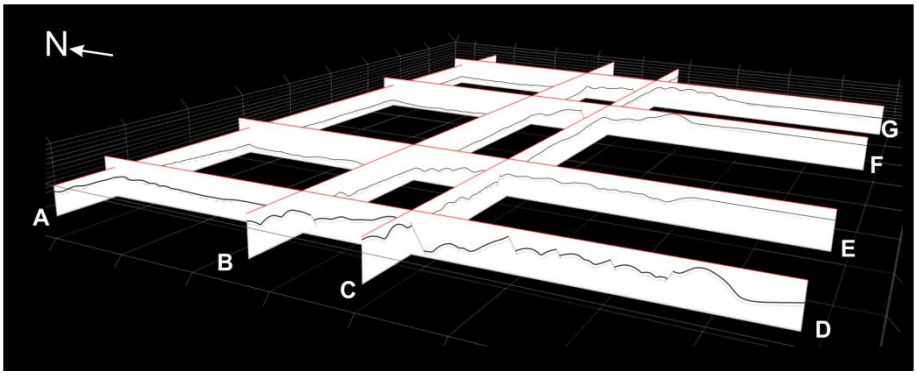

Figure 3. Cross section grid from Figure 1 seen in 3D, after being georeferenced in 3DMove. The maximum extent of the stratigraphy has been digitised as a horizon; ready to project the maximum upper surface between cross sections.

effect on the extent of the missing volume. It is assumed that minor faults, confined

within lithostratigraphic groups, have little effect on the eroded volume and can be ignored. Large extensional faults, as at Worcester, are assumed to be late events that offset all units, which is demonstrated by Cretaceous and younger deposits in the hanging wall.

When using the Arc method (Busk, 1929) to extrapolate the preferred lithostratigraphic thicknesses (Table 1), it was assumed that all units are conformably overlying one another and that all have been deformed and folded at the same time. It is also assumed that lithostratigraphic thicknesses are constant across the whole study area.

It is unreasonable to assume the coastline has remained in its present location throughout the evolution of the continent. When extrapolating the structural cross sections it is assumed that the lithostratigraphic groups extended out to sea at a similar elevation to that at the coast.

If the maximum upper surfaces do not intersect after georeferencing the cross sections into 3DMove; it is first assumed that construction has strayed off the section line and therefore slight rotations to the cross sections align the top horizons. If this does not align the horizons it is assumed that it is due to slight construction errors and horizons can be edited to intersect using a maximum bias.

RESULTS

Using the c. 140,000 km study area from 19°E, 32°S – 24°E, 35°S and a value of c. 13 km of sediment above the Table Mountain Group; the total volume removed from SW South Africa since the Cretaceous is 1.56×10^6 km^3. This equates to an eroded average of 11 km vertical thickness across the study area. Figure 4 shows a colour coded overlay on top of the study area indicating where the eroded sediment has been removed. The volumes of eroded sediment are closely linked with present day features. The interior Karoo Basin is missing the least material and is clearly defined by the cold colours in the north of the study area. The majority of eroded sediment has come from the mountainous Cape Fold Belt (Fig. 4). A small depression in eroded volume is seen within the Cape Fold Belt to the west of the study area. This is the large extensional Worcester fault and it can be seen to have prevented erosion of the lithostratigraphic units.

DISCUSSION

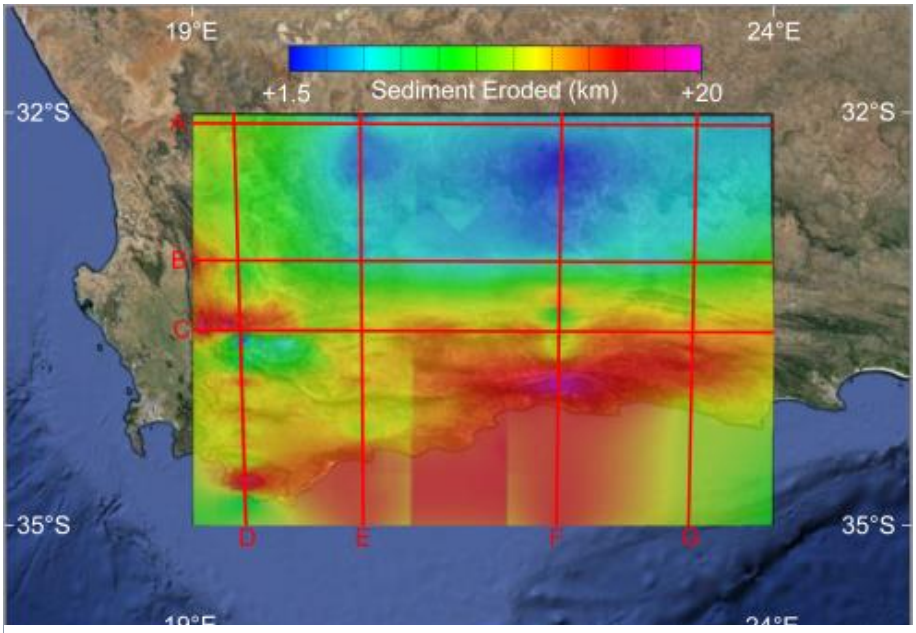

Figure 4. Map of the study area (as in Fig. 1) with coloured overlay image, from 3DMove, showing the extent of the missing sediment. Cold colours indicate areas where little volume of sediment has been removed and warm colours indicate where large volumes of sediment have been removed.

Tinker et al. (2008a, b) studied a similar area along southern South Africa. The maximum vertical thickness value of 7.5km over the 140,000 km^2 area (Tinker et al., 2008b), equates to a total eroded volume of 1.05 x 10^6 km^3. The area examined in this study suggests an additional 3.5 km eroded vertical thickness, equating to a total of 1.56 x 10^6 km^3 of eroded sediment. The value of Tinker et al. (2008a, b) is based on AFTA of only three boreholes across southern South Arica and is therefore a basic estimate, with little constraints. The value obtained from this study provides a maximum volume estimate. Similar causes to those suggested by Tinker et al. (2008a) likely explain the order of magnitude difference between the onshore volume of this study, and the calculated offshore value of 268,500 km^3 (Tinker et al., 2008a); however a large factor may be due to the poor knowledge of active drainage basins and the locations of their sinks over the period of erosion.

Refinements can be made to this estimate, and further constraints can be added to reduce the approximated total maximum volume of eroded sediment; discussed below.

To improve this estimate; more structural cross sections, with closer spacing, are needed to improve the upper surface. This will allow better correlation between features and prevent 3DMove from ‘bulk’ interpolation; as seen in the southern central grid square between section lines **E** and **F** in Figure 4.

There are certain assumptions used in this study, discussed above, that may be incorrect and leading to an overestimation. These are;

The Witteberg group pinches out in the Clanwilliam region; in this study it is assumed to be laterally extensive, however this is therefore an over estimate. It is possible that other lithostratigraphic groups are not laterally extensive, such as the Drakensberg, and this needs to be taken into account to better constrain the total maximum volume of eroded sediment. By examining the clast composition of outcrops of the Cretaceous Enon formation, as exposed at Oudtshoorn, it may be possible to determine the lateral extent of the lithostratigraphic groups such as the Drakensberg flood basalts. The implication of this is the quality of offshore reservoirs; eroded Drakensberg makes poor reservoir sediment, whereas the mix of sands and silts of the Karoo Supergroup are likely to make better quality reservoirs.

Thickness variations within the lithostratigraphic groups are indicated by borehole data in the region (Rowsell and De Swardt, 1976), this also questions; how laterally extensive the groups are, and how accurate the preferred chosen thicknesses (Table 1) of these groups are.

Figure 4 shows that a large proportion of sediment has been eroded from the current offshore area, with approximately one fifth of the study area being extrapolated beyond the current shoreline. As discussed above it is unreasonable to assume the coastline has remained in its present location, however there is no evidence beyond the present shoreline to constrain the upper maximum surface; therefore this is a large unknown effecting the calculation.

CONCLUSION

The total maximum volume of eroded sediment determined through this study is *the* maximum value. It is now a case of better constraining this value by inputting the additional constraints, and by doing more detailed studies and tests within and around the study area as discussed above. Nonetheless, the volume of material eroded is an order of magnitude greater than the material found in offshore basins.

REFERENCES

ADAMS, S., TITUS, R., PIETERSEN, K., TREDOUX, G. & HARRIS, C. 2001. Hydrochemical characteristics of aquifers near Sutherland in the Western Karoo, South Africa. *Journal of Hydrology,* 241**,** 91-103.

AL-HAJRI, Y., WHITE, N. & FISHWICK, S. 2009. Scales of transient convective support beneath Africa. *Geology*, 37, 883-886.

BUSK, H. G. 1929. *Earth flexures: their geometry and their representation and*

analysis in geological section with special reference to the problem of oil finding, CUP Archive.

CATUNEANU, O., WOPFNER, H., ERIKSSON, P. G., CAIRNCROSS, B., RUBIDGE, B. S., SMITH, R. M. H. & HANCOX, P. J. 2005. The Karoo basins of south-central Africa. *Journal of African Earth Sciences,* 43**,** 211-253.

GALLAGHER, K. & BROWN, R. 1999. The Mesozoic denudation history of the Atlantic margins of southern Africa and southeast Brazil and the relationship to offshore sedimentation. *Geological Society, London, Special Publications*, 153, 41-53.

JOHNSON, M. 1976. *Stratigraphy and sedimentology of the Cape and Karoo sequences in the Eastern Cape Province.* Rhodes University.

KING, R. C. 2005. The structural evolution of the Cape Fold Belt and southwest Karoo Basin: Implications on sediment storage and routing to the southwest Karoo Basin, South Africa: Unpublished Ph.D. thesis. University of Liverpool, 327p.

KING, R. C., HODGSON, D. M., FLINT, S. S., POTTS, G. J. & VAN LENTE, B. 2009. Development of subaqueous fold belts as a control on the timing and distribution of deepwater sedimentation: an example from the southwest Karoo Basin, South Africa. *External Controls on Deep-water Depositional Systems,* 92**,** 261.

ROWSELL, D. & DE SWARDT, A. 1976. Diagenesis in Cape and Karoo sediments, South Africa, and its bearing on their hydrocarbon potential. *Transactions of the Geological Society of South Africa,* 79**,** 81-145.

SHONE, R. W. & BOOTH, P. W. K. 2005. The Cape Basin, South Africa: A review. *Journal of African Earth Sciences,* 43**,** 196-210.

TINKER, J., DE WIT, M. & BROWN, R. 2008a. Linking source and sink: Evaluating the balance between onshore erosion and offshore sediment accumulation since Gondwana break-up, South Africa. *Tectonophysics,* 455**,** 94-103.

TINKER, J., DE WIT, M. & BROWN, R. 2008b. Mesozoic exhumation of the southern Cape, South Africa, quantified using apatite fission track thermochronology. *Tectonophysics,* 455**,** 77-93.

GOOGLE EARTH 7.0. 2014. SW South Africa, 35°S, 17°E, elevation 900km. [Accessed 15 April 2014].